A CYLINDRICAL SHELL WITH A FIXED END WHICH CONTAINS A CIRCUMFERENTIAL PART-THROUGH OR THROUGH CRACK UNDER GENERAL LOADING

A Ph.D. Thesis
Presented by

Müfit GÜLGEÇ

to
the Graduate School of Natural and Applied Sciences
of Middle East Technical University
in Partial Fulfillment for the Degree of

DOCTOR OF PHILOSOPHY

in

MECHANICAL ENGINEERING

MIDDLE EAST TECHNICAL UNIVERSITY
ANKARA
January, 1993

Approval of the Graduate School of Natural and Applied Sciences.

Prof. Dr. Alpay Ankara
Director

I certify that this thesis satisfies all the requirements as a thesis for the degree of Doctor of Philosophy.

Prof. Dr. Rüknettin Oskay
Chairman of the Department

We certify that we have read this thesis and that in our opinion it is fully adequate, in scope and quality, as a thesis for the degree of Doctor of Philosophy in Mechanical Engineering

Prof. Dr. O. Selçuk Yahşi
Supervisor

Examining Committee in Charge

Prof. Dr. Ömer Gündüz Bilir (Chairman)

Prof. Dr. Orhan Aksoğan

Prof. Dr. Osman Selçuk Yahşi

Prof. Dr. Ruşen Geçit

Assoc. Prof. Dr. Bülent Doyum

ABSTRACT

A CYLINDRICAL SHELL WITH A FIXED END CONTAINING A CIRCUMFERENTIAL PART-THROUGH OR THROUGH CRACK UNDER THE GENERAL LOADING

GÜLGEÇ, Müfit
Ph.D. in Mechanical Engineering
Supervisor: Prof. Dr. O. Selçuk YAHSI
January, 1993, 183 pages

In this study, the problem of a cylindrical shell with a fixed end containing a circumferential part-through or through crack under the general loading is analyzed. The problem is formulated for a specially orthotropic material by using Reissner's shell theory. The part-through problem is treated by using a line-spring model. By using the Fourier integral transform technique ,the problem is reduced to five simultaneous singular integral equations. The system of singular integral equations is further reduced to a system of linear algebraic equations which is solved numerically by using Gauss-Chebyshev quadrature formula. The primary objective is to study the effect of the end constraining on the stress intensity factor which is the main fracture mechanics parameter. Also, the effect of the shell curvature and thickness, material orthotropy, and the Poisson's ratio on the stress intensity factors are investigated.

Keywords: Cylindrical Shell, Circumferential Part-Through Crack, Circumferential Through Crack, Fixed End.

Science Code: 625.03.02

ÖZ

GENEL YÜKLEMENİN ETKİSİNDE BİR UCUNDAN SABİTLENMİŞ KISMİ ÇATLAK VEYA ÇATLAK İHTİVA EDEN SİLİNDİRİK BİR KABUK

GÜLGEÇ, Müfit
Doktora Tezi, Makina Mühendisligi Anabilim Dalı
Tez Yöneticisi: Prof. Dr. O. Selçuk YAHŞI
Ocak, 1993, 183 sayfa

Bu tezde, genel yüklemenin etkisi altında, bir ucundan sabitlenmiş ve çevresel kısmi çatlak veya çatlak ihtiva eden silindirik bir kabuk incelenmiştir. Problem, özel ortotropik bir malzeme için Reissner Kabuk Teorisi kullanılarak formüle edilmiştir. Kısmi çatlak problemi line-spring modeli kullanılarak çozülmüştür. Fourier integral dönüşüm tekniği kullanılarak, problem beş tekil integral denklemine indirgenmiştir. Tekil integral denklemleri daha sonra lineer denklem takımına indirgenmiş ve Gauss-Chebyshev integral denklemi kullanılarak sayısal olarak çozülmüştür. Bu çalışmada asıl amaç, sabit ucun ana kırılma mekaniği parametresi olan gerilme şiddeti çarpanına olan etkisini incelemektir. Ayrıca, kabuk eğriliğinin ve kalınlığının, malzeme ortotropisinin ve Poisson oranının gerilme şiddeti çarpanına etkisi de incelenmiştir.

Anahtar Kelimeler: Silindrik Kabuk, Çevresel Kısmi Çatlak, Çevresel Çatlak, Sabit Uç.

Bilim Dalı Sayısal Kodu: 625.03.02

ACKNOWLEDGEMENTS

I would like to express my deepest gratitude and appreciation to my supervisor Prof. Dr. O. Selçuk Yahşi who inspired and encouraged me in completing this study.

I wish to extend my special thanks to Prof. Dr. Yucel Ercan and Prof. Dr. Ali Durmaz for their invaluable support and encouragement.

I am thankful to my friend Dr. Levend Parnas for his cooperation in discussing and writing this dissertation.

I wish to express my deep sense of gratitude to my parents for their lifelong care and devotion.

I am especially thankful to my wife, Sema, for her long support and encouragemet during the years.

To my lovely dougther, *Sıla*

TABLE OF CONTENTS

Page

ABSTRACT iii

ÖZ iv

ACKNOWLEDGEMENTS v

LIST OF TABLES viii

LIST OF FIGURES xvi

LIST OF SYMBOLS xx

CHAPTER I: INTRODUCTION 1

CHAPTER II: BASIC FORMULATION OF THE PROBLEM 5

CHAPTER III: A CYLINDRICAL SHELL WITH A FIXED END WHICH CONTAINS CIRCUMFERENTIAL THROUGH CRACK 11

3.1 Formulation of the Problem 11

3.2 Numerical Solution Method 39

3.3 Asymptotic Fields Around the Crack Tip 43

3.4 Numerical Results and Discussion 46

CHAPTER IV: A CYLINDRICAL SHELL WITH A FIXED END WHICH CONTAINS A CIRCUMFERENTIAL PART-THROUGH CRACK 52

CHAPTER V: CONCLUSION 68

REFERENCES 147

APPENDICES

APPENDIX A. THE DIMENSIONLESS QUANTITIES 149

APPENDIX B. ASYMPTOTIC VALUES OF KERNELS OF INTEGRAL EQUATIONS 150

APPENDIX C. THE KERNELS OF INTEGRAL EQUATIONS 162

APPENDIX D. EVALUATION OF SINE AND COSINE INTEGRALS 170

APPENDIX E. EDGE CRACK STRESS INTENSITY FACTOR CURVE FITTING 181

VITA 183

LIST OF TABLES

Page

Table 1. Stress Intensity Factor Ratios in an Isotropic Cylindrical Shell with a Fixed End Containing a Circumferential Through Crack Under Uniform Membrane Loading N_{11}; $\nu = 0.3$. 70

Table 2. Stress Intensity Factor Ratios in an Isotropic Cylindrical Shell with a Fixed End Containing a Circumferential Through Crack Under Uniform Membrane Loading N_{11}; $\nu = 0.3$. 71

Table 3. Stress Intensity Factor Ratios in an Isotropic Cylindrical Shell with a Fixed End Containing a Circumferential Through Crack Under Uniform Bending Moment M_{11}; $\nu = 0.3$. 72

Table 4. Stress Intensity Factor Ratios in an Isotropic Cylindrical Shell with a Fixed End Containing a Circumferential Through Crack Under Uniform Bending Moment M_{11}; $\nu = 0.3$. 73

Table 5. Stress Intensity Factor Ratios in an Isotropic Cylindrical Shell with a Fixed End Containing a Circumferential Through Crack Under Uniform Transverse Shear Loading V_1; $\nu = 0.3$. 74

Table 6. Stress Intensity Factor Ratios in an Isotropic Cylindrical Shell with a Fixed End Containing a Circumferential Through Crack Under Uniform Transverse Shear Loading V_1; $\nu = 0.3$. 75

Table 7. Stress Intensity Factor Ratios in an Isotropic Cylindrical Shell with a Fixed End Containing a Circumferential Through Crack Under Uniform Transverse Shear Loading V_1; $\nu = 0.3$. 76

Table 8. Stress Intensity Factor Ratios in an Isotropic Cylindrical Shell with a Fixed End Containing a Circumferential Through Crack Under In-Plane Shear Loading N_{12}; $\nu = 0.3$. 77

Page

Table 9. Stress Intensity Factor Ratios in an Isotropic Cylindrical Shell with a Fixed End Containing a Circumferential Through Crack Under In-Plane Shear Loading N_{12}; $\nu = 0.3$. 78

Table 10. Stress Intensity Factor Ratios in an Isotropic Cylindrical Shell with a Fixed End Containing a Circumferential Through Crack Under In-Plane Shear Loading N_{12}; $\nu = 0.3$. 79

Table 11. Stress Intensity Factor Ratios in an Isotropic Cylindrical Shell with a Fixed End Containing a Circumferential Through Crack Under Uniform Twisting Moment M_{12}; $\nu = 0.3$. 80

Table 12. Stress Intensity Factor Ratios in an Isotropic Cylindrical Shell with a Fixed End Containing a Circumferential Through Crack Under Uniform Twisting Moment M_{12}; $\nu = 0.3$. 81

Table 13. Stress Intensity Factor Ratios in an Isotropic Cylindrical Shell with a Fixed End Containing a Circumferential Through Crack Under Uniform Twisting Moment M_{12}; $\nu = 0.3$. 82

Table 14. The Effect of Poisson's Ratio on the Stress Intensity Factor Ratiosin an Isotropic Cylindrical Shell with a Fixed End Containing a Circumferential Through Crack; l/a=0.5, a/h=1, R/h=5. 83

Table 15. The Effect of Material Orthotropyon the Stress Intensity Factor Ratiosin a Cylindrical Shell with a Fixed End Containing a Circumferential Through Crack; l/a=0.5, a/h=1, R/h=10. 84

Table 16. Mode I Normalized Stress Intensity Factor at the Center of a Semi-Elliptic Circumferential Part-Through Crack in an Isotropic Cylindrical Shell with a Fixed End Subjected to Membrane Loading; $\nu = 0.3$, l/a=0.25 85

Table 17. Mode I Normalized Stress Intensity Factor at the Center of a Semi-Elliptic Circumferential Part-Through Crack in an Isotropic Cylindrical Shell with a Fixed End Subjected to Membrane Loading; $\nu = 0.3$, l/a=0.40 86

Page

Table 18. Mode I Normalized Stress Intensity Factor at the Center of a Semi-Elliptic Circumferential Part-Through Crack in an Isotropic Cylindrical Shell with a Fixed End Subjected to Membrane Loading; $\nu = 0.3$, l/a=0.50 87

Table 19. Mode I Normalized Stress Intensity Factor at the Center of a Semi-Elliptic Circumferential Part-Through Crack in an Isotropic Cylindrical Shell with a Fixed End Subjected to Membrane Loading; $\nu = 0.3$, l/a=1.0 88

Table 20. Mode I Normalized Stress Intensity Factor at the Center of a Semi-Elliptic Circumferential Part-Through Crack in an Isotropic Cylindrical Shell with a Fixed End Subjected to Membrane Loading; $\nu = 0.3$, l/a=1.5 89

Table 21. Mode I Normalized Stress Intensity Factor at the Center of a Semi-Elliptic Circumferential Part-Through Crack in an Isotropic Cylindrical Shell with a Fixed End Subjected to Membrane Loading; $\nu = 0.3$, l/a=2.5 90

Table 22. Mode I Normalized Stress Intensity Factor at the Center of a Semi-Elliptic Circumferential Part-Through Crack in an Isotropic Cylindrical Shell with a Fixed End Subjected to Membrane Loading; $\nu = 0.3$, l/a=5. 91

Table 23. Mode I Normalized Stress Intensity Factor at the Center of a Semi-Elliptic Circumferential Part-Through Crack in an Isotropic Cylindrical Shell with a Fixed End Subjected to Membrane Loading; $\nu = 0.3$, l/a=50. 92

Table 24. Mode I Normalized Stress Intensity Factor at the Center of a Semi-Elliptic Circumferential Part-Through Crack in an Isotropic Cylindrical Shell with a Fixed End Subjected to Bending Moment; $\nu = 0.3$, l/a=0.25 93

Table 25. Mode I Normalized Stress Intensity Factor at the Center of a Semi-Elliptic Circumferential Part-Through Crack in an Isotropic Cylindrical Shell with a Fixed End Subjected to Bending Moment; $\nu = 0.3$, l/a=0.40 94

Table 26. Mode I Normalized Stress Intensity Factor at the Center of a Semi-Elliptic Circumferential Part-Through Crack in an Isotropic Cylindrical Shell with a Fixed End Subjected to Bending Moment; $\nu = 0.3$, l/a=0.50 95

Page

Table 27. Mode I Normalized Stress Intensity Factor at the Center of a Semi-Elliptic Circumferential Part-Through Crack in an Isotropic Cylindrical Shell with a Fixed End Subjected to Bending Moment; $\nu = 0.3$, l/a=1.0 96

Table 28. Mode I Normalized Stress Intensity Factor at the Center of a Semi-Elliptic Circumferential Part-Through Crack in an Isotropic Cylindrical Shell with a Fixed End Subjected to Bending Moment; $\nu = 0.3$, l/a=1.5 97

Table 29. Mode I Normalized Stress Intensity Factor at the Center of a Semi-Elliptic Circumferential Part-Through Crack in an Isotropic Cylindrical Shell with a Fixed End Subjected to Bending Moment; $\nu = 0.3$, l/a=2.5 98

Table 30. Mode I Normalized Stress Intensity Factor at the Center of a Semi-Elliptic Circumferential Part-Through Crack in an Isotropic Cylindrical Shell with a Fixed End Subjected to Bending Moment; $\nu = 0.3$, l/a=5. 99

Table 31. Mode I Normalized Stress Intensity Factor at the Center of a Semi-Elliptic Circumferential Part-Through Crack in an Isotropic Cylindrical Shell with a Fixed End Subjected to Bending Moment; $\nu = 0.3$, l/a=50. 100

Table 32. Mode II Normalized Stress Intensity Factor at the Center of a Semi-Elliptic Circumferential Part-Through Crack in an Isotropic Cylindrical Shell with a Fixed End Subjected to Out-of-Plane Shear; $\nu = 0.3$, l/a=0.25 101

Table 33. Mode II Normalized Stress Intensity Factor at the Center of a Semi-Elliptic Circumferential Part-Through Crack in an Isotropic Cylindrical Shell with a Fixed End Subjected to Out-of-Plane Shear; $\nu = 0.3$, l/a=0.40 102

Table 34. Mode II Normalized Stress Intensity Factor at the Center of a Semi-Elliptic Circumferential Part-Through Crack in an Isotropic Cylindrical Shell with a Fixed End Subjected to Out-of-Plane Shear; $\nu = 0.3$, l/a=0.50 103

Table 35. Mode II Normalized Stress Intensity Factor at the Center of a Semi-Elliptic Circumferential Part-Through Crack in an Isotropic Cylindrical Shell with a Fixed End Subjected to Out-of-Plane Shear; $\nu = 0.3$, l/a=1.0 104

Table 36. Mode II Normalized Stress Intensity Factor at the Center of a Semi-Elliptic Circumferential Part-Through Crack in an Isotropic Cylindrical Shell with a Fixed End Subjected to Out-of-Plane Shear; $\nu = 0.3$, l/a=1.5 105

Table 37. Mode II Normalized Stress Intensity Factor at the Center of a Semi-Elliptic Circumferential Part-Through Crack in an Isotropic Cylindrical Shell with a Fixed End Subjected to Out-of-Plane Shear; $\nu = 0.3$, l/a=2.5 106

Table 38. Mode II Normalized Stress Intensity Factor at the Center of a Semi-Elliptic Circumferential Part-Through Crack in an Isotropic Cylindrical Shell with a Fixed End Subjected to Out-of-Plane Shear; $\nu = 0.3$, l/a=5. 107

Table 39. Mode II Normalized Stress Intensity Factor at the Center of a Semi-Elliptic Circumferential Part-Through Crack in an Isotropic Cylindrical Shell with a Fixed End Subjected to Out-of-Plane Shear; $\nu = 0.3$, l/a=50. 108

Table 40. Mode III Normalized Stress Intensity Factor at the Center of a Semi-Elliptic Circumferential Part-Through Crack in an Isotropic Cylindrical Shell with a Fixed End Subjected to In-Plane Shear; $\nu = 0.3$, l/a=0.25 ... 109

Table 41. Mode III Normalized Stress Intensity Factor at the Center of a Semi-Elliptic Circumferential Part-Through Crack in an Isotropic Cylindrical Shell with a Fixed End Subjected to In-Plane Shear; $\nu = 0.3$, l/a=0.40 ... 110

Table 42. Mode III Normalized Stress Intensity Factor at the Center of a Semi-Elliptic Circumferential Part-Through Crack in an Isotropic Cylindrical Shell with a Fixed End Subjected to In-Plane Shear; $\nu = 0.3$, l/a=0.50 ... 111

Table 43. Mode III Normalized Stress Intensity Factor at the Center of a Semi-Elliptic Circumferential Part-Through Crack in an Isotropic Cylindrical Shell with a Fixed End Subjected to In-Plane Shear; $\nu = 0.3$, l/a=1.0 112

Table 44. Mode III Normalized Stress Intensity Factor at the Center of a Semi-Elliptic Circumferential Part-Through Crack in an Isotropic Cylindrical Shell with a Fixed End Subjected to In-Plane Shear; $\nu = 0.3$, l/a=1.5 113

Table 45. Mode III Normalized Stress Intensity Factor at the Center of a Semi-Elliptic Circumferential Part-Through Crack in an Isotropic Cylindrical Shell with a Fixed End Subjected to In-Plane Shear; $\nu = 0.3$, l/a=2.5 114

Table 46. Mode III Normalized Stress Intensity Factor at the Center of a Semi-Elliptic Circumferential Part-Through Crack in an Isotropic Cylindrical Shell with a Fixed End Subjected to In-Plane Shear; $\nu = 0.3$, l/a=5. 115

Table 47. Mode III Normalized Stress Intensity Factor at the Center of a Semi-Elliptic Circumferential Part-Through Crack in an Isotropic Cylindrical Shell with a Fixed End Subjected to In-Plane Shear; $\nu = 0.3$, l/a=50..... 116

Table 48. Mode III Normalized Stress Intensity Factor at the Center of a Semi-Elliptic Circumferential Part-Through Crack in an Isotropic Cylindrical Shell with a Fixed End Subjected to Twisting; $\nu = 0.3$, l/a=0.25 117

Table 49. Mode III Normalized Stress Intensity Factor at the Center of a Semi-Elliptic Circumferential Part-Through Crack in an Isotropic Cylindrical Shell with a Fixed End Subjected to Twisting; $\nu = 0.3$, l/a=0.40 118

Table 50. Mode III Normalized Stress Intensity Factor at the Center of a Semi-Elliptic Circumferential Part-Through Crack in an Isotropic Cylindrical Shell with a Fixed End Subjected to Twisting; $\nu = 0.3$, l/a=0.50 119

Table 51. Mode III Normalized Stress Intensity Factor at the Center of a Semi-Elliptic Circumferential Part-Through Crack in an Isotropic Cylindrical Shell with a Fixed End Subjected to Twisting; $\nu = 0.3$, l/a=1.0 120

Table 52. Mode III Normalized Stress Intensity Factor at the Center of a Semi-Elliptic Circumferential Part-Through Crack in an Isotropic Cylindrical Shell with a Fixed End Subjected to Twisting; $\nu = 0.3$, l/a=1.5 121

Table 53. Mode III Normalized Stress Intensity Factor at the Center of a Semi-Elliptic Circumferential Part-Through Crack in an Isotropic Cylindrical Shell with a Fixed End Subjected to Twisting; $\nu = 0.3$, l/a=2.5 122

Table 54. Mode III Normalized Stress Intensity Factor at the Center of a Semi-Elliptic Circumferential Part-Through Crack in an Isotropic Cylindrical Shell with a Fixed End Subjected to Twisting; $\nu = 0.3$, l/a=5. 123

Table 55. Mode III Normalized Stress Intensity Factor at the Center of a Semi-Elliptic Circumferential Part-Through Crack in an Isotropic Cylindrical Shell with a Fixed End Subjected to Twisting; $\nu = 0.3$, l/a=50..... 124

Table 56. The Effect of Poisson's Ratio on the Normalized Stress Intensity Factorsat the Center of a Semi-Elliptic Circumferential Part-Through Crack inan Isotropic Cylindrical Shell with a Fixed End; l/a=0.5, a/h=1, R/h=5..... 125

Table 57. The Effect of Material Orthotropy on the Normalized Stress Intensity Factorsat the Center of a Semi-Elliptic Circumferential Part-Through Crack in a Cylindrical Shell with a Fixed End; $\nu = 0.3$, l/a=0.5, a/h=1, R/h=10..... 126

Table E.1. The Compliance Coefficients for $p_1(\xi)$ and $p_2(\xi)$ for Tension and Bending, Respectively..... 182

Table E.2. The Compliance Coeeficients for $p_i(\xi)$, i=3,4,5, for Parabolic In-Plane Shear, Constant Out-of-Plane Shear and Twisting, Respectively..... 182

LIST OF FIGURES

Page

Figure 1. Geometry of a Cylindrical Shell Containing Circumferential Trough Crack with a Fixed End..... 12

Figure 2. Geometry of a Semi-Elliptical Part-Through Crack in a Shell..... 53

Figure 3. The Notation for a Part-Through Crack in Shells..... 55

Figure 4. Development of the Line-Spring Model for a Part-Through Crack..... 64

Figure 5. Stress Intensity Factor Ratio k_{mm} in an Isotropic Cylindrical Shell with a Fixed end Containing a Circumferential Through Crack Under Uniform Membrane Loading; $\nu = 0.3$, $R/h = 5$, ... 127

Figure 6. Stress Intensity Factor Ratio k_{bb} in an Isotropic Cylindrical Shell with a Fixed end Containing a Circumferential Through Crack Under Uniform Bending Moment; $\nu = 0.3$, $R/h = 5$..... 128

Figure 7. Stress Intensity Factor Ratio k_{vv} in an Isotropic Cylindrical Shell with a Fixed end Containing a Circumferential Through Crack Under Uniform Out-of-Plane Shear Loading; $\nu = 0.3$, $R/h = 5$..... 129

Figure 8. Stress Intensity Factor Ratio k_{ss} in an Isotropic Cylindrical Shell with a Fixed end Containing a Circumferential Through Crack Under Uniform In-Plane Shear Loading; $\nu = 0.3$, $R/h = 5$..... 130

Figure 9. Stress Intensity Factor Ratio k_{tt} in an Isotropic Cylindrical Shell with a Fixed end Containing a Circumferential Through Crack Under Uniform Twisting Moment; $\nu = 0.3$, $R/h = 5$..... 131

Figure 10. Stress Intensity Factor Ratio k_{mm} in an Isotropic Cylindrical Shell with a Fixed end Containing a Circumferential Through Crack Under Uniform Membrane Loading; $\nu = 0.3$, $l / a = 0.5$ 132

Figure 11. Stress Intensity Factor Ratio k_{bb} in an Isotropic Cylindrical Shell with a Fixed end Containing a Circumferential Through Crack Under Uniform Bending Moment; $\nu = 0.3$, $l / a = 0.5$ 133

Figure 12. Stress Intensity Factor Ratio k_{vv} in an Isotropic Cylindrical Shell with a Fixed end Containing a Circumferential Through Crack Under Uniform Out-of-Plane Shear Loading; $\nu = 0.3$, $l / a = 0.5$ 134

Figure 13. Stress Intensity Factor Ratio k_{ss} in an Isotropic Cylindrical Shell with a Fixed end Containing a Circumferential Through Crack Under Uniform In-Plane Shear Loading; $\nu = 0.3$, $l / a = 0.5$ 135

Figure 14. Stress Intensity Factor Ratio k_{tt} in an Isotropic Cylindrical Shell with a Fixed end Containing a Circumferential Through Crack Under Uniform Twisting Moment; $\nu = 0.3$, $l / a = 0.5$ 136

Figure 15. Mode I Normalized Stress Intensity Factor at the Center of a Semi-Elliptic Circumferential Outer Part-Through Crack in an Isotropic Cylindrical Shell with a Fixed End Subjected to Membrane Loading; $\nu = 0.3$, $R / h = 5$, $a / h = 1$ 137

Figure 16. Mode I Normalized Stress Intensity Factor at the Center of a Semi-Elliptic Circumferential Outer Part-Through Crack in an Isotropic Cylindrical Shell with a Fixed End Subjected to Bending Moment; $\nu = 0.3$, $R / h = 5$, $a / h = 1$ 138

Figure 17. Mode II Normalized Stress Intensity Factor at the Center of a Semi-Elliptic Circumferential Outer Part-Through Crack in an Isotropic Cylindrical Shell with a Fixed End Subjected to Out-of-Plane Shear; $\nu = 0.3$, $R / h = 5$, $a / h = 1$ 139

Figure 18. Mode III Normalized Stress Intensity Factor at the Center of a Semi-Elliptic Circumferential Outer Part-Through Crack in an Isotropic Cylindrical Shell with a Fixed End Subjected to In-Plane Shear; $\nu = 0.3$, $R/h = 5$, $a/h = 1$ 140

Figure 19. Mode III Normalized Stress Intensity Factor at the Center of a Semi-Elliptic Circumferential Outer Part-Through Crack in an Isotropic Cylindrical Shell with a Fixed End Subjected to Twisting; $\nu = 0.3$, $R/h = 5$, $a/h = 1$ 141

Figure 20. Mode I Normalized Stress Intensity Factor at the Center of a Semi-Elliptic Circumferential Outer Part-Through Crack in an Isotropic Cylindrical Shell with a Fixed End Subjected to Membrane Loading; $\nu = 0.3$, $R/h = 5$, $l_0/h = 0.2$ 142

Figure 21. Mode I Normalized Stress Intensity Factor at the Center of a Semi-Elliptic Circumferential Outer Part-Through Crack in an Isotropic Cylindrical Shell with a Fixed End Subjected to Bending Moment; $\nu = 0.3$, $R/h = 5$, $l_0/h = 0.2$ 143

Figure 22. Mode II Normalized Stress Intensity Factor at the Center of a Semi-Elliptic Circumferential Outer Part-Through Crack in an Isotropic Cylindrical Shell with a Fixed End Subjected to Out-of-Plane Shear; $\nu = 0.3$, $R/h = 5$, $l_0/h = 0.2$ 144

Figure 23. Mode III Normalized Stress Intensity Factor at the Center of a Semi-Elliptic Circumferential Outer Part-Through Crack in an Isotropic Cylindrical Shell with a Fixed End Subjected to In-Plane Shear; $\nu = 0.3$, $R/h = 5$, $l_0/h = 0.2$ 145

Figure 24. Mode III Normalized Stress Intensity Factor at the Center of a Semi-Elliptic Circumferential Outer Part-Through Crack in an Isotropic Cylindrical Shell with a Fixed End Subjected to Twisting; $\nu = 0.3$, $R/h = 5$, $l_0/h = 0.2$ 146

LIST OF SYMBOLS

q	Surface loading
N_{ij}	Membrane resultants
M_{ij}	Moment resultants
V_i	Transverse shear resultants
ε_{ij}	Strain components
X_i	Rectangular coordinates
$Z(X_1, X_2)$	Equation of middle surface
U_1	Displacement component in X_1 - direction
U_2	Displacement component in X_2 - direction
W	Displacement component in X_3 - direction
β_i	Angle of rotation of normals to shell surface
$F(X_1, X_2)$	Stress function
h	Shell thickness
D	Bending stiffness of shell
B	Effective shear modulus
E, ν	Material constants for specially orthotropic shell
c	Orthotropy parameter
R	Radius of shell
a	half of crack length
Ω, Ψ	Unknown auxiliary functions
λ_2	Shell parameter
l'	Distance between crack and circumferential crack
m_j, n_j	Roots of characteristic equations
$R_j(\alpha), S_j(\beta), A_1(\alpha), A_2(\alpha), B_1(\beta)$	Unknown functions
F_{j0}	Known crack surface loads
G_j	New unknown functions defined in terms of derivatives of displacement quantities
q_i	Fourier transform of G_j

τ, η, ρ	Normalized quantities used in numerical integration
k_{ij}	Fredholm kernels of singular integral equations
$h_i(\tau_j)$	Unknown fundamental functions
σ_{ij}	Stress components
k_j	Stress intensity factors
F_i	Net ligament force resultants
G	Energy available for fracture along the crack front
U	Work done by external loads
V	Strain energy
δ_i	Relative crack surface displacements and rotations corresponding to the resultants
r	Radial distance from crack tip
l_0	Maximum depth of semi-elliptical part-through crack
ξ	Ratio of crack depth to shell thickness
C_{ik}	Coefficients of compliance functions

CHAPTER I

INTRODUCTION

Pressure vessels, pipelines, containers, ship hulls etc. are all shell like structures which may fail by fracture. The designers of these components must take this into account as such failures are often catastrophic and endangering lives and the environment. The fracture process typically starts with a small material defect or weld imperfection that grows in fatigue which is driven by mechanical or environmental conditions. Eventually the flaw may be characterized as a macroscopic surface crack. This surface or part-through crack then continues its growth through the thickness, leading to failure by leaking or an unstable fracture.

In the discipline of fracture mechanics, one usually assumes an initial flaw configuration, and then seeks to obtain certain fracture parameters that are believed to govern the tendency of crack to grow. In the case of brittle fractures and more importantly, fracture by fatigue, the stress intensity factor is the most commonly used parameter.

Up to now, fracture mechanics research as applied to cylindrical containers and pipelines has dealt mostly with longitudinal flaws in the component. There is, of course, a good reason for this, namely, in pressurized cylinders under normal operating conditions, the hoop stress is by far the dominant stress component. On the other hand, any secondary load caused by known and unforeseen factors would be primarily in the axial direction. Some of the sources of these stresses are support misalignment, variety of thermal fluctuations, earthquake, vehicle vibrations and installations mistakes, which cause the different loading conditions. One may also pointed out that axial stresses would be much more time-varying than basically pressure induced hoop stresses and hence would tend to facilitate the formation and propagation of fatigue cracks in the circumferential direction.

Due to the three-dimensional nature of the problem, the crack problem in shells appears to be, at least at the present time, analytically intractable. However, the through crack problem can be treated within the confines of various shell theories. In fracture problems related to shells, the classical shell theory has been used in most of the existing solutions. In the classical shell theory, the transverse shear effects are neglected and eighth order classical shell theory is used to formulate the problem. Due to this approximation, one can have only four boundary conditions on the shell boundary. Hence, the crack surface boundary conditions are approximated by using the Kirchhoff assumption (i.e. instead of satisfying the conditions M_{ns}, $V = 0$ separately, the condition $V + \partial M_{ns}/\partial s = 0$ is satisfied where n,s are the coordinates normal and parallel to the crack surface, M_{ns} is the twisting moment and V is the transverse shear).

The first analysis of cracks in shells was presented by Folias in 1965 for a cracked sphere [1], [2] and for an axially cracked cylinder [3]. The circumferential cracked cylinder was investigated in 1967 [4]. The results in these papers are asymptotic in nature for short cracks. A shallow shell theory was also used which linearizes the governing equations.

In late 1960's Erdogan and Kibler [5] provided a more complete solution to the problems studied by Folias. In this study, shallow shell equations are employed, the numerical techniques for the solution of the singular integral equations are exact.

The major shortcoming of these early shell solutions, was the neglect of transverse shear deformation. In shells, since extension and bending are coupled, the elasticity concept of stress intensity factor cannot be used with these 8th order theories without redefinition. It was Sih and Hagendorf [6] in 1974 who first solved cracked shell problems by including the transverse shear effects. Later papers, which include the transverse shear effect use the shallow shell equations given by Naghdi [7], provided more exact and extensive results. For axially cracked cylinder, Krenk [8], and for the circumferentially cracked cylinder, Delale and Erdogan [9]. It was shown in these papers that the asymptotic stress field obtained is compatible with the solution obtained by the theory of elasticity; therefore standard fracture parameters such as stress intensity factors could be used. The skew-symmetric shell problem was studied by Delale [10] and it was shown that the mode II and III stress intensity

factors also have the same elasticity definition. Therefore, it appears that the simplest shell theory that may be used to study cracks in shells to obtain stress intensity factors, is the one that includes transverse shear deformation [11,12,7]. In 1983, Yahsi and Erdogan [13] solved the shallow shell problem for an arbitrarily oriented crack with respect to a principal line of curvature. They used Reissner's higher order shell theory which was used by Delale and Erdogan [9], but the analysis involved the in-plane and out-of-plane stress, moment and shear resultants because of the generality of the problem.

The problem of surface cracks in shells is inherently a three-dimensional elasticity problem that appears to be analytically intractable. There are, however ,some numerical solutions based on the techniques of finite elements [14], [15] or boundary integral equations [16]. Rice [17], [18] introduced the so-called line-spring model which transformed the part through crack into a through crack by making use of the plane strain solution for an edge-cracked strip. This model has been shown to give very good results in spite of its simplicity. Therefore, within the limitations of this model, both through and part-through crack problems can be solved with the same plate or shell theory formulation. Delale and Erdogan [19] have used the samemodel, with a shallow shell formulation to predict stress intensity factors for surface cracks in cylinders. In the study of Joseph and Erdogan [20], the problem of shallow shell containing a surface crack and subjected to general loading conditions by using line-spring model is considered. They used the displacement quantities as unknowns, rather than their derivatives which were used in most of similar investigations.

The above mentioned solutions for part-through or through crack problems, which are based on either the classical shallow shell theory or a Reissner type transverse shear theory have all been given for infinite shells in the sense that the crack is assumed to be located sufficiently far from the boundaries and all other sources of stress disturbances so that all interaction effects may be neglected. The first analysis of fixed end problem was presented by Yahsi and Erdogan in 1985 for a pressurized cylindrical shell which contains an axial part-through or through crack [21].

The primary objective of this dissertation is to study the influence of a stiffened end on the stress intensity factors in a cylindrical shell containing a

circumferential through or a part-through crack under general loading conditions. Such problems may arise in pipes and cylindrical containers having flanges or end plates the stiffnesses of which are very high in comparison with those of the shell itself. Thus, in formulating the problem it may be assumed that the end of the shell is "fixed", that is all components of displacement and rotation vectors are zero. Then the problem is formulated for a specially orthotropic material by using Fourier integral transform technique. Similar to other crack problems, this mixed boundary value problem is reduced to a system of five simultaneous singular integral equations and they are solved numerically.

CHAPTER II

BASIC FORMULATION OF THE PROBLEM

In this problem the general shallow shell equations developed in [7] for an isotropic medium will be used. The equilibrium equations for a shallow shell may be expressed as,

$$N_{ij,j}=0 \tag{2.1}$$

$$V_{i,j}+\left(Z_{,i}\cdot N_{ij}\right),_j+q\left(X_1,X_2\right) \tag{2.2}$$

$$M_{ij,j}-V_i=0\ ,\quad (i,j=1,2) \tag{2.3}$$

where X_1, X_2, X_3 are the rectangular coordinates, X_1, X_2 plane being tangent to the middle surface of the shell, $Z=Z(X_1,X_2)$ is the equation of the middle surface, q is the surface loading, and N_{ij}, M_{ij} and V_i (i,j=1,2) are respectively , membrane, moment and transverse shear resultants. The indicial notation and the summation convention are used in the formulation of the problem. The components of strains can be given by

$$\varepsilon_{ij}=\frac{1}{2}\left[U_{i,j}+U_{j,i}+Z_{,i}W_{,j}+Z_{,j}W_{,i}\right]\ ,\quad (i,j=1,2) \tag{2.4}$$

where U_1, U_2 and W are the displacement components in X_1, X_2 and Z directions. The normals of the shell in its original configuration change directions by the angles β_1 and β_2. The slope of the middle surface changes by $W_{,i}$, and thus the effect of the transverse shear is expressed by

$$\theta_i=W_{,i}+\beta_i\ ,\quad i=1,2 \tag{2.5}$$

If U_1 and U_2 are eliminated from equation (2.4), a compatibility equation can be obtained in the following form

$$e_{ik}e_{jl}\left(\varepsilon_{ij,kl}+Z_{,ij}W_{kl}\right)=0 \tag{2.6}$$

where e_{ik} is the permutation symbol (i.e. $e_{11}=e_{22}=0$ and $e_{12}=-e_{21}=1$) By using of the stress function $F(X_1,X_2)$ defined by

$$N_{ij}=e_{ik}e_{jl}F_{,kl} \tag{2.7}$$

the equilibrium equation (2.1) is satisfied. If the generalized Hooke's law, which is expressed as

$$\varepsilon_{ij}=a_{ijkl}N_{kl}/h \tag{2.8}$$

is used, the equations (2.2) and (2.6) reduce to

$$M_{ij,ij}+Z_{,ij}e_{ik}e_{jl}F_{,kl}+q=0 \tag{2.9}$$

$$e_{im}e_{jn}e_{kp}e_{lq}a_{ijkl}F_{,mnpq}+hZ_{,ij}e_{ik}e_{jl}W_{,kl}=0 \tag{2.10}$$

Even with simple geometries for anisotropic materials the differential equations are not tractable. However, as shown in [8] if one assumes a special orthotropy, the related differential operators in these equations can be factorized and the problem can be made analytically tractable. This factorization condition can be expressed as follows;

$$2G_{12}=\left(E_1E_2\right)^{1/2}\Big/\left[1+\left(\nu_1\nu_2\right)^{1/2}\right] \tag{2.11}$$

where E_1, E_2, ν_1, ν_2 and G_{12} are the material constants of the orthotropic material. The material which satisfies the condition (2.11) is called "specially orthotropic".

Defining

$$E=\sqrt{E_1E_2},\ \nu=\sqrt{\nu_1\nu_2},\ c=\left(E_1/E_2\right)^{1/2} \tag{2.12}$$

the relations between stress and displacement quantities in the shell may be expressed as

$$\begin{aligned}\varepsilon_{11}&=\frac{1}{hE}\left(\frac{N_{11}}{c^2}-\nu N_{22}\right)\\ \varepsilon_{12}&=\frac{1+\nu}{hE}N_{12}\\ \varepsilon_{22}&=\frac{1}{hE}\left(c^2N_{22}-\nu N_{11}\right)\end{aligned} \tag{2.13}$$

By using the assumption of linear variation of stress components σ_{ij} over the thickness, the moment resultants can be expressed by

$$\begin{aligned}M_{11}&=D\left(c^2\beta_{1,1}+\nu\beta_{2,2}\right)\\ M_{12}&=\frac{D\left(1-\nu\right)}{2}\left(\beta_{1,2}+\beta_{2,1}\right)\\ M_{22}&=D\left(\nu\beta_{1,1}+\beta_{2,2}/c^2\right)\end{aligned} \tag{2.14}$$

where $D=Eh^3/12(1-\nu^2)$ and B is the effective shear modulus. Referring to [12], it will be assumed that

$$B=\frac{5}{6}\frac{E}{2(1+\nu)} \tag{2.15}$$

Defining now the operator

$$\nabla_c^2=c\frac{\partial^2}{\partial X_1^2}+\frac{\partial^2}{c\partial X_2^2} \tag{2.16}$$

equations (2.9), (2.10) and (2.3) may be reduced to

$$\nabla_c^2\nabla_c^2 F + hE\left(\frac{\partial^2 Z}{\partial X_1^2}\frac{\partial^2}{\partial X_2^2} - 2\frac{\partial^2 Z}{\partial X_1 \partial X_2}\frac{\partial^2}{\partial X_1 \partial X_2} + \frac{\partial^2 Z}{\partial X_2^2}\frac{\partial^2}{\partial X_1^2}\right)W = 0 \tag{2.17}$$

$$D\nabla_c^2\nabla_c^2 W - \left(1 - \frac{D}{Bh}\nabla_c^2\right)\left(\frac{\partial^2 Z}{\partial X_1^2}\frac{\partial^2}{\partial X_2^2} - 2\frac{\partial^2 Z}{\partial X_1 \partial X_2}\frac{\partial^2}{\partial X_1 \partial X_2} + \frac{\partial^2 Z}{\partial X_2^2}\frac{\partial^2}{\partial X_1^2}\right)F = \left(1 - \frac{D}{Bh}\nabla_c^2\right)q \tag{2.18}$$

$$\beta_1 + \frac{\partial W}{\partial X_1} = \frac{D}{hB}\left[\nabla_c^2\beta_1 + \frac{(1+\nu)}{2c}\frac{\partial}{\partial X_2}\left(\frac{\partial \beta_2}{\partial X_1} - \frac{\partial \beta_1}{\partial X_2}\right)\right] \tag{2.19}$$

$$\beta_2 + \frac{\partial W}{\partial X_2} = \frac{D}{hB}\left[\nabla_c^2\beta_2 + c\frac{(1+\nu)}{2}\frac{\partial}{\partial X_1}\left(\frac{\partial \beta_1}{\partial X_2} - \frac{\partial \beta_2}{\partial X_1}\right)\right] \tag{2.20}$$

Equations (2.17)-(2.20) provide the formulation for an arbitrary shallow shell in terms of the unknown functions F, W, β_1 and β_2.

Now let us assume that in the domain of interest the curvatures of the shell are constant. Then in (2.17) and (2.18) the terms involving Z may be replaced by

$$\frac{\partial^2 Z}{\partial X_1^2} = -\frac{1}{R_1}$$

$$\frac{\partial^2 Z}{\partial X_2^2} = -\frac{1}{R_2}$$

$$\frac{\partial^2 Z}{\partial X_1 \partial X_2} = -\frac{1}{R_{12}} \tag{2.21}$$

Also, following [13], if one introduces the dimensionless quantities given in Appendix A, equations (2.17)-(2.20) may further be simplified to

$$\nabla^4\Phi-\frac{1}{\lambda^2}\left(\lambda_1^2\frac{\partial^2}{\partial y^2}-2\lambda_{12}^2\frac{\partial^2}{\partial x\partial y}+\lambda_2^2\frac{\partial^2}{\partial x^2}\right)w=0 \tag{2.22}$$

$$\nabla^4 w-\lambda^2\left(1-\kappa\nabla^2\right)\left(\lambda_1^2\frac{\partial^2}{\partial y^2}-2\lambda_{12}^2\frac{\partial^2}{\partial x\partial y}+\lambda_2^2\frac{\partial^2}{\partial x^2}\right)\Phi=\lambda^4\left(1-\kappa\nabla^2\right)\frac{a}{h}q \tag{2.23}$$

$$\left(1-\kappa\nabla^2\right)\beta_x+\frac{\partial w}{\partial x}=\kappa\frac{1+\nu}{2}\frac{\partial}{\partial y}\left(\frac{\partial\beta_y}{\partial x}-\frac{\partial\beta_x}{\partial y}\right) \tag{2.24}$$

$$\left(1-\kappa\nabla^2\right)\beta_y+\frac{\partial w}{\partial y}=\kappa\frac{1+\nu}{2}\frac{\partial}{\partial x}\left(\frac{\partial\beta_x}{\partial y}-\frac{\partial\beta_y}{\partial x}\right) \tag{2.25}$$

The constant a used in Appendix A to normalize various quantities is a characteristic length parameter in the shell. Usually in crack problems the shell is assumed to be "infinitely large" and a is taken to be half of the crack length.

Introducing new unknown functions Ω and Ψ defined as follows

$$\Omega(x,y)=\frac{\partial\beta_x}{\partial y}-\frac{\partial\beta_y}{\partial x} \tag{2.26}$$

$$\Psi(x,y)=\kappa\left(\frac{\partial\beta_x}{\partial x}+\frac{\partial\beta_y}{\partial y}\right)-w \tag{2.27}$$

equations (2.24) and (2.25) may be expressed as follows

$$\beta_x=\kappa\nabla^2\beta_x-\frac{\partial w}{\partial x}-\kappa\frac{1+\nu}{2}\frac{\partial\Omega}{\partial y} \tag{2.28a}$$

$$\beta_y=\kappa\nabla^2\beta_y-\frac{\partial w}{\partial y}+\kappa\frac{1+\nu}{2}\frac{\partial\Omega}{\partial x} \tag{2.28b}$$

Then by using equations (2.26) and (2.27), $\nabla^2\beta_x$ and $\nabla^2\beta_y$ terms in (2.28a,b) can be written as follows

$$\nabla^2\beta_x = \frac{\partial\Omega}{\partial y} + \frac{\partial^2\beta_x}{\partial x^2} + \frac{\partial^2\beta_y}{\partial x\partial y} \tag{2.29a}$$

$$\nabla^2\beta_y = -\frac{\partial\Omega}{\partial x} + \frac{\partial^2\beta_y}{\partial y^2} + \frac{\partial^2\beta_x}{\partial x\partial y} \tag{2.29b}$$

Finally from equations (2.28a,b), and (2.29a,b), following relations can be obtained

$$\beta_x = \frac{\partial\Psi}{\partial x} - \kappa\frac{1-\nu}{2}\frac{\partial\Omega}{\partial y} \tag{2.30a}$$

$$\beta_y = \frac{\partial\Psi}{\partial y} - \kappa\frac{1-\nu}{2}\frac{\partial\Omega}{\partial x} \tag{2.30b}$$

In (2.30a,b), eliminating Ω and then using (2.27) the following differential equation can be found

$$\kappa\nabla^2\Psi - \Psi - w = 0 \tag{2.31}$$

Similarly, by eliminating w, equations (2.28a,b) yield

$$\kappa\frac{1-\nu}{2}\nabla^2\Omega - \Omega = 0 \tag{2.32}$$

The solution of the shell problem must then satisfy the differential equations (2.22), (2.23), (2.31) and (2.32) and all the necessary boundary conditions.

CHAPTER III

A CYLINDRICAL SHELL WITH A FIXED END WHICH CONTAINS A CIRCUMFERENTIAL THROUGH CRACK

3.1. Formulation of the Problem

Consider a specially orthotropic cylindrical shell with a fixed end which contains a circumferential through crack of length $2a$ as shown in Figure 1. Let the shell be loaded with membrane forces, moments and transverse shear forces far away from the crack region, and let the surface loading q be zero.

To solve the problem, one may first consider a cylindrical shell without a crack which is fixed at $X_1 = 0$ plane and which is subjected to the given set of external loads. Since the problem under consideration is linear, the solution of the cracked shell problem may then be obtained by adding to this uncracked shell results a perturbation solution obtained from the cracked shell with a fixed end by using equal and opposite stress, moment and shear force resultants from the first solution as the crack surface tractions.

For a cylindrical shell with a circumferential crack, $\lambda_1 = 0 = \lambda_{12}$, and equations (2.17), (2.18), (2.31) and (2.32) simplify to the following set of differential equations

$$\nabla^4 \Phi - \left(\frac{\lambda_2}{\lambda}\right)^2 \frac{\partial^2 w}{\partial x^2} = 0 \tag{3.1.1}$$

$$\nabla^4 w + \left(\lambda\lambda_2\right)^2 \left(1 - \kappa\nabla^2\right) \frac{\partial^2 \Phi}{\partial x^2} = 0 \tag{3.1.2}$$

$$\kappa\nabla^2 \Psi - \Psi - w = 0 \tag{3.1.3}$$

$$\kappa \frac{1-\nu}{2} \nabla^2 \Omega - \Omega = 0 \tag{3.1.4}$$

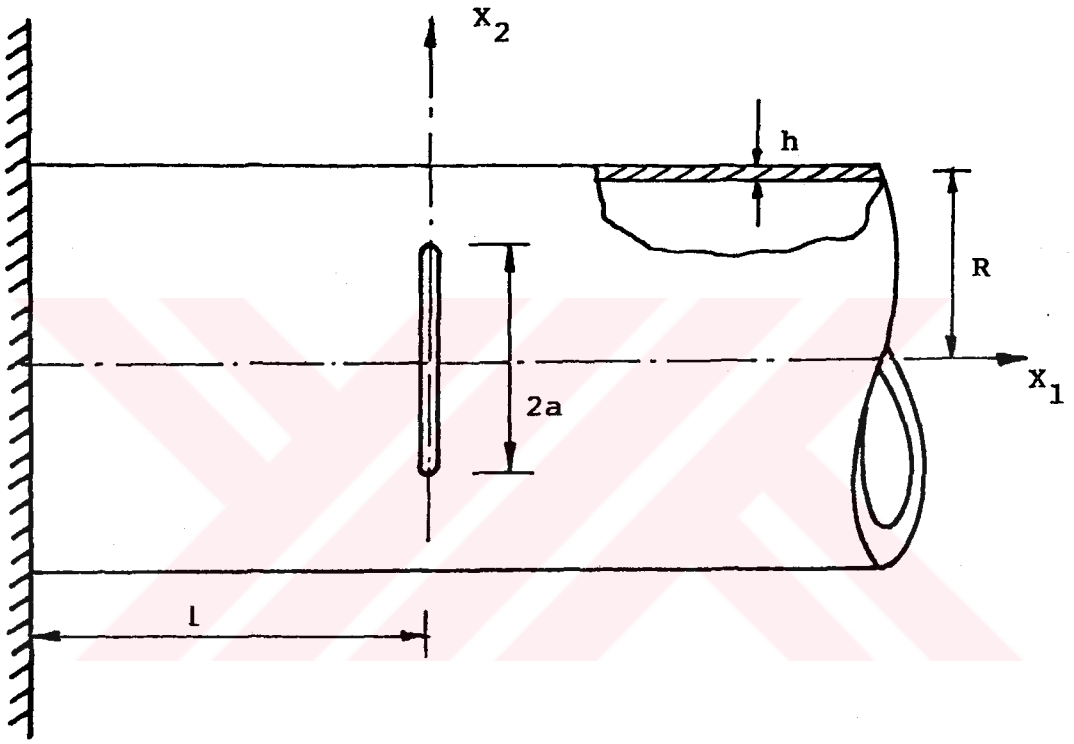

Figure 1. Geometry of a Cylindrical Shell Containing Circumferential Through Crack with a Fixed End

By eliminating Φ from equations (3.1.1) and (3.1.2), following equations can be obtained

$$\nabla^4\nabla^4 w+\lambda_2^4\left(1-\kappa\nabla^2\right)\frac{\partial^4 w}{\partial x^4}=0 \tag{3.1.5}$$

In the present study, the primary interest is in the problem of a cylindrical shell with a fixed end which contains a circumferential crack. So, for the shallow shell under consideration the solution of (3.1.5) may be expressed as

$$w(x,y)=\frac{1}{2\pi}\int_{-\infty}^{+\infty} f_1(x,\alpha)e^{-i\alpha y}\,d\alpha+\frac{1}{2\pi}\int_{-\infty}^{+\infty} f_2(x,\beta)e^{-i\beta y}\,d\beta \tag{3.1.6}$$

Assuming the solution of the ordinary differential equations resulting from (3.1.6) and (3.1.5) of the form

$$f_1(x,\alpha)=R(\alpha)e^{mx} \tag{3.1.7}$$

$$f_2(x,\beta)=S(\beta)e^{n(x+l')} \tag{3.1.8}$$

the characteristic equations giving m and n may be obtained as follows:

$$m^8-\left(\kappa\lambda_2^4+4\alpha^2\right)m^6+\left(6\alpha^4+\lambda_2^4+\alpha^2\kappa\lambda_2^4\right)m^4-4\alpha^6m^2+\alpha^8=0 \tag{3.1.9}$$

$$n^8-\left(\kappa\lambda_2^4+4\beta^2\right)n^6+\left(6\beta^4+\lambda_2^4+\beta^2\kappa\lambda_2^4\right)n^4-4\beta^6n^2+\beta^8=0 \tag{3.1.10}$$

It should be emphasized that the roots of (3.1.9) and (3.1.10) are in general complex, and, of course, are not known as a function of α and β in closed form. Note that, ordered properly, the roots of (3.1.9) and (3.1.10) have the following property

$$\mathrm{Re}(m_j)<0,\quad m_{j+4}=-m_j,\ j=1,2,3,4 \tag{3.1.11}$$

$$\mathrm{Re}(n_j)<0,\quad n_{j+4}=-n_j,\ j=1,2,3,4 \tag{3.1.12}$$

then the solution of $f_1(x,\alpha)$ and $f_2(x,\beta)$, which also satisfy the regularity condition at $x = \pm\infty$ may be expressed as

$$f_1(x,\alpha) = \begin{cases} \sum_{j=1}^{4} R_j(\alpha) e^{m_j x} & x > 0 \\ \sum_{j=5}^{8} R_j(\alpha) e^{m_j x} & x < 0 \end{cases} \tag{3.1.13}$$

$$f_2(x,\beta) = \sum_{j=1}^{4} S_j(\beta) e^{n_j(x+l')} \quad x > 0 \tag{3.1.14}$$

Similarly, by expressing the solution

$$\Phi(x,y) = \frac{1}{2\pi}\int_{-\infty}^{+\infty} g_1(x,\alpha) e^{-i\alpha y}\, d\alpha + \frac{1}{2\pi}\int_{-\infty}^{+\infty} g_2(x,\beta) e^{-i\beta y}\, d\beta \tag{3.1.15}$$

from (3.1.1) and (3.1.13), (3.1.14), the functions g_1 and g_2 may be obtained as

$$g_1(x,\alpha) = \begin{cases} \sum_{j=1}^{4} R_j(\alpha) K_j e^{m_j x} & x > 0 \\ \sum_{j=5}^{8} R_j(\alpha) K_j e^{m_j x} & x < 0 \end{cases} \tag{3.1.16}$$

$$g_2(x,\beta) = \sum_{j=1}^{4} S_j(\beta) M_j e^{n_j(x+l')} \quad x > 0 \tag{3.1.17}$$

where

$$K_j = \left(\frac{m_j}{p_j}\right)^2 \left(\frac{\lambda_2}{\lambda}\right)^2 \tag{3.1.18}$$

$$M_j = \left(\frac{n_j}{s_j}\right)^2 \left(\frac{\lambda_2}{\lambda}\right)^2 \tag{3.1.19}$$

$$p_j = m_j^2 - \alpha^2 \tag{3.1.20}$$

$$s_j = n_j^2 - \beta^2 \tag{3.1.21}$$

Expressing now Ω in the form

$$\Omega(x,y) = \frac{1}{2\pi}\int_{-\infty}^{+\infty} h_1(x,\alpha)e^{-i\alpha y}\,d\alpha + \frac{1}{2\pi}\int_{-\infty}^{+\infty} h_2(x,\beta)e^{-i\beta y}\,d\beta \tag{3.1.22}$$

and assuming that

$$\begin{aligned} h_1(x,\alpha) &= A(\alpha,r)e^{rx} \\ h_2(x,\beta) &= B(\beta,t)e^{tx} \end{aligned} \tag{3.1.23}$$

from (3.1.24), it can be shown that the functions h_1 and h_2 satisfying the conditions at $x = \pm\infty$ may be expressed as

$$h_1(x,\alpha) = \begin{cases} A_1 e^{r_1 x} & x > 0 \\ A_2 e^{r_2 x} & x < 0 \end{cases} \tag{3.1.24}$$

$$h_2(x,\beta) = B_1(\beta)e^{t_1(x+l')} \qquad x > 0 \tag{3.1.25}$$

where

$$\begin{aligned} r_1 &= -r_2 = -\left[\alpha^2 + \frac{2}{\kappa(1-\nu)}\right]^{1/2} \\ t_1 &= -\left[\beta^2 + \frac{2}{\kappa(1-\nu)}\right]^{1/2} \end{aligned} \tag{3.1.26}$$

Finally, it may be shown that the remaining differential equation (3.1.3) will also be satisfied and the solution will have the proper behavior at $x = \pm\infty$, if it is assumed that

$$\Psi(x,y) = \frac{1}{2\pi}\int_{-\infty}^{+\infty} \theta_1(x,\alpha)e^{-i\alpha y}\,d\alpha + \frac{1}{2\pi}\int_{-\infty}^{+\infty} \theta_2(x,\beta)e^{-i\beta y}\,d\beta \tag{3.1.27}$$

$$\theta_1(x,\alpha)=\begin{cases}\sum_{j=1}^{4}\dfrac{R_j(\alpha)}{\kappa p_j-1}e^{m_j x} & x>0\\ \sum_{j=5}^{8}\dfrac{R_j(\alpha)}{\kappa p_j-1}e^{m_j x} & x<0\end{cases} \tag{3.1.28}$$

$$\theta_2(x,\beta)=\sum_{j=1}^{4}\frac{S_j(\alpha)}{\kappa s_j-1}e^{n_j(x+l')} \quad x>0 \tag{3.1.29}$$

Thus, the problem is reduced to the determination of the unknown functions $R_j(\alpha)$ (j=1,...,8), $S_j(\beta)$ (j=1,..,4), $A_j(\alpha)$ (j=1,2) and $B_1(\beta)$ from the boundary conditions of the problem.

As mentioned earlier, the only external loads in the problem are the self-equilibrating force and moment resultants on the crack surfaces. Therefore ,these fifteen unknowns are obtained by using the following continuity and boundary conditions:

$$\lim_{x\to 0^+} N_{xx}-\lim_{x\to 0^-} N_{xx}=0 \quad -\infty<y<+\infty \tag{3.1.30}$$

$$\lim_{x\to 0^+} M_{xx}-\lim_{x\to 0^-} M_{xx}=0 \quad -\infty<y<+\infty \tag{3.1.31}$$

$$\lim_{x\to 0^+} V_x-\lim_{x\to 0^-} V_x=0 \quad -\infty<y<+\infty \tag{3.1.32}$$

$$\lim_{x\to 0^+} N_{xy}-\lim_{x\to 0^-} N_{xy}=0 \quad -\infty<y<+\infty \tag{3.1.33}$$

$$\lim_{x\to 0^+} M_{xy}-\lim_{x\to 0^-} M_{xy}=0 \quad -\infty<y<+\infty \tag{3.1.34}$$

$$\lim_{x\to -l'} u=0 \quad -\infty<y<+\infty \tag{3.1.35}$$

$$\lim_{x\to -l'} \beta_x=0 \quad -\infty<y<+\infty \tag{3.1.36}$$

$$\lim_{x\to -\ell'} w = 0 \qquad -\infty < y < +\infty \qquad (3.1.37)$$

$$\lim_{x\to -\ell'} v = 0 \qquad -\infty < y < +\infty \qquad (3.1.38)$$

$$\lim_{x\to -\ell'} \beta_y = 0 \qquad -\infty < y < +\infty \qquad (3.1.39)$$

$$\begin{aligned} &\lim_{x\to 0^+} N_{xx} + \lim_{x\to 0^-} N_{xx} = 2F_{10}(y) && |y| < \sqrt{c} \\ &\lim_{x\to 0^+} u - \lim_{x\to 0^-} u = 0 && |y| > \sqrt{c} \end{aligned} \qquad (3.1.40a,b)$$

$$\begin{aligned} &\lim_{x\to 0^+} M_{xx} + \lim_{x\to 0^-} M_{xx} = 2F_{20}(y) && |y| < \sqrt{c} \\ &\lim_{x\to 0^+} \beta_x - \lim_{x\to 0^-} \beta_x = 0 && |y| > \sqrt{c} \end{aligned} \qquad (3.1.41a,b)$$

$$\begin{aligned} &\lim_{x\to 0^+} V_x + \lim_{x\to 0^-} V_x = 2F_{30}(y) && |y| < \sqrt{c} \\ &\lim_{x\to 0^+} w - \lim_{x\to 0^-} w = 0 && |y| > \sqrt{c} \end{aligned} \qquad (3.1.42a,b)$$

$$\begin{aligned} &\lim_{x\to 0^+} N_{xy} + \lim_{x\to 0^-} N_{xy} = 2F_{40}(y) && |y| < \sqrt{c} \\ &\lim_{x\to 0^+} v - \lim_{x\to 0^-} v = 0 && |y| > \sqrt{c} \end{aligned} \qquad (3.1.43a,b)$$

$$\begin{aligned} &\lim_{x\to 0^+} M_{xy} + \lim_{x\to 0^-} M_{xy} = 2F_{50}(y) && |y| < \sqrt{c} \\ &\lim_{x\to 0^+} \beta_y - \lim_{x\to 0^-} \beta_y = 0 && |y| > \sqrt{c} \end{aligned} \qquad (3.1.44a,b)$$

where F_{j0} (j=1,...,5) are known crack surface loads.

Using (3.1.6), and (3.1.13)-(3.1.29), from the basic expressions given in Chapter 2, the components of the stress and moment resultants and, the displacements and rotations may be obtained as:

$$N_{xx}(x,y)=\begin{cases}-\dfrac{1}{2\pi}\displaystyle\int_{-\infty}^{+\infty}\alpha^2\sum_{j=1}^{4}K_jR_j(\alpha)e^{m_jx}e^{-i\alpha y}\,d\alpha- \\ \dfrac{1}{2\pi}\displaystyle\int_{-\infty}^{+\infty}\beta^2\sum_{j=1}^{4}M_jS_j(\beta)e^{n_j(x+l')}e^{-\beta y}\,d\beta\ , \quad x>0 \\ \\ -\dfrac{1}{2\pi}\displaystyle\int_{-\infty}^{+\infty}\alpha^2\sum_{j=5}^{8}K_jR_j(\alpha)e^{m_jx}e^{-i\alpha y}\,d\alpha- \\ \dfrac{1}{2\pi}\displaystyle\int_{-\infty}^{+\infty}\beta^2\sum_{j=1}^{4}M_jS_j(\beta)e^{n_j(x+l')}e^{-\beta y}\,d\beta\ , \quad x<0\end{cases} \tag{3.1.45}$$

$$M_{xx}(x,y)=\begin{cases}\dfrac{1}{2\pi}\dfrac{a}{h\lambda^4}\displaystyle\int_{-\infty}^{+\infty}\sum_{j=1}^{4}\frac{(1-\nu)\alpha^2+p_j}{\kappa p_j-1}R_j(\alpha)e^{m_jx}e^{-i\alpha y}\,d\alpha- \\ \dfrac{1}{2\pi}\dfrac{a}{h\lambda^4}\dfrac{\kappa(1-\nu)^2}{2}\displaystyle\int_{-\infty}^{+\infty}iA_1(\alpha)\alpha r_1e^{r_1x}e^{-i\alpha y}\,d\alpha+ \\ \dfrac{1}{2\pi}\dfrac{a}{h\lambda^4}\displaystyle\int_{-\infty}^{+\infty}\sum_{j=1}^{4}\frac{(1-\nu)\beta^2+s_j}{\kappa s_j-1}S_j(\beta)e^{n_j(x+l')}e^{-\beta y}\,d\beta- \\ \dfrac{1}{2\pi}\dfrac{a}{h\lambda^4}\dfrac{\kappa(1-\nu)^2}{2}\displaystyle\int_{-\infty}^{+\infty}iB_1(\beta)\beta t_1e^{t_1(x+l')}e^{-\beta y}\,d\beta\ , \quad x>0 \\ \\ \dfrac{1}{2\pi}\dfrac{a}{h\lambda^4}\displaystyle\int_{-\infty}^{+\infty}\sum_{j=5}^{8}\frac{(1-\nu)\alpha^2+p_j}{\kappa p_j-1}R_j(\alpha)e^{m_jx}e^{-i\alpha y}\,d\alpha- \\ \dfrac{1}{2\pi}\dfrac{a}{h\lambda^4}\dfrac{\kappa(1-\nu)^2}{2}\displaystyle\int_{-\infty}^{+\infty}iA_2(\alpha)\alpha r_2e^{r_2x}e^{-i\alpha y}\,d\alpha+ \\ \dfrac{1}{2\pi}\dfrac{a}{h\lambda^4}\displaystyle\int_{-\infty}^{+\infty}\sum_{j=1}^{4}\frac{(1-\nu)\beta^2+s_j}{\kappa s_j-1}S_j(\beta)e^{n_j(x+l')}e^{-\beta y}\,d\beta- \\ \\ \dfrac{1}{2\pi}\dfrac{a}{h\lambda^4}\dfrac{\kappa(1-\nu)^2}{2}\displaystyle\int_{-\infty}^{+\infty}iB_1(\beta)\beta t_1e^{t_1(x+l')}e^{-\beta y}\,d\beta\ , \quad x<0\end{cases} \tag{3.1.46}$$

$$V_x(x,y)=\begin{cases}\dfrac{1}{2\pi}\displaystyle\int_{-\infty}^{+\infty}\sum_{j=1}^{4}\frac{\kappa p_j m_j}{\kappa p_j-1}R_j(\alpha)e^{m_j x}e^{-i\alpha y}\,d\alpha- \\ \quad\dfrac{1}{2\pi}\dfrac{\kappa(1-\nu)}{2}\displaystyle\int_{-\infty}^{+\infty}iA_1(\alpha)\alpha e^{r_1 x}e^{-i\alpha y}\,d\alpha+ \\ \quad\dfrac{1}{2\pi}\displaystyle\int_{-\infty}^{+\infty}\sum_{j=1}^{4}\frac{\kappa s_j n_j}{\kappa s_j-1}S_j(\beta)e^{n_j(x+l')}e^{-\beta y}\,d\beta- \\ \quad\dfrac{1}{2\pi}\dfrac{\kappa(1-\nu)}{2}\displaystyle\int_{-\infty}^{+\infty}iB_1(\beta)\beta e^{t_1(x+l')}e^{-\beta y}\,d\beta\ ,\quad x>0 \\ \\ \dfrac{1}{2\pi}\displaystyle\int_{-\infty}^{+\infty}\sum_{j=5}^{8}\frac{\kappa p_j m_j}{\kappa p_j-1}R_j(\alpha)e^{m_j x}e^{-i\alpha y}\,d\alpha- \\ \quad\dfrac{1}{2\pi}\dfrac{\kappa(1-\nu)}{2}\displaystyle\int_{-\infty}^{+\infty}iA_2(\alpha)\alpha e^{r_2 x}e^{-i\alpha y}\,d\alpha+ \\ \quad\dfrac{1}{2\pi}\displaystyle\int_{-\infty}^{+\infty}\sum_{j=1}^{4}\frac{\kappa s_j n_j}{\kappa s_j-1}S_j(\beta)e^{n_j(x+l')}e^{-\beta y}\,d\beta- \\ \quad\dfrac{1}{2\pi}\dfrac{\kappa(1-\nu)}{2}\displaystyle\int_{-\infty}^{+\infty}iB_1(\beta)\beta e^{t_1(x+l')}e^{-\beta y}\,d\beta\ ,\quad x<0\end{cases} \tag{3.1.47}$$

$$N_{xy}(x,y)=\begin{cases}\dfrac{i}{2\pi}\displaystyle\int_{-\infty}^{+\infty}\alpha\sum_{j=1}^{4}K_j R_j(\alpha)m_j e^{m_j x}e^{-i\alpha y}\,d\alpha+ \\ \quad\dfrac{i}{2\pi}\displaystyle\int_{-\infty}^{+\infty}\beta\sum_{j=1}^{4}M_j S_j(\beta)n_j e^{n_j(x+l')}e^{-\beta y}\,d\beta\ ,\quad x>0 \\ \\ \dfrac{i}{2\pi}\displaystyle\int_{-\infty}^{+\infty}\alpha\sum_{j=5}^{8}K_j R_j(\alpha)m_j e^{m_j x}e^{-i\alpha y}\,d\alpha+ \\ \quad\dfrac{i}{2\pi}\displaystyle\int_{-\infty}^{+\infty}\beta\sum_{j=1}^{4}M_j S_j(\beta)n_j e^{n_j(x+l')}e^{-\beta y}\,d\beta\ ,\quad x<0\end{cases} \tag{3.1.48}$$

$$M_{xy}(x,y)=\begin{cases}
-\dfrac{1}{2\pi}\dfrac{(1-\nu)a}{h\lambda^4}\displaystyle\int_{-\infty}^{+\infty} i\alpha\sum_{j=1}^{4}\frac{m_j}{\kappa p_j-1}R_j(\alpha)e^{m_j x}e^{-i\alpha y}\,d\alpha- \\
\dfrac{1}{2\pi}\dfrac{a\kappa}{h\lambda^4}\dfrac{(1-\nu)^2}{4}\displaystyle\int_{-\infty}^{+\infty}\left(\alpha^2+r_1^2\right)A_1(\alpha)e^{r_1 x}e^{-i\alpha y}\,d\alpha- \\
\dfrac{1}{2\pi}\dfrac{(1-\nu)a}{h\lambda^4}\displaystyle\int_{-\infty}^{+\infty} i\beta\sum_{j=1}^{4}\frac{n_j}{\kappa s_j-1}S_j(\beta)e^{n_j(x+l')}e^{-i\beta y}\,d\beta- \\
\dfrac{1}{2\pi}\dfrac{a\kappa}{h\lambda^4}\dfrac{(1-\nu)^2}{4}\displaystyle\int_{-\infty}^{+\infty}\left(\beta^2+t_1^2\right)B_1(\beta)e^{t_1(x+l')}e^{-i\beta y}\,d\beta\ , \quad x>0 \\
\\
-\dfrac{1}{2\pi}\dfrac{(1-\nu)a}{h\lambda^4}\displaystyle\int_{-\infty}^{+\infty} i\alpha\sum_{j=5}^{8}\frac{m_j}{\kappa p_j-1}R_j(\alpha)e^{m_j x}e^{-i\alpha y}\,d\alpha- \\
\dfrac{1}{2\pi}\dfrac{a\kappa}{h\lambda^4}\dfrac{(1-\nu)^2}{4}\displaystyle\int_{-\infty}^{+\infty}\left(\alpha^2+r_2^2\right)A_2(\alpha)e^{r_2 x}e^{-i\alpha y}\,d\alpha- \\
\dfrac{1}{2\pi}\dfrac{(1-\nu)a}{h\lambda^4}\displaystyle\int_{-\infty}^{+\infty} i\beta\sum_{j=1}^{4}\frac{n_j}{\kappa s_j-1}S_j(\beta)e^{n_j(x+l')}e^{-i\beta y}\,d\beta- \\
\dfrac{1}{2\pi}\dfrac{a\kappa}{h\lambda^4}\dfrac{(1-\nu)^2}{4}\displaystyle\int_{-\infty}^{+\infty}\left(\beta^2+t_1^2\right)B_1(\beta)e^{t_1(x+l')}e^{-i\beta y}\,d\beta\ , \quad x<0
\end{cases} \tag{3.1.49}$$

$$N_{xy}(x,y)=\begin{cases}
\dfrac{1}{2\pi}\displaystyle\int_{-\infty}^{+\infty}\sum_{j=1}^{4}K_j R_j(\alpha)m_j^2 e^{m_j x}e^{-i\alpha y}\,d\alpha+ \\
\quad\dfrac{1}{2\pi}\displaystyle\int_{-\infty}^{+\infty}\sum_{j=1}^{4}M_j S_j(\beta)n_j^2 e^{n_j(x+l')}e^{-i\beta y}\,d\beta\ , \quad x>0 \\
\\
\dfrac{1}{2\pi}\displaystyle\int_{-\infty}^{+\infty}\sum_{j=5}^{8}K_j R_j(\alpha)m_j^2 e^{m_j x}e^{-i\alpha y}\,d\alpha+ \\
\quad\dfrac{1}{2\pi}\displaystyle\int_{-\infty}^{+\infty}\sum_{j=1}^{4}M_j S_j(\beta)n_j^2 e^{n_j(x+l')}e^{-i\beta y}\,d\beta\ , \quad x<0
\end{cases} \tag{3.1.50}$$

$$M_{yy}(x,y)=\begin{cases}\dfrac{1}{2\pi}\dfrac{a}{h\lambda^4}\displaystyle\int_{-\infty}^{+\infty}\sum_{j=1}^{4}\frac{\nu p_j-(1-\nu)\alpha^2}{\kappa p_j-1}R_j(\alpha)e^{m_j x}e^{-i\alpha y}\,d\alpha+\\ \dfrac{1}{2\pi}\dfrac{a}{h\lambda^4}\dfrac{\kappa(1-\nu)^2}{2}\displaystyle\int_{-\infty}^{+\infty}iA_1(\alpha)\alpha r_1 e^{r_1 x}e^{-i\alpha y}\,d\alpha+\\ \dfrac{1}{2\pi}\dfrac{a}{h\lambda^4}\displaystyle\int_{-\infty}^{+\infty}\sum_{j=1}^{4}\frac{\nu s_j-(1-\nu)\beta^2}{\kappa s_j-1}S_j(\beta)e^{n_j(x+l')}e^{-i\beta y}\,d\beta+\\ \dfrac{1}{2\pi}\dfrac{a}{h\lambda^4}\dfrac{\kappa(1-\nu)^2}{2}\displaystyle\int_{-\infty}^{+\infty}iB_1(\beta)\beta t_1 e^{t_1(x+l')}e^{-i\beta y}\,d\beta\ ,\quad x>0\\ \dfrac{1}{2\pi}\dfrac{a}{h\lambda^4}\displaystyle\int_{-\infty}^{+\infty}\sum_{j=5}^{8}\frac{\nu p_j-(1-\nu)\alpha^2}{\kappa p_j-1}R_j(\alpha)e^{m_j x}e^{-i\alpha y}\,d\alpha+\\ \dfrac{1}{2\pi}\dfrac{a}{h\lambda^4}\dfrac{\kappa(1-\nu)^2}{2}\displaystyle\int_{-\infty}^{+\infty}iA_2(\alpha)\alpha r_2 e^{r_2 x}e^{-i\alpha y}\,d\alpha+\\ \dfrac{1}{2\pi}\dfrac{a}{h\lambda^4}\displaystyle\int_{-\infty}^{+\infty}\sum_{j=1}^{4}\frac{\nu s_j-(1-\nu)\beta^2}{\kappa s_j-1}S_j(\beta)e^{n_j(x+l')}e^{-i\beta y}\,d\beta+\\ \dfrac{1}{2\pi}\dfrac{a}{h\lambda^4}\dfrac{\kappa(1-\nu)^2}{2}\displaystyle\int_{-\infty}^{+\infty}iB_1(\beta)\beta t_1 e^{t_1(x+l')}e^{-i\beta y}\,d\beta\ ,\quad x<0\end{cases}\tag{3.1.51}$$

$$V_y(x,y)=\begin{cases}
-\dfrac{1}{2\pi}\displaystyle\int_{-\infty}^{+\infty} i\alpha \sum_{j=1}^{4}\frac{\kappa p_j}{\kappa p_j-1}R_j(\alpha)e^{m_j x}e^{-i\alpha y}\,d\alpha - \\
\quad \dfrac{1}{2\pi}\dfrac{\kappa(1-\nu)}{2}\displaystyle\int_{-\infty}^{+\infty} A_1(\alpha)r_1 e^{r_1 x}e^{-i\alpha y}\,d\alpha - \\
\quad \dfrac{1}{2\pi}\displaystyle\int_{-\infty}^{+\infty} i\beta \sum_{j=1}^{4}\frac{\kappa s_j}{\kappa s_j-1}S_j(\beta)e^{n_j(x+l')}e^{-\beta y}\,d\beta - \\
\quad \dfrac{1}{2\pi}\dfrac{\kappa(1-\nu)}{2}\displaystyle\int_{-\infty}^{+\infty} B_1(\beta)t_1 e^{t_1(x+l')}e^{-\beta y}\,d\beta\,, \quad x>0 \\
-\dfrac{1}{2\pi}\displaystyle\int_{-\infty}^{+\infty} i\alpha \sum_{j=5}^{8}\frac{\kappa p_j}{\kappa p_j-1}R_j(\alpha)e^{m_j x}e^{-i\alpha y}\,d\alpha - \\
\quad \dfrac{1}{2\pi}\dfrac{\kappa(1-\nu)}{2}\displaystyle\int_{-\infty}^{+\infty} A_2(\alpha)r_2 e^{r_2 x}e^{-i\alpha y}\,d\alpha - \\
\quad \dfrac{1}{2\pi}\displaystyle\int_{-\infty}^{+\infty} i\beta \sum_{j=1}^{4}\frac{\kappa s_j}{\kappa s_j-1}S_j(\beta)e^{n_j(x+l')}e^{-\beta y}\,d\beta - \\
\quad \dfrac{1}{2\pi}\dfrac{\kappa(1-\nu)}{2}\displaystyle\int_{-\infty}^{+\infty} B_1(\beta)t_1 e^{t_1(x+l')}e^{-\beta y}\,d\beta\,, \quad x<0
\end{cases} \tag{3.1.52}$$

$$u(x,y)=\begin{cases}
-\frac{1}{2\pi}\int_{-\infty}^{+\infty}\sum_{j=1}^{4}R_j\left[(2+\nu)K_jm_j-K_j\frac{m_j^3}{\alpha^2}+\left(\frac{\lambda_2}{\lambda}\right)^2\frac{m_j}{\alpha^2}\right]e^{m_jx}e^{-i\alpha y}\,d\alpha- \\
\frac{1}{2\pi}\int_{-\infty}^{+\infty}\sum_{j=1}^{4}S_j\left[(2+\nu)M_jn_j-M_j\frac{n_j^3}{\beta^2}+\left(\frac{\lambda_2}{\lambda}\right)^2\frac{n_j}{\beta^2}\right]e^{n_j(x+l)}e^{-i\alpha y}\,d\alpha\,, \quad x>0 \\
-\frac{1}{2\pi}\int_{-\infty}^{+\infty}\sum_{j=5}^{8}R_j\left[(2+\nu)K_jm_j-K_j\frac{m_j^3}{\alpha^2}+\left(\frac{\lambda_2}{\lambda}\right)^2\frac{m_j}{\alpha^2}\right]e^{m_jx}e^{-i\alpha y}\,d\alpha- \\
\frac{1}{2\pi}\int_{-\infty}^{+\infty}\sum_{j=1}^{4}S_j\left[(2+\nu)M_jn_j-M_j\frac{n_j^3}{\beta^2}+\left(\frac{\lambda_2}{\lambda}\right)^2\frac{n_j}{\beta^2}\right]e^{n_j(x+l)}e^{-i\alpha y}\,d\alpha\,, \quad x<0
\end{cases} \tag{3.1.53}$$

$$\beta_x(x,y)=\begin{cases}\dfrac{1}{2\pi}\displaystyle\int_{-\infty}^{+\infty}\left[\sum_{j=1}^{4}\frac{R_j m_j}{\kappa p_j-1}e^{m_j x}-\frac{\kappa(1-\nu)}{2}A_1(\alpha)\alpha i e^{r_1 x}\right]e^{-\alpha y}\,d\alpha+\\ \quad\dfrac{1}{2\pi}\displaystyle\int_{-\infty}^{+\infty}\left[\sum_{j=1}^{4}\frac{S_j n_j}{\kappa s_j-1}e^{n_j(x+l)}-\right.\\ \qquad\left.\frac{\kappa(1-\nu)}{2}B_1(\beta)\beta i e^{t_1(x+l)}\right]e^{-\beta y}\,d\beta\ ,\quad x>0\\ \dfrac{1}{2\pi}\displaystyle\int_{-\infty}^{+\infty}\left[\sum_{j=5}^{8}\frac{R_j m_j}{\kappa p_j-1}e^{m_j x}-\frac{\kappa(1-\nu)}{2}A_2(\alpha)\alpha i e^{r_2 x}\right]e^{-\alpha y}\,d\alpha+\\ \quad\dfrac{1}{2\pi}\displaystyle\int_{-\infty}^{+\infty}\left[\sum_{j=1}^{4}\frac{S_j n_j}{\kappa s_j-1}e^{n_j(x+l)}-\right.\\ \qquad\left.\frac{\kappa(1-\nu)}{2}B_1(\beta)\beta i e^{t_1(x+l)}\right]e^{-\beta y}\,d\beta\ ,\quad x<0\end{cases}\qquad 3.1.54)$$

$$w(x,y)=\begin{cases}\dfrac{1}{2\pi}\displaystyle\int_{-\infty}^{+\infty}\sum_{j=1}^{4}R_j e^{m_j x}e^{-\alpha y}\ d\alpha+\\ \quad\dfrac{1}{2\pi}\displaystyle\int_{-\infty}^{+\infty}\sum_{j=1}^{4}S_j e^{n_j(x+l)}e^{-\alpha y}\,d\alpha\ ,\quad x>0\\ \dfrac{1}{2\pi}\displaystyle\int_{-\infty}^{+\infty}\sum_{j=5}^{8}R_j e^{m_j x}e^{-\alpha y}\ d\alpha+\\ \quad\dfrac{1}{2\pi}\displaystyle\int_{-\infty}^{+\infty}\sum_{j=1}^{4}S_j e^{n_j(x+l)}e^{-\beta y}\ d\beta\ ,\quad x<0\end{cases}\qquad (3.1.55)$$

$$
v(x,y)=\begin{cases}
\dfrac{i}{2\pi}\displaystyle\int_{-\infty}^{+\infty}\sum_{j=1}^{4}R_j\left[\frac{K_j m_j^2}{\alpha}+\nu\alpha K_j-\left(\frac{\lambda_2}{\lambda}\right)^2\frac{1}{\alpha}\right]e^{m_j x}e^{-i\alpha y}\,d\alpha+ \\
\dfrac{i}{2\pi}\displaystyle\int_{-\infty}^{+\infty}\sum_{j=1}^{4}S_j\left[\frac{M_j n_j^2}{\beta}+\nu\beta M_j-\left(\frac{\lambda_2}{\lambda}\right)^2\frac{1}{\beta}\right]e^{n_j(x+l')}e^{-i\beta y}\,d\beta, \quad x>0 \\
\dfrac{i}{2\pi}\displaystyle\int_{-\infty}^{+\infty}\sum_{j=5}^{8}R_j\left[\frac{K_j m_j^2}{\alpha}+\nu\alpha K_j-\left(\frac{\lambda_2}{\lambda}\right)^2\frac{1}{\alpha}\right]e^{m_j x}e^{-i\alpha y}\,d\alpha+ \\
\dfrac{i}{2\pi}\displaystyle\int_{-\infty}^{+\infty}\sum_{j=1}^{4}S_j\left[\frac{M_j n_j^2}{\beta}+\nu\beta M_j-\left(\frac{\lambda_2}{\lambda}\right)^2\frac{1}{\beta}\right]e^{n_j(x+l')}e^{-i\beta y}\,d\beta, \quad x<0
\end{cases}
\tag{3.1.56}
$$

$$\beta_y(x,y)=\begin{cases}
-\frac{1}{2\pi}\int_{-\infty}^{+\infty}\left[i\alpha\sum_{j=1}^{4}\frac{R_j}{\kappa p_j-1}e^{m_j x}+\frac{\kappa(1-\nu)}{2}A_1(\alpha)r_1e^{r_1 x}\right]e^{-i\alpha y}\,d\alpha- \\
\quad\frac{1}{2\pi}\int_{-\infty}^{+\infty}\left[i\beta\sum_{j=1}^{4}\frac{S_j}{\kappa s_j-1}e^{n_j(x+l')}+\right. \\
\qquad\left.\frac{\kappa(1-\nu)}{2}B_1(\beta)t_1e^{t_1(x+l')}\right]e^{-i\beta y}d\beta\ , \quad x>0 \\
-\frac{1}{2\pi}\int_{-\infty}^{+\infty}\left[i\alpha\sum_{j=5}^{8}\frac{R_j}{\kappa p_j-1}e^{m_j x}+\frac{\kappa(1-\nu)}{2}A_2(\alpha)r_2e^{r_2 x}\right]e^{-i\alpha y}\,d\alpha- \\
\quad\frac{1}{2\pi}\int_{-\infty}^{+\infty}\left[i\beta\sum_{j=1}^{4}\frac{S_j}{\kappa s_j-1}e^{n_j(x+l')}+\right. \\
\qquad\left.\frac{\kappa(1-\nu)}{2}B_1(\beta)t_1e^{t_1(x+l')}\right]e^{-i\beta y}d\beta\ , \quad x<0
\end{cases} \tag{3.1.57}$$

From (3.1.40)-(3.1.44), it is seen that mixed boundary conditions are given in terms of complementary stress and displacement quantities and the displacement quantities would be the natural new unknown functions in the system of integral equations to be derived. However, in order to avoid kernels with strong singularities in the resulting integral equations, it is necessary that the new unknown functions be selected as the derivatives of the displacement quantities rather than displacements and rotations themselves. In the present problem, the derivation of the integral equations and the asymptotic analysis become relatively simple if the complementary displacement quantities (which are the new unknowns) are selected as follows:

$$G_1(y)=\lim_{x\to 0^+}\frac{\partial u}{\partial y}-\lim_{x\to 0^-}\frac{\partial u}{\partial y}\ , \quad -\infty<y<+\infty \tag{3.1.58}$$

$$G_2(y)=\lim_{x\to 0^+}\frac{\partial \beta_x}{\partial y}-\lim_{x\to 0^-}\frac{\partial \beta_x}{\partial y}\ , \quad -\infty<y<+\infty \tag{3.1.59}$$

$$G_3(y)=\lim_{x\to 0^+}\frac{\partial w}{\partial y}-\lim_{x\to 0^-}\frac{\partial w}{\partial y}\ , \quad -\infty<y<+\infty \tag{3.1.60}$$

$$G_4(y) = \lim_{x\to 0^+}\left[\frac{\partial u}{\partial y} - \left(\frac{\lambda_2}{\lambda}\right)^2 y\frac{\partial w}{\partial y}\right] - \lim_{x\to 0^-}\left[\frac{\partial u}{\partial y} - \left(\frac{\lambda_2}{\lambda}\right)^2 y\frac{\partial w}{\partial y}\right], \quad -\infty < y < +\infty \quad (3.1.61)$$

$$G_5(y) = \lim_{x\to 0^+}\frac{\partial \beta_y}{\partial y} - \lim_{x\to 0^-}\frac{\partial \beta_y}{\partial y}, \quad -\infty < y < +\infty \quad (3.1.62)$$

By using the dimensionless quantities given in Appendix A, the functions G_j (j=1,..,5) may be expressed in terms of the unknown functions R_j (j=1,...,8) and A_j(j=1,2) as follows [13]:

$$G_1(y) = \frac{1}{2\pi}\int_{-\infty}^{+\infty}\frac{i}{\alpha}\left[\sum_{j=1}^{4}\left(\frac{\lambda_2^2}{\lambda^2} - K_j p_j\right) m_j R_j(\alpha) - \sum_{j=5}^{8}\left(\frac{\lambda_2^2}{\lambda^2} - K_j p_j\right) m_j R_j(\alpha)\right] e^{-i\alpha y}\, d\alpha, \quad (3.1.63)$$

$$G_2(y) = \frac{1}{2\pi}\int_{-\infty}^{+\infty} -i\alpha\left[\sum_{j=1}^{4}\frac{R_j(\alpha) m_j}{\kappa p_j - 1} - \sum_{j=5}^{8}\frac{R_j(\alpha) m_j}{\kappa p_j - 1}\right] e^{-i\alpha y}\, d\alpha - \frac{1}{2\pi}\int_{-\infty}^{+\infty}\frac{\alpha^2\kappa(1-\nu)}{2}\left[A_1(\alpha) - A_2(\alpha)\right] e^{-i\alpha y}\, d\alpha, \quad (3.1.64)$$

$$G_3(y) = -\frac{1}{2\pi}\int_{-\infty}^{+\infty} i\alpha\left[\sum_{j=1}^{4} R_j(\alpha) - \sum_{j=5}^{8} R_j(\alpha)\right] e^{-i\alpha y}\, d\alpha, \quad (3.1.65)$$

$$G_4(y) = \frac{1}{2\pi}\int_{-\infty}^{+\infty}\left\{\sum_{j=1}^{4} R_j(\alpha) K_j\left[p_j + (1+\nu)\alpha^2\right] - \sum_{j=5}^{8} R_j(\alpha) K_j\left[p_j + (1+\nu)\alpha^2\right]\right\} e^{-i\alpha y}\, d\alpha, \quad (3.1.66)$$

$$G_5(y) = -\frac{1}{2\pi}\int_{-\infty}^{+\infty}\alpha^2\left[\sum_{j=1}^{4}\frac{R_j(\alpha)}{\kappa p_j - 1} - \sum_{j=5}^{8}\frac{R_j(\alpha)}{\kappa p_j - 1}\right]e^{-i\alpha y}\,d\alpha + \frac{1}{2\pi}\int_{-\infty}^{+\infty}\frac{\kappa(1-\nu)}{2}i\alpha\left[r_1 A_1(\alpha) - r_2 A_2(\alpha)\right]e^{-i\alpha y}\,d\alpha \tag{3.1.67}$$

Substituting from (3.1.45)-(3.1.49) into (3.1.30)-(3.1.34) and (3.1.53)-(3.1.57) into (3.1.35)-(3.1.39) and inverting the results, the homogeneous boundary conditions (3.1.30)-(3.1.39) become

$$\sum_{j=1}^{4} K_j R_j(\alpha) - \sum_{j=5}^{8} K_j R_j(\alpha) = 0 \tag{3.1.68}$$

$$\sum_{j=1}^{4}\frac{\left[p_j + (1+\nu)\alpha^2\right]}{\kappa p_j - 1}R_j(\alpha) - \sum_{j=5}^{8}\frac{\left[p_j + (1+\nu)\alpha^2\right]}{\kappa p_j - 1}R_j(\alpha) - \frac{\kappa(1-\nu)^2 i\alpha}{2}\left[r_1 A_1(\alpha) - r_2 A_2(\alpha)\right] = 0 \tag{3.1.69}$$

$$\sum_{j=1}^{4}\frac{p_j m_j}{\kappa p_j - 1}R_j(\alpha) - \sum_{j=5}^{8}\frac{p_j m_j}{\kappa p_j - 1}R_j(\alpha) - \frac{(1-\nu)i\alpha}{2}\left[A_1(\alpha) - A_2(\alpha)\right] = 0 \tag{3.1.70}$$

$$\sum_{j=1}^{4} K_j m_j R_j(\alpha) - \sum_{j=5}^{8} K_j m_j R_j(\alpha) = 0 \tag{3.1.71}$$

$$i\alpha\sum_{j=1}^{4}\frac{m_j R_j(\alpha)}{\kappa p_j - 1} - i\alpha\sum_{j=5}^{8}\frac{m_j R_j(\alpha)}{\kappa p_j - 1} + \frac{\kappa(1-\nu)i\alpha}{4}\left(\alpha^2 + r_1^2\right)\left[A_1(\alpha) - A_2(\alpha)\right] = 0 \tag{3.1.72}$$

$$\sum_{j=5}^{8}\left[\left(2+\nu\right)K_j m_j - K_j\frac{m_j^3}{\alpha^2} + \left(\frac{\lambda_2}{\lambda}\right)^2\frac{m_j}{\alpha^2}\right]R_j e^{-m_j l'} + \sum_{j=1}^{4}\left[\left(2+\nu\right)M_j n_j - M_j\frac{n_j^3}{\beta^2} + \left(\frac{\lambda_2}{\lambda}\right)^2\frac{n_j}{\beta^2}\right]S_j = 0 \tag{3.1.73}$$

$$\sum_{j=5}^{8}\frac{R_j m_j}{\kappa p_j - 1}e^{m_j t} - \frac{\kappa(1-\nu)}{2}A_2(\alpha)\beta i + \sum_{j=1}^{4}\frac{S_j n_j}{\kappa s_j - 1} - \frac{\kappa(1-\nu)}{2}B_1(\beta)\beta i = 0 \qquad (3.1.74)$$

$$\sum_{j=5}^{8}R_j e^{m_j t} + \sum_{j=1}^{4}S_j = 0 \qquad (3.1.75)$$

$$\sum_{j=5}^{8}\left[\frac{K_j m_j}{\alpha} + \nu\alpha K_j - \left(\frac{\lambda_2}{\lambda}\right)^2\frac{1}{\alpha}\right]R_j e^{m_j t} + \sum_{j=1}^{4}\left[\frac{M_j n_j}{\beta} - \nu\beta M_j + \left(\frac{\lambda_2}{\lambda}\right)^2\frac{1}{\beta}\right]S_j = 0 \qquad (3.1.76)$$

$$i\alpha\sum_{j=5}^{8}\frac{R_j}{\kappa p_j - 1}e^{m_j t} + \frac{\kappa(1-\nu)}{2}A_2(\alpha)t_2 e^{t_2 t} + i\beta\sum_{j=1}^{4}\frac{S_j}{\kappa s_j - 1} + \frac{\kappa(1-\nu)}{2}B_2(\beta)t_1 = 0 \qquad (3.1.77)$$

Also, inverting the Fourier integrals (3.1.63)-(3.1.67) and observing that $G_i = 0$ (i=1,...,5) for $-\infty < y < -\sqrt{c}$, $\sqrt{c} < y < \infty$, following expressions may be obtained

$$q_1(\alpha) = \left(\frac{\lambda_2}{\lambda}\right)^2\frac{q_2(\alpha)}{\alpha^2} - \frac{i}{\alpha}\left[\sum_{j=1}^{4}K_j p_j m_j R_j(\alpha) - \sum_{j=5}^{8}K_j p_j m_j R_j(\alpha)\right] \qquad (3.1.78)$$

$$q_2(\alpha) = \frac{A_1(\alpha) - A_1(\alpha)}{2} = i\alpha\left[\sum_{j=1}^{4}m_j R_j(\alpha) - \sum_{j=5}^{8}m_j R_j(\alpha)\right] \qquad (3.1.79)$$

$$q_3(\alpha) = -i\alpha\left[\sum_{j=1}^{4}R_j(\alpha) - \sum_{j=5}^{8}R_j(\alpha)\right] \qquad (3.1.80)$$

$$q_4(\alpha) = \sum_{j=1}^{4}p_j K_j R_j(\alpha) - \sum_{j=5}^{8}p_j K_j R_j(\alpha) \qquad (3.1.81)$$

$$q_5(\alpha) = \frac{1}{(1-\nu)}\left[\sum_{j=1}^{4}\frac{p_j R_j(\alpha)}{\kappa p_j - 1} - \sum_{j=5}^{8}\frac{p_j R_j(\alpha)}{\kappa p_j - 1}\right] \tag{3.1.82}$$

where

$$q_1(\alpha) = \int_{-\sqrt{c}}^{+\sqrt{c}} G_1(t) e^{-\kappa t t}\, dt \tag{3.1.83}$$

$$q_2(\alpha) = \int_{-\sqrt{c}}^{+\sqrt{c}} G_2(t) e^{-\kappa t t}\, dt \tag{3.1.84}$$

$$q_3(\alpha) = \int_{-\sqrt{c}}^{+\sqrt{c}} G_3(t) e^{-\kappa t t}\, dt \tag{3.1.85}$$

$$q_4(\alpha) = \int_{-\sqrt{c}}^{+\sqrt{c}} G_4(t) e^{-\kappa t t}\, dt \tag{3.1.86}$$

$$q_5(\alpha) = \int_{-\sqrt{c}}^{+\sqrt{c}} G_5(t) e^{-\kappa t t}\, dt \tag{3.1.87}$$

The algebraic equations (3.1.68)-(3.1.77) can now be solved to give R_j(j=1,...,8), S_j(j=1,...,4), A_j (j=1,2) and B_1 in terms of $q_1,\ldots,q_5$ as follows:

$$R_j(\alpha) = \Big[Q_j(\alpha) q_1(\alpha) + N_j(\alpha) q_2(\alpha) + C_j(\alpha) q_3(\alpha) + D_j(\alpha) q_4(\alpha) + Y_j(\alpha) q_5(\alpha)\Big], \qquad j = 1,2,\ldots,8 \tag{3.1.88}$$

$$S_j(\beta) = \Big[Q_j^*(\beta) q_1(\beta) + N_j^*(\beta) q_2(\beta) + C_j^*(\beta) q_3(\beta) + D_j^*(\beta) q_4(\beta) + Y_j^*(\beta) q_5(\beta)\Big], \qquad j = 1,2,3,4 \tag{3.1.89}$$

$$A_1(\alpha) = U_1(\alpha) q_1(\alpha) + U_2(\alpha) q_2(\alpha) + U_3(\alpha) q_3(\alpha) + U_4(\alpha) q_4(\alpha) + U_5(\alpha) q_5(\alpha) \tag{3.1.90}$$

$$B_1(\beta) = U_1^*(\beta)q_1(\beta) + U_2^*(\beta)q_2(\beta) + U_3^*(\beta)q_3(\beta) + U_4^*(\beta)q_4(\beta) + U_5^*(\beta)q_5(\beta) \qquad (3.1.91)$$

$$A_2(\alpha) = V_1(\alpha)q_1(\alpha) + V_2(\alpha)q_2(\alpha) + V_3(\alpha)q_3(\alpha) + V_4(\alpha)q_4(\alpha) + V_5(\alpha)q_5(\alpha) \qquad (3.1.92)$$

where $Q_j(\alpha)$, $N_j(\alpha)$, $C_j(\alpha)$, $D_j(\alpha)$, $Y_j(\alpha)$ (j=1,...,8), $Q_j^*(\beta)$, $N_j^*(\beta)$, $C_j^*(\beta)$, $D_j^*(\beta)$, $Y_j^*(\beta)$ (j=1,...,4), $U_i(\alpha)$ (i=1,...,5), $U_i^*(\beta)$ (i=1,...,5) and $V_i(\beta)$ (i=1,...,5) are known functions and are given implicitly by the system of equations (3.1.63)-(3.1.77). Then all the unknowns of the problem are expressed in terms of $G_1,...,G_5$.

It can be seen that the equations (3.1.40a), (3.1.41a), (3.1.42a), (3.1.43a), (3.1.44a) related to the crack surface loading would then give the integral equations to determine $G_1,...,G_5$. By substituting (3.1.45)-(3.1.49) into (3.1.40a)-(3.1.44a) following integral equations can be obtained:

$$\lim_{x\to 0^+}\left\{-\frac{1}{2\pi}\int_{-\infty}^{+\infty}\alpha^2\sum_{j=1}^{4}K_jR_j(\alpha)e^{m_jx}e^{-i\alpha y}\,d\alpha - \frac{1}{2\pi}\int_{-\infty}^{+\infty}\beta^2\sum_{j=1}^{4}M_jS_j(\beta)e^{n_j(x+l)}e^{-i\beta y}\,d\beta\right\} +$$
$$\lim_{x\to 0^-}\left\{-\frac{1}{2\pi}\int_{-\infty}^{+\infty}\alpha^2\sum_{j=5}^{8}K_jR_j(\alpha)e^{m_jx}e^{-i\alpha y}\,d\alpha - \frac{1}{2\pi}\int_{-\infty}^{+\infty}\beta^2\sum_{j=1}^{4}M_jS_j(\beta)e^{n_j(x+l)}e^{-i\beta y}\,d\beta\right\} = 2F_{10}(y)\ ,\quad -\sqrt{c} < y < \sqrt{c} \qquad (3.1.93)$$

$$\lim_{x\to 0^+}\frac{1}{2\pi}\frac{a}{h\lambda^4}\left\{\int_{-\infty}^{+\infty}\sum_{j=1}^{4}\frac{p_j+(1-\nu)\alpha^2}{\kappa p_j-1}R_j(\alpha)e^{m_j x}e^{-i\alpha y}\,d\alpha-\right.$$
$$\frac{\kappa(1-\nu)^2}{2}\int_{-\infty}^{+\infty}A_1(\alpha)i\alpha r_1 e^{r_1 x}e^{-i\alpha y}\,d\alpha+$$
$$\int_{-\infty}^{+\infty}\sum_{j=1}^{4}\frac{s_j+(1-\nu)\beta^2}{\kappa s_j-1}S_j(\beta)e^{n_j(x+l)}e^{-i\beta y}\,d\beta-$$
$$\left.\frac{\kappa(1-\nu)^2}{2}\int_{-\infty}^{+\infty}B_1(\beta)i\beta t_1 e^{t_1(x+l)}e^{-i\beta y}\,d\beta\right\}+$$
$$\lim_{x\to 0^-}\frac{1}{2\pi}\frac{a}{h\lambda^4}\left\{\int_{-\infty}^{+\infty}\sum_{j=5}^{8}\frac{p_j+(1-\nu)\alpha^2}{\kappa p_j-1}R_j(\alpha)e^{m_j x}e^{-i\alpha y}\,d\alpha-\right.$$
$$\frac{\kappa(1-\nu)^2}{2}\int_{-\infty}^{+\infty}A_2(\alpha)i\alpha r_2 e^{r_2 x}e^{-i\alpha y}\,d\alpha+$$
$$\int_{-\infty}^{+\infty}\sum_{j=1}^{4}\frac{s_j+(1-\nu)\beta^2}{\kappa s_j-1}S_j(\beta)e^{n_j(x+l)}e^{-i\beta y}\,d\beta-$$
$$\left.\frac{\kappa(1-\nu)^2}{2}\int_{-\infty}^{+\infty}B_1(\beta)i\beta t_1 e^{t_1(x+l)}e^{-i\beta y}\,d\beta\right\}=2F_{20}(y)\ ,\qquad -\sqrt{c}<y<\sqrt{c}\tag{3.1.94}$$

$$\lim_{x\to 0^+}\frac{1}{2\pi}\left\{\int_{-\infty}^{+\infty}\sum_{j=1}^{4}\frac{\kappa p_j m_j R_j(\alpha)}{\kappa p_j-1}e^{m_j x}e^{-i\alpha y}\,d\alpha-\frac{\kappa(1-\nu)}{2}\int_{-\infty}^{+\infty}A_1(\alpha)i\alpha e^{r_1 x}e^{-i\alpha y}\,d\alpha+\right.$$
$$\left.\int_{-\infty}^{+\infty}\sum_{j=1}^{4}\frac{\kappa s_j n_j S_j(\beta)}{\kappa s_j-1}e^{n_j(x+l)}e^{-i\beta y}\,d\beta-\frac{\kappa(1-\nu)}{2}\int_{-\infty}^{+\infty}B_1(\beta)i\beta e^{t_1(x+l)}e^{-i\beta y}\,d\beta\right\}+$$
$$\lim_{x\to 0^-}\frac{1}{2\pi}\left\{\int_{-\infty}^{+\infty}\sum_{j=5}^{8}\frac{\kappa p_j m_j R_j(\alpha)}{\kappa p_j-1}e^{m_j x}e^{-i\alpha y}\,d\alpha-\frac{\kappa(1-\nu)}{2}\int_{-\infty}^{+\infty}A_2(\alpha)i\alpha e^{r_2 x}e^{-i\alpha y}\,d\alpha+\right.$$
$$\left.\int_{-\infty}^{+\infty}\sum_{j=1}^{4}\frac{\kappa s_j n_j S_j(\beta)}{\kappa s_j-1}e^{n_j(x+l)}e^{-i\beta y}\,d\beta-\frac{\kappa(1-\nu)}{2}\int_{-\infty}^{+\infty}B_1(\beta)i\beta e^{t_1(x+l)}e^{-i\beta y}\,d\beta\right\}$$
$$=2F_{30}(y)\ ,\qquad -\sqrt{c}<y<\sqrt{c}\tag{3.1.95}$$

$$\lim_{x\to 0^+}\frac{i}{2\pi}\left\{\int_{-\infty}^{+\infty}\alpha\sum_{j=1}^{4}K_j m_j R_j(\alpha)e^{m_j x}e^{-i\alpha y}\,d\alpha+\int_{-\infty}^{+\infty}\beta\sum_{j=1}^{4}M_j n_j S_j(\beta)e^{n_j(x+l)}e^{-i\beta y}\,d\beta+\right.$$
$$\lim_{x\to 0^-}\frac{i}{2\pi}\left\{\int_{-\infty}^{+\infty}\alpha\sum_{j=51}^{8}K_j m_j R_j(\alpha)e^{m_j x}e^{-i\alpha y}\,d\alpha+\int_{-\infty}^{+\infty}\beta\sum_{j=1}^{4}M_j n_j S_j(\beta)e^{n_j(x+l)}e^{-i\beta y}\,d\beta\right.$$
$$=2F_{40}(y)\ ,\qquad -\sqrt{c}<y<\sqrt{c}\tag{3.1.96}$$

$$
\begin{aligned}
&-\lim_{x\to 0^+}\frac{1}{2\pi}\frac{d(1-\nu)}{h\lambda^4}\left\{\int_{-\infty}^{+\infty} i\alpha\sum_{j=1}^{4}\frac{m_j R_j(\alpha)}{\kappa p_j-1}e^{m_j x}e^{-i\alpha y}\,d\alpha-\right.\\
&\frac{\kappa(1-\nu)}{4}\int_{-\infty}^{+\infty}\left(\alpha^2+r_1^2\right)A_1(\alpha)e^{r_1 x}e^{-i\alpha y}\,d\alpha+\int_{-\infty}^{+\infty} i\beta\sum_{j=1}^{4}\frac{n_j S_j(\beta)}{\kappa s_j-1}e^{n_j(x+l')}e^{-i\beta y}\,d\beta+\\
&\left.\frac{\kappa(1-\nu)}{4}\int_{-\infty}^{+\infty}\left(\beta^2+t_1^2\right)B_1(\beta)e^{t_1(x+l')}e^{-i\beta y}\,d\beta\right\}-\\
&\lim_{x\to 0^-}\frac{1}{2\pi}\frac{d(1-\nu)}{h\lambda^4}\left\{\int_{-\infty}^{+\infty} i\alpha\sum_{j=5}^{8}\frac{m_j R_j(\alpha)}{\kappa p_j-1}e^{m_j x}e^{-i\alpha y}\,d\alpha+\right.\\
&\frac{\kappa(1-\nu)}{4}\int_{-\infty}^{+\infty}\left(\alpha^2+r_2^2\right)A_2(\alpha)e^{r_2 x}e^{-i\alpha y}\,d\alpha+\int_{-\infty}^{+\infty} i\beta\sum_{j=1}^{4}\frac{n_j S_j(\beta)}{\kappa s_j-1}e^{n_j(x+l')}e^{-i\beta y}\,d\beta+\\
&\left.\frac{\kappa(1-\nu)}{4}\int_{-\infty}^{+\infty}\left(\beta^2+t_1^2\right)B_1(\beta)e^{t_1(x+l')}e^{-i\beta y}\,d\beta\right\}=2F_{50}(y)\ ,\quad -\sqrt{c}<y<\sqrt{c}
\end{aligned}
\tag{3.1.97}
$$

By using equations (3.1.83)-(3.1.87) and (3.1.88)-(3.1.92) and observing that $G_j(y)=0$ for $|y|>\sqrt{c}$ (j=1,...,5}, equations (3.1.93)-(3.1.97) can be written as

$$
\begin{aligned}
&\lim_{x\to 0^+}\int_{-\sqrt{c}}^{+\sqrt{c}}\sum_{j=1}^{5}G_j(t)\,dt\left\{\int_{-\infty}^{+\infty}O_{k_j}(\alpha,x)e^{-i(t-y)\alpha}\,d\alpha+\int_{-\infty}^{+\infty}Z_{k_j}(\beta,x)e^{-i(t-y)\beta}\,d\beta\right\}+\\
&\lim_{x\to 0^-}\int_{-\sqrt{c}}^{+\sqrt{c}}\sum_{j=1}^{5}G_j(t)\,dt\left\{\int_{-\infty}^{+\infty}O^*_{k_j}(\alpha,x)e^{-i(t-y)\alpha}\,d\alpha+\int_{-\infty}^{+\infty}Z^*_{k_j}(\beta,x)e^{-i(t-y)\beta}\,d\beta\right\}\\
&\qquad=2F_k(y)\ ,\quad k=1,2,\ldots,5
\end{aligned}
\tag{3.1.98}
$$

where O_{kj}, O^*_{kj}, Z_{kj}, and Z^*_{kj} are complicated but known functions and contain exponential damping terms of the form $e^{m_j x}$ (j=1,...,8), $e^{n_j(x+l')}$(j=1,...,4), $e^{r_j x}$(j=1,2) and $e^{t_1(x+l')}$ However, in the limiting case of $x\to 0$ for $y=t$ and also the case of $(x,l')\to 0$ for $(y,t)\to 0$, this damping does not insure the convergence of the inner integrals if the functions O_{kj}, O^*_{kj}, Z_{kj}, and Z^*_{kj} do not decay sufficiently fast as $|\alpha,\beta|\to\infty$ in equation (3.1.98). For this particular problem, the case of $(x,l')\to 0$ for $(y,t)\to 0$, (i.e. circumferential crack touches the fixed end), is not taken into consideration. To extract the singularities for the case of $x\to 0$ for $y=t$, (i.e. circumferential crack does not touch the fixed end), asymptotic behavior of the inner integrals has to be examined. This can be done in closed form by first extracting the

asymptotic values of $m_j(\alpha)$, $n_j(\beta)$, $r_j(\alpha)$ and $t_1(\beta)$ from the characteristic equations (3.1.9), (3.1.10) and (3.1.26) and then by substituting these values into the expressions of O_{kj}, O^*_{kj}, Z_{kj}, and Z^*_{kj} . From the characteristic equations it can be shown that for large values of $|\alpha|$ and β, we have,

$$m_j(\alpha) = -|\alpha|\left(1+\frac{p_j}{2\alpha^2}-\frac{p_j^2}{8\alpha^4}+.....\right), \quad (j=1,...,4) \tag{3.1.99}$$

$$m_j(\alpha) = |\alpha|\left(1+\frac{p_j}{2\alpha^2}-\frac{p_j^2}{8\alpha^4}+.....\right), \quad (j=5,...,8) \tag{3.1.100}$$

$$n_j(\beta) = -\beta\left(1+\frac{s_j}{2\beta^2}-\frac{s_j^2}{8\beta^4}+.....\right), \quad (j=1,...,4) \tag{3.1.101}$$

$$r_1(\alpha) = -|\alpha|\left(1+\frac{1}{\kappa(1-\nu)\alpha^2}-.....\right), \tag{3.1.102}$$

$$r_2(\alpha) = |\alpha|\left(1+\frac{1}{\kappa(1-\nu)\alpha^2}-.....\right), \tag{3.1.103}$$

$$t_1(\beta) = -\beta\left(1+\frac{1}{\kappa(1-\nu)\beta^2}-.....\right), \tag{3.1.104}$$

The asymptotic values of O_{kj}, O^*_{kj}, Z_{kj}, and Z^*_{kj} for large values of $|\alpha|$ and β, may then be obtained by using (3.1.99)-(3.1.104). It should be noticed that as $x \to 0$, the second inner integrals in (3.1.98) are convergent because of the exponential damping term $e^{-\beta|r'}$. By adding and subtracting the asymptotic values O_{kj}, and Z_{kj},for large values of $|\alpha|$, the singular parts of the kernels can be separated. As an example, consider the equation (3.1.96). It can be rewritten as follows:

$$\lim_{x\to 0^+}\frac{i}{2\pi}\int_{-\infty}^{+\infty}\alpha\left(\sum_{j=1}^{4}K_j m_j R_j(\alpha)e^{m_j x}+\sum_{j=5}^{8}K_j m_j R_j(\alpha)e^{-m_j x}\right)e^{-i\alpha y}\,d\alpha+$$
$$\lim_{x\to 0^+}\frac{i}{\pi}\int_{-\infty}^{+\infty}\beta\sum_{j=1}^{4}M_j n_j S_j(\beta)e^{n_j(x+l)}e^{-i\beta y}\,d\beta=2F_{40}(y) \qquad (3.1.105)$$

If one notices the equation (3.1.73), it is clear that

$$\sum_{j=1}^{4}M_j n_j S_j(\beta)=-\sum_{j=5}^{8}K_j m_j R_j(\alpha)e^{-m_j l} \qquad (3.1.106)$$

Substituing (3.1.106) into (3.1.105) and using the asymptotic expansion of m_j given in (3.1.99) and (3.1.100), and separating the leading terms in the right hand side of equation, (3.1.105) can be expressed as

$$T_1=\lim_{x\to 0^+}\int_{-\infty}^{+\infty}\frac{i\alpha}{2\pi}\sum_{j=1}^{4}K_j m_j R_j(\alpha)e^{-|\alpha|x}e^{-i\alpha y}\,d\alpha+$$
$$\lim_{x\to 0^+}\int_{-\infty}^{+\infty}\frac{i\alpha}{2\pi}\sum_{j=5}^{8}K_j m_j R_j(\alpha)e^{-|\alpha|(x+2l)}e^{-i\alpha y}\,d\alpha \qquad (3.1.107)$$

It should be noticed that as $x\to 0$, the second integral in (3.1.107) is convergent because of the exponential damping term $e^{-2\alpha l'}$. So it is seen that to separate the singular part of (3.1.107), the asymptotic value of $\sum_{1}^{8}K_j m_j R_j$ as $|\alpha|\to\infty$ should be known. By using (3.1.99) and (3.1.100), $\sum_{1}^{8}K_j m_j R_j$ can be expressed as

$$\sum_{j=1}^{8}K_j m_j R_j(\alpha)=-\alpha\,sign(\alpha)\left\{\left[\sum_{j=1}^{4}K_j R_j(\alpha)-\sum_{j=5}^{8}K_j R_j(\alpha)\right]+\right.$$
$$\left.+\frac{1}{2\alpha^2}\left[\sum_{j=1}^{4}K_j p_j R_j(\alpha)-\sum_{j=5}^{8}K_j p_j R_j(\alpha)\right]+\cdots\cdots\right\} \qquad (3.1.108)$$

From (3.1.68), we know that $\sum_{1}^{4}K_j R_j-\sum_{5}^{8}K_j R_j=0$, so equation (3.1.108) can be rewritten as

$$\sum_{j=1}^{8} K_j m_j R_j(\alpha) = -\frac{sign(\alpha)}{2\alpha}\left\{\left[\sum_{j=1}^{4} K_j p_j R_j(\alpha) - \sum_{j=5}^{8} K_j p_j R_j(\alpha)\right] - \ldots\ldots\right\} \quad (3.1.109)$$

Also by using (3.1.81) and neglecting the lower order terms, equation (3.1.109) can be expressed as follows:

$$\sum_{1}^{8} K_j m_j R_j(\alpha) = -\frac{sign(\alpha)}{2\alpha} q_4 \quad (3.1.110)$$

Then, equation (3.1.107), can be rewritten as

$$\begin{aligned}
&\lim_{x\to 0^+} \int_{-\infty}^{+\infty} \left[i\alpha \left(\sum_{j=1}^{4} K_j m_j R_j(\alpha) e^{m_j x} + \sum_{j=5}^{8} K_j m_j R_j(\alpha) e^{-m_j x} \right) + \right. \\
&\qquad \left. \frac{i}{2} sign(\alpha) q_4(\alpha) e^{-|\alpha| x} \right] e^{-i\alpha y} d\alpha - \\
&\lim_{x\to 0^+} \int_{-\infty}^{+\infty} \frac{i}{2} sign(\alpha) q_4(\alpha) e^{-|\alpha| x} e^{-i\alpha y} d\alpha - \\
&\lim_{x\to 0^+} \int_{-\infty}^{+\infty} 2i\alpha \sum_{j=5}^{8} K_j m_j R_j(\alpha) e^{-m_j(x+2l)} e^{-i\alpha y} d\alpha = 4\pi F_{40}(y)
\end{aligned} \quad (3.1.111)$$

If the expression of $q_4(\alpha)$ given in (3.1.86) is substituted into (3.1.111) one obtains,

$$\begin{aligned}
&\lim_{x\to 0^+} \int_{-\infty}^{+\infty} \left[i\alpha \left(\sum_{j=1}^{4} K_j m_j R_j(\alpha) e^{m_j x} + \sum_{j=5}^{8} K_j m_j R_j(\alpha) e^{-m_j x} \right) + \right. \\
&\qquad \left. \frac{i}{2} sign(\alpha) q_4(\alpha) e^{-|\alpha| x} \right] e^{-i\alpha y} d\alpha - \\
&\lim_{x\to 0^+} \int_{-\infty}^{+\infty} \frac{i}{2} sign(\alpha) \int_{-\sqrt{c}}^{+\sqrt{c}} G_4(t) e^{i\alpha(t-y)} e^{-|\alpha| x} dt\, d\alpha - \\
&\lim_{x\to 0^+} \int_{-\infty}^{+\infty} 2i\alpha \sum_{j=5}^{8} K_j m_j R_j(\alpha) e^{-m_j(x+2l)} e^{-i\alpha y} d\alpha = 4\pi F_{40}(y)
\end{aligned} \quad (3.1.112)$$

By changing the order of integration, (3.1.112) can be rewritten as

$$\lim_{x\to 0^+}\int_{-\infty}^{+\infty}\left[i\alpha\left(\sum_{j=1}^{4}K_j m_j R_j(\alpha)e^{m_j x}+\sum_{j=5}^{8}K_j m_j R_j(\alpha)e^{-m_j x}\right)+\frac{i}{2}sign(\alpha)q_4(\alpha)e^{-|\alpha|x}\right]e^{-i\alpha y}d\alpha-$$

$$\lim_{x\to 0^+}\int_{-\sqrt{c}}^{+\sqrt{c}}G_4(t)\,dt\int_{-\infty}^{+\infty}\frac{i}{2}sign(\alpha)e^{i\alpha(t-y)}e^{-|\alpha|x}\,d\alpha-$$

$$\lim_{x\to 0^+}\int_{-\infty}^{+\infty}2i\alpha\sum_{j=5}^{8}K_j m_j R_j(\alpha)e^{-m_j(x+2l)}e^{-i\alpha y}\,d\alpha=4\pi F_{40}(y) \qquad (3.1.113)$$

Finally, by evaluating the second integral as follows

$$\int_{-\infty}^{+\infty}\frac{i}{2}sign(\alpha)e^{i\alpha(t-y)}e^{-|\alpha|x}\,d\alpha=-\int_{0}^{\infty}\sin\left[\alpha(t-y)\right]e^{-\alpha x}\,d\alpha=-\frac{(t-y)}{(t-y)^2+x^2} \qquad (3.1.114)$$

and by taking the limit $x\to 0^+$, the singular integral equation (3.1.113) is reduced to the following form

$$\int_{-\sqrt{c}}^{+\sqrt{c}}\frac{G_4(t)}{(t-y)}dt+\int_{-\infty}^{+\infty}\left[i\alpha\sum_{j=1}^{8}K_j m_j R_j+\frac{i}{2}sign(\alpha)q_4(\alpha)\right]e^{-i\alpha y}d\alpha-$$

$$\int_{-\infty}^{+\infty}2i\alpha\sum_{j=5}^{8}K_j m_j R_j e^{-2m_j l'}e^{-i\alpha y}\,d\alpha=4\pi F_{40}(y)\ ,\quad -\sqrt{c}<y<\sqrt{c} \qquad (3.1.115)$$

where the second and third integrals are now uniformly convergent. Finally by using (3.1.88), the equation (3.1.115) is reduced to the following form

$$\int_{-\sqrt{c}}^{+\sqrt{c}}\frac{G_4(t)}{(t-y)}dt+\sum_{j=1}^{5}\int_{-\sqrt{c}}^{+\sqrt{c}}k_{4j}(y,t)G_j(t)\,dt=4\pi F_{40}(y)\ ,\quad -\sqrt{c}<y<\sqrt{c} \qquad (3.1.116)$$

Similarly, the remaining integral equations can be reduced to the following singular integral equations.

$$\int_{-\sqrt{c}}^{+\sqrt{c}}\frac{G_1(t)}{(t-y)}dt+\sum_{j=1}^{5}\int_{-\sqrt{c}}^{+\sqrt{c}}k_{1j}(y,t)G_j(t)dt=4\pi F_{10}(y)\ ,\quad -\sqrt{c}<y<\sqrt{c} \qquad (3.1.117)$$

$$\frac{1-\nu^2}{\lambda^4}\int_{-\sqrt{c}}^{+\sqrt{c}}\frac{G_2(t)}{(t-y)}dt+\sum_{j=1}^{5}\int_{-\sqrt{c}}^{+\sqrt{c}}k_{2j}(y,t)G_j(t)dt=4\pi\frac{h}{a}F_{20}(y),\ -\sqrt{c}<y<\sqrt{c} \quad (3.1.118)$$

$$\int_{-\sqrt{c}}^{+\sqrt{c}}\frac{G_3(t)}{(t-y)}dt+\sum_{j=1}^{5}\int_{-\sqrt{c}}^{+\sqrt{c}}k_{3j}(y,t)G_j(t)dt=2\pi F_{30}(y)\ ,\quad -\sqrt{c}<y<\sqrt{c} \quad (3.1.119)$$

$$\frac{1-\nu^2}{\lambda^4}\int_{-\sqrt{c}}^{+\sqrt{c}}\frac{G_5(t)}{(t-y)}dt+\sum_{j=1}^{5}\int_{-\sqrt{c}}^{+\sqrt{c}}k_{5j}(y,t)G_j(t)\,dt=4\pi\frac{h}{a}F_{50}(y),\ -\sqrt{c}<y<\sqrt{c} \quad (3.1.120)$$

where the kernels $k_{ij}(y,t)$ (i,j=1,...,5) are bounded in the interval $-\sqrt{c}\le(y,t)\le\sqrt{c}$ and their expressions can be found in Appendix B. To complete the formulation of the problem, one must also require the single-valuedness of the rotations and displacements. In order to get the continuity of the displacements outside the crack, $G_1,...,G_5$ must satisfy the following conditions:

$$\int_{-\sqrt{c}}^{+\sqrt{c}}G_1(t)\,dt=0 \quad (3.1.121)$$

$$\int_{-\sqrt{c}}^{+\sqrt{c}}G_2(t)\,dt=0 \quad (3.1.122)$$

$$\int_{-\sqrt{c}}^{+\sqrt{c}}G_3(t)\,dt=0 \quad (3.1.123)$$

$$\int_{-\sqrt{c}}^{+\sqrt{c}}\left[G_4(t)+\left(\frac{\lambda_2}{\lambda}\right)^2 tG_3(t)\right]dt=0 \quad (3.1.124)$$

$$\int_{-\sqrt{c}}^{+\sqrt{c}}G_5(t)\,dt=0 \quad (3.1.125)$$

Thus, by solving the singular integral equations (3.1.116)-(3.1.120) with the single-valuedness conditions (3.1.121)-(3.1.125), the unknown functions $G_j(y)$, (j=1,...,5) can be found.

3.2 Numerical Solution Method

To solve the system of singular integral equations, (3.1.105)-(3.1.109) , the quadrature technique given in [22] will be used.

It is convenient to apply the technique to these singular integral equations, they should be normalized. To do so, the following normalized quantities are introduced:

$$\tau = t/\sqrt{c} \ , \quad -\sqrt{c} < t < \sqrt{c}$$
$$-1 < \tau < 1 \tag{3.2.1}$$

$$\eta = y/\sqrt{c} \ , \quad -\sqrt{c} < t < \sqrt{c}$$
$$-1 < \eta < 1 \tag{3.2.2}$$

$$\rho = x/\sqrt{c} \ , \quad -\infty < x < \infty$$
$$-\infty < \rho < \infty \tag{3.2.3}$$

$$H_i(\tau) = G_i(\sqrt{c}\tau) \ , \quad (i = 1,\ldots,5) \tag{3.2.4}$$

By using the normalized quantities given in (3.2.1)-(3.2.4), the equations (3.1.105)-(3.1.114) can be rewritten as follows

$$\int_{-1}^{1} \frac{H_1(\tau)}{\tau-\eta} d\tau + \sqrt{c} \int_{-1}^{1} \sum_{j=1}^{5} k_{1j}(\sqrt{c}\eta, \sqrt{c}\tau) H_j(\tau) d\tau = 4\pi F_{10}(\sqrt{c}\eta) \ ,$$
$$-1 < \eta < 1 \tag{3.2.5}$$

$$\frac{1-\nu^2}{\lambda^4} \int_{-1}^{1} \frac{H_2(\tau)}{\tau-\eta} d\tau + \sqrt{c} \int_{-1}^{1} \sum_{j=1}^{5} k_{2j}(\sqrt{c}\eta, \sqrt{c}\tau) H_j(\tau) d\tau = 4\pi \frac{h}{a} F_{20}(\sqrt{c}\eta) \ ,$$
$$-1 < \eta < 1 \tag{3.2.6}$$

$$\int_{-1}^{1}\frac{H_3(\tau)}{\tau-\eta}\,d\tau+\sqrt{c}\int_{-1}^{1}\sum_{j=1}^{5}k_{3j}(\sqrt{c}\eta,\sqrt{c}\tau)H_j(\tau)\,d\tau=2\pi F_{30}(\sqrt{c}\eta)\ ,$$

$$-1<\eta<1 \qquad (3.2.7)$$

$$\int_{-1}^{1}\frac{H_4(\tau)}{\tau-\eta}\,d\tau+\sqrt{c}\int_{-1}^{1}\sum_{j=1}^{5}k_{4j}(\sqrt{c}\eta,\sqrt{c}\tau)H_j(\tau)\,d\tau=4\pi F_{40}(\sqrt{c}\eta)\ ,$$

$$-1<\eta<1 \qquad (3.2.8)$$

$$\frac{1-\nu^2}{\lambda^4}\int_{-1}^{1}\frac{H_5(\tau)}{\tau-\eta}\,d\tau+\sqrt{c}\int_{-1}^{1}\sum_{j=1}^{5}k_{5j}(\sqrt{c}\eta,\sqrt{c}\tau)H_j(\tau)\,d\tau=4\pi\frac{h}{a}F_{50}(\sqrt{c}\eta)\ ,$$

$$-1<\eta<1 \qquad (3.2.9)$$

$$\int_{-1}^{1}H_1(\tau)\,d\tau=0 \qquad (3.2.10)$$

$$\int_{-1}^{1}H_2(\tau)\,d\tau=0 \qquad (3.2.11)$$

$$\int_{-1}^{1}H_3(\tau)\,d\tau=0 \qquad (3.2.12)$$

$$\int_{-1}^{1}\left[H_4(\tau)+\left(\frac{\lambda_2}{\lambda}\right)^2\sqrt{c}\,\tau H_3(\tau)\right]d\tau=0 \qquad (3.2.13)$$

$$\int_{-1}^{1}H_5(\tau)\,d\tau=0 \qquad (3.2.14)$$

In equations (3.2.5)-(3.2.9), the kernels k_{ij} (i,j=1,...,5) are in the form of infinite integrals. To evaluate these integrals, it is possible to use one of the known integration techniques. However, before evaluating the value of the integrals, it is possible to find the asymptotic value of the integrand as the variable of integration approaches infinity. From the asymptotic analysis, it is found that the integrands of

the kernels are not exponentially decaying functions for large values of the variable of the integration. To be able to cope with the convergency problem, these infinite integrals will be evaluated as follows,

$$I=\int_0^A F(\alpha)\,d\alpha+\int_A^\infty \Phi(\alpha)\,d\alpha \qquad (3.2.15)$$

where A is a large enough number and $\Phi(\alpha)$ is the asymptotic value of $F(\alpha)$ as $\alpha\to\infty$. To solve the problem, in addition to numerical evaluation of the first integral in equation (3.2.15), the values of the second integral is found in closed form by sine and cosine integral as stated in [23].Further details of the evaluation of $\Phi(\alpha)$ is given in Appendix D.

The crack tips, $\tau=\pm1$, are the points of singularity. Behavior of the unknown functions H_j (j=1,...,5) in the neighborhood of these singular points is one of the main objectives in solving the problem. Since the unknown functions $H_j(\tau)$ (j=1,...,5) are infinite but integrable at $\tau=\pm1$, the index of equations (3.2.5)-(3.2.9) is +1. The fundamental functions $G_j(\tau)$ will then be in the following form [22]

$$H_j(\tau)=h_j(\tau)(1-\tau^2)^{-1/2}\ ,\quad (j=1,\ldots,5) \qquad (3.2.16)$$

where $h_j(\tau)$ (j=1,...,5) are bounded in $-1\le\tau\le1$. Observing that $(1-\tau^2)^{-1/2}$ is the weight of Chebyshev polynomials of the first kind and applying the Gauss-Chebyshev integration formulas, equations (3.2.5)-(3.2.14) can be reduced to the following set of simultaneous algebraic equations:

$$\sum_{j=1}^{n}\left[\frac{h_1(\tau_j)}{\tau_j-\eta_i}+\sqrt{c}\sum_{m=1}^{5}k_{1m}(\sqrt{c}\eta_i,\sqrt{c}\tau_j)h_m(\tau_j)\right]w_j=4\pi F_{10}(\sqrt{c}\eta_i)\ ,$$
$$i=1,\ldots,n-1 \qquad (3.2.17)$$

$$\sum_{j=1}^{n}\left[\frac{1-\nu^2}{\lambda^4}\frac{h_2(\tau_j)}{\tau_j-\eta_i}+\sqrt{c}\sum_{m=1}^{5}k_{2m}(\sqrt{c}\eta_i,\sqrt{c}\tau_j)h_m(\tau_j)\right]w_j=4\pi\frac{h}{a}F_{20}(\sqrt{c}\eta_i)\ ,$$
$$i=1,\ldots,n-1 \qquad (3.2.18)$$

$$\sum_{j=1}^{n}\left[\frac{h_3(\tau_j)}{\tau_j-\eta_i}+\sqrt{c}\sum_{m=1}^{5}k_{3m}(\sqrt{c}\eta_i,\sqrt{c}\tau_j)h_m(\tau_j)\right]w_j=2\pi F_{30}(\sqrt{c}\eta_i)\ ,$$

$$i=1,\ldots,n-1 \qquad (3.2.19)$$

$$\sum_{j=1}^{n}\left[\frac{h_4(\tau_j)}{\tau_j-\eta_i}+\sqrt{c}\sum_{m=1}^{5}k_{4m}(\sqrt{c}\eta_i,\sqrt{c}\tau_j)h_m(\tau_j)\right]w_j=4\pi F_{40}(\sqrt{c}\eta_i),$$

$$i=1,\ldots,n-1 \qquad (3.2.20)$$

$$\sum_{j=1}^{n}\left[\frac{1-\nu^2}{\lambda^4}\frac{h_5(\tau_j)}{\tau_j-\eta_i}+\sqrt{c}\sum_{m=1}^{5}k_{5m}(\sqrt{c}\eta_i,\sqrt{c}\tau_j)h_m(\tau_j)\right]w_j=4\pi F_{50}(\sqrt{c}\eta_i),$$

$$i=1,\ldots,n-1 \qquad (3.2.21)$$

$$\sum_{j=1}^{n}h_1(\tau_j)w_j=0 \qquad (3.2.22)$$

$$\sum_{j=1}^{n}h_2(\tau_j)w_j=0 \qquad (3.2.23)$$

$$\sum_{j=1}^{n}h_3(\tau_j)w_j=0 \qquad (3.2.24)$$

$$\sum_{j=1}^{n}\left[h_4(\tau_j)+\left(\frac{\lambda_2}{\lambda}\right)^2\sqrt{c}\ \tau_j h_3(\tau_j)\right]w_j=0 \qquad (3.2.25)$$

$$\sum_{j=1}^{n}h_5(\tau_j)w_j=0 \qquad (3.2.26)$$

where

$$\tau_j=\cos(\pi\frac{j-1}{n-1})\ ,\quad j=1,\ldots,n \qquad (3.2.27)$$

$$\eta_i=\cos(\pi\frac{2i-1}{2n-2})\ ,\quad i=1,\ldots,n-1 \qquad (3.2.28)$$

$$w_1 = w_n = \frac{\pi}{2(n-1)}\ ,\quad w_j = \frac{\pi}{n-1}\ ,\quad j = 2,\ldots,n-1 \qquad (3.2.29)$$

By solving the set of 5n simultaneous algebraic equations given in (3.2.17)-(3.2.26), 5n discrete values for $h_i(\tau_j)$ (i=1,...,5; j=1,...,n) can be found. By using these values, it is possible to find every physical quantities of the problem.

3.3 Asymptotic Fields Around the Crack Tips

In order to obtain the asymptotic stress field in a neighborhood of the crack tip, the following formula is used [24]

$$\int_{-1}^{1} \frac{h(\tau)}{\sqrt{1-\tau^2}} e^{i\alpha\tau} d\tau = \left(\frac{\pi}{2|\alpha|}\right)^{1/2} \left\{ h(1)\exp\left[i\left(\alpha - \frac{\pi}{4}\frac{\alpha}{|\alpha|}\right)\right] + h(-1)\exp\left[-i\left(\alpha - \frac{\pi}{4}\frac{\alpha}{|\alpha|}\right)\right] + O\left(\frac{1}{|\alpha|}\right)\right\}, \quad (|\alpha| \to \infty) \qquad (3.3.1)$$

Using the asymptotic expansions of m_j (j=1,...,8), n_j (j=1,...,4) r_1, r_2 and t_1 given in (3.1.99)-(3.1.104) and equations (3.3.1), (3.1.45)-(3.1.52), one can obtain the asymptotic expressions for stress and moment resultants around the crack tip $\eta = 1$, $\rho = 0$. The leading terms of the asymptotic stress and moment resultants may be expressed as

$$N_{xx} \cong \frac{h_1(1)}{4\sqrt{2\pi}} \int_0^{\infty} \frac{1}{\sqrt{\alpha}} \left(1 + \alpha|\rho|\right) e^{-\alpha|\rho|} \sin\left[\alpha(1-\eta) - \frac{\pi}{4}\right] d\alpha\ , \qquad (3.3.2)$$

$$N_{yy} \cong \frac{h_1(1)}{4\sqrt{2\pi}} \int_0^{\infty} \frac{1}{\sqrt{\alpha}} \left(1 - \alpha|\rho|\right) e^{-\alpha|\rho|} \sin\left[\alpha(1-\eta) - \frac{\pi}{4}\right] d\alpha\ , \qquad (3.3.3)$$

$$N_{xy} \cong \frac{h_4(1)}{4\sqrt{2\pi}} \int_0^{\infty} \frac{1}{\sqrt{\alpha}} \left(1 - \alpha|\rho|\right) e^{-\alpha|\rho|} \sin\left[\alpha(1-\eta) - \frac{\pi}{4}\right] d\alpha\ , \qquad (3.3.4)$$

$$M_{xx} \cong \frac{h}{12a}\frac{h_2(1)}{4\sqrt{2\pi}}\int_0^\infty \frac{1}{\sqrt{\alpha}}\left(1+\alpha|\rho|\right)e^{-\alpha|\rho|}\sin\left[\alpha(1-\eta)-\frac{\pi}{4}\right]d\alpha\ , \quad (3.3.5)$$

$$M_{yy} \cong \frac{h}{12a}\frac{h_2(1)}{4\sqrt{2\pi}}\int_0^\infty \frac{1}{\sqrt{\alpha}}\left(1-\alpha|\rho|\right)e^{-\alpha|\rho|}\sin\left[\alpha(1-\eta)-\frac{\pi}{4}\right]d\alpha\ , \quad (3.3.6)$$

$$M_{xy} \cong \frac{h}{12a}\frac{h_5(1)}{4\sqrt{2\pi}}\int_0^\infty \frac{1}{\sqrt{\alpha}}\left(1-\alpha|\rho|\right)e^{-\alpha|\rho|}\sin\left[\alpha(1-\eta)-\frac{\pi}{4}\right]d\alpha\ , \quad (3.3.7)$$

$$V_x \cong \frac{h_3(1)}{2\sqrt{2\pi}}\int_0^\infty \frac{e^{-\alpha|\rho|}}{\sqrt{\alpha}}\sin\left[\alpha(1-\eta)-\frac{\pi}{4}\right]d\alpha\ , \quad (3.3.8)$$

$$V_y \cong \frac{h_3(1)}{2\sqrt{2\pi}}\int_0^\infty \frac{e^{-\alpha|\rho|}}{\sqrt{\alpha}}\cos\left[\alpha(1-\eta)-\frac{\pi}{4}\right]d\alpha \quad (3.3.9)$$

Defining the new coordinates r, θ in η, ρ plane by $\rho = r\sin\theta$, $\eta - 1 = r\cos\theta$ and using the relation [25]

$$\int_0^\infty z^{\mu-1}e^{-sz}\begin{Bmatrix}\sin\\ \cos\end{Bmatrix}(rz)\,dz = \frac{\Gamma(\mu)}{(s^2+r^2)^{\mu/2}}\begin{Bmatrix}\sin\\ \cos\end{Bmatrix}\left(\mu\tan^{-1}\frac{r}{s}\right)\ , \quad (s>0,\ \mu>0) \quad (3.3.10)$$

equations (3.3.2)-(3..3.9) can be reduced to the following form

$$N_{xx} = -\frac{h_1(1)}{4\sqrt{2r}}\left[\frac{5}{4}\cos\frac{\theta}{2} - \frac{1}{4}\cos\frac{5\theta}{2}\right], \quad (3.3.11)$$

$$N_{yy} = -\frac{h_1(1)}{4\sqrt{2r}}\left[\frac{3}{4}\cos\frac{\theta}{2} + \frac{1}{4}\cos\frac{5\theta}{2}\right], \quad (3.3.12)$$

$$N_{xy} = -\frac{h_4(1)}{4\sqrt{2r}}\left[\frac{3}{4}\cos\frac{\theta}{2} + \frac{1}{4}\cos\frac{5\theta}{2}\right], \quad (3.3.13)$$

$$M_{xx} = -\frac{h_2(1)}{4\sqrt{2r}}\frac{h}{12a}\left[\frac{5}{4}\cos\frac{\theta}{2} - \frac{1}{4}\cos\frac{5\theta}{2}\right], \tag{3.3.14}$$

$$M_{yy} = -\frac{h_2(1)}{4\sqrt{2r}}\frac{h}{12a}\left[\frac{3}{4}\cos\frac{\theta}{2} + \frac{1}{4}\cos\frac{5\theta}{2}\right], \tag{3.3.15}$$

$$M_{xy} = -\frac{h_5(1)}{4\sqrt{2r}}\frac{h}{12a}\left[\frac{3}{4}\cos\frac{\theta}{2} + \frac{1}{4}\cos\frac{5\theta}{2}\right], \tag{3.3.16}$$

$$V_x = -\frac{h_3(1)}{2\sqrt{2r}}\cos\frac{\theta}{2}, \tag{3.3.17}$$

$$V_y = \frac{h_3(1)}{2\sqrt{2r}}\sin\frac{\theta}{2} \tag{3.3.18}$$

By observing that the membrane and bending components of the stresses are given by (see Appendix A)

$$\sigma_{ij}^m = N_{ij}\ ,\ \sigma_{ij}^b = \frac{12az}{h}M_{ij}\ ,\ (i,j = x,y) \tag{3.3.19}$$

from equations (3.3.11)-(3.3.16), the asymptotic stress distribution may be obtained as,

$$\sigma_{xx} = -\frac{h_1(1) + zh_2(1)}{4\sqrt{2r}}\left[\frac{5}{4}\cos\frac{\theta}{2} - \frac{1}{4}\cos\frac{5\theta}{2}\right], \tag{3.3.20}$$

$$\sigma_{yy} = -\frac{h_1(1) + zh_2(1)}{4\sqrt{2r}}\left[\frac{3}{4}\cos\frac{\theta}{2} + \frac{1}{4}\cos\frac{5\theta}{2}\right], \tag{3.3.21}$$

$$\sigma_{xy} = -\frac{h_4(1) + zh_5(1)}{4\sqrt{2r}}\left[\frac{3}{4}\cos\frac{\theta}{2} + \frac{1}{4}\cos\frac{5\theta}{2}\right], \tag{3.3.22}$$

similarly, for the transverse shear stresses by using

$$\sigma_{iz} = \frac{3}{2} V_i \left[1 - \left(\frac{az}{h/2} \right)^2 \right], \quad (i = x, y) \tag{3.3.23}$$

the following asymptotic stress distribution can be found

$$\sigma_{xz} = -\frac{3}{2} \frac{h_3(1)}{2\sqrt{2r}} \cos\frac{\theta}{2} \left[1 - \left(\frac{az}{h/2} \right)^2 \right], \tag{3.3.24}$$

$$\sigma_{yz} = -\frac{3}{2} \frac{h_3(1)}{2\sqrt{2r}} \sin\frac{\theta}{2} \left[1 - \left(\frac{az}{h/2} \right)^2 \right] \tag{3.3.25}$$

3.4 Numerical Results and Discussion

For the problem under consideration, Modes I, II and III stress intensity factors at the crack tip are defined by:

$$k_j(x_3) = \lim_{x_2 \to a} \sqrt{2(x-a)}\ \sigma_{1j}(0, x_2, x_3), \quad (j = 1,2,3) \tag{3.4.1}$$

Then, from equations (3.3.20), (3.3.22), (3.3.24) and Appendix A, the stress intensity factors can be written as

$$k_1(x_3) = -\frac{cE}{4}\sqrt{a} \left[h_1(1) + \frac{x_3}{a} h_2(1) \right], \tag{3.4.2}$$

$$k_2(x_3) = -\frac{E}{4}\sqrt{a} \left[h_4(1) + \frac{x_3}{a} h_5(1) \right], \tag{3.4.3}$$

$$k_3(x_3) = -\frac{3}{4} B\sqrt{a}\sqrt{c} h_3(1) \left[1 - \left(\frac{x_3}{h/2a} \right)^2 \right], \tag{3.4.4}$$

The main interest in this study is the evaluation of the stress intensity factors in shells for various crack geometries and loading conditions. For each crack geometry the problem is solved by assuming only one of the possible crack surface loadings to be non zero at a time. For a general loading the results may then be obtained by superposition. From (3.4.2) and (3.4.3) it is seen that the in-plane stress intensity factors k_1 and k_2 have "membrane" and "bending" components, since h_1 and h_4 are related to the membrane and h_2 and h_5 are related to the bending stresses. For simplicity, the related stress intensity factors are defined separately. The calculated results are normalized with respect to a standard stress intensity factor $\sigma_j\sqrt{a}$ (j=1,...,5) where σ_j stands for any of the following five nominal ("membrane", "bending", "transverse shear", "in-plane shear" and "twisting") stresses:

$$\sigma_1 = \frac{N_{11}}{h}\ ,\quad \sigma_2 = \frac{6M_{11}}{h^2}\ ,\quad \sigma_3 = \frac{3}{2}\frac{V_1}{h}\ ,\quad \sigma_4 = \frac{N_{12}}{h}\ ,\quad \sigma_5 = \frac{6M_{12}}{h^2} \qquad (3.4.5)$$

where crack lies in X_2X_3 plane and N_{11}, M_{11}, V_1, N_{12} and M_{12} are the crack surface tractions.

The normalized stress intensity factors are then defined and calculated in terms of $h_j(1)$ (j=1,...,5) as follows:

$$k_{mm} = \frac{k_1(0)}{\sigma_1\sqrt{a}} = -\frac{cE}{4\sigma_1}h_1(1)\ , \qquad (3.4.6)$$

$$k_{bm} = \frac{k_1(0)}{\sigma_2\sqrt{a}} = -\frac{cE}{4\sigma_2}h_1(1)\ , \qquad (3.4.7)$$

$$k_{mb} = \frac{k_1(h/2) - k_1(0)}{\sigma_1\sqrt{a}} = -\frac{cE}{4\sigma_1}\frac{h}{2a}h_2(1)\ , \qquad (3.4.8)$$

$$k_{bb} = \frac{k_1(h/2) - k_1(0)}{\sigma_2\sqrt{a}} = -\frac{cE}{4\sigma_2}\frac{h}{2a}h_2(1)\ , \qquad (3.4.9)$$

$$k_{w} = \frac{k_3(0)}{\sigma_3\sqrt{a}} = -\frac{3}{4}\frac{B}{\sigma_3}\sqrt{c}h_3(1) \ , \tag{3.4.10}$$

$$k_{sv} = \frac{k_3(0)}{\sigma_4\sqrt{a}} = -\frac{3}{4}\frac{B}{\sigma_4}\sqrt{c}h_3(1) \ , \tag{3.4.11}$$

$$k_{tw} = \frac{k_3(0)}{\sigma_5\sqrt{a}} = -\frac{3}{4}\frac{B}{\sigma_5}\sqrt{c}h_3(1) \ , \tag{3.4.12}$$

$$k_{us} = \frac{k_2(0)}{\sigma_3\sqrt{a}} = -\frac{E}{4\sigma_3}h_4(1) \ , \tag{3.4.13}$$

$$k_{ss} = \frac{k_2(0)}{\sigma_4\sqrt{a}} = -\frac{E}{4\sigma_4}h_4(1) \ , \tag{3.4.14}$$

$$k_{ts} = \frac{k_2(0)}{\sigma_5\sqrt{a}} = -\frac{E}{4\sigma_5}h_4(1) \ , \tag{3.4.15}$$

$$k_{ut} = \frac{k_2(h/2) - k_2(0)}{\sigma_3\sqrt{a}} = -\frac{E}{4\sigma_3}\frac{h}{2a}h_5(1) \ , \tag{3.4.16}$$

$$k_{st} = \frac{k_2(h/2) - k_2(0)}{\sigma_4\sqrt{a}} = -\frac{E}{4\sigma_4}\frac{h}{2a}h_5(1) \ , \tag{3.4.17}$$

$$k_{tt} = \frac{k_2(h/2) - k_2(0)}{\sigma_5\sqrt{a}} = -\frac{E}{4\sigma_5}\frac{h}{2a}h_5(1) \tag{3.4.18}$$

where for each individual loading σ_j is given by (3.4.5).In the case of uniform crack surface loads N_{11}, M_{11}, V_1, N_{12} and M_{12}, referring to (3.1.40a)-(3.1.44a), Appendix A, and (3.4.5) the input functions of the system of integral equations (3.1.105)-(3.1.109) are given by

$$F_{10}(y)=\frac{\sigma_1}{cE}\ ,\ F_{20}(y)=\frac{\sigma_2}{6cE}\ ,\ F_{30}(y)=\frac{2}{3}\frac{\sigma_3}{B\sqrt{c}}\ ,$$

$$F_{40}(y)=\frac{\sigma_4}{6E}\ ,\ F_{50}(y)=\frac{\sigma_5}{6E}\ , \qquad (3.4.19)$$

The normalized stress intensity factors are obtained for various values of the dimensionless length parameters h/R, a/h and l/a of the problem and they are given in Tables 1 through 13 and Figures 5 through 15. In all of these examples it is assumed that the material is isotropic and Poisson's ratio is ν=0.3. To show the material orthotropy on the stress intensity factors , graphite, a strongly orthotropic material, is considered and results are given in Table 15 for l/a=0.5, a/h=1 and R/h=10. Also the effect of Poisson's ratio on the stress intensity factors is analyzed and results are tabulated in Table 14 for l/a=0.5, a/h=1 and R/h=5.

From the Tables 1 through 15 and Figures 5 through 15, one can make the following observations:

As $l/a\to\infty$, the values of the stress intensity factor ratios are in excellent agreement with the results given for infinite cylinder in [9] and [13].

If the crack surface is under the effect of uniform membrane loading, the membrane component of the stress intensity factor ratio, k_{mm} is larger than k_{bm}. The value of k_{mm} increases with decreasing R/h and increasing a/h ratios as shown in Table 1 and Figure 10. When the crack approaches to the fixed end, i.e. l/a gets smaller, significant increase in k_{mm} can be observed in Figure 5. For small a/h ratios, increase in k_{mm} is larger as the crack approaches to the fixed end.

If the crack surface is under uniform bending moment, the bending stress intensity factor ratio k_{bb} is the dominant one. The value of k_{bb} decreases with decreasing R/h and a/h ratios. The effect of the fixed end on k_{bb} decreases as crack length increases.

In the shell theories used the stress intensity factor in a shell containing a through crack and subjected to pure bending is found to be function of the thickness coordinate X_3 meaning that for $X_3<0$, the stress intensity factor would be

negative. Therefore the through crack bending results would be meaningful only if the shell is also under tension and the applied loads satisfy following inequality

$$\frac{\sigma_1}{\sigma_2} \geq \frac{k_1^b(h/2)}{\sigma_2^\infty \sqrt{a}} \tag{3.4.20}$$

It is then clear that if the shell under pure bending or if the tensile stress is not sufficiently high to satisfy the above inequality, the crack surfaces may be in contact on the compression side. In this case the problem may be treated as a part-through crack problem with the crack forming a cusp along the boundary of contact region.

Equations (3.2.7), (3.2.8) and (3.2.9), respectively, correspond to transverse shear, uniform in-plane shear and twisting moment loading of the shell with a fixed end containing a circumferential crack. Since the integral equations are coupled, for each loading there will be a primary and two secondary stress intensity factors. In each case primary stress intensity factor are normalized with respect to both secondary stress intensity factors and primary stress intensity factor obtained from the corresponding two dimensional elasticity solution of the infinite plate with a central crack problem.

In the case of uniform transverse shear loading, the twisting moment component and the transverse shear component of the stress intensity factor ratios k_{tv} and k_{vv} are the dominant factors, and k_{vv} increases with increasing R/h. For large a/h ratios, as crack gets closer to fixed end, k_{vv} values decrease. For small a/h ratios, a weak interaction between fixed end and circumferential crack can be observed in Figure 7.

Tables 8 through 10 show some sample results for a cylindrical shell subjected to uniform membrane shear loading N_{12}^∞ away from the crack region. This represents by far the most important antisymmetric loading in practice as in, for example, cylinders subjected to torsion. The stress intensity factor ratio k_{ss} is the dominant component and its value increases as h/R and a/h increases. As l/a ratio gets smaller, k_{ss} values increase and as l/a gets larger, it asymptotically approaches the results obtained for infinite cylindrical shells.

In the case of twisting moment, the twisting component of the stress intensity factor ratio k_{II} is the dominant one and its value is practically insensitive to the change in h/R ratio but it increases with decreasing a/h values. The effect of the fixed end in reducing the stress intensity factor k_{II} can be observed in Figure 14.

The effect of Poisson's ratio ν on the stress intensity factors for a specific geometry a/h=1, R/h=5 and l/a=0.5 is shown in Table 14. From the table the effect of Poisson's ratio on the primary stress intensity factors does not seem to be very significant. Even though under membrane loading, the effect of ν (varying between 0 and 0.5) on k_{bm} may be as high as 40% , for practical variations in ν and for most crack geometries, the influence of Poisson's ratio is not expected to be significant.

It should be noted that the Poisson's ratio ν in isotropic shells and $\nu = \sqrt{\nu_1 \nu_2}$ and orthotropy parameter $c = (E_1/E_2)^{1/4}$ in specially orthotropic shells appear in the expressions of the kernels of the integral equations. Thus, in general, to investigate the effect of the material orthotropy on the stress intensity factors both ν and c must be varied. However, as seen from table 14, the influence of ν is rather insignificant. Therefore, to study the effect of material orthotropy it may be sufficient to vary c only. The effect of material orthotropy on the stress intensity factors is shown in Table 15 for a/h=1, R/h=10 and l/a=0.5. It is seen that all stress intensity factor ratios are affected considerably by the material orthotropy. Except, the twisting component of stress intensity factor ratio, k_{II}, when E_1 / E_2<1 the values of stress intensity factor ratios are smaller than that of isotropic case, and if E_1 / E_2>1 then they are larger than that of isotropic case.

CHAPTER IV

A CYLINDRICAL SHELL WITH A FIXED END WHICH CONTAINS A CIRCUMFERENTIAL PART-THROUGH CRACK

In this part of the study, a cylindrical shell with a fixed end which contains a circumferential part-through crack subjected to the five possible loadings is considered. The problem will be treated by using the line-spring model [17].

The local geometry of the surface crack for the cylindrical shell under consideration is shown in Figure 2. Let $\sigma_{ij}^{n}(0,X_2,X_3)$, (j=1,2,3) be the stresses acting on the net ligament ($X_1=0,\ -a<X_2<a,\ -h/2<X_3<[h/2-l(X_2)]$). Let the net ligament stresses σ_{ij}^{n} be statically equivalent to the resultants $N_{11}(0,X_2)$, $M_{11}(0,X_2)$, $V_1(0,X_2)$, $N_{12}(0,X_2)$, $M_{12}(0,X_2)$ acting on the neutral surface $X_3=0$ along ($X_1=0,\ -a<X_2<a$). Note that in expressing the boundary conditions for the three dimensional surface crack problem the conditions of zero displacements on the uncracked part of the boundary $X_1=0$ may be replaced by the traction boundary conditions $\sigma_{ij}(0,X_2,X_3)=\sigma_{ij}^{n}(0,X_2,X_3)$, provided that σ_{ij}^{n} are known. One of the major assumptions in developing the line spring model is that the net ligament tractions σ_{ij}^{n} (which are unknown functions of X_2 and X_3) may be replaced by their statically equivalent resultants N_{11}, M_{11}, V_1, N_{12} and M_{12} which are now functions of only one variable, X_2. This assumption also implies that, for the purpose of determining the unknown resultants, the part-through crack problem may be replaced by a through crack problem. If the following matrix is defined

$$\left[F_i(y)\right]^T=\left\{\frac{N_{11}}{Ehc},\frac{M_{11}}{Eh^2c},\frac{12(1+\nu)V_1}{5Eh\sqrt{c}},\frac{N_{12}}{Eh},\frac{M_{12}}{Eh^2}\right\},\quad (i=1,\ldots,5)\qquad (4.1)$$

by taking into consideration the contribution coming from the net ligament stresses , the system of singular integral equations (3.1.105)-(3.1.109) may now be modified as

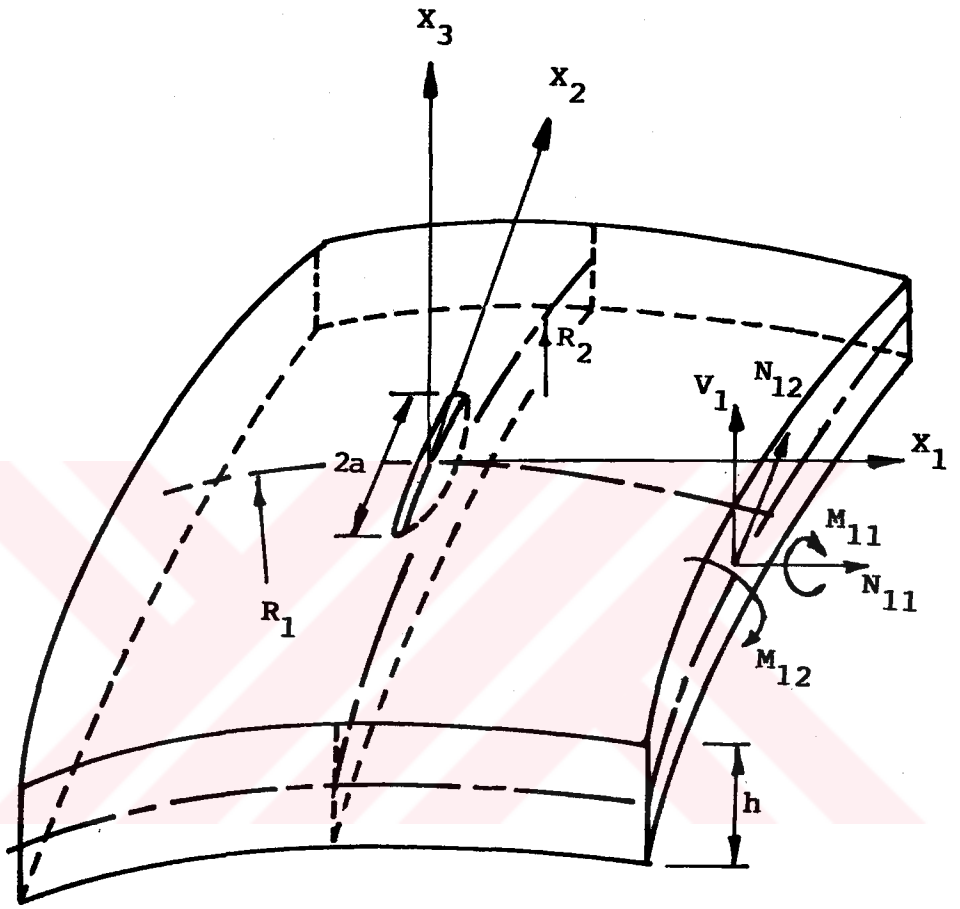

Figure 2. Geometry of a Semi-Elliptical Part-Through Crack in a Shell

$$\int_{-\sqrt{c}}^{+\sqrt{c}} \frac{G_1(t)}{(t-y)}dt + \sum_{j=1}^{5}\int_{-\sqrt{c}}^{+\sqrt{c}} k_{1j}(y,t)G_j(t)dt = 4\pi\left[F_{10}(y) - F_1(y)\right], \quad -\sqrt{c} < y < \sqrt{c} \tag{4.2}$$

$$\frac{1-\nu^2}{\lambda^4}\int_{-\sqrt{c}}^{+\sqrt{c}} \frac{G_2(t)}{(t-y)}dt + \sum_{j=1}^{5}\int_{-\sqrt{c}}^{+\sqrt{c}} k_{2j}(y,t)G_j(t)dt = 4\pi\frac{h}{a}\left[F_{20}(y) - F_2(y)\right], \quad -\sqrt{c} < y < \sqrt{c} \tag{4.3}$$

$$\int_{-\sqrt{c}}^{+\sqrt{c}} \frac{G_3(t)}{(t-y)}dt + \sum_{j=1}^{5}\int_{-\sqrt{c}}^{+\sqrt{c}} k_{3j}(y,t)G_j(t)dt = 2\pi\left[F_{30}(y) - F_3(y)\right], \quad -\sqrt{c} < y < \sqrt{c} \tag{4.4}$$

$$\int_{-\sqrt{c}}^{+\sqrt{c}} \frac{G_4(t)}{(t-y)}dt + \sum_{j=1}^{5}\int_{-\sqrt{c}}^{+\sqrt{c}} k_{4j}(y,t)G_j(t)dt = 4\pi\left[F_{40}(y) - F_4(y)\right], \quad -\sqrt{c} < y < \sqrt{c} \tag{4.5}$$

$$\frac{1-\nu^2}{\lambda^4}\int_{-\sqrt{c}}^{+\sqrt{c}} \frac{G_5(t)}{(t-y)}dt + \sum_{j=1}^{5}\int_{-\sqrt{c}}^{+\sqrt{c}} k_{5j}(y,t)G_j(t)dt = 4\pi\frac{h}{a}\left[F_{50}(y) - F_5(y)\right], \quad -\sqrt{c} < y < \sqrt{c} \tag{4.6}$$

To solve the integral equations (4.2)-(4.6), the two sets of unknown functions G_j and F_j (j=1,...,5) must be somehow related. The key to this relationship is another important assumption made in developing the model to the effect that the stress intensity factors at a location X_2 along the crack front (Figure 3) may be approximated by the corresponding Modes I, II and III values obtained from the plane elasticity solution of a strip containing an edge crack of depth $l(X_2)$ and subjected to stress and moment resultants $[N_{11}(X_2), M_{11}(X_2)]$, $V_1(X_2)$ and $[N_{12}(X_2), M_{12}(X_2)]$ away from the crack region. To obtain the relationship between the functions G_j and F_j (j=1,...,5), the energy G available for fracture along the crack front is expressed in two ways. First, it is noted that for coplanar crack growth G is equivalent to the crack closure energy per unit thickness which may be expressed in terms of the stress intensity factors as follows:

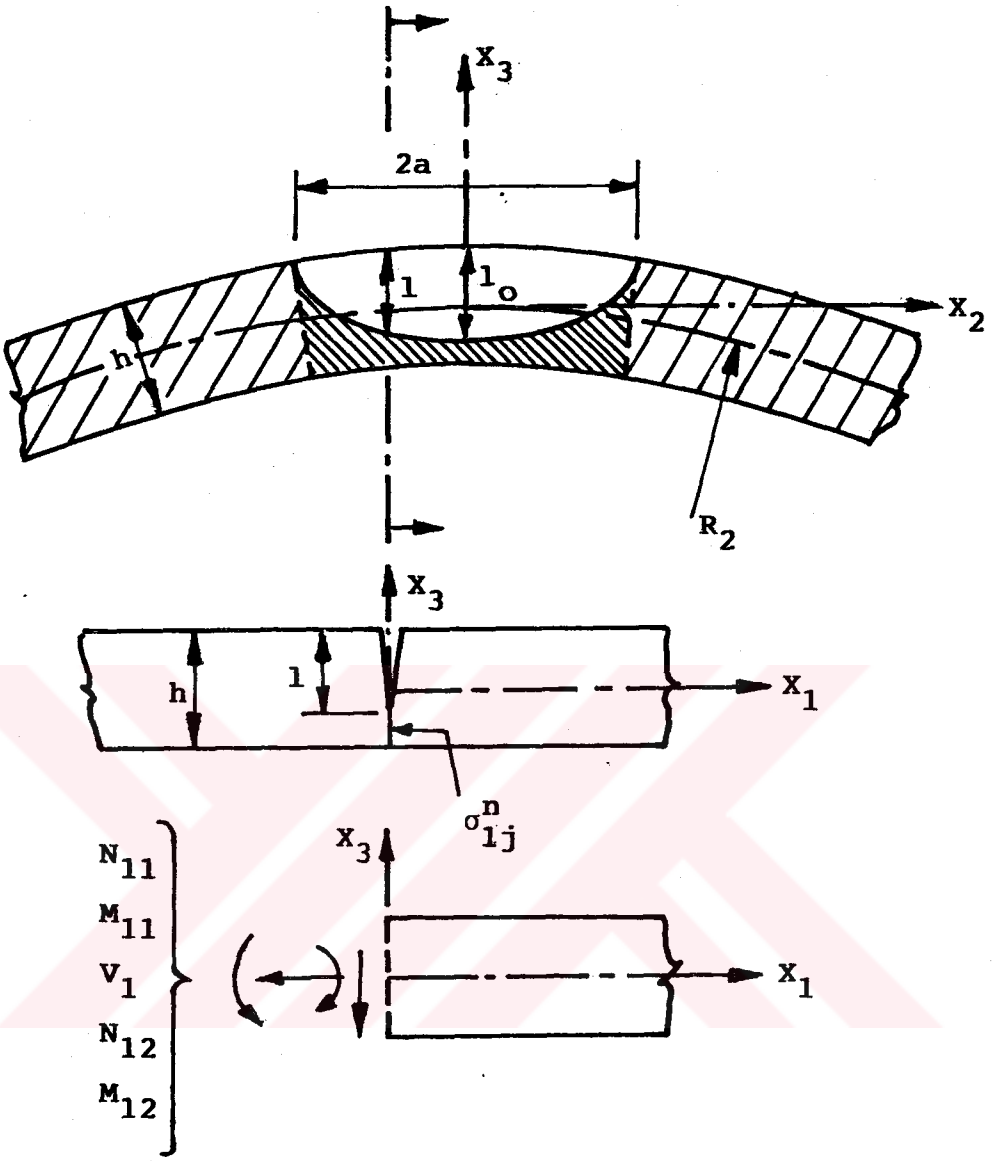

Figure 3. The Notation for a Part-Through Crack in Shells

$$G=\frac{\partial}{\partial l}\left(U-V\right)=\frac{\pi\left(1-\nu^2\right)}{E}\left[k_1^2+k_2^2+\frac{1}{1-\nu}k_3^2\right] \tag{4.7}$$

where U is the work done by the external loads, V is the strain energy, and k_1, k_2 and k_3 are, respectively, the Modes I, II, and III stress intensity factor defined by (3.4.1).

Referring now to Figure 3, let δ_j be the relative crack surface displacements and rotations corresponding to the resultants, f_i (i=1,...,5) defined by

$$\begin{aligned}\left\{f_i\right\}^T &=\left\{N_{11},M_{11},V_1,N_{12},M_{12}\right\}\\ &=\left\{EhcF_1,\ Ech^2F_2,\ \frac{5Eh\sqrt{c}}{12\left(1+\nu\right)}F_3,\ EhF_4,\ Eh^2F_5\right\}\ (i=1,\ldots,5)\end{aligned} \tag{4.8}$$

$$\left\{\delta_i\right\}^T=\left\{u_1^+-u_1^-,\ \beta_1^+-\beta_1^-,\ W^+-W^-,\ u_2^+-u_2^-,\ \beta_2^+-\beta_2^-\right\}\ (i=1,\ldots,5) \tag{4.9}$$

Also, let $d\delta_i$ be the change in δ_i (i=1,...,5) as the crack length increases from $l+dl$ under "fixed load" conditions. From Figure 3 it may then be seen that the changes in U and V may be expressed as

$$dU=\sum_{j=1}^{5}F_i\,d\delta_i\ , \tag{4.10}$$

$$dV=\sum_{j=1}^{5}\left[\frac{1}{2}F_i\left(\delta_i+d\delta_i\right)-\frac{1}{2}F_i\delta_i\right]=\frac{1}{2}\sum_{j=1}^{5}F_i\,d\delta_i \tag{4.11}$$

giving the energy available for crack growth dl as

$$d(U-V)=\frac{1}{2}\sum_{i=1}^{5}F_i\,d\delta_i\ . \tag{4.12}$$

By observing that under constant loads,

$$d\delta_i = \frac{\partial \delta_i}{\partial l} dl \,, \quad (i = 1,\ldots,5) \,, \tag{4.13}$$

from (4.7), (4.12) and (4.13), it follows that

$$G = \frac{\partial}{\partial l}(U - V) = \frac{1}{2}\sum_{i=1}^{5} F_i \frac{\partial \delta_i}{\partial l} \,, \tag{4.14}$$

and

$$\frac{1}{2}\sum_{i=1}^{5} F_i \frac{\partial \delta_i}{\partial l} = \frac{\pi(1-\nu)}{E}\left[k_1^2 + k_2^2 + \frac{1}{1-\nu}k_3^2\right] \tag{4.15}$$

It will be now assumed that the plane edge crack problem under (uniform) resultants f_i away from the crack region shown in Figure 3 has been solved and the stress intensity factors are known as functions of l/h. Defining the stress amplitudes in the shell by

$$\begin{aligned}\{\sigma_i\}^T &= \left\{\frac{N_{11}}{h}, \frac{6M_{11}}{h^2}, \frac{3V_1}{2h}, \frac{N_{12}}{h}, \frac{6M_{12}}{h^2}\right\} \\ &= \left\{\frac{f_1}{h}, \frac{6f_2}{h^2}, \frac{3f_3}{2h}, \frac{f_4}{h}, \frac{6f_5}{h^2}\right\}, \quad (i = 1,\ldots,5)\end{aligned} \tag{4.16}$$

we express the stress intensity factors as

$$k_1 = \sqrt{h}\left[\sigma_1 p_1(\xi) + \sigma_2 p_2(\xi)\right] \,, \tag{4.17}$$

$$k_2 = \sqrt{h}\left[\sigma_3 p_3(\xi)\right] \,, \tag{4.18}$$

$$k_3 = \sqrt{h}\left[\sigma_4 p_4(\xi) + \sigma_5 p_5(\xi)\right] \tag{4.19}$$

where $\xi = l/h$ and p_i (i=1,...,5) are known functions given in Appendix E. From (4.7) and (3.4.1) it is seen that

$$G=\frac{\pi h(1-\nu^2)}{E}\Big[\sigma_1^2p_1^2+2\sigma_1\sigma_2p_1p_2+\sigma_2^2p_2^2+\sigma_3^2p_3^2+\frac{1}{1-\nu}\left(\sigma_4^2p_4^2+2\sigma_4\sigma_5p_4p_5+\sigma_5^2p_5^2\right)\Big]$$
$$=\{\sigma\}^T[P]\{\sigma\} \tag{4.20}$$

The matrix $\{\sigma\}$ is given by (4.16) and the square matrix $[P]$ is defined by

$$[P]=\frac{\pi h(1-\nu^2)}{E}\begin{bmatrix} p_1^2 & p_1p_2 & 0 & 0 & 0 \\ p_1p_2 & p_2^2 & 0 & 0 & 0 \\ 0 & 0 & p_3^2 & 0 & 0 \\ 0 & 0 & 0 & p_4^2/(1-\nu) & p_4p_5/(1-\nu) \\ 0 & 0 & 0 & p_4p_5/(1-\nu) & p_5^2/(1-\nu) \end{bmatrix} \tag{4.21}$$

In terms of the matrices $\{\delta\}$ and $\{\sigma\}$ defined by (4.9) and (4.16) from (4.14), G may also be expressed as

$$G=\frac{1}{2}\{f\}^T\frac{\partial}{\partial l}\{\delta\}=\{\sigma\}^T\frac{1}{2}[d]\frac{\partial}{\partial l}\{\delta\} \tag{4.22}$$

where the diagonal matrix $[d]$ is given by

$$[d]=diag\left[h,h^2/6,2h/3,h,h^2/6\right] \tag{4.23}$$

From (4.20) and (4.22) it now follows that

$$\frac{1}{2}[d]\frac{\partial}{\partial l}\{\delta\}=[P]\{\sigma\} \tag{4.24}$$

By observing that $[C]$ is constant, $\{\delta\}=0$ for $l=0$, $[P]$ is a function of l and $\{\sigma\}$ is independent of l, from (4.24), following expression can be obtained

$$\frac{1}{2}[c]\{\delta\}=\left(\int_0^l[P]dl\right)\{\sigma\}=h\left(\int_0^\xi[P(\xi)]d\xi\right)\{\sigma\} \tag{4.25}$$

From (4.21), if the following matrix is defined

$$[A]=[\alpha_{ij}]=\frac{E}{\pi h(1-\nu^2)}\int_0^{\xi}[P(\xi)]\,d\xi \tag{4.26}$$

$$\alpha_{ij}=\int_0^{\xi}p_i p_j\,d\xi\ ,\quad (i,j=1,2)\ \ and\ \ (i=j=3) \tag{4.27}$$

$$\alpha_{ij}=\int_0^{\xi}p_i p_j\,d\xi\ ,\quad (i,j=4,5) \tag{4.28}$$

equation (4.25) becomes

$$\frac{E}{\pi h^2(1-\nu^2)}[A]^{-1}\frac{1}{2}[d]\{\delta\}=\{\sigma\} \tag{4.29}$$

which, considering the definitions of $\{\sigma\}$ and $\{F\}$ given by (4.16) and (4.1) and $\{\delta\}$ and $\{G\}$ given by (4.9) and (3.1.58)-(3.1.62) provides the needed relationship between $\{F\}$ and $\{G\}$.

Equation (4.29) has the information that is needed for substitution into integral equations of the form of (4.2)-(4.6). First it must be non-dimensionalized. This is done according to the definitions in Appendix A.

Since the crack lies in a principal plane of curvature of the shell, the crack opening displacements and rotations become,

$$\delta_1=2\left|\mu_1\right|\ ,\ \delta_2=2\left|\beta_1\right|\ ,\ \delta_3=2\left|W\right|\ ,\ \delta_4=2\left|\mu_2\right|\ ,\ \delta_5=2\left|\beta_2\right| \tag{4.30}$$

Then, the final non-dimensional result is obtained as

$$F_1=\frac{1}{\pi c^{3/2}(1-\nu^2)}\left(\gamma_{11}\frac{a}{h}u+\gamma_{12}\frac{1}{6}\beta_x\right), \tag{4.31}$$

$$F_2 = \frac{1}{6\pi c^{3/2}(1-\nu^2)}\left(\gamma_{21}\frac{a}{h}u + \gamma_{22}\frac{1}{6}\beta_x\right), \tag{4.32}$$

$$F_3 = \frac{16}{15\pi\sqrt{c}(1-\nu^2)}\ \gamma_{33}\frac{a}{h}w\ , \tag{4.33}$$

$$F_4 = \frac{\sqrt{c}}{\pi(1-\nu^2)}\left(\gamma_{44}\frac{a}{h}v + \gamma_{45}\frac{1}{6}\beta_y\right), \tag{4.34}$$

$$F_5 = \frac{\sqrt{c}}{6\pi(1-\nu^2)}\left(\gamma_{54}\frac{a}{h}v + \gamma_{55}\frac{1}{6}\beta_y\right) \tag{4.35}$$

where

$$\gamma_{11} = \frac{\alpha_{22}}{\Delta_1},\ \gamma_{12} = \gamma_{21} = -\frac{\alpha_{12}}{\Delta_1},\ \gamma_{22} = \frac{\alpha_{11}}{\Delta_1},\ \gamma_{33} = -\frac{1}{\alpha_{33}},\ \gamma_{44} = \frac{\alpha_{55}}{\Delta_2},$$
$$\gamma_{45} = \gamma_{54} = -\frac{\alpha_{45}}{\Delta_2},\ \gamma_{55} = \frac{\alpha_{44}}{\Delta_2},\ \Delta_1 = \alpha_{11}\alpha_{22} - \alpha_{12}^2,\ \Delta_2 = \alpha_{44}\alpha_{55} - \alpha_{45}^2 \tag{4.36}$$

If the crack opening displacements and the rotations are expressed in terms of G_j (j=1,...,5) and using (4.31)-(4.35), the final form of the system of integral equations are obtained as

$$\int_{-\sqrt{c}}^{+\sqrt{c}} \frac{G_1(t)}{t-y}\,dt + \sum_{j=1}^{5}\int_{-\sqrt{c}}^{+\sqrt{c}} k_{1j}(y,t)G_j(t)\,dt + \frac{4}{c^{3/2}(1-\nu^2)}\left[\gamma_{11}\frac{a}{h}\int_{-\sqrt{c}}^{y} G_1(t)\,dt + \gamma_{12}\frac{1}{6}\int_{-\sqrt{c}}^{y} G_2(t)\,dt\right] = 4\pi F_{10}(y)\ ,\quad -\sqrt{c} < y < \sqrt{c} \tag{4.37}$$

$$\frac{(1-\nu^2)}{\lambda^4}\int_{-\sqrt{c}}^{+\sqrt{c}} \frac{G_2(t)}{t-y}\,dt + \sum_{j=1}^{5}\int_{-\sqrt{c}}^{+\sqrt{c}} k_{2j}(y,t)G_j(t)\,dt + \frac{2}{3c^{3/2}(1-\nu^2)}\left[\gamma_{21}\frac{a}{h}\int_{-\sqrt{c}}^{y} G_1(t)\,dt + \gamma_{22}\frac{1}{6}\frac{h}{a}\int_{-\sqrt{c}}^{y} G_2(t)\,dt\right] = 4\pi\frac{h}{a}F_{20}(y)\ ,\quad -\sqrt{c} < y < \sqrt{c} \tag{4.38}$$

$$\int_{-\sqrt{c}}^{+\sqrt{c}} \frac{G_3(t)}{t-y}\,dt+\sum_{j=1}^{5}\int_{-\sqrt{c}}^{+\sqrt{c}} k_{3j}(y,t)G_j(t)\,dt+\frac{10}{27\sqrt{c}(1-\nu)}\left[\gamma_{33}\frac{a}{h}\int_{-\sqrt{c}}^{y} G_3(t)\,dt\right]=$$
$$2\pi F_{30}(y)\ ,\quad -\sqrt{c}<y<\sqrt{c} \tag{4.39}$$

$$\int_{-\sqrt{c}}^{+\sqrt{c}} \frac{G_4(t)}{t-y}\,dt+\sum_{j=1}^{5}\int_{-\sqrt{c}}^{+\sqrt{c}} k_{4j}(y,t)G_j(t)\,dt+\frac{4\sqrt{c}}{(1-\nu^2)}\left[\gamma_{44}\frac{a}{h}\int_{-\sqrt{c}}^{y} G_4(t)\,dt+\right.$$
$$\left.\gamma_{44}\frac{a}{h}\int_{-\sqrt{c}}^{y}\left(\frac{\lambda_2}{\lambda}\right)^2 tG_3(t)\,dt+\gamma_{45}\frac{1}{6}\int_{-\sqrt{c}}^{y} G_5(t)\,dt\right]=4\pi F_{40}(y)\ ,\quad -\sqrt{c}<y<\sqrt{c} \tag{4.40}$$

$$\frac{(1-\nu^2)}{\lambda^4}\int_{-\sqrt{c}}^{+\sqrt{c}} \frac{G_5(t)}{t-y}\,dt+\sum_{j=1}^{5}\int_{-\sqrt{c}}^{+\sqrt{c}} k_{5j}(y,t)G_j(t)\,dt+\frac{2\sqrt{c}}{3(1-\nu^2)}\left[\gamma_{54}\int_{-\sqrt{c}}^{y} G_4(t)\,dt+\right.$$
$$\left.\gamma_{54}\int_{-\sqrt{c}}^{y}\left(\frac{\lambda_2}{\lambda}\right)^2 t\,G_3(t)\,dt+\gamma_{55}\frac{1}{6}\frac{h}{a}\int_{-\sqrt{c}}^{y} G_5(t)\,dt\right]=4\pi\frac{h}{a}F_{50}(y)\ ,\quad -\sqrt{c}<y<\sqrt{c} \tag{4.41}$$

where the Fredholm kernels k_{ij} (i,j=1,...,5) are given in Appendix C.

After normalizing the interval $(-\sqrt{c},\sqrt{c})$ and by using the numerical solution method given in Section 3.2, the singular integral equation (4.37) through (4.41) are solved for G_j (j=1,...,5).Then the crack surface displacements and rotations are evaluated as follows:

$$u(+0,y)=\int_{-\sqrt{c}}^{y} G_1(t)\,dt\ ,$$
$$\beta_x(+0,y)=\int_{-\sqrt{c}}^{y} G_2(t)\,dt\ ,$$
$$w(+0,y)=\int_{-\sqrt{c}}^{y} G_3(t)\,dt\ ,$$
$$v(+0,y)=\int_{-\sqrt{c}}^{y}\left[G_4(t)+\left(\frac{\lambda_2}{\lambda}\right)^2 tG_3(t)\right]dt\ ,$$
$$\beta_y(+0,y)=\int_{-\sqrt{c}}^{y} G_5(t)\,dt \tag{4.42}$$

By using (4.16), (4.1) and (4.31)-(4.35), σ_j (j=1,...,5) can be written as

$$\sigma_1 = \frac{E}{\pi\sqrt{c}(1-\nu^2)}\left(\gamma_{11}\frac{a}{h}u + \gamma_{12}\frac{1}{6}\beta_x\right),$$
$$\sigma_2 = \frac{E}{\pi\sqrt{c}(1-\nu^2)}\left(\gamma_{21}\frac{a}{h}u + \gamma_{22}\frac{1}{6}\beta_x\right),$$
$$\sigma_3 = \frac{2E}{3\pi(1-\nu^2)}\gamma_{33}\frac{a}{h}w,$$
$$\sigma_4 = \frac{\sqrt{c}E}{\pi(1-\nu^2)}\left(\gamma_{44}\frac{a}{h}v + \gamma_{45}\frac{1}{6}\beta_y\right),$$
$$\sigma_5 = \frac{\sqrt{c}E}{\pi(1-\nu^2)}\left(\gamma_{54}\frac{a}{h}v + \gamma_{55}\frac{1}{6}\beta_y\right) \qquad (4.43)$$

The stress intensity factors k_1, k_2 and k_3 may then be obtained by substituting from (4.42) and (4.43) into (4.17)-(4.19).

In the solution of singular integral equations (4.37)-(4.41), the input functions F_{j0} (j=1,...,5) are the same ones given in (3.4.19). Even though $l(X_2) = l\left(ay/\sqrt{c}\right)$ describing the crack shape can be any single-valued function, the problem is solved only for a semi-elliptic surface crack given by

$$l(X_2) = l_0\sqrt{1 - X_2^2 c/a^2}, \quad -a < X_2 < a \qquad (4.44)$$

The normalizing stress intensity factors are obtained from the solution of the corresponding edge cracked strip shown in Figure 4. Under the same specified perturbation load as for the shell. The normalizing stress intensity factor k_{1m}, k_{1b}, k_{2v}, k_{3s} and k_{3t} are corresponding value for the plane strain problem, under membrane loading N_{11}^{∞}, bending moment M_{11}^{∞}, out-of plane shear V_1^{∞}, in-plane shear N_{12}^{∞} and twisting moment M_{12}^{∞}, respectively, are defined as follows

$$
\begin{aligned}
k_{1m} &= \sigma_1^{\infty}\sqrt{h}p_1(\xi_0)\ , \\
k_{1b} &= \sigma_2^{\infty}\sqrt{h}p_2(\xi_0)\ , \\
k_{2v} &= \sigma_3^{\infty}\sqrt{h}p_3(\xi_0)\ , \\
k_{3s} &= \sigma_4^{\infty}\sqrt{h}p_4(\xi_0)\ , \\
k_{3t} &= \sigma_5^{\infty}\sqrt{h}p_5(\xi_0)\ , \quad \xi_0 = l_0/h
\end{aligned}
\tag{4.45}
$$

where σ_i^{∞} (i=1,...,5) are the stress resultants as given in Appendix A.

The normalized stress intensity factors are calculated at the maximum penetration point of a semi-elliptic inner or outer surface crack in the shell for various combination of R/h, a/h, l_0/h and l/a which are the characteristic dimensionless length parameters of the shell. In all calculations given in this part, it is assumed that the Poisson's ratio ν is 0.3 and the material is isotropic. In addition to this, the effect of material orthotropy and Poisson's ratio on the normalized stress intensity factors is investigated.

Results are presented to emphasize the effect of crack length (a/h), crack depth (l_0/h) and shell curvature (R/h) on the stress intensity factor. Variation of the stress intensity factors is plotted against distance from the fixed end (l/a). First the stress intensity factors for different crack depths (l_0/h) at fixed crack length (a/h=1) and shell curvature (R/h=5) are plotted in Figures 14 through 19. In Figures 20 through 24, variation of the stress intensity factors with crack length (a/h) for fixed crack depth (l_0/h=0.2) and shell curvature (R/h=5) are plotted.

As $l/a \to \infty$, the normalized stress intensity factors are in excellent agreement with the results given for infinite cylinder in [19], [20]. The results given in Tables 16 through 55, it is clear that the part-through crack results are not very sensitive to shell curvature. Consequently, the difference between the stress intensity factors for the crack located inner and outside the shell is not significant.

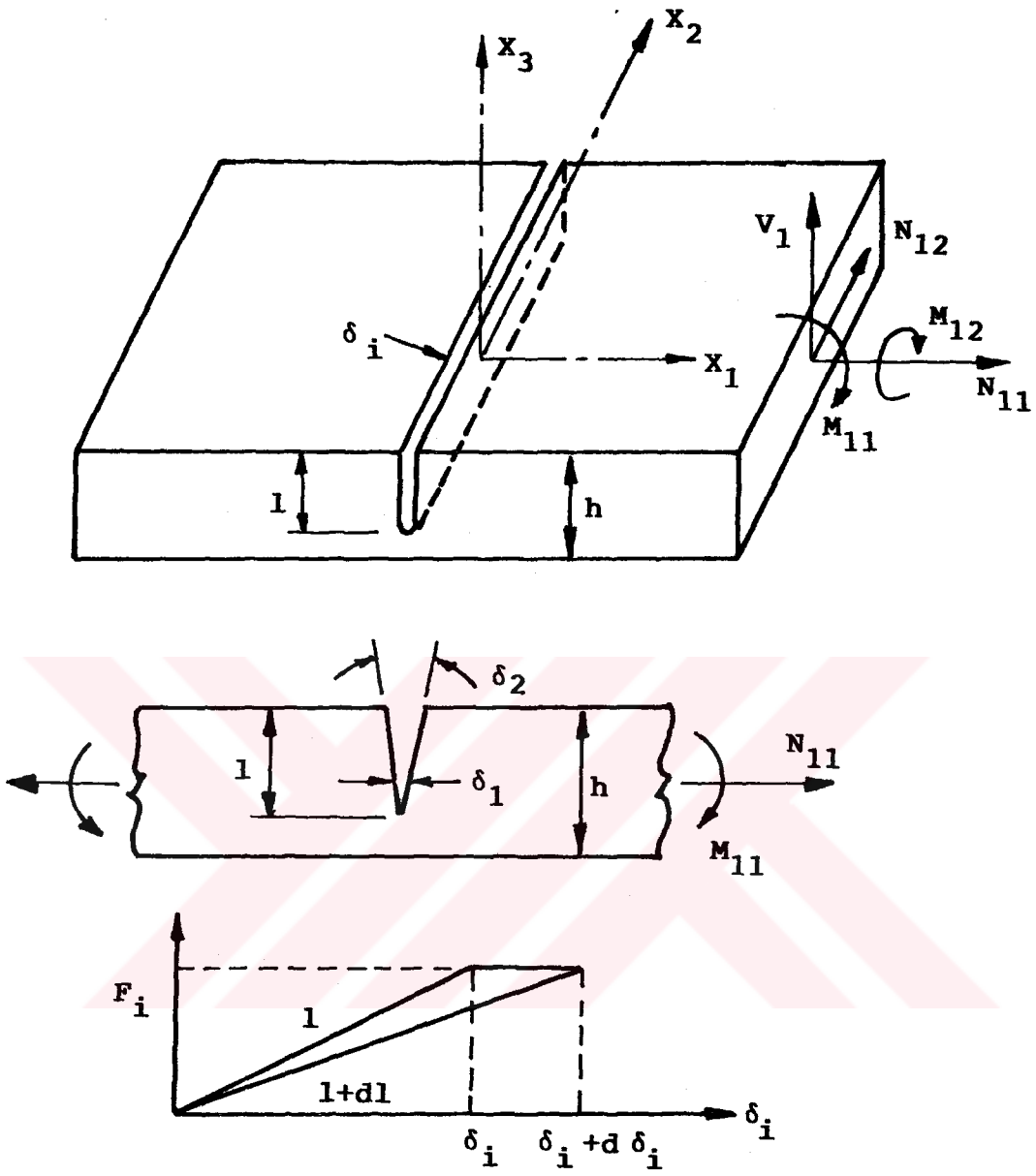

Figure 4. Development of the Line-Spring Model for a Part-Through Crack

Tables 16 through 23 show some sample results for a cylindrical shell subjected to uniform membrane loading, N_{11}^{∞} away from the crack region. The value of normalized stress intensity factor k_1/k_{1m} increases with increasing R/h and decreasing a/h ratios for all crack depths. As seen in this figure, for l_0/h=0.2 and R/h=5 at small a/h values, while crack approaches to the fixed end, an increase in the normalized stress intensity factor can be observed.

If the uniform bending moment M_{11}^{∞} is applied to the shell away from the crack region, the normalized stress intensity factor k_1/k_{1b} increases with increasing R/h and decreasing a/h ratios for all l_0/h values as seen in Tables 24 through 31. As in the case of uniform membrane loading, when crack approaches to the fixed end there seems an increase in the normalized stress intensity factor for small a/h values, and R/h=5 and l_0/h=0.2.

In Tables 27 through 31, for small crack length, a/h=1, the normalized stress intensity factor k_1/k_{1b} changes sign as crack gets deeper. Needless to say, when the stress intensity factor becomes negative, the problem is no longer a simple crack problem and must be treated as a crack-contact problem. In such a case the solution given in this thesis is, of course, not valid. The crack contact problem is highly nonlinear in which the additional unknown function $l(y)$ has to be determined by using the following condition

$$k_1 = \sqrt{h}\left[\sigma_1 p_1(\xi) + \sigma_2 p_2(\xi)\right] = 0 \qquad (4.46)$$

Even though the problem can be solved by a complicated iterative scheme, quite clearly it has no practical value. From a viewpoint of structural failure, the important problems in practice are those of crack opening not crack closing.

Unlike the mode I problem, the three-dimensional modes II and III crack problems are always coupled. For example, in a plate containing a surface crack of finite length $2a$ and a constant depth l_0 and subjected to in-plane shear loading N_{12}^{∞}, even though the primary mode of deformation along the crack front X_3=constant is mode III and X_2=constant mode II, X_2 X_3 being the plane of the crack, the stress intensity factors corresponding to the secondary modes (k_2 along X_3=constant k_3 and along X_2=constant) are not zero. Similarly, for a semi-elliptic surface crack the primary stress intensity factor would be k_3 in the central portion of the crack and k_2

near the ends. It is in the nature of the line-spring model that the "stress intensity factors" k_2 and k_3 are introduced into the model in the X_2 X_3-plane, X_1 being the coordinate perpendicular to the plane of the crack. On the other hand, the conventional definition of the stress intensity factors refers to the local coordinate system X_1', X_2', X_3'at the crack front with $X_1'=X_1$ and X_2' and X_3'being, respectively, tangent and normal to the crack front. Thus, the physically relevant stress intensity factors k_1', k_2', and k_3' may be expressed in terms of k_1, k_2 and k_3 given by line-spring model

$$\begin{aligned} k_1' &= k_1 \\ k_2' &= k_2 \cos\theta - k_3 \sin\theta \\ k_3' &= k_2 \sin\theta + k_3 \cos\theta \end{aligned} \tag{4.47}$$

where θ is the angle between X_3, the normal to the shell and X_3' the normal to the crack front. Since the line-spring model is most accurate in the center of the crack, the normalized stress intensity factors are calculated for the deepest penetration point of the crack (i.e. θ=0°)

Tables 32 through 39 show some example results for a cylindrical shell subjected to vertical shear loading V_1^{∞}. The normalized stress intensity factor for the vertical shear are nearly insensitive to R/h and a/h ratios. As crack approaches to the fixed end, the normalized stress intensity factor k_2/k_{2_v} first increases and then decreases slightly for all a/h ratios at l_0/h=0.2 and R/h=5 as seen in Figure 22.

If the shell under the effect of in-plane shear N_{12}^{∞}, the normalized stress intensity factor k_3/k_{3_s} increases with increasing R/h and a/h ratios for all crack depth values as given in Tables 40 through 47. As crack approaches to the fixed end, a small decrease in the normalized stress intensity factor is observed for different a/h values for l_0/h=0.2 and R/h=5 in Figure 23.

Tables 48 through 55 show the effect of loading of twisting moment on the normalized stress intensity factor. The normalized stress intensity factor k_3/k_{3_t} decreases, as crack approaches to the fixed end for all a/h ratios at l_0/h=0.2 and R/h=5.

Some physical explanation of sign reversal in mode III stress intensity factor k_3 in the cylindrical shell with relatively deep surface cracks under twisting moment is needed (Tables 48 through 55 and Figure 19). Theoretically the problem is a three-dimensional part-through crack problem in which the crack surface traction

$$\sigma_{12}(0,X_2,X_3)=\frac{6M_{12}}{h^2}\frac{X_3}{(h/2)} \quad , \quad |X_2|<a$$
$$[(h/2)-l]<X_3<(h/2) \tag{4.48}$$

is the only external load. Thus in shallow crack the negative shear tractions for $X_3>0$ would dominate giving $k_3(0)>0$. Also, since part of the effect of the shear tractions σ_{12} is balanced by the uncracked portion of the shell $\{X_1=0, |X_2|>0, [(h/2)-l]<X_3<(h/2)\}$, $k_3(0)$ would be less than k_{3t} which is obtained from the anti-plane shear solution with $a\to\infty$. However, for very deep cracks, $l>(h/2)$, the shear traction σ_{12} for $X_3>0$ would be balanced by the uncracked part of the shell, $|X_2|>a$ to a much greater extent than for $X_3<0$ and consequently the influence of the tractions $\sigma_{12}(0,X_2,X_3)$ for $X_3<0$ on the deformation behavior along the crack front near $X_2=0$ would be more dominant. Since $\sigma_{12}>0$ for $X_3<0$, the resulting mode III stress intensity factor would become negative.

For the five possible loading conditions, the influence of Poisson's ratio on the normalized stress intensity factors is given for a geometry of a/h=1 and R/h=5 in Table 56. As in the case of through crack, the effect of ν (varying between 0. and 0.5) on the normalized stress intensity factors is found to be insignificant.

The effect of material orthotropy on the normalized stress intensity factors in a cylindrical shell under five possible loading is given in Table 57. The table shows that the deviation from isotropic results can be considerable.

CHAPTER V

CONCLUSION

In this study, the effect of fixed end on stress intensity factors for a cylindrical shell containing a circumferential through and part-through crack are determined. In the formulation of the problem, the line-spring model is used.The problem is reduced to five simultaneous singular integral equations, and then solved numerically by using Gauss-Chebyshev integration formulas. Normalized stress intensity factors are obtained for five different loading conditions, The results of this work can be summarized as follows ;

- In the through crack problem, under each loading condition (except transverse loading) only one of the stress intensity factors is important, the others are relatively insignificant.

- As crack approaches to the fixed end, considerable increase in the stress intensity factors k_{mm} can be observed for all a/h ratios. Effect of fixed end on the stress intensity factor k_{bb} is significant for small a/h ratios and relatively small as crack length decreases. Influence of the fixed end on the stress intensity factors k_{ss}, k_{vv} and k_{tt} is relatively small.

- The stress intensity factors k_{mm} and k_{ss} increase and k_{bb} decrease with an increase in the h/R and/or a/h ratios. The stress intensity factor k_{vv} decreases with an increase in the h/R ratio regardless of distance from the fixed end. The stress intensity factor k_{tt} is nearly independent of the orientation of the crack and h/R ratio.

- Whereas, in the part through crack problem, the influence of fixed end on mode I stress intensity factors k_1 / k_{1m} and k_1 / k_{1b} is significant, while mode II and III stress intensity factors k_2 / k_{2v}, k_3 / k_{3s} and k_3 / k_{3t} have nearly the same stress intensity factor values as infinitely long cylinders. Therefore, it can be concluded

that the influence of fixed end on Mode II and mode III stress intensity factors is negligible.

- Stress intensity factor for part-through crack are not very sensitive to shell curvature. Consequently, the difference in the stress intensity factors for the crack located inside and outside of the shell are not significant.

- The line-spring model used in the formulation of part-through problem is based on two assumptions. The first involves replacing the net ligament by resultant forces which are functions of X_2 only. The second assumption is that the stress intensity factors along the crack front may be obtained from these resultant forces as though the stress state were one of plane strain. The restriction at the ends of the crack and the crack front curvature, both against this assumption. Since the model is most accurate at the center of the crack, results obtained are best applied to the problems where failure occurs when the surface crack grows through the thickness leading either to leaking or to the development of a through crack which then grows in length to critical size.

- It is shown that the ortothropy of the material has a significant effect on the stress intensity factors.

- The effect of Poisson's ratio on the stress intensity factors does not seem to be very significant.

- It should be emphasized that all solutions presented in this study correspond to the perturbation problem, where constant loading along the length of the crack has been assumed. To make use of the results, the solution to the uncracked shell must first be obtained along the plane of the crack, Then superposition principles apply.

- For the problem of crack touching the fixed end, it is not possible to obtain a solution by current method, because of the change in boundary conditions on crack surfaces. This is a different problem by itself.

- For a future study, the problem of arbitrarily oriented crack with a fixed end can be solved for five possible loadings, which is the general case.

Table 1. Stress Intensity Factor Ratios In An Isotropic Cylindrical Shell With A Fixed End Containing A Circumferential Through Crack Under Uniform Membrane Loading N_{11}; $\nu = 0.3$

k_{mm}

		l/a							
a/h	R/h	0.25	0.4	0.5	1.0	1.5	2.5	5.0	50.
	5	2.455	1.867	1.670	1.282	1.164	1.089	1.052	1.037
	10	2.436	1.852	1.656	1.266	1.146	1.068	1.032	1.018
1	15	2.431	1.849	1.652	1.262	1.141	1.063	1.025	1.012
	25	2.429	1.847	1.651	1.259	1.138	1.059	1.020	1.007
	50	2.428	1.846	1.650	1.258	1.137	1.056	1.017	1.003
	100	2.428	1.846	1.650	1.258	1.136	1.056	1.015	1.001
	5	2.563	1.974	1.778	1.392	1.274	1.193	1.148	1.125
	10	2.473	1.892	1.697	1.313	1.198	1.123	1.084	1.066
2	15	2.451	1.870	1.674	1.289	1.172	1.098	1.061	1.045
	25	2.437	1.856	1.660	1.272	1.154	1.078	1.042	1.028
	50	2.430	1.849	1.653	1.262	1.142	1.064	1.027	1.014
	100	2.428	1.847	1.650	1.259	1.138	1.058	1.020	1.007
	5	2.778	2.171	1.969	1.564	1.432	1.332	1.270	1.237
	10	2.567	1.982	1.787	1.403	1.286	1.205	1.158	1.134
3	15	2.503	1.923	1.728	1.347	1.232	1.156	1.114	1.094
	25	2.461	1.881	1.686	1.303	1.188	1.114	1.076	1.059
	50	2.438	1.857	1.661	1.274	1.156	1.081	1.045	1.030
	100	2.431	1.849	1.653	1.263	1.143	1.065	1.029	1.015
	5	3.412	2.736	2.505	2.000	1.805	1.645	1.538	1.477
	10	2.900	2.285	2.079	1.663	1.520	1.407	1.337	1.298
5	15	2.719	2.124	1.925	1.531	1.404	1.308	1.250	1.219
	25	2.575	1.993	1.798	1.416	1.299	1.217	1.169	1.144
	50	2.479	1.901	1.707	1.326	1.212	1.137	1.097	1.078
	100	2.444	1.864	1.669	1.283	1.167	1.093	1.057	1.041
	5	5.792	4.740	4.319	3.282	2.848	2.459	2.171	1.990
	10	4.234	3.462	3.179	2.500	2.219	1.977	1.807	1.705
10	15	3.663	2.968	2.725	2.172	1.950	1.764	1.637	1.562
	25	3.174	2.534	2.319	1.862	1.691	1.552	1.460	1.409
	50	2.773	2.177	1.977	1.579	1.447	1.346	1.283	1.249
	100	2.567	1.987	1.793	1.413	1.297	1.215	1.167	1.143

Table 2. Stress Intensity Factor Ratios In An Isotropic Cylindrical Shell With A Fixed End Containing A Circumferential Through Crack Under Uniform Membrane Loading N_{11} ; $\nu = 0.3$

k_{bm}

		l/a							
a/h	R/h	0.25	0.4	0.5	1.0	1.5	2.5	5.0	50.
	5	0.192	0.132	0.121	0.105	0.098	0.088	0.080	0.076
	10	0.107	0.073	0.068	0.063	0.063	0.060	0.055	0.052
1	15	0.074	0.050	0.047	0.045	0.046	0.046	0.043	0.040
	25	0.045	0.031	0.029	0.028	0.029	0.031	0.030	0.028
	50	0.023	0.016	0.015	0.015	0.016	0.017	0.018	0.017
	100	0.012	0.008	0.007	0.007	0.008	0.009	0.010	0.010
	5	0.285	0.229	0.208	0.160	0.141	0.126	0.117	0.112
	10	0.205	0.177	0.167	0.142	0.128	0.113	0.103	0.099
2	15	0.151	0.135	0.130	0.118	0.109	0.097	0.088	0.085
	25	0.098	0.089	0.087	0.085	0.082	0.076	0.069	0.065
	50	0.051	0.047	0.047	0.048	0.050	0.049	0.046	0.043
	100	0.026	0.024	0.024	0.026	0.027	0.029	0.029	0.026
	5	0.225	0.160	0.141	0.118	0.111	0.101	0.094	0.090
	10	0.285	0.232	0.211	0.163	0.144	0.129	0.120	0.115
3	15	0.244	0.210	0.197	0.160	0.141	0.125	0.116	0.111
	25	0.175	0.159	0.153	0.135	0.123	0.109	0.100	0.096
	50	0.099	0.093	0.092	0.090	0.087	0.080	0.072	0.069
	100	0.052	0.050	0.050	0.052	0.053	0.053	0.048	0.045
	5	-0.399	-0.297	-0.237	-0.096	-0.064	-0.048	-0.042	-0.042
	10	0.141	0.086	0.078	0.085	0.084	0.078	0.073	0.069
5	15	0.268	0.197	0.174	0.139	0.128	0.116	0.108	0.104
	25	0.290	0.237	0.216	0.168	0.149	0.133	0.124	0.119
	50	0.211	0.191	0.182	0.154	0.138	0.121	0.112	0.108
	100	0.124	0.118	0.117	0.111	0.104	0.094	0.085	0.081
	5	-2.892	-1.861	-1.511	-0.837	-0.625	-0.477	-0.396	-0.359
	10	-1.296	-0.876	-0.703	-0.373	-0.280	-0.222	-0.193	-0.182
10	15	-0.649	-0.465	-0.371	-0.174	-0.126	-0.098	-0.087	-0.083
	25	-0.096	-0.092	-0.069	0.005	0.018	0.022	0.021	0.019
	50	0.259	0.184	0.163	0.136	0.126	0.114	0.107	0.102
	100	0.294	0.245	0.225	0.175	0.155	0.138	0.129	0.124

Table 3. Stress Intensity Factor Ratios In An Isotropic Cylindrical Shell With A Fixed End Containing A Circumferential Through Crack Under Uniform Bending Moment M_{11}; $\nu = 0.3$

k_{mb}

		l/a							
a/h	R/h	0.25	0.4	0.5	1.0	1.5	2.5	5.0	50.
	5	0.086	0.042	0.038	0.032	0.030	0.027	0.025	0.024
	10	0.047	0.023	0.021	0.019	0.019	0.018	0.017	0.016
1	15	0.032	0.016	0.014	0.013	0.014	0.014	0.013	0.012
	25	0.019	0.010	0.009	0.008	0.009	0.009	0.009	0.008
	50	0.010	0.005	0.004	0.004	0.005	0.005	0.005	0.005
	100	0.005	0.002	0.002	0.002	0.002	0.003	0.003	0.003
	5	0.091	0.075	0.069	0.055	0.048	0.042	0.039	0.038
	10	0.058	0.050	0.048	0.042	0.038	0.033	0.031	0.029
2	15	0.041	0.037	0.036	0.033	0.031	0.028	0.025	0.024
	25	0.026	0.024	0.024	0.023	0.023	0.021	0.019	0.018
	50	0.014	0.013	0.013	0.013	0.014	0.013	0.012	0.012
	100	0.007	0.006	0.006	0.007	0.007	0.008	0.008	0.007
	5	0.108	0.087	0.079	0.060	0.053	0.047	0.043	0.041
	10	0.083	0.072	0.067	0.054	0.047	0.042	0.039	0.037
3	15	0.065	0.059	0.056	0.047	0.042	0.037	0.034	0.033
	25	0.044	0.041	0.041	0.037	0.034	0.030	0.027	0.026
	50	0.024	0.023	0.023	0.024	0.023	0.021	0.019	0.018
	100	0.012	0.012	0.013	0.013	0.014	0.014	0.013	0.012
	5	0.102	0.080	0.073	0.057	0.050	0.044	0.040	0.038
	10	0.104	0.084	0.076	0.059	0.052	0.046	0.042	0.040
5	15	0.096	0.081	0.074	0.057	0.050	0.045	0.041	0.040
	25	0.078	0.069	0.065	0.052	0.046	0.041	0.038	0.036
	50	0.049	0.047	0.046	0.041	0.037	0.032	0.030	0.029
	100	0.028	0.028	0.028	0.028	0.026	0.024	0.021	0.021
	5	0.071	0.059	0.055	0.043	0.038	0.033	0.029	0.027
	10	0.085	0.069	0.064	0.050	0.044	0.038	0.034	0.031
10	15	0.093	0.074	0.068	0.053	0.047	0.041	0.037	0.034
	25	0.099	0.079	0.072	0.056	0.049	0.044	0.040	0.038
	50	0.094	0.079	0.072	0.056	0.049	0.044	0.040	0.038
	100	0.071	0.065	0.061	0.050	0.044	0.039	0.036	0.034

Table 4. Stress Intensity Factor Ratios In An Isotropic Cylindrical Shell With A Fixed End Containing A Circumferential Through Crack Under Uniform Bending Moment M_{11} ; $\nu = 0.3$

k_{bb}

		l/a							
a/h	R/h	0.25	0.4	0.5	1.0	1.5	2.5	5.0	50.
	5	1.788	1.105	0.973	0.759	0.702	0.675	0.675	0.675
	10	1.874	1.146	1.012	0.804	0.748	0.714	0.707	0.707
1	15	1.895	1.156	1.022	0.817	0.765	0.731	0.719	0.720
	25	1.907	1.162	1.028	0.826	0.777	0.746	0.731	0.731
	50	1.913	1.165	1.031	0.831	0.784	0.756	0.741	0.739
	100	1.915	1.166	1.032	0.833	0.786	0.760	0.747	0.744
	5	0.952	0.733	0.663	0.541	0.527	0.530	0.530	0.529
	10	1.084	0.855	0.781	0.633	0.598	0.592	0.593	0.593
2	15	1.124	0.897	0.824	0.678	0.636	0.620	0.622	0.622
	25	1.151	0.926	0.856	0.717	0.674	0.650	0.649	0.649
	50	1.165	0.943	0.875	0.745	0.706	0.680	0.672	0.673
	100	1.169	0.948	0.881	0.756	0.721	0.698	0.686	0.686
	5	0.666	0.519	0.476	0.429	0.433	0.433	0.433	0.433
	10	0.863	0.680	0.618	0.514	0.505	0.509	0.508	0.508
3	15	0.943	0.758	0.693	0.568	0.546	0.548	0.548	0.548
	25	1.005	0.824	0.761	0.630	0.595	0.588	0.590	0.590
	50	1.043	0.870	0.811	0.689	0.650	0.629	0.630	0.630
	100	1.056	0.886	0.830	0.718	0.683	0.659	0.653	0.654
	5	0.371	0.319	0.312	0.321	0.323	0.323	0.324	0.324
	10	0.549	0.436	0.406	0.387	0.391	0.391	0.391	0.391
5	15	0.668	0.525	0.481	0.431	0.435	0.436	0.436	0.436
	25	0.800	0.639	0.584	0.493	0.488	0.492	0.491	0.491
	50	0.912	0.756	0.698	0.580	0.555	0.555	0.556	0.556
	100	0.961	0.815	0.762	0.648	0.613	0.599	0.601	0.601
	5	0.197	0.208	0.213	0.220	0.222	0.224	0.225	0.226
	10	0.252	0.246	0.251	0.261	0.263	0.265	0.265	0.266
10	15	0.309	0.280	0.280	0.292	0.293	0.294	0.295	0.295
	25	0.415	0.345	0.332	0.338	0.339	0.339	0.339	0.340
	50	0.602	0.478	0.441	0.408	0.413	0.412	0.412	0.412
	100	0.770	0.625	0.573	0.487	0.483	0.487	0.486	0.486

Table 5. Stress Intensity Factor Ratios In An Isotropic Cylindrical Shell With A Fixed End Containing A Circumferential Through Crack Under Uniform Transverse Shear Loading V_1 ; $\nu = 0.3$

k_{vv}

		l/a							
a/h	R/h	0.25	0.4	0.5	1.0	1.5	2.5	5.0	50.
	5	1.645	1.612	1.589	1.542	1.539	1.547	1.550	1.550
	10	1.727	1.705	1.685	1.643	1.635	1.634	1.637	1.637
1	15	1.744	1.724	1.706	1.666	1.658	1.655	1.657	1.657
	25	1.753	1.734	1.716	1.678	1.671	1.668	1.668	1.668
	50	1.756	1.738	1.721	1.684	1.677	1.674	1.674	1.674
	100	1.757	1.740	1.722	1.686	1.678	1.676	1.675	1.675
	5	1.720	1.628	1.601	1.613	1.646	1.653	1.652	1.652
	10	2.261	2.153	2.110	2.049	2.058	2.072	2.071	2.071
2	15	2.414	2.312	2.269	2.195	2.190	2.198	2.200	2.199
	25	2.503	2.408	2.368	2.292	2.280	2.280	2.283	2.283
	50	2.544	2.453	2.415	2.343	2.329	2.325	2.326	2.326
	100	2.555	2.465	2.427	2.357	2.344	2.339	2.338	2.339
	5	1.276	1.248	1.263	1.368	1.384	1.380	1.380	1.380
	10	2.269	2.135	2.099	2.117	2.156	2.159	2.158	2.157
3	15	2.733	2.569	2.514	2.462	2.487	2.500	2.497	2.497
	25	3.078	2.910	2.847	2.750	2.749	2.760	2.760	2.760
	50	3.262	3.100	3.039	2.931	2.914	2.913	2.915	2.915
	100	3.313	3.155	3.096	2.991	2.971	2.965	2.965	2.965
	5	0.626	0.702	0.746	0.798	0.796	0.795	0.795	0.795
	10	1.461	1.472	1.514	1.662	1.664	1.662	1.661	1.661
5	15	2.249	2.161	2.167	2.309	2.336	2.329	2.329	2.329
	25	3.332	3.112	3.057	3.081	3.129	3.130	3.127	3.127
	50	4.338	4.040	3.940	3.807	3.817	3.832	3.829	3.829
	100	4.729	4.426	4.321	4.144	4.120	4.123	4.124	4.124
	5	0.136	0.167	0.174	0.183	0.181	0.178	0.177	0.177
	10	0.335	0.406	0.427	0.438	0.437	0.435	0.434	0.434
10	15	0.557	0.650	0.694	0.727	0.725	0.724	0.724	0.723
	25	1.104	1.183	1.251	1.365	1.359	1.358	1.358	1.358
	50	2.787	2.622	2.637	2.846	2.863	2.854	2.853	2.853
	100	5.661	4.872	4.686	4.611	4.679	4.675	4.671	4.670

Table 6. Stress Intensity Factor Ratios In An Isotropic Cylindrical Shell With A Fixed End Containing A Circumferential Through Crack Under Uniform Transverse Shear Loading V_1; $\nu = 0.3$

k_{sv}

		l/a							
a/h	R/h	0.25	0.4	0.5	1.0	1.5	2.5	5.0	50.
	5	-0.184	-0.173	-0.169	-0.158	-0.155	-0.153	-0.153	-0.153
	10	-0.097	-0.092	-0.090	-0.085	-0.084	-0.082	-0.082	-0.082
1	15	-0.065	-0.062	-0.061	-0.058	-0.057	-0.056	-0.056	-0.056
	25	-0.039	-0.038	-0.037	-0.035	-0.034	-0.034	-0.034	-0.034
	50	-0.020	-0.019	-0.018	-0.018	-0.017	-0.017	-0.017	-0.017
	100	-0.010	-0.009	-0.009	-0.009	-0.009	-0.009	-0.009	-0.009
	5	-0.516	-0.464	-0.446	-0.418	-0.417	-0.418	-0.418	-0.418
	10	-0.347	-0.318	-0.306	-0.282	-0.276	-0.275	-0.275	-0.275
2	15	-0.248	-0.229	-0.222	-0.205	-0.200	-0.198	-0.198	-0.198
	25	-0.155	-0.144	-0.140	-0.130	-0.127	-0.125	-0.125	-0.125
	50	-0.079	-0.074	-0.072	-0.067	-0.066	-0.065	-0.064	-0.064
	100	-0.040	-0.037	-0.036	-0.034	-0.033	-0.033	-0.033	-0.033
	5	-0.716	-0.648	-0.631	-0.625	-0.627	-0.626	-0.627	-0.627
3	10	-0.674	-0.602	-0.577	-0.538	-0.535	-0.535	-0.535	-0.535
	15	-0.550	-0.495	-0.474	-0.434	-0.428	-0.427	-0.427	-0.427
	25	-0.375	-0.342	-0.329	-0.301	-0.294	-0.291	-0.291	-0.291
	50	-0.200	-0.184	-0.178	-0.164	-0.160	-0.158	-0.157	-0.157
	100	-0.102	-0.094	-0.091	-0.085	-0.083	-0.081	-0.081	-0.081
	5	-0.747	-0.735	-0.743	-0.749	-0.748	-0.750	-0.751	-0.751
	10	-1.023	-0.938	-0.922	-0.925	-0.923	-0.924	-0.925	-0.925
5	15	-1.105	-0.987	-0.953	-0.924	-0.924	-0.923	-0.924	-0.924
	25	-1.018	-0.901	-0.861	-0.797	-0.791	-0.791	-0.791	-0.791
	50	-0.677	-0.607	-0.580	-0.526	-0.513	-0.510	-0.510	-0.510
	100	-0.372	-0.337	-0.324	-0.296	-0.288	-0.283	-0.283	-0.283
	5	-0.681	-0.694	-0.688	-0.678	-0.679	-0.681	-0.682	-0.683
	10	-1.004	-1.040	-1.048	-1.032	-1.034	-1.037	-1.039	-1.039
10	15	-1.285	-1.295	-1.314	-1.308	-1.309	-1.313	-1.315	-1.315
	25	-1.758	-1.670	-1.675	-1.695	-1.689	-1.694	-1.696	-1.696
	50	-2.475	-2.152	-2.076	-2.034	-2.031	-2.029	-2.031	-2.031
	100	-2.638	-2.159	-2.020	-1.825	-1.810	-1.807	-1.807	-1.808

Table 7. Stress Intensity Factor Ratios In An Isotropic Cylindrical Shell With A Fixed End Containing A Circumferential Through Crack Under Uniform Transverse Shear Loading V_1; $\nu = 0.3$

k_{tv}

		l/a							
a/h	R/h	0.25	0.4	0.5	1.0	1.5	2.5	5.0	50.
	5	1.167	0.799	0.678	0.474	0.436	0.425	0.424	0.424
	10	1.228	0.849	0.724	0.511	0.469	0.454	0.453	0.452
1	15	1.240	0.859	0.734	0.519	0.477	0.462	0.459	0.459
	25	1.247	0.865	0.739	0.524	0.482	0.466	0.463	0.463
	50	1.250	0.867	0.741	0.526	0.484	0.468	0.465	0.465
	100	1.250	0.868	0.742	0.526	0.484	0.469	0.466	0.466
	5	1.414	1.084	0.986	0.860	0.856	0.854	0.851	0.851
	10	1.891	1.472	1.341	1.132	1.104	1.102	1.100	1.100
2	15	2.026	1.589	1.452	1.224	1.186	1.178	1.177	1.177
	25	2.105	1.661	1.520	1.286	1.242	1.229	1.228	1.227
	50	2.141	1.694	1.553	1.318	1.272	1.256	1.254	1.254
	100	2.151	1.703	1.562	1.327	1.282	1.265	1.262	1.262
	5	1.152	0.960	0.918	0.912	0.913	0.906	0.905	0.905
	10	2.144	1.746	1.631	1.497	1.501	1.497	1.494	1.494
3	15	2.609	2.134	1.986	1.773	1.759	1.759	1.756	1.756
	25	2.956	2.438	2.273	2.004	1.966	1.962	1.960	1.960
	50	3.141	2.608	2.438	2.151	2.098	2.083	2.082	2.082
	100	3.193	2.657	2.487	2.199	2.144	2.124	2.122	2.122
	5	0.587	0.588	0.609	0.635	0.630	0.628	0.627	0.627
	10	1.566	1.419	1.410	1.476	1.470	1.464	1.462	1.462
5	15	2.500	2.176	2.108	2.125	2.135	2.123	2.121	2.121
	25	3.789	3.227	3.067	2.913	2.930	2.922	2.918	2.918
	50	4.988	4.257	4.024	3.665	3.632	3.633	3.628	3.627
	100	5.455	4.686	4.437	4.017	3.945	3.931	3.929	3.929
	5	0.066	0.090	0.097	0.100	0.098	0.096	0.096	0.096
	10	0.342	0.383	0.401	0.403	0.400	0.398	0.398	0.398
10	15	0.704	0.737	0.772	0.790	0.784	0.782	0.781	0.781
	25	1.635	1.565	1.603	1.688	1.670	1.665	1.664	1.664
	50	4.552	3.874	3.758	3.842	3.839	3.815	3.812	3.812
	100	9.563	7.519	6.994	6.475	6.507	6.483	6.472	6.471

Table 8. Stress Intensity Factor Ratios In An Isotropic Cylindrical Shell With A Fixed End Containing A Circumferential Crack Through Under In-Plane Shear Loading N_{12};; $\nu = 0.3$

k_{vs}

		l/a							
a/h	R/h	0.25	0.4	0.5	1.0	1.5	2.5	5.0	50.
	5	0.175	0.161	0.156	0.146	0.145	0.145	0.146	0.146
	10	0.088	0.081	0.078	0.073	0.073	0.073	0.074	0.074
1	15	0.058	0.054	0.052	0.049	0.049	0.049	0.049	0.049
	25	0.035	0.032	0.031	0.029	0.029	0.030	0.030	0.030
	50	0.018	0.016	0.016	0.015	0.015	0.015	0.015	0.015
	100	0.009	0.008	0.008	0.007	0.007	0.007	0.008	0.008
	5	0.451	0.419	0.406	0.382	0.380	0.383	0.385	0.385
	10	0.226	0.210	0.204	0.194	0.193	0.193	0.194	0.194
2	15	0.151	0.141	0.137	0.130	0.130	0.130	0.130	0.131
	25	0.091	0.085	0.082	0.079	0.079	0.079	0.079	0.079
	50	0.045	0.042	0.041	0.039	0.040	0.040	0.040	0.040
	100	0.023	0.021	0.021	0.020	0.020	0.020	0.020	0.020
	5	0.828	0.767	0.743	0.700	0.699	0.704	0.707	0.708
	10	0.415	0.387	0.376	0.355	0.353	0.355	0.357	0.357
3	15	0.277	0.259	0.252	0.239	0.238	0.239	0.240	0.240
	25	0.167	0.156	0.152	0.145	0.144	0.145	0.145	0.145
	50	0.083	0.078	0.076	0.073	0.073	0.074	0.074	0.074
	100	0.042	0.039	0.038	0.037	0.037	0.038	0.038	0.038
	5	1.883	1.721	1.660	1.573	1.571	1.581	1.590	1.593
	10	0.941	0.869	0.841	0.795	0.795	0.800	0.804	0.805
5	15	0.628	0.583	0.565	0.533	0.533	0.536	0.538	0.539
	25	0.378	0.352	0.342	0.324	0.322	0.324	0.325	0.326
	50	0.189	0.177	0.172	0.165	0.164	0.164	0.165	0.165
	100	0.095	0.089	0.087	0.084	0.084	0.084	0.084	0.084
	5	9.501	7.287	6.692	5.783	5.678	5.744	5.849	5.895
	10	3.636	3.148	2.992	2.769	2.755	2.779	2.804	2.813
10	15	2.359	2.083	1.991	1.866	1.862	1.876	1.888	1.892
	25	1.404	1.257	1.205	1.133	1.133	1.140	1.146	1.148
	50	0.702	0.635	0.611	0.573	0.572	0.576	0.579	0.579
	100	0.352	0.320	0.309	0.291	0.289	0.291	0.292	0.293

Table 9. Stress Intensity Factor Ratios In An Isotropic Cylindrical Shell With A Fixed End Containing A Circumferential Through Crack Under In-Plane Shear Loading $N_{12}; \nu = 0.3$

k_{ss}

		l/a							
a/h	R/h	0.25	0.4	0.5	1.0	1.5	2.5	5.0	50.
	5	1.177	1.070	1.036	0.993	1.003	1.023	1.034	1.036
	10	1.172	1.063	1.028	0.978	0.984	1.001	1.015	1.017
1	15	1.171	1.062	1.026	0.975	0.979	0.994	1.008	1.011
	25	1.171	1.061	1.025	0.972	0.975	0.989	1.003	1.007
	50	1.170	1.061	1.024	0.971	0.973	0.986	0.998	1.003
	100	1.170	1.060	1.024	0.971	0.973	0.985	0.996	1.001
	5	1.208	1.116	1.092	1.083	1.101	1.114	1.120	1.121
	10	1.183	1.079	1.048	1.018	1.034	1.053	1.061	1.063
2	15	1.176	1.070	1.037	0.998	1.010	1.031	1.040	1.042
	25	1.173	1.065	1.030	0.983	0.992	1.011	1.023	1.026
	50	1.171	1.062	1.026	0.975	0.980	0.996	1.010	1.013
	100	1.171	1.061	1.025	0.972	0.975	0.989	1.002	1.007
	5	1.274	1.208	1.197	1.212	1.221	1.228	1.233	1.235
	10	1.207	1.117	1.093	1.089	1.108	1.120	1.125	1.126
3	15	1.190	1.091	1.063	1.044	1.063	1.080	1.086	1.087
	25	1.179	1.074	1.042	1.009	1.024	1.044	1.052	1.054
	50	1.173	1.065	1.030	0.985	0.994	1.014	1.026	1.028
	100	1.171	1.062	1.026	0.976	0.981	0.998	1.011	1.014
	5	1.516	1.509	1.516	1.507	1.501	1.506	1.511	1.514
	10	1.306	1.256	1.253	1.273	1.277	1.283	1.288	1.289
5	15	1.247	1.177	1.164	1.181	1.193	1.200	1.205	1.206
	25	1.207	1.119	1.096	1.096	1.115	1.126	1.131	1.133
	50	1.183	1.082	1.051	1.027	1.045	1.063	1.070	1.071
	100	1.175	1.068	1.034	0.993	1.005	1.026	1.035	1.037
	5	3.748	3.326	3.168	2.852	2.776	2.768	2.798	2.817
	10	1.978	1.975	1.959	1.877	1.856	1.857	1.867	1.873
10	15	1.631	1.636	1.641	1.609	1.599	1.603	1.610	1.613
	25	1.403	1.380	1.387	1.395	1.392	1.397	1.402	1.404
	50	1.262	1.198	1.189	1.210	1.219	1.225	1.230	1.231
	100	1.204	1.115	1.093	1.093	1.112	1.123	1.128	1.129

Table 10. Stress Intensity Factor Ratios In An Isotropic Cylindrical Shell With A Fixed End Containing A Circumferential Through Crack Under Uniform In-Plane Shear Loading N_{12} ; $\nu = 0.3$

k_{ts}

		l/a							
a/h	R/h	0.25	0.4	0.5	1.0	1.5	2.5	5.0	50.
	5	0.024	0.001	-0.007	-0.024	-0.029	-0.029	-0.026	-0.025
	10	0.012	0.000	-0.004	-0.014	-0.018	-0.020	-0.018	-0.017
1	15	0.008	0.000	-0.003	-0.010	-0.013	-0.015	-0.014	-0.013
	25	0.005	0.000	-0.002	-0.006	-0.008	-0.010	-0.010	-0.009
	50	0.002	0.000	-0.001	-0.003	-0.004	-0.006	-0.006	-0.006
	100	0.001	0.000	0.000	-0.002	-0.002	-0.003	-0.004	-0.003
	5	0.139	0.083	0.065	0.034	0.033	0.038	0.040	0.040
	10	0.068	0.039	0.029	0.008	0.004	0.007	0.010	0.010
2	15	0.045	0.025	0.018	0.002	-0.002	-0.001	0.002	0.002
	25	0.027	0.015	0.010	-0.001	-0.004	-0.005	-0.003	-0.002
	50	0.013	0.007	0.005	-0.001	-0.004	-0.005	-0.004	-0.003
	100	0.007	0.004	0.002	-0.001	-0.002	-0.003	-0.004	-0.003
	5	0.386	0.292	0.261	0.216	0.216	0.221	0.224	0.224
	10	0.189	0.139	0.122	0.092	0.091	0.095	0.097	0.098
3	15	0.125	0.091	0.079	0.055	0.053	0.056	0.058	0.059
	25	0.074	0.053	0.045	0.029	0.026	0.027	0.029	0.030
	50	0.037	0.026	0.022	0.012	0.009	0.009	0.010	0.011
	100	0.018	0.013	0.011	0.005	0.003	0.002	0.003	0.003
	5	1.357	1.132	1.059	0.955	0.950	0.958	0.965	0.968
	10	0.664	0.552	0.515	0.459	0.459	0.464	0.467	0.468
5	15	0.439	0.363	0.337	0.295	0.295	0.299	0.302	0.303
	25	0.261	0.214	0.197	0.168	0.167	0.171	0.173	0.173
	50	0.130	0.105	0.096	0.078	0.075	0.078	0.079	0.080
	100	0.064	0.052	0.047	0.036	0.034	0.034	0.036	0.036
	5	17.064	12.476	11.267	9.481	9.288	9.413	9.600	9.679
	10	6.335	5.274	4.947	4.477	4.447	4.490	4.533	4.548
10	15	4.074	3.462	3.267	2.998	2.986	3.011	3.032	3.040
	25	2.407	2.069	1.958	1.803	1.800	1.813	1.824	1.827
	50	1.195	1.032	0.978	0.893	0.892	0.900	0.905	0.907
	100	0.595	0.514	0.487	0.441	0.438	0.443	0.446	0.447

Table 11. Stress Intensity Factor Ratios In An Isotropic Cylindrical Shell With A Fixed End Containing A Circumferential Through Crack Under Uniform Twisting Moment M_{12} ; $\nu = 0.3$

k_{vt}

		l/a							
a/h	R/h	0.25	0.4	0.5	1.0	1.5	2.5	5.0	50.
	5	-0.164	-0.121	-0.106	-0.078	-0.073	-0.070	-0.070	-0.070
	10	-0.164	-0.121	-0.106	-0.079	-0.073	-0.071	-0.070	-0.070
1	15	-0.164	-0.121	-0.106	-0.079	-0.073	-0.071	-0.070	-0.070
	25	-0.164	-0.121	-0.106	-0.079	-0.073	-0.071	-0.070	-0.070
	50	-0.165	-0.121	-0.106	-0.079	-0.073	-0.071	-0.070	-0.070
	100	-0.165	-0.121	-0.106	-0.079	-0.073	-0.071	-0.070	-0.070
	5	-0.132	-0.113	-0.107	-0.095	-0.093	-0.092	-0.091	-0.091
	10	-0.132	-0.113	-0.107	-0.095	-0.093	-0.092	-0.092	-0.091
2	15	-0.132	-0.113	-0.107	-0.095	-0.093	-0.092	-0.092	-0.092
	25	-0.132	-0.113	-0.107	-0.096	-0.093	-0.092	-0.092	-0.092
	50	-0.132	-0.113	-0.107	-0.096	-0.093	-0.092	-0.092	-0.092
	100	-0.132	-0.113	-0.107	-0.096	-0.093	-0.092	-0.092	-0.092
	5	-0.117	-0.106	-0.102	-0.095	-0.094	-0.094	-0.093	-0.093
	10	-0.117	-0.107	-0.103	-0.096	-0.094	-0.094	-0.094	-0.094
3	15	-0.117	-0.107	-0.103	-0.096	-0.095	-0.094	-0.094	-0.094
	25	-0.118	-0.107	-0.103	-0.096	-0.095	-0.094	-0.094	-0.094
	50	-0.118	-0.107	-0.103	-0.096	-0.095	-0.094	-0.094	-0.094
	100	-0.118	-0.107	-0.103	-0.096	-0.095	-0.094	-0.094	-0.094
	5	-0.100	-0.094	-0.092	-0.089	-0.088	-0.088	-0.088	-0.088
	10	-0.100	-0.095	-0.093	-0.089	-0.089	-0.088	-0.088	-0.088
5	15	-0.101	-0.095	-0.093	-0.090	-0.089	-0.089	-0.088	-0.088
	25	-0.101	-0.095	-0.093	-0.090	-0.089	-0.089	-0.089	-0.089
	50	-0.101	-0.095	-0.094	-0.090	-0.089	-0.089	-0.089	-0.089
	100	-0.101	-0.096	-0.094	-0.090	-0.089	-0.089	-0.089	-0.089
	5	-0.094	-0.085	-0.083	-0.078	-0.078	-0.077	-0.078	-0.078
	10	-0.086	-0.082	-0.080	-0.078	-0.077	-0.077	-0.077	-0.077
10	15	-0.085	-0.082	-0.080	-0.078	-0.078	-0.078	-0.078	-0.078
	25	-0.085	-0.082	-0.081	-0.079	-0.079	-0.079	-0.078	-0.078
	50	-0.085	-0.082	-0.081	-0.079	-0.079	-0.079	-0.079	-0.079
	100	-0.085	-0.082	-0.081	-0.080	-0.079	-0.079	-0.079	-0.079

Table 12. Stress Intensity Factor Ratios In An Isotropic Cylindrical Shell With A Fixed End Containing A Circumferential Thriugh Crack Under Uniform Twisting Moment M_{12}; $\nu = 0.3$

k_{st}

		l/a							
a/h	R/h	0.25	0.4	0.5	1.0	1.5	2.5	5.0	50.
	5	-0.004	-0.005	-0.006	-0.009	-0.011	-0.011	-0.010	-0.010
	10	-0.002	-0.003	-0.003	-0.005	-0.006	-0.007	-0.006	-0.006
1	15	-0.001	-0.002	-0.002	-0.004	-0.004	-0.005	-0.005	-0.005
	25	-0.001	-0.001	-0.001	-0.002	-0.003	-0.003	-0.003	-0.003
	50	0.000	-0.001	-0.001	-0.001	-0.001	-0.002	-0.002	-0.002
	100	0.000	0.000	0.000	-0.001	-0.001	-0.001	-0.001	-0.001
	5	-0.007	-0.010	-0.012	-0.014	-0.014	-0.013	-0.013	-0.013
	10	-0.004	-0.006	-0.007	-0.009	-0.010	-0.009	-0.009	-0.009
2	15	-0.003	-0.004	-0.005	-0.007	-0.008	-0.007	-0.007	-0.007
	25	-0.002	-0.003	-0.003	-0.005	-0.005	-0.005	-0.005	-0.005
	50	-0.001	-0.001	-0.002	-0.003	-0.003	-0.003	-0.003	-0.003
	100	0.000	-0.001	-0.001	-0.001	-0.002	-0.002	-0.002	-0.002
	5	-0.010	-0.013	-0.014	-0.015	-0.014	-0.013	-0.013	-0.013
	10	-0.006	-0.008	-0.009	-0.011	-0.010	-0.010	-0.010	-0.009
3	15	-0.004	-0.006	-0.007	-0.009	-0.009	-0.008	-0.008	-0.008
	25	-0.003	-0.004	-0.004	-0.006	-0.006	-0.006	-0.006	-0.006
	50	-0.001	-0.002	-0.002	-0.004	-0.004	-0.004	-0.004	-0.004
	100	-0.001	-0.001	-0.001	-0.002	-0.002	-0.003	-0.002	-0.002
	5	-0.012	-0.014	-0.014	-0.013	-0.013	-0.012	-0.012	-0.012
	10	-0.008	-0.010	-0.010	-0.010	-0.010	-0.009	-0.009	-0.009
5	15	-0.006	-0.008	-0.008	-0.009	-0.008	-0.008	-0.008	-0.008
	25	-0.004	-0.005	-0.006	-0.007	-0.007	-0.006	-0.006	-0.006
	50	-0.002	-0.003	-0.003	-0.005	-0.005	-0.004	-0.004	-0.004
	100	-0.001	-0.002	-0.002	-0.003	-0.003	-0.003	-0.003	-0.003
	5	-0.017	-0.015	-0.014	-0.013	-0.012	-0.012	-0.012	-0.012
	10	-0.010	-0.010	-0.010	-0.009	-0.009	-0.009	-0.009	-0.009
10	15	-0.008	-0.009	-0.009	-0.008	-0.007	-0.007	-0.007	-0.007
	25	-0.006	-0.007	-0.007	-0.006	-0.006	-0.006	-0.006	-0.006
	50	-0.003	-0.004	-0.005	-0.005	-0.005	-0.004	-0.004	-0.004
	100	-0.002	-0.003	-0.003	-0.004	-0.003	-0.003	-0.003	-0.003

Table 13. Stress Intensity Factor Ratios In An Isotropic Cylindrical Shell With A Fixed End Containing A Circumferential Through Crack Under Uniform Twisting Moment M_{12} ; $\nu = 0.3$

k_{II}

		l/a							
a/h	R/h	0.25	0.4	0.5	1.0	1.5	2.5	5.0	50.
	5	0.481	0.504	0.511	0.523	0.524	0.523	0.522	0.522
	10	0.481	0.505	0.512	0.524	0.525	0.525	0.523	0.523
1	15	0.481	0.505	0.512	0.524	0.526	0.525	0.524	0.523
	25	0.481	0.505	0.512	0.524	0.526	0.526	0.524	0.524
	50	0.481	0.505	0.512	0.524	0.526	0.526	0.525	0.524
	100	0.481	0.505	0.512	0.524	0.526	0.526	0.525	0.524
	5	0.327	0.341	0.345	0.351	0.352	0.351	0.351	0.351
	10	0.327	0.342	0.346	0.353	0.353	0.353	0.353	0.353
2	15	0.327	0.342	0.346	0.353	0.354	0.354	0.353	0.353
	25	0.327	0.342	0.346	0.354	0.355	0.354	0.354	0.354
	50	0.327	0.342	0.346	0.354	0.355	0.355	0.354	0.354
	100	0.327	0.342	0.346	0.354	0.355	0.355	0.355	0.354
	5	0.253	0.263	0.266	0.271	0.271	0.271	0.271	0.271
	10	0.254	0.264	0.267	0.272	0.272	0.273	0.272	0.272
3	15	0.254	0.264	0.267	0.272	0.273	0.273	0.273	0.273
	25	0.254	0.264	0.268	0.273	0.274	0.274	0.273	0.273
	50	0.254	0.264	0.268	0.273	0.274	0.274	0.274	0.274
	100	0.254	0.264	0.268	0.274	0.275	0.274	0.274	0.274
	5	0.181	0.187	0.189	0.192	0.193	0.193	0.193	0.193
	10	0.181	0.187	0.189	0.193	0.193	0.194	0.194	0.194
5	15	0.182	0.188	0.190	0.193	0.194	0.194	0.194	0.194
	25	0.182	0.188	0.190	0.193	0.194	0.194	0.194	0.194
	50	0.182	0.188	0.190	0.194	0.194	0.195	0.195	0.195
	100	0.182	0.188	0.190	0.194	0.195	0.195	0.195	0.195
	5	0.056	0.074	0.079	0.087	0.089	0.089	0.088	0.088
	10	0.073	0.082	0.084	0.089	0.090	0.090	0.090	0.090
10	15	0.075	0.082	0.084	0.088	0.089	0.089	0.089	0.089
	25	0.075	0.082	0.084	0.088	0.088	0.089	0.089	0.089
	50	0.075	0.082	0.084	0.087	0.088	0.088	0.088	0.088
	100	0.075	0.082	0.084	0.087	0.088	0.088	0.088	0.088

Table 14. The Effect Of Poisson's Ratio On The Stress Intensity Factor Ratios In An Isotropic Cylindrical Shell With A Fixed End Containing A Circumferential Through Crack, $l/a = 0.5$, $a/h = 1$, $R/h = 5$.

ν	0.0	0.1	0.2	0.3	0.4	0.5
k_{mm}	1.668	1.668	1.669	1.670	1.671	1.671
k_{bm}	0.095	0.102	0.110	0.117	0.125	0.132
k_{mb}	0.027	0.030	0.033	0.035	0.038	0.041
k_{bb}	0.873	0.899	0.922	0.943	0.962	0.978
k_{vv}	1.662	1.647	1.632	1.618	1.605	1.592
k_{sv}	-0.139	-0.150	-0.161	-0.172	-0.183	-0.194
k_{tv}	0.614	0.616	0.617	0.618	0.619	0.619
k_{vs}	0.160	0.159	0.158	0.156	0.155	0.154
k_{ss}	1.035	1.036	1.036	1.036	1.036	1.036
k_{ts}	-0.012	-0.012	-0.012	-0.011	-0.010	-0.009
k_{vt}	-0.111	-0.107	-0.103	-0.100	-0.096	-0.093
k_{st}	-0.008	-0.008	-0.007	-0.007	-0.006	-0.005
k_{tt}	0.478	0.499	0.519	0.538	0.555	0.571

Table 15. The effect of material orthotropy on the stress intensity factor ratios in a cylindrical shell with a fixed end containing a circumferential through crack, $l/a = 0.5$, $a/h = 1$, $R/h = 10$.

E_1/E_2	0.037	1.000	26.667
k_{mm}	1.388	1.656	2.056
k_{bm}	0.048	0.066	0.091
k_{mb}	0.015	0.019	0.025
k_{bb}	0.938	0.978	1.046
k_{vb}	1.449	1.719	2.132
k_{sv}	-0.068	-0.092	-0.138
k_{tv}	0.317	0.662	1.284
k_{vs}	0.067	0.078	0.097
k_{ss}	0.986	1.028	1.102
k_{ts}	-0.013	-0.006	0.010
k_{vt}	-0.069	-0.100	-0.128
k_{st}	-0.004	-0.004	-0.003
k_{tt}	0.652	0.538	0.424

Table 16. Mode I Normalized Stress Intensity Factor at the Center of a Semi-Elliptic Circumferential Part-Through Crack in an Isotropic Cylindrical Shell with a Fixed End Subjected to Membrane Loading; $\nu = 0.3$, $l/a = 0.25$.

$$k_1(0)/k_{1m}$$

		OUTER CRACK				INNER CRACK			
		$\xi_0 = l_0/h$							
a/h	R/h	0.2	0.4	0.6	0.8	0.2	0.4	0.6	0.8
	5	0.966	0.827	0.519	0.147	0.925	0.699	0.376	0.108
	10	0.973	0.846	0.538	0.148	0.933	0.719	0.391	0.109
1	15	0.975	0.853	0.544	0.149	0.936	0.726	0.396	0.110
	25	0.977	0.857	0.549	0.149	0.939	0.731	0.400	0.110
	50	0.978	0.861	0.552	0.149	0.940	0.735	0.404	0.111
	100	0.979	0.863	0.554	0.149	0.941	0.738	0.405	0.111
	5	0.936	0.767	0.497	0.182	0.908	0.685	0.397	0.137
	10	0.947	0.794	0.525	0.188	0.923	0.719	0.426	0.144
2	15	0.951	0.803	0.533	0.190	0.928	0.731	0.438	0.146
	25	0.953	0.809	0.540	0.191	0.932	0.742	0.448	0.149
	50	0.955	0.813	0.544	0.191	0.935	0.749	0.456	0.151
	100	0.956	0.815	0.545	0.191	0.937	0.753	0.460	0.152
	5	0.930	0.759	0.501	0.198	0.906	0.686	0.408	0.151
	10	0.947	0.801	0.547	0.213	0.927	0.734	0.452	0.162
3	15	0.953	0.816	0.564	0.218	0.935	0.753	0.471	0.168
	25	0.957	0.827	0.577	0.222	0.941	0.770	0.490	0.174
	50	0.960	0.835	0.585	0.224	0.946	0.783	0.505	0.179
	100	0.961	0.838	0.589	0.225	0.948	0.790	0.513	0.182
	5	0.919	0.736	0.487	0.206	0.899	0.678	0.412	0.165
	10	0.945	0.800	0.557	0.234	0.927	0.740	0.469	0.180
5	15	0.954	0.827	0.591	0.248	0.939	0.770	0.500	0.190
	25	0.963	0.849	0.621	0.262	0.949	0.798	0.533	0.203
	50	0.968	0.866	0.644	0.273	0.957	0.822	0.565	0.217
	100	0.971	0.873	0.654	0.277	0.961	0.835	0.582	0.225
	5	0.907	0.709	0.465	0.206	0.899	0.684	0.430	0.184
	10	0.933	0.774	0.537	0.237	0.922	0.736	0.477	0.198
10	15	0.946	0.811	0.582	0.260	0.935	0.769	0.512	0.210
	25	0.960	0.850	0.638	0.291	0.949	0.808	0.558	0.229
	50	0.973	0.888	0.696	0.329	0.964	0.850	0.616	0.258
	100	0.979	0.908	0.730	0.354	0.972	0.877	0.659	0.283

Table 17. Mode I Normalized Stress Intensity Factor at the Center of a Semi-Elliptic Circumferential Part-Through Crack in an Isotropic Cylindrical Shell with a Fixed End Subjected to Membrane Loading; $\nu = 0.3$, $l/a = 0.40$.

$k_1(0)/k_{1m}$

		OUTER CRACK				INNER CRACK			
		$\xi_0 = l_0/h$							
a/h	R/h	0.2	0.4	0.6	0.8	0.2	0.4	0.6	0.8
	5	0.902	0.665	0.365	0.107	0.867	0.587	0.298	0.090
	10	0.908	0.677	0.372	0.106	0.876	0.603	0.307	0.090
1	15	0.910	0.681	0.374	0.106	0.880	0.609	0.310	0.090
	25	0.912	0.684	0.375	0.105	0.882	0.613	0.313	0.091
	50	0.913	0.686	0.376	0.105	0.884	0.617	0.315	0.091
	100	0.913	0.687	0.377	0.105	0.885	0.619	0.316	0.091
	5	0.908	0.696	0.420	0.149	0.880	0.625	0.346	0.120
	10	0.920	0.721	0.439	0.150	0.897	0.658	0.370	0.123
2	15	0.924	0.729	0.445	0.151	0.903	0.671	0.380	0.125
	25	0.927	0.735	0.450	0.151	0.908	0.682	0.389	0.127
	50	0.929	0.739	0.453	0.150	0.911	0.691	0.396	0.128
	100	0.929	0.741	0.454	0.150	0.913	0.695	0.400	0.129
	5	0.911	0.708	0.443	0.170	0.885	0.641	0.367	0.135
	10	0.928	0.746	0.477	0.177	0.907	0.685	0.402	0.142
3	15	0.934	0.761	0.490	0.179	0.916	0.705	0.419	0.146
	25	0.939	0.773	0.502	0.181	0.923	0.723	0.436	0.150
	50	0.943	0.781	0.509	0.182	0.929	0.737	0.450	0.154
	100	0.944	0.784	0.512	0.182	0.932	0.745	0.458	0.156
	5	0.910	0.714	0.460	0.190	0.890	0.658	0.392	0.155
	10	0.932	0.764	0.508	0.205	0.914	0.707	0.431	0.163
5	15	0.942	0.788	0.534	0.213	0.925	0.733	0.456	0.169
	25	0.950	0.810	0.559	0.221	0.936	0.761	0.485	0.178
	50	0.957	0.827	0.580	0.228	0.945	0.787	0.515	0.189
	100	0.960	0.836	0.589	0.231	0.950	0.801	0.533	0.196
	5	0.910	0.716	0.470	0.206	0.901	0.690	0.434	0.184
	10	0.933	0.773	0.532	0.232	0.922	0.735	0.474	0.195
10	15	0.944	0.801	0.565	0.246	0.932	0.759	0.498	0.201
	25	0.955	0.831	0.604	0.264	0.943	0.789	0.531	0.212
	50	0.966	0.864	0.649	0.288	0.956	0.825	0.577	0.231
	100	0.973	0.884	0.680	0.305	0.965	0.852	0.616	0.251

Table 18. Mode I Normalized Stress Intensity Factor at the Center of a Semi-Elliptic Circumferential Part-Through Crack in an Isotropic Cylindrical Shell with a Fixed End Subjected to Membrane Loading; $\nu = 0.3$, $l/a = 0.5$.

$k_1(0)/k_{1m}$

		OUTER CRACK				INNER CRACK			
		$\xi_0 = l_0/h$							
a/h	R/h	0.2	0.4	0.6	0.8	0.2	0.4	0.6	0.8
1	5	0.878	0.618	0.328	0.098	0.847	0.554	0.277	0.085
	10	0.884	0.628	0.333	0.097	0.856	0.569	0.285	0.085
	15	0.886	0.631	0.334	0.096	0.859	0.574	0.288	0.085
	25	0.887	0.633	0.335	0.096	0.862	0.579	0.290	0.086
	50	0.888	0.635	0.336	0.096	0.864	0.582	0.292	0.086
	100	0.889	0.636	0.336	0.095	0.865	0.583	0.293	0.086
2	5	0.897	0.670	0.394	0.138	0.870	0.606	0.330	0.114
	10	0.908	0.693	0.410	0.139	0.887	0.637	0.352	0.117
	15	0.912	0.701	0.416	0.139	0.893	0.650	0.361	0.118
	25	0.915	0.707	0.420	0.138	0.898	0.661	0.370	0.120
	50	0.917	0.711	0.422	0.138	0.902	0.670	0.377	0.121
	100	0.918	0.713	0.423	0.138	0.904	0.674	0.381	0.122
3	5	0.904	0.692	0.425	0.161	0.879	0.628	0.356	0.131
	10	0.920	0.726	0.453	0.165	0.900	0.669	0.386	0.135
	15	0.926	0.740	0.464	0.167	0.908	0.688	0.401	0.138
	25	0.931	0.751	0.474	0.168	0.916	0.706	0.417	0.142
	50	0.935	0.759	0.481	0.168	0.922	0.721	0.432	0.146
	100	0.937	0.763	0.484	0.168	0.925	0.729	0.440	0.148
5	5	0.910	0.711	0.455	0.186	0.890	0.656	0.390	0.153
	10	0.929	0.754	0.494	0.196	0.910	0.698	0.422	0.158
	15	0.937	0.774	0.515	0.202	0.921	0.722	0.443	0.163
	25	0.945	0.794	0.536	0.208	0.931	0.748	0.469	0.170
	50	0.952	0.812	0.555	0.213	0.941	0.774	0.497	0.179
	100	0.955	0.820	0.565	0.215	0.946	0.789	0.515	0.186
10	5	0.910	0.716	0.470	0.205	0.902	0.690	0.434	0.183
	10	0.934	0.775	0.533	0.230	0.923	0.737	0.476	0.194
	15	0.944	0.801	0.564	0.243	0.932	0.760	0.499	0.200
	25	0.954	0.828	0.597	0.258	0.942	0.786	0.527	0.209
	50	0.964	0.856	0.634	0.275	0.954	0.819	0.566	0.224
	100	0.970	0.874	0.661	0.289	0.962	0.844	0.602	0.241

Table 19. Mode I Normalized Stress Intensity Factor at the Center of a Semi-Elliptic Circumferential Part-Through Crack in an Isotropic Cylindrical Shell with a Fixed End Subjected to Membrane Loading; $\nu = 0.3$, $l/a = 1.0$.

$$k_1(0)/k_{1m}$$

		OUTER CRACK				INNER CRACK			
		$\xi_0 = l_0/h$							
a/h	R/h	0.2	0.4	0.6	0.8	0.2	0.4	0.6	0.8
	5	0.832	0.537	0.271	0.083	0.812	0.500	0.245	0.077
	10	0.836	0.543	0.272	0.082	0.821	0.513	0.251	0.077
1	15	0.838	0.545	0.272	0.081	0.824	0.518	0.253	0.077
	25	0.839	0.546	0.273	0.081	0.827	0.522	0.255	0.077
	50	0.840	0.547	0.273	0.080	0.829	0.525	0.257	0.077
	100	0.840	0.547	0.273	0.080	0.830	0.527	0.258	0.077
	5	0.878	0.627	0.352	0.120	0.856	0.578	0.307	0.105
	10	0.886	0.641	0.358	0.118	0.869	0.601	0.321	0.106
2	15	0.889	0.646	0.361	0.117	0.875	0.613	0.329	0.106
	25	0.892	0.651	0.363	0.117	0.881	0.623	0.336	0.107
	50	0.894	0.655	0.365	0.116	0.885	0.632	0.343	0.108
	100	0.895	0.656	0.365	0.115	0.888	0.637	0.347	0.109
	5	0.897	0.673	0.401	0.146	0.875	0.618	0.345	0.123
	10	0.907	0.692	0.413	0.145	0.890	0.647	0.363	0.125
3	15	0.911	0.700	0.418	0.144	0.897	0.661	0.374	0.126
	25	0.915	0.708	0.423	0.143	0.904	0.676	0.386	0.128
	50	0.919	0.714	0.427	0.143	0.910	0.690	0.398	0.131
	100	0.920	0.718	0.429	0.142	0.914	0.699	0.406	0.133
	5	0.910	0.710	0.449	0.178	0.891	0.658	0.388	0.149
	10	0.927	0.745	0.479	0.183	0.910	0.696	0.416	0.152
5	15	0.932	0.758	0.490	0.184	0.918	0.714	0.431	0.155
	25	0.937	0.770	0.500	0.185	0.926	0.732	0.448	0.158
	50	0.942	0.780	0.509	0.185	0.933	0.752	0.468	0.164
	100	0.945	0.787	0.515	0.185	0.939	0.766	0.484	0.169
	5	0.910	0.715	0.467	0.201	0.901	0.687	0.430	0.180
	10	0.934	0.774	0.529	0.224	0.923	0.736	0.473	0.190
10	15	0.945	0.801	0.560	0.236	0.933	0.761	0.497	0.196
	25	0.954	0.827	0.591	0.248	0.944	0.788	0.526	0.205
	50	0.962	0.847	0.616	0.257	0.953	0.815	0.558	0.216
	100	0.966	0.858	0.629	0.261	0.959	0.833	0.582	0.226

Table 20. Mode III Normalized Stress Intensity Factor at the Center of a Semi-Elliptic Circumferential Part-Through Crack in an Isotropic Cylindrical Shell with a Fixed End Subjected to Membrane Loading; $\nu = 0.3$, $l/a = 1.5$

$k_1(0)/k_{1m}$

		OUTER CRACK				INNER CRACK			
		$\xi_0 = l_0/h$							
a/h	R/h	0.2	0.4	0.6	0.8	0.2	0.4	0.6	0.8
1	5	0.821	0.519	0.258	0.079	0.805	0.490	0.238	0.075
	10	0.825	0.523	0.258	0.078	0.813	0.501	0.243	0.074
	15	0.826	0.524	0.258	0.077	0.816	0.506	0.245	0.074
	25	0.827	0.525	0.258	0.077	0.819	0.510	0.247	0.075
	50	0.828	0.526	0.258	0.077	0.821	0.513	0.249	0.075
	100	0.828	0.526	0.258	0.076	0.822	0.515	0.250	0.075
2	5	0.876	0.621	0.345	0.116	0.855	0.576	0.305	0.103
	10	0.881	0.630	0.347	0.113	0.867	0.596	0.316	0.103
	15	0.884	0.633	0.348	0.112	0.872	0.605	0.322	0.104
	25	0.886	0.637	0.349	0.111	0.877	0.615	0.328	0.104
	50	0.888	0.639	0.350	0.110	0.881	0.624	0.335	0.105
	100	0.888	0.641	0.350	0.110	0.884	0.629	0.338	0.106
3	5	0.897	0.671	0.397	0.143	0.876	0.618	0.343	0.121
	10	0.906	0.688	0.406	0.140	0.890	0.646	0.362	0.123
	15	0.909	0.693	0.409	0.139	0.896	0.658	0.370	0.124
	25	0.912	0.698	0.411	0.138	0.902	0.671	0.380	0.125
	50	0.914	0.703	0.413	0.136	0.908	0.683	0.391	0.128
	100	0.916	0.705	0.414	0.136	0.911	0.691	0.398	0.129
5	5	0.910	0.708	0.446	0.176	0.891	0.656	0.385	0.147
	10	0.926	0.744	0.476	0.180	0.910	0.696	0.415	0.150
	15	0.932	0.757	0.487	0.181	0.918	0.714	0.430	0.153
	25	0.937	0.767	0.495	0.180	0.926	0.732	0.447	0.156
	50	0.940	0.774	0.500	0.179	0.933	0.749	0.464	0.161
	100	0.942	0.779	0.502	0.178	0.937	0.761	0.477	0.165
10	5	0.910	0.714	0.466	0.200	0.901	0.686	0.428	0.178
	10	0.934	0.773	0.527	0.222	0.923	0.735	0.470	0.188
	15	0.944	0.800	0.558	0.234	0.933	0.760	0.495	0.194
	25	0.954	0.825	0.588	0.245	0.943	0.787	0.524	0.203
	50	0.962	0.847	0.613	0.253	0.953	0.815	0.557	0.214
	100	0.965	0.857	0.625	0.256	0.959	0.834	0.582	0.224

Table 21. Mode I Normalized Stress Intensity Factor at the Center of a Semi-Elliptic Circumferential Part-Through Crack in an Isotropic Cylindrical Shell with a Fixed End Subjected to Membrane Loading; $\nu = 0.3$, $l/a = 2.5$

$k_1(0)/k_{1m}$

		OUTER CRACK				INNER CRACK			
		$\xi_0 = l_0/h$							
a/h	R/h	0.2	0.4	0.6	0.8	0.2	0.4	0.6	0.8
	5	0.817	0.511	0.252	0.077	0.803	0.486	0.236	0.073
	10	0.819	0.512	0.251	0.076	0.810	0.496	0.240	0.073
1	15	0.820	0.513	0.250	0.075	0.812	0.500	0.241	0.073
	25	0.821	0.514	0.250	0.075	0.815	0.504	0.243	0.073
	50	0.821	0.514	0.250	0.074	0.817	0.507	0.245	0.073
	100	0.821	0.514	0.250	0.074	0.818	0.509	0.246	0.073
	5	0.875	0.620	0.342	0.114	0.856	0.576	0.303	0.101
	10	0.880	0.627	0.343	0.111	0.867	0.596	0.315	0.102
2	15	0.882	0.628	0.343	0.109	0.872	0.604	0.320	0.102
	25	0.883	0.630	0.342	0.108	0.876	0.612	0.325	0.103
	50	0.884	0.631	0.342	0.107	0.879	0.619	0.330	0.104
	100	0.885	0.632	0.342	0.107	0.881	0.624	0.334	0.104
	5	0.897	0.670	0.395	0.141	0.875	0.617	0.341	0.120
	10	0.906	0.687	0.404	0.138	0.891	0.646	0.360	0.122
3	15	0.909	0.692	0.406	0.137	0.897	0.659	0.370	0.123
	25	0.911	0.695	0.407	0.135	0.902	0.670	0.379	0.124
	50	0.913	0.697	0.406	0.133	0.907	0.681	0.388	0.126
	100	0.913	0.698	0.406	0.132	0.910	0.688	0.394	0.127
	5	0.910	0.708	0.445	0.174	0.891	0.655	0.384	0.145
	10	0.926	0.743	0.474	0.178	0.910	0.694	0.413	0.149
5	15	0.932	0.756	0.484	0.178	0.918	0.713	0.429	0.152
	25	0.937	0.766	0.492	0.178	0.926	0.732	0.446	0.155
	50	0.940	0.773	0.496	0.176	0.933	0.750	0.464	0.160
	100	0.941	0.776	0.497	0.174	0.937	0.760	0.475	0.163
	5	0.910	0.714	0.465	0.199	0.900	0.686	0.427	0.177
	10	0.934	0.773	0.526	0.221	0.922	0.734	0.469	0.187
10	15	0.944	0.800	0.557	0.232	0.933	0.759	0.493	0.193
	25	0.954	0.825	0.587	0.243	0.943	0.786	0.522	0.201
	50	0.961	0.846	0.611	0.251	0.953	0.814	0.556	0.213
	100	0.965	0.856	0.623	0.253	0.960	0.833	0.581	0.223

Table 22. Mode I Normalized Stress Intensity Factor at the Center of a Semi-Elliptic Circumferential Part-Through Crack in an Isotropic Cylindrical Shell with a Fixed End Subjected to Membrane Loading; $\nu = 0.3$, $l/a = 5.0$

$k_1(0)/k_{1m}$

		OUTER CRACK				INNER CRACK			
		$\xi_0 = l_0/h$							
a/h	R/h	0.2	0.4	0.6	0.8	0.2	0.4	0.6	0.8
	5	0.817	0.510	0.250	0.076	0.803	0.486	0.235	0.073
	10	0.818	0.510	0.249	0.075	0.809	0.495	0.239	0.073
1	15	0.818	0.509	0.248	0.074	0.812	0.498	0.240	0.073
	25	0.818	0.509	0.247	0.074	0.814	0.502	0.242	0.073
	50	0.818	0.509	0.246	0.073	0.816	0.504	0.243	0.073
	100	0.819	0.509	0.246	0.073	0.817	0.506	0.244	0.073
	5	0.875	0.619	0.341	0.113	0.855	0.575	0.302	0.101
	10	0.880	0.626	0.342	0.110	0.867	0.595	0.314	0.101
2	15	0.882	0.627	0.341	0.108	0.872	0.604	0.319	0.102
	25	0.883	0.628	0.340	0.107	0.876	0.612	0.325	0.102
	50	0.883	0.629	0.339	0.106	0.879	0.618	0.329	0.103
	100	0.883	0.628	0.338	0.105	0.881	0.622	0.332	0.103
	5	0.897	0.670	0.394	0.140	0.875	0.616	0.340	0.119
	10	0.906	0.686	0.402	0.137	0.890	0.645	0.359	0.121
3	15	0.909	0.691	0.404	0.136	0.897	0.658	0.369	0.122
	25	0.911	0.695	0.405	0.134	0.902	0.670	0.378	0.123
	50	0.912	0.696	0.405	0.132	0.907	0.681	0.387	0.125
	100	0.913	0.697	0.404	0.131	0.910	0.687	0.393	0.126
	5	0.910	0.708	0.444	0.174	0.890	0.654	0.383	0.145
	10	0.926	0.743	0.473	0.177	0.910	0.694	0.412	0.148
5	15	0.932	0.756	0.483	0.178	0.918	0.712	0.428	0.151
	25	0.937	0.766	0.491	0.177	0.926	0.731	0.445	0.154
	50	0.940	0.772	0.495	0.175	0.933	0.749	0.463	0.159
	100	0.941	0.775	0.496	0.173	0.937	0.760	0.475	0.162
	5	0.910	0.714	0.465	0.199	0.900	0.685	0.426	0.176
	10	0.934	0.773	0.526	0.221	0.922	0.734	0.468	0.186
10	15	0.944	0.800	0.557	0.232	0.933	0.759	0.492	0.192
	25	0.954	0.825	0.586	0.243	0.943	0.786	0.521	0.200
	50	0.961	0.846	0.611	0.250	0.953	0.814	0.555	0.212
	100	0.965	0.856	0.622	0.252	0.959	0.833	0.580	0.222

Table 23. Mode I Normalized Stress Intensity Factor at the Center of a Semi-Elliptic Circumferential Part-Through Crack in an Isotropic Cylindrical Shell with a Fixed End Subjected to Membrane Loading; $\nu = 0.3$, $l/a = 50$

$$k_1(0)/k_{1m}$$

		OUTER CRACK				INNER CRACK			
		$\xi_0 = l_0/h$							
a/h	R/h	0.2	0.4	0.6	0.8	0.2	0.4	0.6	0.8
	5	0.817	0.509	0.250	0.076	0.803	0.486	0.234	0.073
	10	0.818	0.509	0.248	0.074	0.809	0.495	0.238	0.072
1	15	0.818	0.509	0.247	0.074	0.812	0.498	0.240	0.072
	25	0.818	0.509	0.246	0.073	0.814	0.501	0.241	0.072
	50	0.818	0.508	0.246	0.073	0.816	0.504	0.243	0.072
	100	0.818	0.508	0.245	0.073	0.817	0.505	0.244	0.072
	5	0.875	0.619	0.341	0.113	0.855	0.575	0.302	0.100
	10	0.880	0.626	0.341	0.110	0.867	0.595	0.314	0.101
2	15	0.882	0.627	0.341	0.108	0.872	0.603	0.319	0.101
	25	0.883	0.628	0.340	0.107	0.876	0.611	0.324	0.102
	50	0.883	0.628	0.339	0.106	0.879	0.618	0.329	0.103
	100	0.883	0.628	0.338	0.105	0.881	0.622	0.332	0.103
	5	0.897	0.669	0.394	0.140	0.875	0.616	0.340	0.119
	10	0.906	0.686	0.402	0.137	0.890	0.645	0.359	0.120
3	15	0.909	0.691	0.404	0.135	0.896	0.658	0.368	0.122
	25	0.911	0.694	0.405	0.134	0.902	0.670	0.378	0.123
	50	0.912	0.696	0.404	0.132	0.907	0.681	0.387	0.125
	100	0.913	0.696	0.403	0.130	0.910	0.687	0.393	0.126
	5	0.910	0.708	0.444	0.173	0.890	0.654	0.382	0.144
	10	0.926	0.743	0.473	0.177	0.910	0.693	0.411	0.148
5	15	0.932	0.756	0.483	0.177	0.918	0.712	0.427	0.150
	25	0.937	0.766	0.491	0.177	0.926	0.731	0.444	0.154
	50	0.940	0.772	0.495	0.175	0.933	0.749	0.462	0.159
	100	0.941	0.775	0.495	0.173	0.937	0.760	0.474	0.162
	5	0.910	0.714	0.465	0.198	0.900	0.685	0.426	0.176
	10	0.934	0.773	0.526	0.221	0.922	0.733	0.468	0.186
10	15	0.944	0.800	0.556	0.232	0.933	0.758	0.492	0.192
	25	0.954	0.825	0.586	0.242	0.943	0.786	0.521	0.200
	50	0.961	0.846	0.611	0.250	0.953	0.814	0.554	0.211
	100	0.965	0.856	0.622	0.252	0.959	0.833	0.580	0.222

Table 24. Mode I Normalized Stress Intensity Factor at the Center of a Semi-Elliptic Circumferential Part-Through Crack in an Isotropic Cylindrical Shell with a Fixed End Subjected to Bending Moment; $\nu = 0.3$, $l/a = 0.25$.

$k_1(0)/k_{1b}$

		OUTER CRACK				INNER CRACK			
		$\xi_0 = l_0/h$							
a/h	R/h	0.2	0.4	0.6	0.8	0.2	0.4	0.6	0.8
	5	0.965	0.815	0.469	0.075	0.921	0.666	0.293	0.023
	10	0.973	0.838	0.493	0.078	0.930	0.689	0.312	0.025
1	15	0.975	0.845	0.501	0.078	0.933	0.698	0.319	0.026
	25	0.977	0.851	0.507	0.078	0.936	0.705	0.325	0.026
	50	0.978	0.855	0.512	0.079	0.938	0.710	0.329	0.027
	100	0.979	0.857	0.514	0.079	0.938	0.712	0.331	0.027
	5	0.932	0.741	0.432	0.108	0.902	0.645	0.311	0.052
	10	0.945	0.774	0.467	0.116	0.919	0.686	0.348	0.061
2	15	0.948	0.784	0.478	0.118	0.924	0.701	0.363	0.064
	25	0.951	0.792	0.487	0.120	0.929	0.714	0.376	0.068
	50	0.953	0.797	0.492	0.120	0.932	0.723	0.386	0.071
	100	0.954	0.799	0.494	0.120	0.934	0.728	0.391	0.072
	5	0.925	0.727	0.429	0.121	0.899	0.644	0.320	0.065
	10	0.944	0.779	0.489	0.140	0.922	0.702	0.375	0.079
3	15	0.951	0.797	0.510	0.148	0.931	0.725	0.400	0.087
	25	0.955	0.811	0.527	0.153	0.938	0.745	0.423	0.094
	50	0.959	0.820	0.539	0.156	0.943	0.761	0.442	0.101
	100	0.960	0.824	0.543	0.157	0.945	0.769	0.452	0.105
	5	0.912	0.696	0.404	0.122	0.891	0.631	0.319	0.075
	10	0.940	0.773	0.493	0.158	0.921	0.706	0.389	0.095
5	15	0.951	0.806	0.536	0.177	0.934	0.741	0.429	0.109
	25	0.960	0.834	0.575	0.195	0.946	0.775	0.470	0.125
	50	0.967	0.854	0.604	0.210	0.955	0.804	0.510	0.142
	100	0.970	0.863	0.617	0.215	0.959	0.819	0.532	0.153
	5	0.898	0.661	0.369	0.111	0.890	0.635	0.334	0.091
	10	0.927	0.738	0.457	0.151	0.915	0.696	0.393	0.110
10	15	0.942	0.782	0.514	0.179	0.930	0.735	0.435	0.125
	25	0.957	0.829	0.584	0.219	0.945	0.781	0.492	0.149
	50	0.971	0.875	0.658	0.267	0.961	0.832	0.564	0.185
	100	0.978	0.900	0.701	0.299	0.970	0.863	0.617	0.217

Table 25. Mode I Normalized Stress Intensity Factor at the Center of a Semi-Elliptic Circumferential Part-Through Crack in an Isotropic Cylindrical Shell with a Fixed End Subjected to Bending Moment; $\nu = 0.3$, $l/a = 0.40$.

$$k_1(0)/k_{1b}$$

		OUTER CRACK				INNER CRACK			
		$\xi_0 = l_0/h$							
a/h	R/h	0.2	0.4	0.6	0.8	0.2	0.4	0.6	0.8
	5	0.897	0.629	0.281	0.028	0.859	0.536	0.197	0.004
	10	0.904	0.643	0.290	0.027	0.869	0.555	0.209	0.005
1	15	0.906	0.648	0.293	0.026	0.873	0.562	0.213	0.005
	25	0.908	0.651	0.295	0.026	0.875	0.568	0.217	0.005
	50	0.909	0.654	0.296	0.026	0.877	0.572	0.220	0.005
	100	0.910	0.655	0.296	0.025	0.878	0.574	0.221	0.006
	5	0.902	0.658	0.339	0.069	0.872	0.576	0.249	0.033
	10	0.915	0.689	0.364	0.072	0.890	0.616	0.280	0.038
2	15	0.919	0.699	0.373	0.073	0.897	0.631	0.293	0.040
	25	0.923	0.707	0.379	0.073	0.902	0.644	0.304	0.043
	50	0.925	0.712	0.383	0.073	0.906	0.655	0.314	0.045
	100	0.926	0.714	0.384	0.072	0.908	0.660	0.318	0.046
	5	0.904	0.669	0.361	0.089	0.876	0.591	0.271	0.047
	10	0.923	0.716	0.405	0.099	0.900	0.645	0.314	0.056
3	15	0.930	0.734	0.423	0.103	0.910	0.668	0.336	0.061
	25	0.936	0.749	0.438	0.106	0.918	0.690	0.357	0.067
	50	0.940	0.758	0.448	0.107	0.925	0.708	0.376	0.072
	100	0.941	0.763	0.452	0.107	0.928	0.717	0.386	0.075
	5	0.903	0.671	0.373	0.105	0.881	0.607	0.296	0.066
	10	0.927	0.732	0.436	0.126	0.907	0.666	0.345	0.076
5	15	0.938	0.761	0.469	0.137	0.919	0.698	0.376	0.085
	25	0.947	0.788	0.501	0.148	0.932	0.731	0.412	0.096
	50	0.954	0.810	0.528	0.158	0.942	0.762	0.449	0.110
	100	0.958	0.820	0.541	0.162	0.948	0.780	0.472	0.119
	5	0.902	0.669	0.376	0.113	0.893	0.642	0.340	0.093
10	10	0.927	0.737	0.453	0.146	0.915	0.695	0.390	0.107
	15	0.939	0.770	0.495	0.165	0.926	0.724	0.419	0.116
	25	0.951	0.808	0.545	0.189	0.939	0.759	0.459	0.130
	50	0.963	0.847	0.603	0.220	0.953	0.803	0.517	0.154
	100	0.971	0.872	0.642	0.243	0.962	0.835	0.565	0.179

Table 26. Mode III Normalized Stress Intensity Factor at the Center of a Semi-Elliptic Circumferential Part-Through Crack in an Isotropic Cylindrical Shell with a Fixed End Subjected to Bending Moment; $\nu = 0.3$, $l/a = 0.50$.

$k_1(0)/k_{1b}$

		OUTER CRACK				INNER CRACK			
		$\xi_0 = l_0/h$							
a/h	R/h	0.2	0.4	0.6	0.8	0.2	0.4	0.6	0.8
	5	0.870	0.573	0.236	0.017	0.837	0.497	0.172	0.000
	10	0.877	0.585	0.242	0.016	0.847	0.515	0.182	0.000
1	15	0.879	0.589	0.244	0.016	0.851	0.521	0.186	0.000
	25	0.881	0.592	0.245	0.015	0.853	0.526	0.189	0.000
	50	0.882	0.594	0.246	0.015	0.855	0.530	0.192	0.001
	100	0.883	0.594	0.246	0.014	0.856	0.532	0.193	0.001
	5	0.890	0.628	0.309	0.058	0.861	0.552	0.230	0.027
	10	0.903	0.657	0.330	0.059	0.879	0.591	0.257	0.031
2	15	0.907	0.667	0.337	0.059	0.886	0.606	0.270	0.033
	25	0.911	0.674	0.343	0.059	0.892	0.620	0.281	0.035
	50	0.913	0.679	0.346	0.058	0.896	0.630	0.290	0.037
	100	0.914	0.681	0.347	0.058	0.898	0.636	0.295	0.038
	5	0.897	0.651	0.340	0.079	0.870	0.576	0.257	0.042
	10	0.915	0.692	0.376	0.086	0.893	0.625	0.295	0.049
3	15	0.922	0.709	0.392	0.088	0.902	0.648	0.315	0.053
	25	0.927	0.723	0.405	0.090	0.911	0.670	0.335	0.058
	50	0.931	0.733	0.414	0.091	0.918	0.688	0.353	0.063
	100	0.933	0.738	0.418	0.091	0.921	0.697	0.363	0.066
	5	0.902	0.668	0.369	0.102	0.881	0.606	0.293	0.064
	10	0.923	0.720	0.420	0.116	0.903	0.656	0.334	0.071
5	15	0.933	0.746	0.447	0.124	0.915	0.685	0.360	0.078
	25	0.942	0.770	0.474	0.133	0.926	0.716	0.393	0.087
	50	0.949	0.791	0.499	0.140	0.937	0.747	0.428	0.099
	100	0.953	0.801	0.511	0.143	0.943	0.765	0.451	0.107
	5	0.902	0.670	0.377	0.113	0.893	0.642	0.340	0.092
	10	0.928	0.740	0.455	0.146	0.916	0.698	0.392	0.107
10	15	0.939	0.771	0.495	0.163	0.927	0.725	0.420	0.115
	25	0.950	0.804	0.537	0.182	0.938	0.756	0.455	0.127
	50	0.961	0.838	0.585	0.206	0.951	0.795	0.504	0.146
	100	0.968	0.860	0.619	0.224	0.960	0.825	0.548	0.167

Table 27. Mode I Normalized Stress Intensity Factor at the Center of a Semi-Elliptic Circumferential Part-Through Crack in an Isotropic Cylindrical Shell with a Fixed End Subjected to Bending Moment; $\nu = 0.3$, $l/a = 1.0$.

$k_1(0)/k_{1b}$

		OUTER CRACK				INNER CRACK			
		$\xi_0 = l_0/h$							
a/h	R/h	0.2	0.4	0.6	0.8	0.2	0.4	0.6	0.8
	5	0.820	0.476	0.165	0.001	0.798	0.432	0.132	-0.008
	10	0.825	0.483	0.167	-0.001	0.808	0.448	0.140	-0.008
1	15	0.827	0.486	0.168	-0.001	0.812	0.454	0.143	-0.008
	25	0.829	0.488	0.168	-0.002	0.815	0.459	0.146	-0.008
	50	0.829	0.489	0.168	-0.002	0.817	0.463	0.148	-0.008
	100	0.830	0.489	0.168	-0.003	0.818	0.465	0.149	-0.007
	5	0.869	0.578	0.258	0.037	0.845	0.519	0.202	0.017
	10	0.878	0.595	0.266	0.035	0.860	0.548	0.220	0.019
2	15	0.882	0.602	0.270	0.034	0.866	0.561	0.230	0.020
	25	0.885	0.608	0.273	0.033	0.872	0.574	0.239	0.021
	50	0.887	0.612	0.275	0.033	0.877	0.585	0.248	0.023
	100	0.888	0.614	0.276	0.032	0.880	0.591	0.252	0.024
	5	0.890	0.629	0.312	0.063	0.865	0.564	0.244	0.035
	10	0.901	0.652	0.328	0.063	0.882	0.598	0.267	0.037
3	15	0.905	0.662	0.335	0.062	0.890	0.615	0.281	0.040
	25	0.910	0.672	0.342	0.062	0.897	0.634	0.296	0.042
	50	0.913	0.680	0.348	0.061	0.904	0.651	0.312	0.046
	100	0.915	0.684	0.350	0.061	0.908	0.661	0.322	0.048
	5	0.903	0.668	0.363	0.094	0.882	0.608	0.291	0.060
	10	0.921	0.711	0.402	0.102	0.903	0.653	0.327	0.065
5	15	0.927	0.727	0.417	0.105	0.912	0.675	0.346	0.069
	25	0.933	0.741	0.430	0.106	0.920	0.697	0.367	0.074
	50	0.938	0.754	0.443	0.107	0.929	0.720	0.392	0.081
	100	0.941	0.763	0.451	0.108	0.935	0.737	0.412	0.087
	5	0.902	0.668	0.373	0.109	0.892	0.640	0.336	0.089
	10	0.928	0.739	0.451	0.140	0.916	0.697	0.388	0.103
10	15	0.940	0.772	0.491	0.157	0.928	0.727	0.419	0.112
	25	0.950	0.803	0.531	0.173	0.939	0.759	0.454	0.123
	50	0.959	0.828	0.564	0.185	0.950	0.790	0.494	0.137
	100	0.963	0.842	0.581	0.191	0.956	0.812	0.524	0.149

Table 28. Mode I Normalized Stress Intensity Factor at the Center of a Semi-Elliptic Circumferential Part-Through Crack in an Isotropic Cylindrical Shell with a Fixed End Subjected to Bending Moment; $\nu = 0.3$, $l/a = 1.5$

$$k_1(0)/k_{1b}$$

		OUTER CRACK				INNER CRACK			
		$\xi_0 = l_0/h$							
a/h	R/h	0.2	0.4	0.6	0.8	0.2	0.4	0.6	0.8
	5	0.808	0.454	0.149	-0.003	0.790	0.419	0.124	-0.010
	10	0.813	0.459	0.150	-0.005	0.799	0.433	0.131	-0.010
1	15	0.814	0.461	0.150	-0.006	0.803	0.439	0.134	-0.010
	25	0.815	0.462	0.150	-0.006	0.806	0.444	0.136	-0.010
	50	0.816	0.463	0.150	-0.007	0.809	0.448	0.138	-0.010
	100	0.816	0.464	0.150	-0.007	0.810	0.450	0.140	-0.010
	5	0.867	0.571	0.249	0.033	0.844	0.517	0.199	0.015
	10	0.873	0.582	0.253	0.030	0.857	0.541	0.214	0.016
2	15	0.876	0.586	0.254	0.028	0.863	0.553	0.221	0.017
	25	0.878	0.590	0.256	0.027	0.868	0.564	0.230	0.018
	50	0.880	0.594	0.257	0.026	0.873	0.575	0.238	0.019
	100	0.881	0.595	0.257	0.025	0.876	0.581	0.242	0.020
	5	0.889	0.627	0.308	0.060	0.866	0.565	0.242	0.033
	10	0.900	0.648	0.321	0.058	0.882	0.598	0.265	0.035
3	15	0.903	0.654	0.324	0.056	0.889	0.613	0.277	0.037
	25	0.906	0.660	0.327	0.055	0.895	0.628	0.289	0.039
	50	0.909	0.666	0.330	0.053	0.901	0.643	0.302	0.042
	100	0.910	0.669	0.332	0.053	0.905	0.653	0.312	0.044
	5	0.903	0.666	0.359	0.091	0.882	0.606	0.288	0.058
	10	0.921	0.709	0.398	0.099	0.903	0.653	0.325	0.063
5	15	0.927	0.726	0.413	0.101	0.912	0.675	0.345	0.067
	25	0.933	0.738	0.424	0.101	0.921	0.697	0.366	0.072
	50	0.936	0.747	0.431	0.100	0.928	0.717	0.387	0.077
	100	0.939	0.753	0.435	0.099	0.933	0.732	0.404	0.082
	5	0.902	0.668	0.372	0.108	0.892	0.638	0.334	0.088
	10	0.928	0.738	0.449	0.138	0.916	0.696	0.386	0.101
10	15	0.940	0.770	0.488	0.154	0.927	0.725	0.416	0.110
	25	0.950	0.801	0.527	0.169	0.939	0.757	0.452	0.120
	50	0.959	0.827	0.561	0.181	0.950	0.791	0.493	0.135
	100	0.963	0.840	0.576	0.185	0.957	0.813	0.524	0.148

Table 29. Mode I Normalized Stress Intensity Factor at the Center of a Semi-Elliptic Circumferential Part-Through Crack in an Isotropic Cylindrical Shell with a Fixed End Subjected to Bending Moment; $\nu = 0.3$, $l/a = 2.5$

$k_1(0)/k_{1b}$

		OUTER CRACK				INNER CRACK			
		$\xi_0 = l_0/h$							
a/h	R/h	0.2	0.4	0.6	0.8	0.2	0.4	0.6	0.8
	5	0.804	0.445	0.142	-0.006	0.788	0.415	0.121	-0.011
	10	0.806	0.447	0.141	-0.007	0.796	0.427	0.126	-0.011
1	15	0.807	0.448	0.140	-0.008	0.799	0.432	0.129	-0.011
	25	0.808	0.448	0.140	-0.009	0.802	0.436	0.131	-0.011
	50	0.809	0.449	0.140	-0.009	0.804	0.440	0.133	-0.011
	100	0.809	0.449	0.139	-0.009	0.806	0.443	0.134	-0.011
	5	0.866	0.569	0.245	0.030	0.845	0.517	0.197	0.014
	10	0.872	0.578	0.247	0.027	0.857	0.541	0.212	0.015
2	15	0.874	0.580	0.247	0.025	0.862	0.551	0.219	0.015
	25	0.875	0.582	0.247	0.023	0.867	0.560	0.226	0.016
	50	0.876	0.584	0.247	0.022	0.871	0.569	0.232	0.017
	100	0.877	0.585	0.246	0.021	0.873	0.575	0.237	0.018
	5	0.889	0.625	0.305	0.058	0.866	0.563	0.240	0.031
	10	0.899	0.646	0.317	0.055	0.882	0.598	0.264	0.034
3	15	0.903	0.653	0.321	0.054	0.889	0.613	0.276	0.036
	25	0.905	0.657	0.322	0.051	0.895	0.627	0.288	0.038
	50	0.907	0.660	0.322	0.049	0.900	0.640	0.299	0.040
	100	0.908	0.661	0.322	0.048	0.904	0.648	0.307	0.042
	5	0.902	0.665	0.358	0.090	0.882	0.604	0.286	0.056
	10	0.921	0.708	0.396	0.097	0.903	0.652	0.323	0.061
5	15	0.927	0.724	0.410	0.098	0.912	0.674	0.343	0.065
	25	0.932	0.737	0.421	0.098	0.921	0.697	0.365	0.070
	50	0.936	0.746	0.427	0.096	0.928	0.718	0.387	0.076
	100	0.938	0.749	0.429	0.094	0.933	0.731	0.401	0.080
	5	0.902	0.668	0.371	0.107	0.892	0.637	0.332	0.086
	10	0.928	0.737	0.448	0.137	0.916	0.695	0.384	0.100
10	15	0.940	0.770	0.487	0.152	0.927	0.724	0.414	0.108
	25	0.950	0.801	0.526	0.167	0.939	0.756	0.450	0.119
	50	0.959	0.826	0.558	0.179	0.950	0.790	0.491	0.133
	100	0.963	0.839	0.574	0.182	0.957	0.813	0.523	0.146

Table 30. Mode I Normalized Stress Intensity Factor at the Center of a Semi-Elliptic Circumferential Part-Through Crack in an Isotropic Cylindrical Shell with a Fixed End Subjected to Bending Moment; $\nu = 0.3$, $l/a = 5.0$.

$$k_1(0)/k_{1b}$$

		OUTER CRACK				INNER CRACK			
		$\xi_0 = l_0/h$							
a/h	R/h	0.2	0.4	0.6	0.8	0.2	0.4	0.6	0.8
	5	0.803	0.443	0.140	-0.007	0.789	0.415	0.120	-0.012
	10	0.805	0.444	0.138	-0.009	0.796	0.426	0.125	-0.012
1	15	0.805	0.443	0.137	-0.009	0.798	0.430	0.127	-0.012
	25	0.805	0.443	0.136	-0.010	0.801	0.434	0.129	-0.012
	50	0.806	0.443	0.135	-0.010	0.803	0.437	0.131	-0.011
	100	0.806	0.443	0.135	-0.011	0.804	0.439	0.132	-0.011
	5	0.866	0.568	0.244	0.029	0.844	0.516	0.196	0.013
	10	0.872	0.577	0.246	0.026	0.857	0.541	0.211	0.014
2	15	0.873	0.579	0.245	0.024	0.862	0.551	0.218	0.015
	25	0.875	0.580	0.245	0.022	0.867	0.560	0.225	0.016
	50	0.875	0.581	0.243	0.021	0.870	0.568	0.231	0.017
	100	0.875	0.581	0.242	0.020	0.873	0.573	0.235	0.017
	5	0.889	0.625	0.304	0.057	0.865	0.562	0.238	0.031
	10	0.899	0.645	0.316	0.054	0.882	0.597	0.263	0.033
3	15	0.902	0.652	0.319	0.052	0.889	0.612	0.275	0.035
	25	0.905	0.656	0.320	0.050	0.895	0.627	0.287	0.037
	50	0.907	0.659	0.320	0.048	0.901	0.640	0.298	0.039
	100	0.907	0.659	0.319	0.046	0.903	0.648	0.306	0.041
	5	0.902	0.665	0.357	0.089	0.881	0.604	0.285	0.055
	10	0.921	0.708	0.395	0.096	0.903	0.651	0.322	0.061
5	15	0.927	0.724	0.409	0.097	0.912	0.673	0.341	0.064
	25	0.932	0.737	0.420	0.097	0.920	0.696	0.363	0.069
	50	0.936	0.745	0.426	0.095	0.928	0.717	0.386	0.075
	100	0.938	0.748	0.427	0.093	0.933	0.731	0.401	0.080
	5	0.902	0.667	0.371	0.107	0.892	0.637	0.331	0.086
	10	0.928	0.737	0.448	0.136	0.916	0.694	0.383	0.099
10	15	0.940	0.770	0.487	0.152	0.927	0.724	0.413	0.107
	25	0.950	0.801	0.525	0.167	0.938	0.756	0.448	0.118
	50	0.959	0.826	0.558	0.178	0.950	0.789	0.490	0.132
	100	0.963	0.839	0.573	0.181	0.957	0.812	0.521	0.145

Table 31. Mode I Normalized Stress Intensity Factor at the Center of a Semi-Elliptic Circumferential Part-Through Crack in an Isotropic Cylindrical Shell with a Fixed End Subjected to Bending Moment; $\nu = 0.3$, $l/a = 50.0$.

$$k_1(0)/k_{1b}$$

		OUTER CRACK				INNER CRACK			
		$\xi_0 = l_0/h$							
a/h	R/h	0.2	0.4	0.6	0.8	0.2	0.4	0.6	0.8
	5	0.803	0.443	0.139	-0.007	0.788	0.415	0.120	-0.012
	10	0.805	0.443	0.137	-0.009	0.795	0.426	0.125	-0.012
1	15	0.805	0.443	0.136	-0.010	0.798	0.430	0.127	-0.012
	25	0.805	0.443	0.135	-0.010	0.801	0.434	0.129	-0.012
	50	0.805	0.442	0.134	-0.011	0.802	0.437	0.131	-0.012
	100	0.805	0.442	0.134	-0.011	0.803	0.439	0.132	-0.012
	5	0.866	0.568	0.244	0.029	0.844	0.516	0.195	0.013
	10	0.872	0.577	0.245	0.025	0.857	0.540	0.211	0.014
2	15	0.873	0.579	0.245	0.024	0.862	0.550	0.218	0.014
	25	0.874	0.580	0.244	0.022	0.867	0.560	0.224	0.015
	50	0.875	0.580	0.243	0.020	0.870	0.568	0.231	0.016
	100	0.875	0.580	0.241	0.019	0.873	0.573	0.234	0.017
	5	0.889	0.625	0.304	0.057	0.865	0.562	0.238	0.030
	10	0.899	0.645	0.316	0.054	0.882	0.596	0.262	0.033
3	15	0.902	0.652	0.319	0.052	0.889	0.612	0.274	0.035
	25	0.905	0.656	0.320	0.050	0.895	0.627	0.286	0.037
	50	0.906	0.658	0.320	0.048	0.900	0.640	0.298	0.039
	100	0.907	0.659	0.318	0.046	0.903	0.648	0.305	0.041
	5	0.902	0.665	0.357	0.089	0.881	0.603	0.284	0.055
	10	0.921	0.708	0.395	0.096	0.902	0.650	0.321	0.060
5	15	0.927	0.724	0.409	0.097	0.912	0.673	0.341	0.064
	25	0.932	0.736	0.420	0.097	0.920	0.696	0.363	0.069
	50	0.936	0.745	0.426	0.095	0.928	0.717	0.385	0.075
	100	0.938	0.748	0.427	0.093	0.933	0.730	0.400	0.079
	5	0.902	0.667	0.371	0.107	0.892	0.637	0.331	0.085
	10	0.928	0.737	0.447	0.136	0.916	0.694	0.383	0.099
10	15	0.940	0.770	0.487	0.151	0.927	0.723	0.412	0.107
	25	0.950	0.801	0.525	0.166	0.938	0.756	0.448	0.117
	50	0.959	0.826	0.558	0.178	0.950	0.789	0.489	0.132
	100	0.963	0.839	0.573	0.181	0.957	0.812	0.521	0.145

Table 32. Mode II Normalized Stress Intensity Factor at the Center of a Semi-Elliptic Circumferential Part-Through Crack in an Isotropic Cylindrical Shell with a Fixed End Subjected to Out-of-Plane Shear; $\nu = 0.3$, $l/a = 0.25$.

$$k_2(0)/k_{2v}$$

		OUTER CRACK				INNER CRACK			
		$\xi_0 = l_0/h$							
a/h	R/h	0.2	0.4	0.6	0.8	0.2	0.4	0.6	0.8
	5	0.996	0.958	0.865	0.714	0.996	0.958	0.866	0.717
	10	0.996	0.958	0.865	0.715	0.996	0.958	0.866	0.718
1	15	0.996	0.958	0.864	0.715	0.996	0.958	0.866	0.717
	25	0.996	0.958	0.864	0.714	0.996	0.958	0.866	0.717
	50	0.996	0.958	0.864	0.714	0.996	0.958	0.865	0.717
	100	0.996	0.957	0.864	0.714	0.996	0.958	0.865	0.716
	5	0.999	0.987	0.954	0.880	0.999	0.987	0.954	0.882
	10	0.999	0.987	0.955	0.885	0.999	0.987	0.955	0.886
2	15	0.999	0.987	0.955	0.886	0.999	0.987	0.955	0.887
	25	0.999	0.987	0.955	0.886	0.999	0.987	0.955	0.887
	50	0.999	0.987	0.955	0.886	0.999	0.987	0.955	0.887
	100	0.999	0.987	0.955	0.885	0.999	0.987	0.955	0.887
	5	0.999	0.994	0.977	0.935	0.999	0.994	0.977	0.934
	10	0.999	0.994	0.979	0.942	0.999	0.994	0.979	0.942
3	15	0.999	0.994	0.980	0.943	0.999	0.994	0.980	0.943
	25	0.999	0.994	0.980	0.944	0.999	0.994	0.980	0.944
	50	0.999	0.994	0.980	0.944	0.999	0.994	0.980	0.944
	100	0.999	0.994	0.980	0.943	0.999	0.994	0.980	0.944
	5	1.000	0.998	0.990	0.969	1.000	0.997	0.989	0.967
	10	1.000	0.998	0.993	0.977	1.000	0.998	0.992	0.976
5	15	1.000	0.998	0.993	0.979	1.000	0.998	0.993	0.978
	25	1.000	0.998	0.993	0.980	1.000	0.998	0.993	0.979
	50	1.000	0.998	0.993	0.980	1.000	0.998	0.993	0.980
	100	1.000	0.998	0.993	0.980	1.000	0.998	0.993	0.980
	5	1.000	1.000	0.998	0.992	1.000	1.000	0.998	0.991
	10	1.000	1.000	0.998	0.994	1.000	0.999	0.998	0.993
10	15	1.000	1.000	0.998	0.995	1.000	0.999	0.998	0.994
	25	1.000	1.000	0.999	0.996	1.000	1.000	0.998	0.995
	50	1.000	1.000	0.999	0.996	1.000	1.000	0.999	0.996
	100	1.000	1.000	0.999	0.996	1.000	1.000	0.999	0.996

Table 33. Mode II Normalized Stress Intensity Factor at the Center of a Semi-Elliptic Circumferential Part-Through Crack in an Isotropic Cylindrical Shell with a Fixed End Subjected to Out-of-Plane Shear; $\nu = 0.3$, $l/a = 0.40$.

$$k_2(0)/k_{2\nu}$$

		OUTER CRACK				INNER CRACK			
		$\xi_0 = l_0/h$							
a/h	R/h	0.2	0.4	0.6	0.8	0.2	0.4	0.6	0.8
	5	0.996	0.955	0.856	0.700	0.996	0.955	0.857	0.702
	10	0.996	0.955	0.857	0.702	0.996	0.955	0.857	0.703
1	15	0.996	0.955	0.857	0.702	0.996	0.955	0.857	0.703
	25	0.996	0.955	0.856	0.702	0.996	0.955	0.857	0.703
	50	0.996	0.955	0.856	0.702	0.996	0.955	0.857	0.703
	100	0.996	0.955	0.856	0.701	0.996	0.955	0.857	0.702
	5	0.999	0.986	0.949	0.870	0.999	0.986	0.949	0.872
	10	0.999	0.986	0.952	0.878	0.999	0.986	0.952	0.879
2	15	0.999	0.987	0.952	0.880	0.999	0.987	0.953	0.881
	25	0.999	0.987	0.952	0.880	0.999	0.987	0.953	0.881
	50	0.999	0.987	0.952	0.880	0.999	0.987	0.953	0.881
	100	0.999	0.987	0.952	0.880	0.999	0.987	0.953	0.881
	5	0.999	0.993	0.974	0.926	0.999	0.993	0.973	0.926
	10	0.999	0.994	0.977	0.937	0.999	0.994	0.977	0.937
3	15	0.999	0.994	0.978	0.939	0.999	0.994	0.978	0.940
	25	0.999	0.994	0.978	0.941	0.999	0.994	0.979	0.941
	50	0.999	0.994	0.979	0.941	0.999	0.994	0.979	0.941
	100	0.999	0.994	0.979	0.941	0.999	0.994	0.979	0.941
	5	1.000	0.997	0.989	0.965	1.000	0.997	0.988	0.962
	10	1.000	0.998	0.991	0.974	1.000	0.998	0.991	0.973
5	15	1.000	0.998	0.992	0.976	1.000	0.998	0.992	0.976
	25	1.000	0.998	0.993	0.978	1.000	0.998	0.992	0.978
	50	1.000	0.998	0.993	0.979	1.000	0.998	0.993	0.979
	100	1.000	0.998	0.993	0.979	1.000	0.998	0.993	0.979
	5	1.000	1.000	0.998	0.993	1.000	1.000	0.998	0.991
10	10	1.000	0.999	0.998	0.994	1.000	0.999	0.998	0.992
	15	1.000	1.000	0.998	0.994	1.000	0.999	0.998	0.993
	25	1.000	1.000	0.998	0.995	1.000	1.000	0.998	0.995
	50	1.000	1.000	0.999	0.996	1.000	1.000	0.999	0.996
	100	1.000	1.000	0.999	0.996	1.000	1.000	0.999	0.996

Table 34. Mode II Normalized Stress Intensity Factor at the Center of a Semi-Elliptic Circumferential Part-Through Crack in an Isotropic Cylindrical Shell with a Fixed End Subjected to Out-of-Plane Shear; $\nu = 0.3$, $l/a = 0.5$.

$k_2(0)/k_{2\nu}$

		OUTER CRACK				INNER CRACK			
		$\xi_0 = l_0/h$							
a/h	R/h	0.2	0.4	0.6	0.8	0.2	0.4	0.6	0.8
	5	0.996	0.954	0.853	0.695	0.996	0.954	0.854	0.697
	10	0.996	0.954	0.854	0.698	0.996	0.955	0.855	0.699
1	15	0.996	0.954	0.854	0.698	0.996	0.955	0.855	0.699
	25	0.996	0.954	0.854	0.698	0.996	0.955	0.855	0.699
	50	0.996	0.954	0.854	0.698	0.996	0.955	0.855	0.699
	100	0.996	0.954	0.854	0.698	0.996	0.954	0.854	0.699
	5	0.999	0.985	0.947	0.866	0.999	0.985	0.947	0.868
	10	0.999	0.986	0.951	0.876	0.999	0.986	0.951	0.877
2	15	0.999	0.986	0.951	0.878	0.999	0.986	0.952	0.879
	25	0.999	0.986	0.952	0.879	0.999	0.986	0.952	0.879
	50	0.999	0.986	0.952	0.879	0.999	0.986	0.952	0.879
	100	0.999	0.986	0.952	0.879	0.999	0.986	0.952	0.879
	5	0.999	0.993	0.973	0.923	0.999	0.993	0.972	0.923
	10	0.999	0.994	0.977	0.935	0.999	0.994	0.976	0.935
3	15	0.999	0.994	0.978	0.938	0.999	0.994	0.977	0.938
	25	0.999	0.994	0.978	0.940	0.999	0.994	0.978	0.940
	50	0.999	0.994	0.978	0.940	0.999	0.994	0.978	0.940
	100	0.999	0.994	0.978	0.940	0.999	0.994	0.978	0.941
	5	1.000	0.997	0.989	0.964	1.000	0.997	0.987	0.962
	10	1.000	0.998	0.991	0.973	1.000	0.997	0.990	0.972
5	15	1.000	0.998	0.992	0.976	1.000	0.998	0.992	0.975
	25	1.000	0.998	0.992	0.978	1.000	0.998	0.992	0.977
	50	1.000	0.998	0.993	0.978	1.000	0.998	0.993	0.978
	100	1.000	0.998	0.993	0.979	1.000	0.998	0.993	0.979
	5	1.000	1.000	0.998	0.992	1.000	0.999	0.998	0.991
	10	1.000	0.999	0.998	0.994	1.000	0.999	0.998	0.992
10	15	1.000	1.000	0.998	0.994	1.000	0.999	0.998	0.993
	25	1.000	1.000	0.998	0.995	1.000	1.000	0.998	0.994
	50	1.000	1.000	0.999	0.996	1.000	1.000	0.998	0.996
	100	1.000	1.000	0.999	0.996	1.000	1.000	0.999	0.996

Table 35. Mode II Normalized Stress Intensity Factor at the Center of a Semi-Elliptic Circumferential Part-Through Crack in an Isotropic Cylindrical Shell with a Fixed End Subjected to Out-of-Plane Shear; $\nu = 0.3$, $l/a = 1.0$.

$$k_2(0)/k_{2\nu}$$

		OUTER CRACK				INNER CRACK			
		$\xi_0 = l_0/h$							
a/h	R/h	0.2	0.4	0.6	0.8	0.2	0.4	0.6	0.8
	5	0.996	0.953	0.848	0.687	0.996	0.953	0.849	0.688
	10	0.996	0.953	0.851	0.693	0.996	0.954	0.851	0.693
1	15	0.996	0.954	0.852	0.694	0.996	0.954	0.852	0.694
	25	0.996	0.954	0.852	0.694	0.996	0.954	0.852	0.694
	50	0.996	0.954	0.852	0.694	0.996	0.954	0.852	0.694
	100	0.996	0.954	0.852	0.694	0.996	0.954	0.852	0.694
	5	0.999	0.985	0.944	0.860	0.999	0.985	0.944	0.861
	10	0.999	0.986	0.949	0.872	0.999	0.986	0.949	0.872
2	15	0.999	0.986	0.950	0.874	0.999	0.986	0.950	0.875
	25	0.999	0.986	0.951	0.876	0.999	0.986	0.951	0.876
	50	0.999	0.986	0.951	0.877	0.999	0.986	0.951	0.877
	100	0.999	0.986	0.951	0.877	0.999	0.986	0.951	0.877
	5	0.999	0.992	0.972	0.921	0.999	0.992	0.971	0.920
	10	0.999	0.993	0.976	0.933	0.999	0.993	0.975	0.933
3	15	0.999	0.994	0.977	0.936	0.999	0.994	0.977	0.936
	25	0.999	0.994	0.977	0.938	0.999	0.994	0.977	0.938
	50	0.999	0.994	0.978	0.939	0.999	0.994	0.978	0.939
	100	0.999	0.994	0.978	0.939	0.999	0.994	0.978	0.939
	5	1.000	0.997	0.989	0.964	1.000	0.997	0.987	0.961
	10	1.000	0.998	0.991	0.973	1.000	0.997	0.990	0.971
5	15	1.000	0.998	0.992	0.975	1.000	0.998	0.991	0.974
	25	1.000	0.998	0.992	0.977	1.000	0.998	0.992	0.976
	50	1.000	0.998	0.993	0.978	1.000	0.998	0.992	0.978
	100	1.000	0.998	0.993	0.978	1.000	0.998	0.993	0.978
	5	1.000	1.000	0.998	0.992	1.000	0.999	0.998	0.990
	10	1.000	0.999	0.998	0.994	1.000	0.999	0.998	0.992
10	15	1.000	1.000	0.998	0.994	1.000	0.999	0.998	0.993
	25	1.000	1.000	0.998	0.995	1.000	0.999	0.998	0.994
	50	1.000	1.000	0.999	0.996	1.000	1.000	0.998	0.995
	100	1.000	1.000	0.999	0.996	1.000	1.000	0.999	0.996

Table 36. Mode II Normalized Stress Intensity Factor at the Center of a Semi-Elliptic Circumferential Part-Through Crack in an Isotropic Cylindrical Shell with a Fixed End Subjected to Out-of-Plane Shear; $\nu = 0.3$, $l/a = 1.5$.

$k_2(0)/k_{2\nu}$

		OUTER CRACK				INNER CRACK			
		$\xi_0 = l_0/h$							
a/h	R/h	0.2	0.4	0.6	0.8	0.2	0.4	0.6	0.8
	5	0.996	0.952	0.847	0.685	0.996	0.953	0.848	0.686
	10	0.996	0.953	0.850	0.691	0.996	0.953	0.851	0.692
1	15	0.996	0.953	0.851	0.693	0.996	0.954	0.851	0.693
	25	0.996	0.954	0.851	0.693	0.996	0.954	0.852	0.693
	50	0.996	0.954	0.852	0.694	0.996	0.954	0.852	0.694
	100	0.996	0.954	0.852	0.694	0.996	0.954	0.852	0.694
	5	0.999	0.985	0.944	0.860	0.999	0.985	0.944	0.861
	10	0.999	0.986	0.949	0.871	0.999	0.986	0.949	0.872
2	15	0.999	0.986	0.950	0.874	0.999	0.986	0.950	0.874
	25	0.999	0.986	0.950	0.876	0.999	0.986	0.950	0.876
	50	0.999	0.986	0.951	0.876	0.999	0.986	0.951	0.877
	100	0.999	0.986	0.951	0.877	0.999	0.986	0.951	0.877
	5	0.999	0.992	0.972	0.921	0.999	0.992	0.971	0.920
	10	0.999	0.993	0.976	0.933	0.999	0.993	0.975	0.932
3	15	0.999	0.994	0.977	0.936	0.999	0.994	0.976	0.936
	25	0.999	0.994	0.977	0.938	0.999	0.994	0.977	0.938
	50	0.999	0.994	0.978	0.939	0.999	0.994	0.978	0.939
	100	0.999	0.994	0.978	0.939	0.999	0.994	0.978	0.939
	5	1.000	0.997	0.989	0.964	1.000	0.997	0.987	0.961
	10	1.000	0.998	0.991	0.973	1.000	0.997	0.990	0.971
5	15	1.000	0.998	0.992	0.975	1.000	0.998	0.991	0.974
	25	1.000	0.998	0.992	0.977	1.000	0.998	0.992	0.976
	50	1.000	0.998	0.993	0.978	1.000	0.998	0.992	0.978
	100	1.000	0.998	0.993	0.978	1.000	0.998	0.993	0.978
	5	1.000	1.000	0.998	0.992	1.000	0.999	0.998	0.990
	10	1.000	0.999	0.998	0.994	1.000	0.999	0.997	0.992
10	15	1.000	1.000	0.998	0.994	1.000	0.999	0.998	0.993
	25	1.000	1.000	0.998	0.995	1.000	0.999	0.998	0.994
	50	1.000	1.000	0.999	0.996	1.000	1.000	0.998	0.995
	100	1.000	1.000	0.999	0.996	1.000	1.000	0.999	0.996

Table 37. Mode II Normalized Stress Intensity Factor at the Center of a Semi-Elliptic Circumferential Part-Through Crack in an Isotropic Cylindrical Shell with a Fixed End Subjected to Out-of-Plane Shear; $\nu = 0.3$, $l/a = 2.5$.

$$k_2(0)/k_{2V}$$

		OUTER CRACK				INNER CRACK			
		$\xi_0 = l_0/h$							
a/h	R/h	0.2	0.4	0.6	0.8	0.2	0.4	0.6	0.8
	5	0.996	0.952	0.847	0.685	0.996	0.952	0.847	0.685
	10	0.996	0.953	0.850	0.691	0.996	0.953	0.850	0.691
1	15	0.996	0.953	0.851	0.692	0.996	0.953	0.851	0.692
	25	0.996	0.954	0.851	0.693	0.996	0.954	0.851	0.693
	50	0.996	0.954	0.851	0.693	0.996	0.954	0.851	0.693
	100	0.996	0.954	0.851	0.693	0.996	0.954	0.851	0.693
	5	0.999	0.985	0.944	0.860	0.999	0.985	0.944	0.861
	10	0.999	0.986	0.949	0.871	0.999	0.986	0.949	0.872
2	15	0.999	0.986	0.950	0.874	0.999	0.986	0.950	0.874
	25	0.999	0.986	0.950	0.875	0.999	0.986	0.950	0.876
	50	0.999	0.986	0.951	0.876	0.999	0.986	0.951	0.876
	100	0.999	0.986	0.951	0.877	0.999	0.986	0.951	0.877
	5	0.999	0.992	0.972	0.921	0.999	0.992	0.971	0.920
	10	0.999	0.993	0.976	0.933	0.999	0.993	0.975	0.932
3	15	0.999	0.994	0.977	0.936	0.999	0.994	0.976	0.936
	25	0.999	0.994	0.977	0.938	0.999	0.994	0.977	0.938
	50	0.999	0.994	0.978	0.939	0.999	0.994	0.978	0.939
	100	0.999	0.994	0.978	0.939	0.999	0.994	0.978	0.939
	5	1.000	0.997	0.989	0.964	1.000	0.997	0.987	0.961
	10	1.000	0.998	0.991	0.973	1.000	0.997	0.990	0.971
5	15	1.000	0.998	0.992	0.975	1.000	0.998	0.991	0.974
	25	1.000	0.998	0.992	0.977	1.000	0.998	0.992	0.976
	50	1.000	0.998	0.993	0.978	1.000	0.998	0.992	0.978
	100	1.000	0.998	0.993	0.978	1.000	0.998	0.993	0.978
	5	1.000	1.000	0.998	0.992	1.000	0.999	0.998	0.990
	10	1.000	0.999	0.998	0.994	1.000	0.999	0.997	0.992
10	15	1.000	1.000	0.998	0.994	1.000	0.999	0.998	0.993
	25	1.000	1.000	0.998	0.995	1.000	0.999	0.998	0.994
	50	1.000	1.000	0.999	0.996	1.000	1.000	0.998	0.995
	100	1.000	1.000	0.999	0.996	1.000	1.000	0.999	0.996

Table 38. Mode II Normalized Stress Intensity Factor at the Center of a Semi-Elliptic Circumferential Part-Through Crack in an Isotropic Cylindrical Shell with a Fixed End Subjected to Out-of-Plane Shear; $\nu = 0.3$, $l/a = 5.0$.

$$k_2(0)/k_{2\nu}$$

		OUTER CRACK				INNER CRACK			
		$\xi_0 = l_0/h$							
a/h	R/h	0.2	0.4	0.6	0.8	0.2	0.4	0.6	0.8
	5	0.996	0.952	0.847	0.685	0.996	0.952	0.847	0.685
	10	0.996	0.953	0.850	0.691	0.996	0.953	0.850	0.691
1	15	0.996	0.953	0.851	0.692	0.996	0.953	0.851	0.692
	25	0.996	0.954	0.851	0.693	0.996	0.954	0.851	0.693
	50	0.996	0.954	0.851	0.693	0.996	0.954	0.851	0.693
	100	0.996	0.954	0.851	0.693	0.996	0.954	0.851	0.693
	5	0.999	0.985	0.944	0.860	0.999	0.985	0.944	0.861
	10	0.999	0.986	0.949	0.871	0.999	0.986	0.949	0.872
2	15	0.999	0.986	0.950	0.874	0.999	0.986	0.950	0.874
	25	0.999	0.986	0.950	0.875	0.999	0.986	0.950	0.876
	50	0.999	0.986	0.951	0.876	0.999	0.986	0.951	0.876
	100	0.999	0.986	0.951	0.877	0.999	0.986	0.951	0.877
	5	0.999	0.992	0.972	0.921	0.999	0.992	0.971	0.920
	10	0.999	0.993	0.976	0.933	0.999	0.993	0.975	0.932
3	15	0.999	0.994	0.977	0.936	0.999	0.994	0.976	0.936
	25	0.999	0.994	0.977	0.938	0.999	0.994	0.977	0.938
	50	0.999	0.994	0.978	0.939	0.999	0.994	0.978	0.939
	100	0.999	0.994	0.978	0.939	0.999	0.994	0.978	0.939
	5	1.000	0.997	0.989	0.964	1.000	0.997	0.987	0.961
	10	1.000	0.998	0.991	0.973	1.000	0.997	0.990	0.971
5	15	1.000	0.998	0.992	0.975	1.000	0.998	0.991	0.974
	25	1.000	0.998	0.992	0.977	1.000	0.998	0.992	0.976
	50	1.000	0.998	0.993	0.978	1.000	0.998	0.992	0.978
	100	1.000	0.998	0.993	0.978	1.000	0.998	0.993	0.978
	5	1.000	1.000	0.998	0.992	1.000	0.999	0.998	0.990
	10	1.000	0.999	0.998	0.994	1.000	0.999	0.997	0.992
10	15	1.000	1.000	0.998	0.994	1.000	0.999	0.998	0.993
	25	1.000	1.000	0.998	0.995	1.000	0.999	0.998	0.994
	50	1.000	1.000	0.999	0.996	1.000	1.000	0.998	0.995
	100	1.000	1.000	0.999	0.996	1.000	1.000	0.999	0.996

Table 39. Mode II Normalized Stress Intensity Factor at the Center of a Semi-Elliptic Circumferential Part-Through Crack in an Isotropic Cylindrical Shell with a Fixed End Subjected to Out-of-Plane Shear; $\nu = 0.3$, $l/a = 50$.

$$k_2(0)/k_{2v}$$

		OUTER CRACK				INNER CRACK			
		$\xi_0 = l_0/h$							
a/h	R/h	0.2	0.4	0.6	0.8	0.2	0.4	0.6	0.8
	5	0.996	0.952	0.847	0.685	0.996	0.952	0.847	0.685
	10	0.996	0.953	0.850	0.691	0.996	0.953	0.850	0.691
1	15	0.996	0.953	0.851	0.692	0.996	0.953	0.851	0.692
	25	0.996	0.954	0.851	0.693	0.996	0.954	0.851	0.693
	50	0.996	0.954	0.851	0.693	0.996	0.954	0.851	0.693
	100	0.996	0.954	0.851	0.693	0.996	0.954	0.851	0.693
	5	0.999	0.985	0.944	0.860	0.999	0.985	0.944	0.861
	10	0.999	0.986	0.949	0.871	0.999	0.986	0.949	0.872
2	15	0.999	0.986	0.950	0.874	0.999	0.986	0.950	0.874
	25	0.999	0.986	0.950	0.875	0.999	0.986	0.950	0.876
	50	0.999	0.986	0.951	0.876	0.999	0.986	0.951	0.876
	100	0.999	0.986	0.951	0.877	0.999	0.986	0.951	0.877
	5	0.999	0.992	0.972	0.921	0.999	0.992	0.971	0.920
	10	0.999	0.993	0.976	0.933	0.999	0.993	0.975	0.932
3	15	0.999	0.994	0.977	0.936	0.999	0.994	0.976	0.936
	25	0.999	0.994	0.977	0.938	0.999	0.994	0.977	0.938
	50	0.999	0.994	0.978	0.939	0.999	0.994	0.978	0.939
	100	0.999	0.994	0.978	0.939	0.999	0.994	0.978	0.939
	5	1.000	0.997	0.989	0.964	1.000	0.997	0.987	0.961
	10	1.000	0.998	0.991	0.973	1.000	0.997	0.990	0.971
5	15	1.000	0.998	0.992	0.975	1.000	0.998	0.991	0.974
	25	1.000	0.998	0.992	0.977	1.000	0.998	0.992	0.976
	50	1.000	0.998	0.993	0.978	1.000	0.998	0.992	0.978
	100	1.000	0.998	0.993	0.978	1.000	0.998	0.993	0.978
	5	1.000	1.000	0.998	0.992	1.000	0.999	0.998	0.990
	10	1.000	0.999	0.998	0.994	1.000	0.999	0.997	0.992
10	15	1.000	1.000	0.998	0.994	1.000	0.999	0.998	0.993
	25	1.000	1.000	0.998	0.995	1.000	0.999	0.998	0.994
	50	1.000	1.000	0.999	0.996	1.000	1.000	0.998	0.995
	100	1.000	1.000	0.999	0.996	1.000	1.000	0.999	0.996

Table 40. Mode III Normalized Stress Intensity Factor at the Center of a Semi-Elliptic Circumferential Part-Through Crack in an Isotropic Cylindrical Shell with a Fixed End Subjected to In-Plane Shear; $\nu = 0.3$, $l/a = 0.25$.

$$k_3(0)/k_{3s}$$

		OUTER CRACK				INNER CRACK			
		$\xi_0 = l_0/h$							
a/h	R/h	0.2	0.4	0.6	0.8	0.2	0.4	0.6	0.8
	5	0.773	0.617	0.589	0.539	0.794	0.649	0.621	0.551
	10	0.773	0.617	0.589	0.538	0.793	0.648	0.620	0.549
1	15	0.773	0.617	0.589	0.537	0.793	0.647	0.619	0.549
	25	0.773	0.617	0.589	0.537	0.793	0.647	0.619	0.548
	50	0.773	0.617	0.589	0.537	0.792	0.647	0.618	0.548
	100	0.773	0.617	0.589	0.537	0.792	0.646	0.618	0.548
	5	0.820	0.680	0.667	0.662	0.836	0.708	0.699	0.682
	10	0.821	0.681	0.667	0.661	0.835	0.706	0.695	0.677
2	15	0.821	0.682	0.668	0.660	0.834	0.705	0.694	0.676
	25	0.821	0.682	0.668	0.661	0.834	0.704	0.693	0.675
	50	0.821	0.682	0.669	0.661	0.834	0.703	0.692	0.675
	100	0.822	0.683	0.669	0.661	0.833	0.703	0.692	0.674
	5	0.831	0.699	0.697	0.722	0.844	0.723	0.726	0.743
	10	0.831	0.699	0.697	0.718	0.843	0.720	0.722	0.737
3	15	0.832	0.700	0.697	0.718	0.843	0.719	0.720	0.735
	25	0.832	0.701	0.698	0.718	0.842	0.718	0.719	0.733
	50	0.833	0.701	0.699	0.718	0.842	0.717	0.718	0.732
	100	0.833	0.702	0.699	0.718	0.841	0.717	0.717	0.731
	5	0.838	0.713	0.725	0.785	0.848	0.731	0.748	0.805
	10	0.838	0.712	0.722	0.777	0.847	0.729	0.744	0.796
5	15	0.838	0.713	0.722	0.775	0.846	0.728	0.742	0.792
	25	0.839	0.713	0.722	0.774	0.846	0.727	0.740	0.789
	50	0.839	0.714	0.723	0.774	0.845	0.726	0.738	0.787
	100	0.839	0.715	0.724	0.774	0.845	0.725	0.737	0.786
	5	0.843	0.725	0.752	0.852	0.846	0.732	0.761	0.861
	10	0.842	0.723	0.747	0.839	0.847	0.732	0.759	0.852
10	15	0.842	0.722	0.744	0.833	0.847	0.732	0.758	0.847
	25	0.842	0.722	0.743	0.829	0.847	0.731	0.756	0.842
	50	0.842	0.722	0.742	0.826	0.847	0.730	0.754	0.838
	100	0.842	0.723	0.743	0.825	0.846	0.730	0.752	0.835

Table 41. Mode III Normalized Stress Intensity Factor at the Center of a Semi-Elliptic Circumferential Part-Through Crack in an Isotropic Cylindrical Shell with a Fixed End Subjected to In-Plane Shear Loading; $\nu = 0.3$, $l/a = 0.40$.

$k_3(0)/k_{3s}$

		OUTER CRACK				INNER CRACK			
		$\xi_0 = l_0/h$							
a/h	R/h	0.2	0.4	0.6	0.8	0.2	0.4	0.6	0.8
	5	0.780	0.616	0.575	0.512	0.802	0.650	0.608	0.526
	10	0.779	0.616	0.575	0.511	0.800	0.648	0.606	0.523
1	15	0.779	0.616	0.575	0.510	0.800	0.648	0.605	0.523
	25	0.779	0.617	0.575	0.510	0.799	0.647	0.605	0.522
	50	0.779	0.617	0.575	0.510	0.799	0.646	0.604	0.522
	100	0.779	0.617	0.576	0.510	0.799	0.646	0.604	0.522
	5	0.821	0.677	0.656	0.639	0.838	0.707	0.690	0.661
	10	0.821	0.678	0.656	0.636	0.836	0.704	0.685	0.655
2	15	0.822	0.678	0.656	0.636	0.835	0.702	0.683	0.653
	25	0.822	0.679	0.657	0.636	0.835	0.701	0.682	0.652
	50	0.822	0.680	0.658	0.636	0.834	0.700	0.681	0.651
	100	0.823	0.680	0.658	0.636	0.834	0.700	0.680	0.651
	5	0.831	0.696	0.689	0.705	0.845	0.722	0.721	0.730
	10	0.831	0.696	0.688	0.699	0.844	0.719	0.715	0.720
3	15	0.832	0.697	0.688	0.697	0.843	0.717	0.713	0.717
	25	0.832	0.698	0.689	0.697	0.842	0.716	0.711	0.715
	50	0.833	0.699	0.690	0.697	0.842	0.715	0.709	0.713
	100	0.833	0.699	0.690	0.698	0.841	0.714	0.708	0.712
	5	0.837	0.712	0.722	0.779	0.848	0.731	0.747	0.801
	10	0.838	0.710	0.717	0.766	0.847	0.729	0.741	0.787
5	15	0.838	0.711	0.717	0.762	0.847	0.727	0.738	0.782
	25	0.838	0.711	0.716	0.760	0.846	0.726	0.735	0.778
	50	0.839	0.712	0.717	0.759	0.845	0.725	0.733	0.774
	100	0.839	0.713	0.718	0.760	0.845	0.724	0.732	0.772
	5	0.843	0.725	0.752	0.852	0.846	0.732	0.761	0.862
	10	0.842	0.723	0.746	0.839	0.847	0.732	0.759	0.852
10	15	0.842	0.722	0.743	0.831	0.847	0.732	0.757	0.846
	25	0.842	0.721	0.741	0.824	0.847	0.731	0.755	0.839
	50	0.842	0.721	0.740	0.819	0.847	0.730	0.752	0.832
	100	0.842	0.721	0.740	0.817	0.846	0.729	0.750	0.829

Table 42. Mode III Normalized Stress Intensity Factor at the Center of a Semi-Elliptic Circumferential Part-Through Crack in an Isotropic Cylindrical Shell with a Fixed End Subjected to In-Plane Shear; $\nu = 0.3$, $l/a = 0.5$.

$k_3(0)/k_{3s}$

		OUTER CRACK				INNER CRACK			
		$\xi_0 = l_0/h$							
a/h	R/h	0.2	0.4	0.6	0.8	0.2	0.4	0.6	0.8
	5	0.784	0.618	0.571	0.503	0.804	0.650	0.603	0.517
	10	0.784	0.618	0.571	0.501	0.803	0.648	0.600	0.514
1	15	0.784	0.618	0.571	0.501	0.802	0.647	0.600	0.514
	25	0.784	0.618	0.572	0.501	0.802	0.647	0.599	0.513
	50	0.784	0.619	0.572	0.501	0.802	0.646	0.598	0.513
	100	0.784	0.619	0.572	0.501	0.801	0.646	0.598	0.512
	5	0.822	0.677	0.653	0.632	0.838	0.706	0.686	0.655
	10	0.822	0.678	0.653	0.629	0.836	0.702	0.681	0.648
2	15	0.823	0.678	0.653	0.628	0.835	0.701	0.679	0.646
	25	0.823	0.679	0.654	0.628	0.835	0.700	0.678	0.644
	50	0.824	0.680	0.655	0.628	0.834	0.699	0.676	0.643
	100	0.824	0.680	0.655	0.629	0.834	0.698	0.676	0.643
	5	0.831	0.696	0.688	0.701	0.845	0.722	0.719	0.726
	10	0.832	0.696	0.686	0.694	0.844	0.718	0.713	0.715
3	15	0.832	0.697	0.686	0.692	0.843	0.716	0.710	0.711
	25	0.833	0.698	0.687	0.691	0.842	0.715	0.708	0.709
	50	0.833	0.698	0.688	0.691	0.842	0.714	0.706	0.707
	100	0.834	0.699	0.688	0.692	0.841	0.713	0.705	0.706
	5	0.838	0.712	0.722	0.779	0.848	0.731	0.746	0.801
	10	0.838	0.711	0.717	0.764	0.847	0.728	0.740	0.786
5	15	0.838	0.711	0.716	0.759	0.847	0.727	0.737	0.779
	25	0.839	0.711	0.715	0.756	0.846	0.725	0.734	0.774
	50	0.839	0.712	0.716	0.755	0.845	0.724	0.731	0.770
	100	0.840	0.713	0.717	0.755	0.845	0.723	0.730	0.768
	5	0.843	0.725	0.752	0.852	0.846	0.732	0.761	0.862
	10	0.842	0.723	0.747	0.839	0.847	0.732	0.759	0.852
10	15	0.842	0.722	0.744	0.832	0.847	0.732	0.757	0.846
	25	0.842	0.721	0.741	0.824	0.847	0.731	0.754	0.838
	50	0.842	0.721	0.739	0.818	0.847	0.730	0.751	0.831
	100	0.842	0.721	0.739	0.815	0.846	0.729	0.749	0.827

Table 43. Mode III Normalized Stress Intensity Factor at the Center of a Semi-Elliptic Circumferential Part-Through Crack in an Isotropic Cylindrical Shell with a Fixed End Subjected to In-PLane Shear; $\nu = 0.3$, $l/a = 1.0$.

$$k_3(0)/k_{3s}$$

		OUTER CRACK				INNER CRACK			
		$\xi_0 = l_0/h$							
a/h	R/h	0.2	0.4	0.6	0.8	0.2	0.4	0.6	0.8
	5	0.793	0.626	0.570	0.490	0.806	0.647	0.592	0.501
	10	0.794	0.627	0.570	0.488	0.805	0.645	0.588	0.498
1	15	0.794	0.627	0.570	0.488	0.804	0.644	0.587	0.497
	25	0.794	0.627	0.571	0.488	0.804	0.643	0.586	0.496
	50	0.795	0.628	0.571	0.488	0.804	0.643	0.586	0.496
	100	0.795	0.628	0.571	0.488	0.803	0.642	0.585	0.496
	5	0.824	0.680	0.654	0.629	0.836	0.702	0.680	0.647
	10	0.825	0.681	0.653	0.622	0.835	0.698	0.673	0.637
2	15	0.826	0.681	0.653	0.621	0.834	0.697	0.671	0.634
	25	0.826	0.682	0.654	0.620	0.833	0.695	0.669	0.632
	50	0.827	0.683	0.654	0.620	0.833	0.694	0.667	0.630
	100	0.827	0.684	0.655	0.621	0.832	0.693	0.666	0.629
	5	0.833	0.698	0.691	0.702	0.844	0.719	0.716	0.723
	10	0.833	0.698	0.688	0.692	0.842	0.715	0.708	0.709
3	15	0.834	0.699	0.687	0.689	0.842	0.713	0.705	0.704
	25	0.835	0.700	0.687	0.687	0.841	0.712	0.702	0.700
	50	0.835	0.701	0.688	0.686	0.840	0.710	0.699	0.697
	100	0.836	0.701	0.688	0.686	0.840	0.709	0.698	0.695
	5	0.838	0.713	0.724	0.781	0.847	0.729	0.745	0.800
	10	0.839	0.712	0.719	0.766	0.846	0.727	0.738	0.784
5	15	0.839	0.712	0.718	0.761	0.846	0.725	0.734	0.777
	25	0.840	0.713	0.717	0.756	0.845	0.723	0.731	0.770
	50	0.840	0.713	0.716	0.753	0.844	0.722	0.727	0.764
	100	0.841	0.714	0.717	0.752	0.844	0.720	0.725	0.761
	5	0.843	0.725	0.752	0.852	0.846	0.732	0.761	0.861
	10	0.842	0.723	0.747	0.839	0.847	0.732	0.758	0.851
10	15	0.842	0.723	0.745	0.833	0.847	0.731	0.756	0.845
	25	0.842	0.722	0.742	0.826	0.846	0.730	0.753	0.838
	50	0.843	0.722	0.741	0.819	0.846	0.729	0.750	0.830
	100	0.843	0.722	0.740	0.816	0.846	0.728	0.747	0.824

Table 44. Mode III Normalized Stress Intensity Factor at the Center of a Semi-Elliptic Circumferential Part-Through Crack in an Isotropic Cylindrical Shell with a Fixed End Subjected to In-Plane Shear; $\nu = 0.3$, $l/a = 1.5$

$k_3(0)/k_{3s}$

		OUTER CRACK				INNER CRACK			
		$\xi_0 = l_0/h$							
a/h	R/h	0.2	0.4	0.6	0.8	0.2	0.4	0.6	0.8
	5	0.796	0.629	0.572	0.490	0.805	0.645	0.589	0.499
	10	0.797	0.630	0.572	0.488	0.804	0.643	0.585	0.495
1	15	0.797	0.630	0.572	0.488	0.804	0.642	0.584	0.494
	25	0.797	0.631	0.573	0.487	0.803	0.641	0.583	0.493
	50	0.798	0.631	0.573	0.487	0.803	0.640	0.582	0.492
	100	0.798	0.632	0.574	0.488	0.803	0.640	0.582	0.492
	5	0.825	0.682	0.657	0.631	0.835	0.700	0.678	0.646
	10	0.826	0.683	0.655	0.624	0.834	0.696	0.671	0.636
2	15	0.827	0.683	0.655	0.622	0.833	0.695	0.669	0.633
	25	0.827	0.684	0.655	0.621	0.833	0.693	0.666	0.630
	50	0.828	0.685	0.656	0.621	0.832	0.692	0.665	0.627
	100	0.828	0.685	0.657	0.621	0.832	0.691	0.664	0.627
	5	0.833	0.699	0.692	0.704	0.843	0.718	0.715	0.723
	10	0.834	0.700	0.689	0.694	0.842	0.714	0.707	0.709
3	15	0.835	0.700	0.689	0.691	0.841	0.712	0.703	0.703
	25	0.835	0.701	0.689	0.688	0.840	0.710	0.700	0.699
	50	0.836	0.702	0.689	0.687	0.840	0.709	0.698	0.695
	100	0.836	0.702	0.689	0.687	0.839	0.708	0.696	0.693
	5	0.838	0.714	0.724	0.781	0.847	0.729	0.744	0.799
	10	0.839	0.713	0.720	0.767	0.846	0.726	0.737	0.784
5	15	0.839	0.713	0.719	0.762	0.845	0.725	0.734	0.777
	25	0.840	0.713	0.718	0.758	0.845	0.723	0.730	0.770
	50	0.841	0.714	0.718	0.755	0.844	0.721	0.726	0.764
	100	0.841	0.715	0.718	0.753	0.844	0.720	0.724	0.760
	5	0.843	0.725	0.752	0.852	0.846	0.732	0.761	0.861
	10	0.842	0.723	0.747	0.839	0.847	0.732	0.758	0.851
10	15	0.842	0.723	0.745	0.833	0.847	0.731	0.756	0.845
	25	0.842	0.722	0.743	0.826	0.846	0.730	0.753	0.838
	50	0.843	0.722	0.741	0.820	0.846	0.729	0.750	0.830
	100	0.843	0.723	0.740	0.817	0.846	0.727	0.747	0.824

Table 45. Mode III Normalized Stress Intensity Factor at the Center of a Semi-Elliptic Circumferential Part-Through Crack in an Isotropic Cylindrical Shell with a Fixed End Subjected to In-Plane Shear; $\nu = 0.3$, $l/a = 2.5$.

$k_3(0)/k_{3s}$

		OUTER CRACK				INNER CRACK			
		$\xi_0 = l_0/h$							
a/h	R/h	0.2	0.4	0.6	0.8	0.2	0.4	0.6	0.8
	5	0.797	0.631	0.574	0.492	0.805	0.644	0.587	0.498
	10	0.798	0.632	0.574	0.489	0.803	0.641	0.583	0.494
1	15	0.798	0.633	0.574	0.488	0.803	0.640	0.582	0.492
	25	0.799	0.633	0.575	0.488	0.802	0.639	0.581	0.491
	50	0.799	0.634	0.575	0.488	0.802	0.638	0.580	0.491
	100	0.799	0.634	0.575	0.488	0.802	0.638	0.579	0.490
	5	0.826	0.683	0.658	0.632	0.835	0.700	0.677	0.646
	10	0.827	0.684	0.657	0.626	0.833	0.695	0.670	0.636
2	15	0.828	0.685	0.657	0.624	0.833	0.694	0.668	0.632
	25	0.828	0.685	0.657	0.623	0.832	0.692	0.665	0.629
	50	0.829	0.686	0.658	0.622	0.831	0.691	0.663	0.626
	100	0.829	0.687	0.658	0.622	0.831	0.690	0.662	0.625
	5	0.833	0.700	0.692	0.704	0.843	0.718	0.714	0.722
	10	0.834	0.700	0.690	0.695	0.841	0.713	0.706	0.708
3	15	0.835	0.701	0.690	0.692	0.841	0.711	0.703	0.703
	25	0.836	0.702	0.690	0.690	0.840	0.710	0.700	0.698
	50	0.836	0.703	0.690	0.688	0.839	0.708	0.697	0.694
	100	0.837	0.703	0.691	0.688	0.839	0.707	0.695	0.692
	5	0.839	0.714	0.724	0.781	0.847	0.729	0.744	0.799
	10	0.839	0.713	0.720	0.767	0.846	0.726	0.737	0.783
5	15	0.839	0.713	0.719	0.762	0.845	0.724	0.733	0.776
	25	0.840	0.714	0.718	0.758	0.845	0.722	0.730	0.770
	50	0.841	0.715	0.718	0.756	0.844	0.720	0.726	0.763
	100	0.841	0.715	0.719	0.754	0.843	0.719	0.724	0.760
	5	0.843	0.725	0.752	0.852	0.846	0.732	0.760	0.861
	10	0.842	0.723	0.747	0.839	0.847	0.732	0.758	0.851
10	15	0.842	0.723	0.745	0.833	0.847	0.731	0.756	0.845
	25	0.842	0.722	0.743	0.826	0.846	0.730	0.753	0.837
	50	0.843	0.722	0.741	0.820	0.846	0.729	0.749	0.829
	100	0.843	0.723	0.741	0.817	0.845	0.727	0.747	0.824

Table 46. Mode III Normalized Stress Intensity Factor at the Center of a Semi-Elliptic Circumferential Part-Through Crack in an Isotropic Cylindrical Shell with a Fixed End Subjected to In-Plane Shear; $\nu = 0.3$, $l/a = 5.0$.

$k_3(0)/k_{3s}$

		OUTER CRACK				INNER CRACK			
		$\xi_0 = l_0/h$							
a/h	R/h	0.2	0.4	0.6	0.8	0.2	0.4	0.6	0.8
1	5	0.797	0.632	0.575	0.492	0.804	0.643	0.586	0.498
	10	0.799	0.633	0.575	0.490	0.803	0.640	0.582	0.494
	15	0.799	0.634	0.576	0.489	0.802	0.639	0.581	0.492
	25	0.799	0.634	0.576	0.489	0.802	0.638	0.580	0.491
	50	0.800	0.635	0.576	0.489	0.801	0.637	0.579	0.490
	100	0.800	0.635	0.577	0.489	0.801	0.637	0.578	0.490
2	5	0.826	0.683	0.658	0.632	0.835	0.699	0.677	0.645
	10	0.827	0.684	0.657	0.626	0.833	0.695	0.670	0.635
	15	0.828	0.685	0.657	0.625	0.832	0.693	0.667	0.632
	25	0.828	0.686	0.658	0.624	0.832	0.692	0.665	0.629
	50	0.829	0.687	0.658	0.623	0.831	0.690	0.663	0.626
	100	0.829	0.687	0.659	0.623	0.831	0.690	0.661	0.625
3	5	0.833	0.700	0.692	0.704	0.843	0.717	0.714	0.722
	10	0.835	0.701	0.690	0.695	0.841	0.713	0.706	0.708
	15	0.835	0.701	0.690	0.692	0.840	0.711	0.702	0.703
	25	0.836	0.702	0.690	0.690	0.840	0.709	0.699	0.698
	50	0.837	0.703	0.691	0.689	0.839	0.708	0.696	0.694
	100	0.837	0.704	0.691	0.689	0.838	0.707	0.695	0.692
5	5	0.839	0.714	0.724	0.781	0.847	0.729	0.744	0.798
	10	0.839	0.713	0.720	0.767	0.846	0.726	0.737	0.783
	15	0.840	0.713	0.719	0.762	0.845	0.724	0.733	0.776
	25	0.840	0.714	0.718	0.758	0.845	0.722	0.729	0.769
	50	0.841	0.715	0.718	0.756	0.844	0.720	0.726	0.763
	100	0.841	0.715	0.719	0.755	0.843	0.719	0.724	0.760
10	5	0.843	0.725	0.752	0.852	0.846	0.732	0.760	0.861
	10	0.842	0.723	0.747	0.839	0.847	0.732	0.758	0.851
	15	0.842	0.723	0.745	0.833	0.847	0.731	0.756	0.845
	25	0.842	0.722	0.743	0.826	0.846	0.730	0.753	0.837
	50	0.843	0.722	0.741	0.820	0.846	0.729	0.749	0.829
	100	0.843	0.723	0.741	0.817	0.845	0.727	0.747	0.824

Table 47. Mode III Normalized Stress Intensity Factor at the Center of a Semi-Elliptic Circumferential Part-Through Crack in an Isotropic Cylindrical Shell with a Fixed End Subjected to In-Plane Shear; $\nu = 0.3$, $l/a = 50.0$.

$k_3(0)/k_{3s}$

		OUTER CRACK				INNER CRACK			
		$\xi_0 = l_0/h$							
a/h	R/h	0.2	0.4	0.6	0.8	0.2	0.4	0.6	0.8
	5	0.797	0.632	0.575	0.492	0.804	0.643	0.586	0.498
	10	0.799	0.633	0.576	0.490	0.803	0.640	0.582	0.494
1	15	0.799	0.634	0.576	0.490	0.802	0.639	0.581	0.492
	25	0.800	0.635	0.576	0.489	0.802	0.638	0.580	0.491
	50	0.800	0.635	0.577	0.489	0.801	0.637	0.579	0.490
	100	0.800	0.636	0.577	0.489	0.801	0.637	0.578	0.490
	5	0.826	0.683	0.658	0.632	0.835	0.699	0.677	0.645
	10	0.827	0.684	0.657	0.626	0.833	0.695	0.670	0.635
2	15	0.828	0.685	0.657	0.625	0.832	0.693	0.667	0.632
	25	0.828	0.686	0.658	0.624	0.832	0.692	0.665	0.629
	50	0.829	0.687	0.659	0.623	0.831	0.690	0.663	0.626
	100	0.829	0.687	0.659	0.623	0.831	0.689	0.661	0.625
	5	0.833	0.700	0.692	0.704	0.843	0.717	0.714	0.722
	10	0.835	0.701	0.690	0.695	0.841	0.713	0.706	0.708
3	15	0.835	0.701	0.690	0.692	0.840	0.711	0.702	0.703
	25	0.836	0.702	0.690	0.690	0.840	0.709	0.699	0.698
	50	0.837	0.703	0.691	0.689	0.839	0.708	0.696	0.694
	100	0.837	0.704	0.691	0.689	0.838	0.707	0.695	0.692
	5	0.839	0.714	0.724	0.781	0.847	0.729	0.744	0.799
	10	0.839	0.713	0.720	0.767	0.846	0.726	0.737	0.783
5	15	0.840	0.713	0.719	0.762	0.845	0.724	0.733	0.776
	25	0.840	0.714	0.718	0.758	0.845	0.722	0.729	0.769
	50	0.841	0.715	0.718	0.756	0.844	0.720	0.726	0.763
	100	0.841	0.715	0.719	0.755	0.843	0.719	0.723	0.760
	5	0.843	0.725	0.752	0.852	0.846	0.732	0.760	0.861
	10	0.842	0.723	0.747	0.839	0.847	0.732	0.758	0.851
10	15	0.842	0.723	0.745	0.833	0.847	0.731	0.756	0.845
	25	0.842	0.722	0.743	0.826	0.846	0.730	0.753	0.837
	50	0.843	0.722	0.741	0.820	0.846	0.729	0.749	0.829
	100	0.843	0.723	0.741	0.817	0.845	0.727	0.747	0.824

Table 48. Mode III Normalized Stress Intensity Factor at the Center of a Semi-Elliptic Circumferential Part-Through Crack in an Isotropic Cylindrical Shell with a Fixed End Subjected to Twisting; $\nu = 0.3$, $l/a = 0.25$.

$$k_3(0)/k_{3t}$$

		OUTER CRACK				INNER CRACK			
		$\xi_0 = l_0/h$							
a/h	R/h	0.2	0.4	0.6	0.8	0.2	0.4	0.6	0.8
	5	0.751	0.500	0.291	-0.208	0.774	0.543	0.356	-0.084
	10	0.750	0.500	0.291	-0.210	0.773	0.541	0.353	-0.091
1	15	0.750	0.500	0.291	-0.210	0.773	0.540	0.352	-0.093
	25	0.750	0.500	0.291	-0.209	0.772	0.539	0.351	-0.094
	50	0.750	0.500	0.292	-0.209	0.772	0.539	0.350	-0.096
	100	0.750	0.500	0.292	-0.209	0.772	0.539	0.350	-0.096
	5	0.801	0.578	0.412	0.077	0.819	0.614	0.472	0.204
	10	0.801	0.579	0.414	0.076	0.817	0.611	0.466	0.188
2	15	0.802	0.580	0.415	0.078	0.816	0.610	0.463	0.182
	25	0.802	0.580	0.416	0.080	0.816	0.609	0.461	0.178
	50	0.802	0.581	0.417	0.082	0.816	0.608	0.460	0.174
	100	0.802	0.581	0.418	0.083	0.815	0.607	0.459	0.172
	5	0.812	0.599	0.455	0.209	0.827	0.631	0.508	0:330
	10	0.813	0.600	0.455	0.203	0.825	0.627	0.500	0.307
3	15	0.813	0.601	0.456	0.203	0.825	0.626	0.497	0.298
	25	0.814	0.602	0.457	0.205	0.824	0.624	0.495	0.291
	50	0.814	0.603	0.459	0.208	0.824	0.623	0.492	0.285
	100	0.814	0.603	0.460	0.211	0.823	0.622	0.491	0.282
	5	0.819	0.615	0.493	0.343	0.830	0.639	0.533	0.437
	10	0.819	0.615	0.488	0.321	0.829	0.636	0.526	0.412
5	15	0.820	0.615	0.488	0.316	0.829	0.635	0.522	0.400
	25	0.820	0.616	0.489	0.315	0.828	0.633	0.519	0.389
	50	0.821	0.617	0.490	0.317	0.827	0.632	0.516	0.379
	100	0.821	0.618	0.491	0.320	0.827	0.631	0.514	0.374
	5	0.824	0.630	0.528	0.470	0.828	0.637	0.540	0.494
	10	0.823	0.627	0.521	0.441	0.829	0.638	0.539	0.486
10	15	0.823	0.626	0.517	0.426	0.829	0.638	0.538	0.478
	25	0.823	0.625	0.514	0.413	0.829	0.637	0.535	0.467
	50	0.824	0.625	0.513	0.405	0.829	0.636	0.532	0.454
	100	0.824	0.626	0.514	0.405	0.828	0.635	0.530	0.446

Table 49. Mode III Normalized Stress Intensity Factor at the Center of a Semi-Elliptic Circumferential Part-Through Crack in an Isotropic Cylindrical Shell with a Fixed End Subjected to Twisting; $\nu = 0.3$, $l/a = 0.40$.

$$k_3(0)/k_{3t}$$

		OUTER CRACK				INNER CRACK			
		$\xi_0 = l_0/h$							
a/h	R/h	0.2	0.4	0.6	0.8	0.2	0.4	0.6	0.8
1	5	0.757	0.498	0.268	-0.287	0.782	0.544	0.337	-0.161
	10	0.757	0.498	0.269	-0.287	0.780	0.541	0.333	-0.171
	15	0.757	0.498	0.269	-0.287	0.779	0.540	0.331	-0.174
	25	0.757	0.498	0.270	-0.286	0.779	0.539	0.330	-0.176
	50	0.757	0.498	0.270	-0.285	0.779	0.539	0.329	-0.177
	100	0.757	0.498	0.270	-0.285	0.778	0.538	0.328	-0.178
2	5	0.801	0.573	0.392	0.005	0.820	0.613	0.459	0.146
	10	0.802	0.574	0.393	0.001	0.818	0.608	0.450	0.122
	15	0.802	0.575	0.394	0.002	0.818	0.607	0.447	0.114
	25	0.803	0.576	0.396	0.005	0.817	0.605	0.444	0.107
	50	0.803	0.576	0.397	0.007	0.816	0.604	0.442	0.103
	100	0.803	0.577	0.398	0.009	0.816	0.604	0.441	0.100
3	5	0.812	0.595	0.441	0.156	0.828	0.630	0.501	0.294
	10	0.812	0.596	0.439	0.142	0.826	0.626	0.491	0.261
	15	0.813	0.597	0.440	0.141	0.825	0.624	0.487	0.248
	25	0.814	0.598	0.441	0.142	0.825	0.622	0.483	0.238
	50	0.814	0.599	0.443	0.146	0.824	0.620	0.480	0.230
	100	0.814	0.600	0.444	0.148	0.824	0.620	0.478	0.226
5	5	0.819	0.614	0.487	0.323	0.830	0.639	0.531	0.429
	10	0.819	0.612	0.479	0.286	0.830	0.636	0.522	0.392
	15	0.819	0.612	0.478	0.276	0.829	0.634	0.518	0.374
	25	0.820	0.613	0.478	0.271	0.828	0.632	0.513	0.358
	50	0.820	0.614	0.479	0.272	0.828	0.631	0.509	0.345
	100	0.821	0.615	0.481	0.274	0.827	0.629	0.506	0.337
10	5	0.824	0.630	0.528	0.470	0.828	0.637	0.540	0.497
	10	0.823	0.627	0.520	0.438	0.829	0.638	0.539	0.487
	15	0.823	0.625	0.515	0.418	0.829	0.638	0.538	0.476
	25	0.823	0.624	0.510	0.397	0.829	0.637	0.535	0.461
	50	0.823	0.624	0.508	0.383	0.829	0.636	0.530	0.442
	100	0.824	0.625	0.508	0.379	0.828	0.635	0.527	0.429

Table 50. Mode III Normalized Stress Intensity Factor at the Center of a Semi-Elliptic Circumferential Part-Through Crack in an Isotropic Cylindrical Shell with a Fixed End Subjected to Twisting; $\nu = 0.3$, $l/a = 0.5$.

$k_3(0)/k_{3t}$

		OUTER CRACK				INNER CRACK			
		$\xi_0 = l_0/h$							
a/h	R/h	0.2	0.4	0.6	0.8	0.2	0.4	0.6	0.8
	5	0.761	0.499	0.262	-0.316	0.784	0.544	0.328	-0.196
	10	0.761	0.500	0.263	-0.316	0.783	0.541	0.323	-0.207
1	15	0.761	0.500	0.263	-0.316	0.782	0.540	0.321	-0.210
	25	0.761	0.500	0.264	-0.315	0.782	0.539	0.320	-0.213
	50	0.761	0.500	0.264	-0.314	0.781	0.538	0.319	-0.215
	100	0.761	0.501	0.264	-0.313	0.781	0.538	0.319	-0.215
	5	0.802	0.572	0.387	-0.016	0.820	0.612	0.453	0.124
	10	0.803	0.573	0.388	-0.022	0.818	0.607	0.443	0.096
2	15	0.803	0.574	0.389	-0.022	0.818	0.605	0.440	0.087
	25	0.804	0.575	0.390	-0.020	0.817	0.603	0.437	0.079
	50	0.804	0.576	0.392	-0.017	0.816	0.602	0.434	0.074
	100	0.804	0.577	0.393	-0.015	0.816	0.601	0.433	0.071
	5	0.812	0.595	0.438	0.144	0.828	0.629	0.498	0.283
	10	0.813	0.595	0.435	0.125	0.826	0.625	0.487	0.244
3	15	0.813	0.596	0.436	0.122	0.825	0.623	0.482	0.229
	25	0.814	0.597	0.437	0.122	0.824	0.621	0.478	0.217
	50	0.815	0.598	0.439	0.126	0.824	0.619	0.474	0.208
	100	0.815	0.599	0.440	0.129	0.823	0.618	0.473	0.203
	5	0.819	0.614	0.488	0.322	0.830	0.638	0.531	0.427
	10	0.819	0.612	0.478	0.279	0.829	0.636	0.521	0.386
5	15	0.819	0.612	0.476	0.266	0.829	0.634	0.516	0.366
	25	0.820	0.613	0.475	0.259	0.828	0.632	0.511	0.347
	50	0.821	0.614	0.476	0.258	0.828	0.630	0.506	0.331
	100	0.821	0.615	0.478	0.260	0.827	0.628	0.503	0.323
	5	0.824	0.630	0.528	0.469	0.828	0.637	0.540	0.497
	10	0.824	0.627	0.520	0.438	0.829	0.638	0.539	0.487
10	15	0.823	0.625	0.515	0.418	0.829	0.638	0.537	0.476
	25	0.823	0.624	0.510	0.396	0.829	0.637	0.534	0.459
	50	0.824	0.624	0.507	0.378	0.829	0.636	0.529	0.438
	100	0.824	0.624	0.507	0.372	0.828	0.634	0.525	0.423

Table 51. Mode III Normalized Stress Intensity Factor at the Center of a Semi-Elliptic Circumferential Part-Through Crack in an Isotropic Cylindrical Shell with a Fixed End Subjected to Twisting; $\nu = 0.3$, $l/a = 1.0$.

$$k_3(0)/k_{3t}$$

		OUTER CRACK				INNER CRACK			
		$\xi_0 = l_0/h$							
a/h	R/h	0.2	0.4	0.6	0.8	0.2	0.4	0.6	0.8
	5	0.772	0.510	0.261	-0.353	0.787	0.540	0.307	-0.269
	10	0.772	0.511	0.262	-0.355	0.785	0.537	0.300	-0.284
1	15	0.773	0.512	0.262	-0.354	0.784	0.535	0.298	-0.289
	25	0.773	0.512	0.263	-0.353	0.784	0.534	0.296	-0.293
	50	0.773	0.513	0.264	-0.352	0.784	0.533	0.295	-0.295
	100	0.773	0.513	0.265	-0.351	0.783	0.533	0.294	-0.297
	5	0.805	0.576	0.390	-0.024	0.818	0.606	0.441	0.088
	10	0.806	0.577	0.388	-0.040	0.817	0.601	0.429	0.050
2	15	0.807	0.578	0.388	-0.042	0.816	0.599	0.424	0.037
	25	0.807	0.579	0.389	-0.042	0.815	0.597	0.420	0.026
	50	0.808	0.581	0.391	-0.040	0.815	0.596	0.417	0.018
	100	0.808	0.581	0.392	-0.038	0.814	0.595	0.416	0.014
	5	0.814	0.598	0.442	0.151	0.826	0.626	0.492	0.265
	10	0.815	0.598	0.437	0.121	0.825	0.621	0.478	0.217
3	15	0.815	0.599	0.436	0.112	0.824	0.619	0.472	0.197
	25	0.816	0.600	0.437	0.108	0.823	0.616	0.467	0.180
	50	0.817	0.601	0.438	0.109	0.822	0.614	0.462	0.166
	100	0.817	0.602	0.439	0.111	0.822	0.613	0.460	0.159
	5	0.820	0.616	0.490	0.329	0.829	0.637	0.528	0.421
	10	0.820	0.614	0.482	0.288	0.828	0.633	0.517	0.377
5	15	0.820	0.614	0.479	0.271	0.828	0.631	0.511	0.354
	25	0.821	0.614	0.477	0.258	0.827	0.629	0.505	0.330
	50	0.822	0.615	0.477	0.250	0.827	0.627	0.499	0.308
	100	0.822	0.616	0.478	0.249	0.826	0.625	0.495	0.295
	5	0.824	0.630	0.528	0.468	0.828	0.637	0.540	0.496
	10	0.824	0.627	0.520	0.439	0.829	0.638	0.539	0.485
10	15	0.824	0.626	0.516	0.421	0.829	0.637	0.536	0.473
	25	0.824	0.625	0.512	0.401	0.829	0.636	0.533	0.456
	50	0.824	0.625	0.509	0.382	0.828	0.635	0.527	0.432
	100	0.825	0.625	0.508	0.372	0.828	0.633	0.523	0.413

Table 52. Mode III Normalized Stress Intensity Factor at the Center of a Semi-Elliptic Circumferential Part-Through Crack in an Isotropic Cylindrical Shell with a Fixed End Subjected to Twisting; $\nu = 0.3$, $l/a = 1.5$

$k_3(0)/k_{3t}$

		OUTER CRACK				INNER CRACK			
		$\xi_0 = l_0/h$							
a/h	R/h	0.2	0.4	0.6	0.8	0.2	0.4	0.6	0.8
	5	0.774	0.514	0.266	-0.349	0.786	0.537	0.301	-0.285
	10	0.775	0.516	0.266	-0.352	0.784	0.533	0.294	-0.302
1	15	0.776	0.516	0.267	-0.352	0.784	0.532	0.291	-0.308
	25	0.776	0.517	0.268	-0.351	0.783	0.531	0.289	-0.312
	50	0.777	0.518	0.269	-0.350	0.783	0.530	0.287	-0.315
	100	0.777	0.518	0.269	-0.349	0.782	0.529	0.287	-0.317
	5	0.806	0.579	0.394	-0.014	0.817	0.604	0.438	0.081
	10	0.807	0.580	0.392	-0.031	0.816	0.599	0.425	0.041
2	15	0.808	0.581	0.392	-0.035	0.815	0.597	0.420	0.026
	25	0.809	0.582	0.393	-0.037	0.814	0.595	0.416	0.014
	50	0.809	0.583	0.394	-0.036	0.814	0.593	0.412	0.004
	100	0.810	0.584	0.395	-0.034	0.813	0.592	0.410	-0.001
	5	0.814	0.599	0.445	0.158	0.825	0.625	0.489	0.261
	10	0.815	0.600	0.441	0.130	0.824	0.619	0.476	0.213
3	15	0.816	0.601	0.440	0.122	0.823	0.617	0.469	0.192
	25	0.817	0.602	0.440	0.116	0.822	0.615	0.464	0.173
	50	0.817	0.603	0.441	0.114	0.822	0.612	0.459	0.157
	100	0.818	0.604	0.442	0.115	0.821	0.611	0.456	0.149
	5	0.820	0.616	0.491	0.330	0.829	0.636	0.527	0.418
	10	0.820	0.615	0.483	0.291	0.828	0.633	0.516	0.374
5	15	0.821	0.615	0.481	0.277	0.828	0.631	0.510	0.351
	25	0.821	0.616	0.480	0.265	0.827	0.628	0.503	0.327
	50	0.822	0.616	0.479	0.257	0.826	0.626	0.497	0.303
	100	0.823	0.617	0.480	0.254	0.826	0.624	0.493	0.289
	5	0.824	0.630	0.528	0.468	0.828	0.637	0.540	0.495
	10	0.824	0.627	0.521	0.439	0.829	0.637	0.538	0.484
10	15	0.824	0.626	0.517	0.421	0.829	0.637	0.536	0.472
	25	0.824	0.626	0.513	0.402	0.828	0.636	0.532	0.454
	50	0.824	0.626	0.510	0.385	0.828	0.634	0.526	0.430
	100	0.825	0.626	0.509	0.376	0.827	0.632	0.522	0.412

Table 53. Mode III Normalized Stress Intensity Factor at the Center of a Semi-Elliptic Circumferential Part-Through Crack in an Isotropic Cylindrical Shell with a Fixed End Subjected to Twisting; $\nu = 0.3$, $l/a = 2.5$.

$k_3(0)/k_{3t}$

		OUTER CRACK				INNER CRACK			
		$\xi_0 = l_0/h$							
a/h	R/h	0.2	0.4	0.6	0.8	0.2	0.4	0.6	0.8
	5	0.776	0.517	0.270	-0.340	0.785	0.535	0.297	-0.291
	10	0.777	0.519	0.271	-0.345	0.783	0.531	0.290	-0.310
1	15	0.778	0.519	0.271	-0.345	0.782	0.530	0.287	-0.317
	25	0.778	0.520	0.272	-0.345	0.782	0.528	0.285	-0.322
	50	0.778	0.521	0.273	-0.344	0.781	0.527	0.283	-0.326
	100	0.779	0.521	0.274	-0.343	0.781	0.527	0.282	-0.327
	5	0.807	0.580	0.396	-0.008	0.817	0.603	0.436	0.077
	10	0.808	0.582	0.395	-0.023	0.815	0.598	0.423	0.038
2	15	0.809	0.583	0.396	-0.026	0.814	0.595	0.418	0.022
	25	0.809	0.584	0.396	-0.029	0.814	0.593	0.413	0.009
	50	0.810	0.585	0.397	-0.029	0.813	0.592	0.409	-0.003
	100	0.810	0.586	0.398	-0.028	0.812	0.591	0.407	-0.008
	5	0.815	0.600	0.446	0.159	0.825	0.624	0.488	0.258
	10	0.816	0.601	0.443	0.135	0.823	0.619	0.474	0.210
3	15	0.816	0.602	0.442	0.128	0.823	0.616	0.468	0.189
	25	0.817	0.603	0.443	0.123	0.822	0.614	0.462	0.170
	50	0.818	0.604	0.443	0.121	0.821	0.611	0.457	0.153
	100	0.818	0.605	0.444	0.121	0.821	0.610	0.454	0.143
	5	0.820	0.616	0.491	0.330	0.829	0.636	0.526	0.416
	10	0.820	0.615	0.484	0.292	0.828	0.632	0.515	0.372
5	15	0.821	0.615	0.482	0.278	0.827	0.630	0.509	0.349
	25	0.822	0.616	0.481	0.268	0.827	0.628	0.503	0.325
	50	0.822	0.617	0.481	0.262	0.826	0.625	0.496	0.301
	100	0.823	0.618	0.481	0.259	0.825	0.624	0.492	0.287
	5	0.824	0.630	0.528	0.468	0.828	0.637	0.540	0.495
	10	0.824	0.627	0.521	0.439	0.829	0.637	0.538	0.483
10	15	0.824	0.626	0.517	0.421	0.829	0.637	0.536	0.471
	25	0.824	0.626	0.513	0.402	0.828	0.636	0.532	0.453
	50	0.824	0.626	0.510	0.386	0.828	0.634	0.526	0.429
	100	0.825	0.626	0.510	0.378	0.827	0.632	0.521	0.410

Table 54. Mode III Normalized Stress Intensity Factor at the Center of a Semi-Elliptic Circumferential Part-Through Crack in an Isotropic Cylindrical Shell with a Fixed End Subjected to Twisting; $\nu = 0.3$, $l/a = 5.0$.

$k_3(0)/k_{3t}$

		OUTER CRACK				INNER CRACK			
		$\xi_0 = l_0/h$							
a/h	R/h	0.2	0.4	0.6	0.8	0.2	0.4	0.6	0.8
	5	0.776	0.518	0.272	-0.336	0.784	0.534	0.296	-0.293
	10	0.778	0.520	0.273	-0.339	0.782	0.530	0.288	-0.312
1	15	0.778	0.521	0.274	-0.340	0.782	0.528	0.285	-0.319
	25	0.779	0.522	0.275	-0.340	0.781	0.527	0.283	-0.325
	50	0.779	0.523	0.275	-0.340	0.781	0.526	0.281	-0.329
	100	0.779	0.523	0.276	-0.339	0.781	0.525	0.280	-0.332
	5	0.807	0.580	0.397	-0.007	0.817	0.603	0.435	0.076
	10	0.808	0.582	0.396	-0.021	0.815	0.597	0.422	0.036
2	15	0.809	0.583	0.397	-0.023	0.814	0.595	0.417	0.020
	25	0.810	0.585	0.398	-0.024	0.813	0.593	0.412	0.007
	50	0.810	0.586	0.399	-0.024	0.813	0.591	0.408	-0.005
	100	0.811	0.587	0.400	-0.024	0.812	0.590	0.406	-0.011
	5	0.815	0.600	0.446	0.159	0.825	0.624	0.488	0.257
	10	0.816	0.601	0.443	0.135	0.823	0.618	0.474	0.208
3	15	0.817	0.602	0.443	0.129	0.823	0.616	0.467	0.188
	25	0.817	0.603	0.443	0.125	0.822	0.613	0.461	0.168
	50	0.818	0.605	0.445	0.124	0.821	0.611	0.456	0.152
	100	0.819	0.606	0.446	0.124	0.820	0.609	0.453	0.142
	5	0.820	0.616	0.491	0.330	0.829	0.636	0.526	0.416
	10	0.820	0.615	0.484	0.292	0.828	0.632	0.515	0.371
5	15	0.821	0.615	0.482	0.278	0.827	0.630	0.509	0.348
	25	0.822	0.616	0.481	0.268	0.827	0.628	0.502	0.324
	50	0.823	0.617	0.481	0.262	0.826	0.625	0.496	0.300
	100	0.823	0.618	0.482	0.261	0.825	0.623	0.491	0.286
	5	0.824	0.630	0.528	0.468	0.828	0.637	0.540	0.495
	10	0.824	0.627	0.521	0.439	0.829	0.637	0.538	0.483
10	15	0.824	0.626	0.517	0.421	0.829	0.637	0.536	0.471
	25	0.824	0.626	0.513	0.402	0.828	0.636	0.532	0.453
	50	0.824	0.626	0.510	0.386	0.828	0.634	0.526	0.429
	100	0.825	0.626	0.510	0.378	0.827	0.632	0.521	0.410

Table 55. Mode III Normalized Stress Intensity Factor at the Center of a Semi-Elliptic Circumferential Part-Through Crack in an Isotropic Cylindrical Shell with a Fixed End Subjected to Twisting; $\nu = 0.3$, $l/a = 50.0$.

$k_3(0)/k_{3t}$

		OUTER CRACK				INNER CRACK			
		$\xi_0 = l_0/h$							
a/h	R/h	0.2	0.4	0.6	0.8	0.2	0.4	0.6	0.8
	5	0.777	0.518	0.272	-0.336	0.784	0.534	0.296	-0.294
	10	0.778	0.520	0.273	-0.339	0.782	0.530	0.288	-0.313
1	15	0.778	0.521	0.274	-0.339	0.782	0.528	0.285	-0.320
	25	0.779	0.522	0.275	-0.338	0.781	0.527	0.282	-0.326
	50	0.779	0.523	0.276	-0.338	0.781	0.526	0.280	-0.330
	100	0.780	0.523	0.277	-0.337	0.780	0.525	0.279	-0.333
	5	0.807	0.580	0.397	-0.008	0.817	0.603	0.435	0.076
	10	0.808	0.582	0.396	-0.021	0.815	0.597	0.422	0.035
2	15	0.809	0.583	0.397	-0.023	0.814	0.595	0.417	0.020
	25	0.810	0.585	0.398	-0.024	0.813	0.593	0.412	0.006
	50	0.810	0.586	0.399	-0.023	0.812	0.591	0.408	-0.005
	100	0.811	0.587	0.401	-0.022	0.812	0.590	0.405	-0.012
	5	0.815	0.600	0.446	0.159	0.825	0.624	0.488	0.257
	10	0.816	0.601	0.443	0.135	0.823	0.618	0.474	0.208
3	15	0.817	0.602	0.443	0.129	0.823	0.616	0.467	0.187
	25	0.817	0.603	0.443	0.125	0.822	0.613	0.461	0.168
	50	0.818	0.605	0.445	0.124	0.821	0.611	0.456	0.151
	100	0.819	0.606	0.446	0.125	0.820	0.609	0.453	0.141
	5	0.820	0.616	0.491	0.330	0.829	0.636	0.526	0.416
	10	0.820	0.615	0.484	0.292	0.828	0.632	0.515	0.371
5	15	0.821	0.615	0.482	0.278	0.827	0.630	0.509	0.348
	25	0.822	0.616	0.481	0.268	0.827	0.628	0.502	0.324
	50	0.823	0.617	0.481	0.262	0.826	0.625	0.496	0.300
	100	0.823	0.618	0.482	0.261	0.825	0.623	0.491	0.285
	5	0.824	0.630	0.528	0.468	0.828	0.637	0.540	0.495
	10	0.824	0.627	0.521	0.439	0.829	0.637	0.538	0.483
10	15	0.824	0.626	0.517	0.421	0.829	0.637	0.536	0.471
	25	0.824	0.626	0.513	0.402	0.828	0.636	0.532	0.453
	50	0.824	0.626	0.510	0.386	0.828	0.634	0.526	0.429
	100	0.825	0.626	0.510	0.378	0.827	0.632	0.521	0.410

Table 56. The Effect of Poisson's Ratio on the Normalized Stress Intensity Factors at the Center of a Semi-Elliptical Part-Through Crack in an Isotropic Cylindrical Shell with a Fixed End, $l/a = 0.5$, $a/h = 1$, $R/h = 5$.

		OUTER CRACK				INNER CRACK			
		ξ_0							
ν		0.2	0.4	0.6	0.8	0.2	0.4	0.6	0.8
	k_1/k_{1m}	0.855	0.582	0.309	0.099	0.845	0.561	0.292	0.094
	k_1/k_{1b}	0.845	0.530	0.212	0.018	0.835	0.506	0.191	0.011
0.0	k_2/k_{2v}	0.994	0.936	0.806	0.623	0.994	0.936	0.806	0.624
	k_3/k_{3s}	0.810	0.652	0.602	0.530	0.816	0.662	0.612	0.535
	k_3/k_{3t}	0.790	0.543	0.314	-0.251	0.797	0.557	0.336	-0.211
	k_1/k_{1m}	0.862	0.592	0.315	0.099	0.851	0.570	0.297	0.094
	k_1/k_{1b}	0.853	0.543	0.219	0.018	0.842	0.516	0.196	0.011
0.1	k_2/k_{2v}	0.994	0.941	0.819	0.643	0.994	0.942	0.820	0.644
	k_3/k_{3s}	0.803	0.642	0.589	0.512	0.809	0.651	0.598	0.516
	k_3/k_{3t}	0.783	0.530	0.294	-0.291	0.789	0.544	0.314	-0.256
	k_1/k_{1m}	0.869	0.605	0.324	0.101	0.859	0.582	0.304	0.096
	k_1/k_{1b}	0.862	0.558	0.230	0.020	0.850	0.530	0.205	0.012
0.2	k_2/k_{2v}	0.995	0.947	0.834	0.665	0.995	0.947	0.835	0.665
	k_3/k_{3s}	0.796	0.632	0.577	0.495	0.802	0.641	0.585	0.498
	k_3/k_{3t}	0.775	0.518	0.275	-0.328	0.781	0.530	0.293	-0.296
	k_1/k_{1m}	0.879	0.622	0.336	0.104	0.868	0.597	0.314	0.098
	k_1/k_{1b}	0.872	0.578	0.245	0.024	0.860	0.548	0.218	0.015
0.3	k_2/k_{2v}	0.996	0.953	0.850	0.689	0.996	0.953	0.850	0.690
	k_3/k_{3s}	0.790	0.623	0.565	0.479	0.795	0.631	0.573	0.482
	k_3/k_{3t}	0.768	0.506	0.257	-0.361	0.774	0.517	0.273	-0.333
	k_1/k_{1m}	0.889	0.643	0.353	0.109	0.878	0.617	0.329	0.102
	k_1/k_{1b}	0.883	0.602	0.265	0.029	0.871	0.571	0.235	0.019
0.4	k_2/k_{2v}	0.996	0.959	0.866	0.716	0.996	0.959	0.867	0.717
	k_3/k_{3s}	0.784	0.614	0.555	0.465	0.788	0.621	0.561	0.467
	k_3/k_{3t}	0.761	0.495	0.240	-0.390	0.767	0.505	0.255	-0.367
	k_1/k_{1m}	0.902	0.670	0.375	0.117	0.891	0.643	0.349	0.108
	k_1/k_{1b}	0.897	0.633	0.292	0.036	0.885	0.601	0.259	0.025
0.5	k_2/k_{2v}	0.997	0.965	0.884	0.747	0.997	0.966	0.885	0.748
	k_3/k_{3s}	0.777	0.605	0.545	0.452	0.781	0.611	0.550	0.453
	k_3/k_{3t}	0.755	0.484	0.225	-0.417	0.759	0.493	0.237	-0.398

Table 57. The Effect of Material Orthotropy on the Normalized Stress Intensity Factors at the Center of a Semi-Elliptical Part-Through Crack in a Cylindrical Shell with a Fixed End, $\nu = 0.3$, $l/a = 0.5$, $a/h = 1$, $R/h = 10$.

		OUTER CRACK				INNER CRACK			
		ξ_0							
E_1/E_2		0.2	0.4	0.6	0.8	0.2	0.4	0.6	0.8
	k_1/k_{1m}	0.931	0.739	0.441	0.140	0.929	0.731	0.431	0.136
	k_1/k_{1b}	0.928	0.711	0.368	0.060	0.925	0.701	0.356	0.055
0.037	k_2/k_{2v}	0.995	0.943	0.822	0.647	0.995	0.943	0.823	0.648
	k_3/k_{3s}	0.662	0.348	0.046	-0.661	0.666	0.355	0.054	-0.648
	k_3/k_{3t}	0.693	0.501	0.432	0.321	0.697	0.506	0.435	0.322
	k_1/k_{1m}	0.871	0.609	0.327	0.103	0.865	0.596	0.316	0.099
	k_1/k_{1b}	0.863	0.562	0.234	0.021	0.857	0.547	0.220	0.017
1.000	k_2/k_{2v}	0.996	0.955	0.856	0.702	0.996	0.955	0.857	0.702
	k_3/k_{3s}	0.783	0.525	0.268	-0.375	0.786	0.531	0.277	-0.360
	k_3/k_{3t}	0.803	0.636	0.570	0.476	0.806	0.640	0.575	0.478
	k_1/k_{1m}	0.784	0.483	0.250	0.083	0.774	0.467	0.239	0.080
	k_1/k_{1b}	0.771	0.416	0.142	0.005	0.760	0.398	0.128	0.004
26.667	k_2/k_{2v}	0.997	0.968	0.893	0.764	0.997	0.968	0.893	0.764
	k_3/k_{3s}	0.864	0.676	0.492	0.045	0.866	0.680	0.499	0.058
	k_3/k_{3t}	0.877	0.752	0.704	0.644	0.878	0.755	0.707	0.646

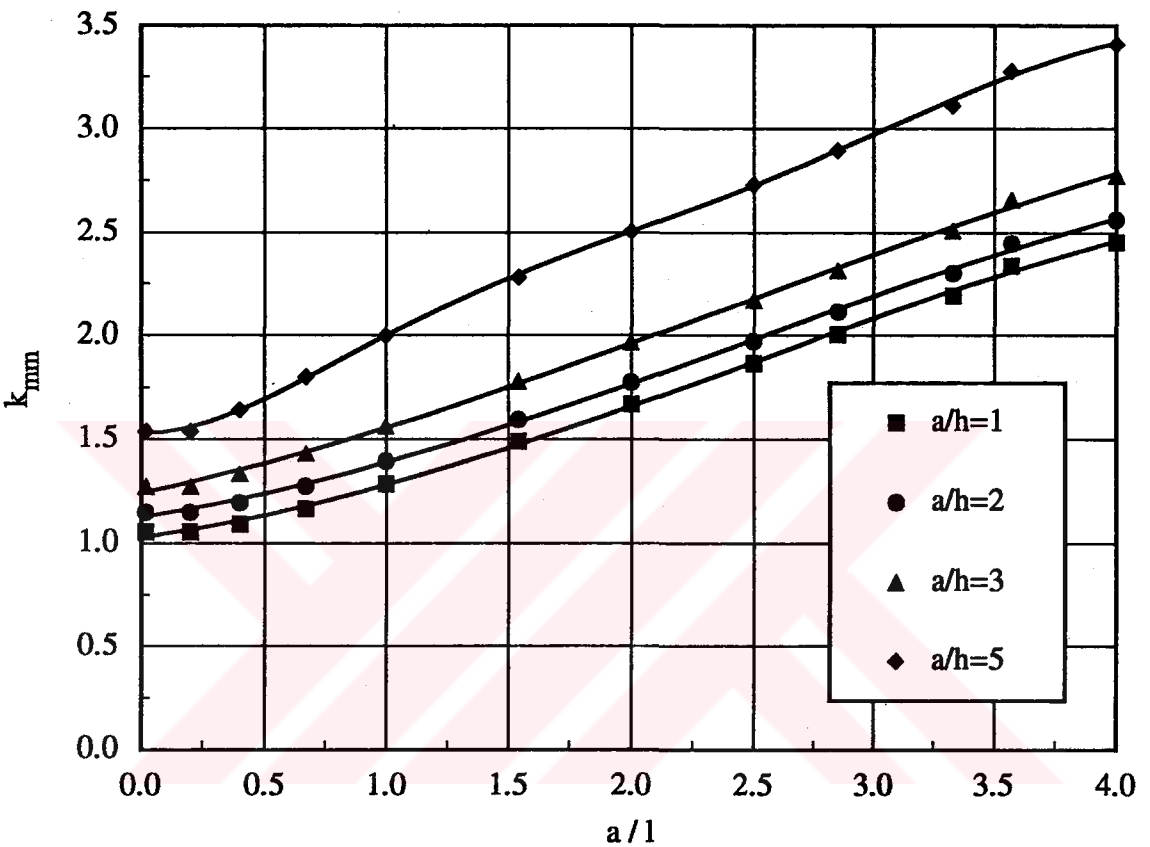

Figure 5. Stress Intensity Factor Ratio k_{mm} in an Isotropic Cylindrical Shell with a Fixed end Containing a Circumferential Through Crack Under Uniform Membrane Loading; $\nu = 0.3$, $R/h = 5$.

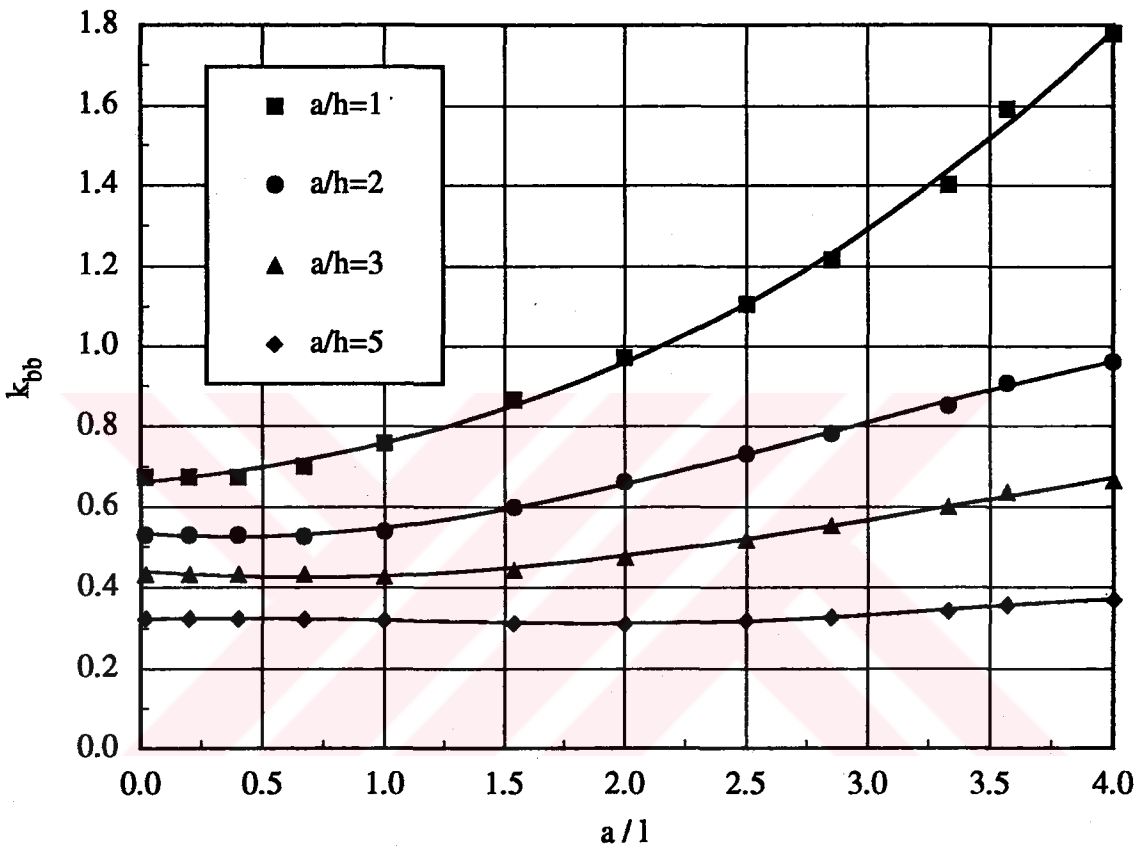

Figure 6. Stress Intensity Factor Ratio k_{bb} in an Isotropic Cylindrical Shell with a Fixed end Containing a Circumferential Through Crack Under Uniform Bending Moment; $\nu = 0.3$, $R/h = 5$.

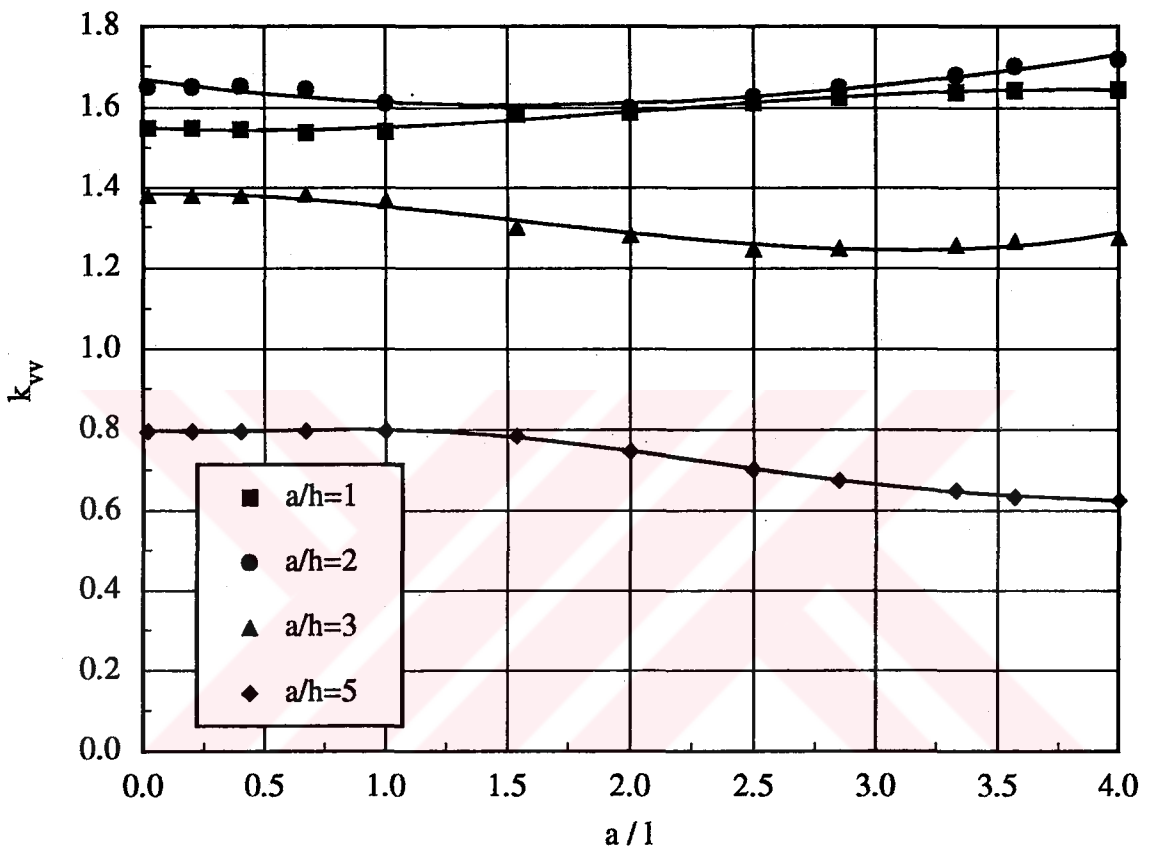

Figure 7. Stress Intensity Factor Ratio k_{vv} in an Isotropic Cylindrical Shell with a Fixed end Containing a Circumferential Through Crack Under Uniform Out-of-Plane Shear Loading; $\nu = 0.3$, $R/h = 5$.

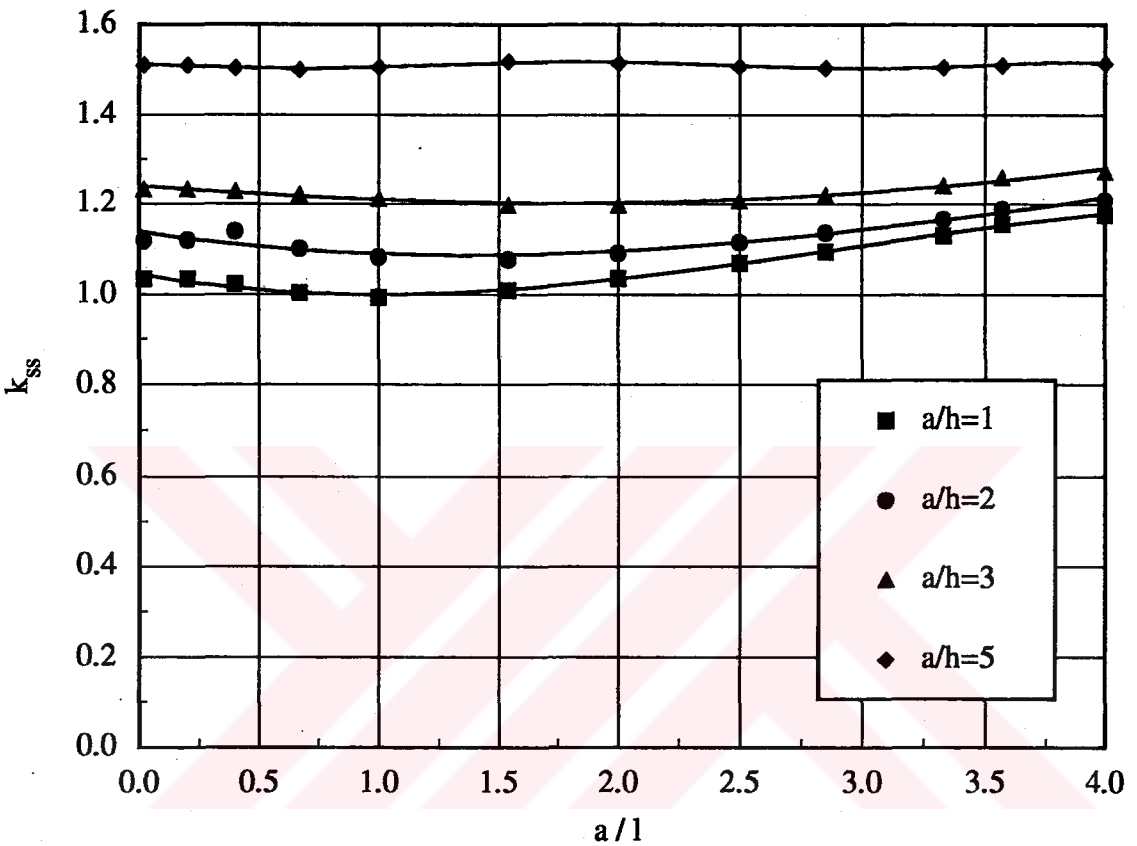

Figure 8. Stress Intensity Factor Ratio k_{ss} in an Isotropic Cylindrical Shell with a Fixed end Containing a Circumferential Through Crack Under Uniform In-Plane Shear Loading; $\nu = 0.3$, $R/h = 5$.

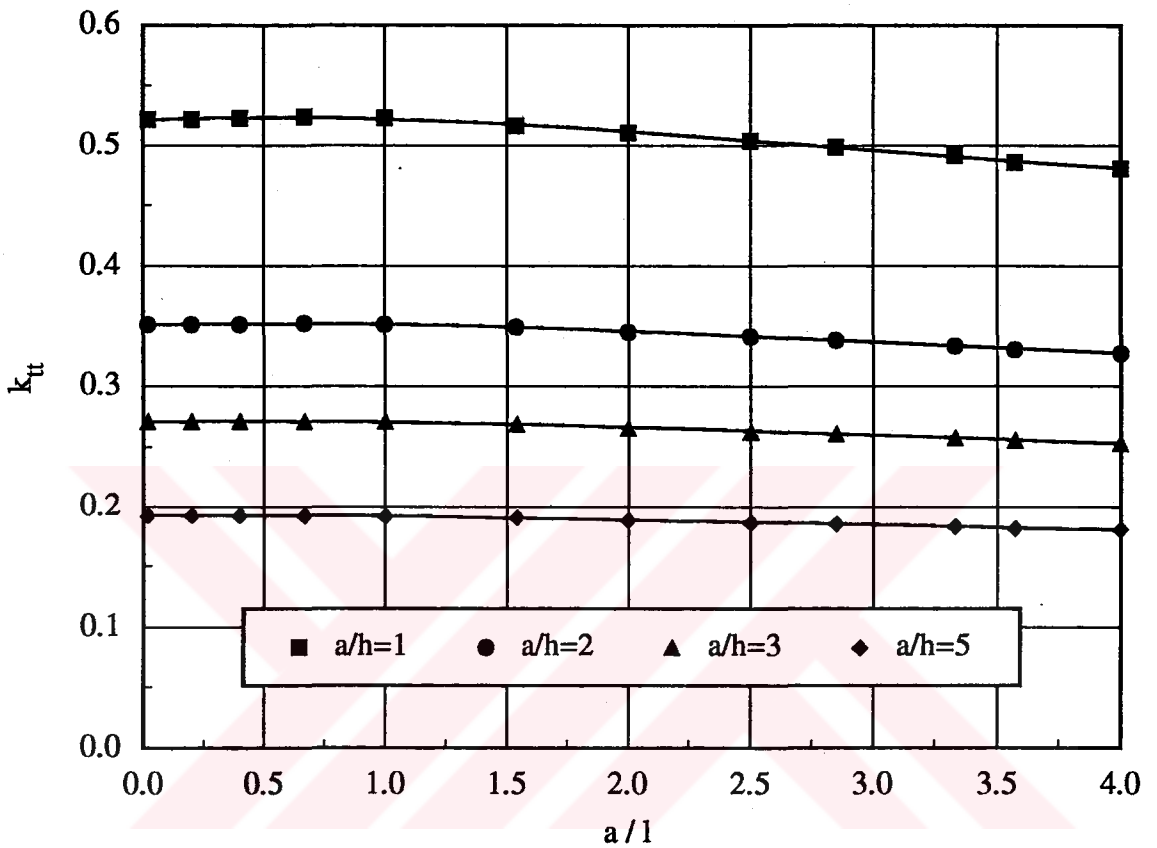

Figure 9. Stress Intensity Factor Ratio k_{tt} in an Isotropic Cylindrical Shell with a Fixed end Containing a Circumferential Through Crack Under Uniform Twisting Moment; $\nu = 0.3$, $R/h = 5$.

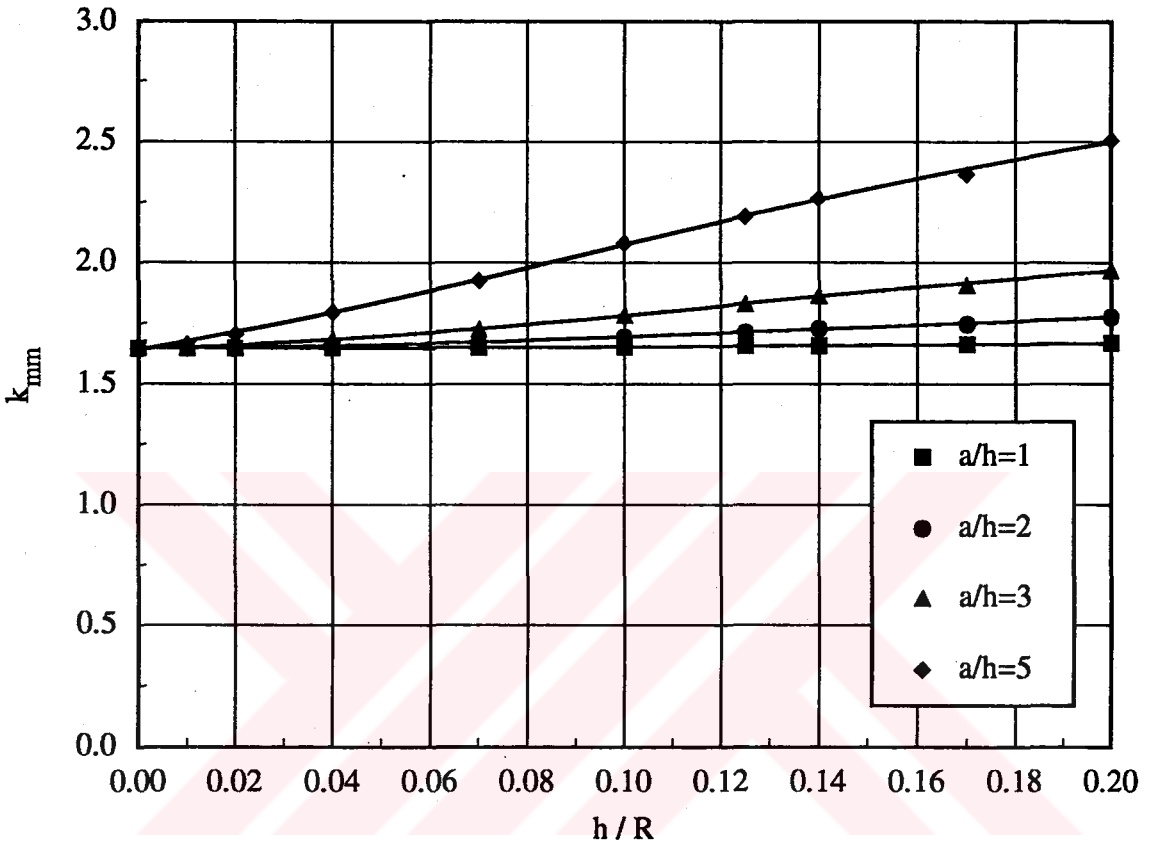

Figure 10. Stress Intensity Factor Ratio k_{mm} in an Isotropic Cylindrical Shell with a Fixed end Containing a Circumferential Through Crack Under Uniform Membrane Loading; $\nu = 0.3$, $l / a = 0.5$.

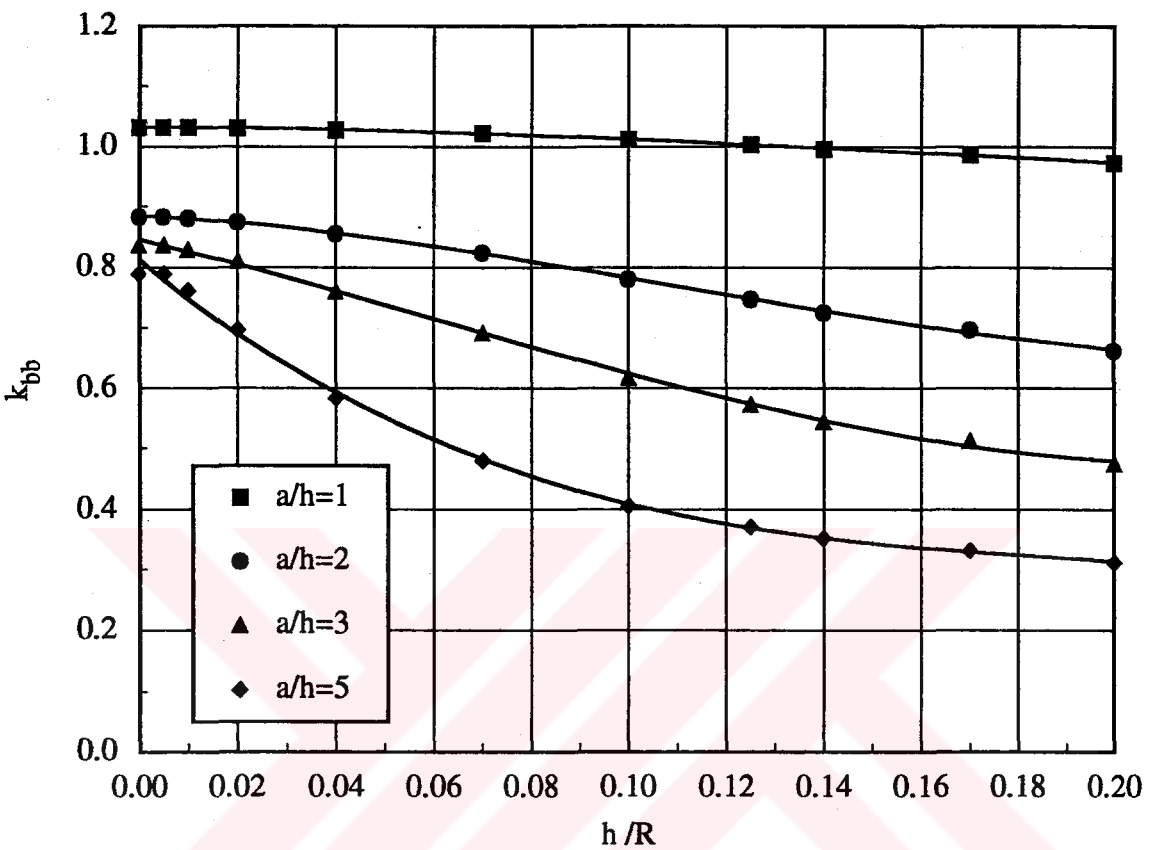

Figure 11. Stress Intensity Factor Ratio k_{bb} in an Isotropic Cylindrical Shell with a Fixed end Containing a Circumferential Through Crack Under Uniform Bending Moment; $\nu = 0.3$, $l / a = 0.5$.

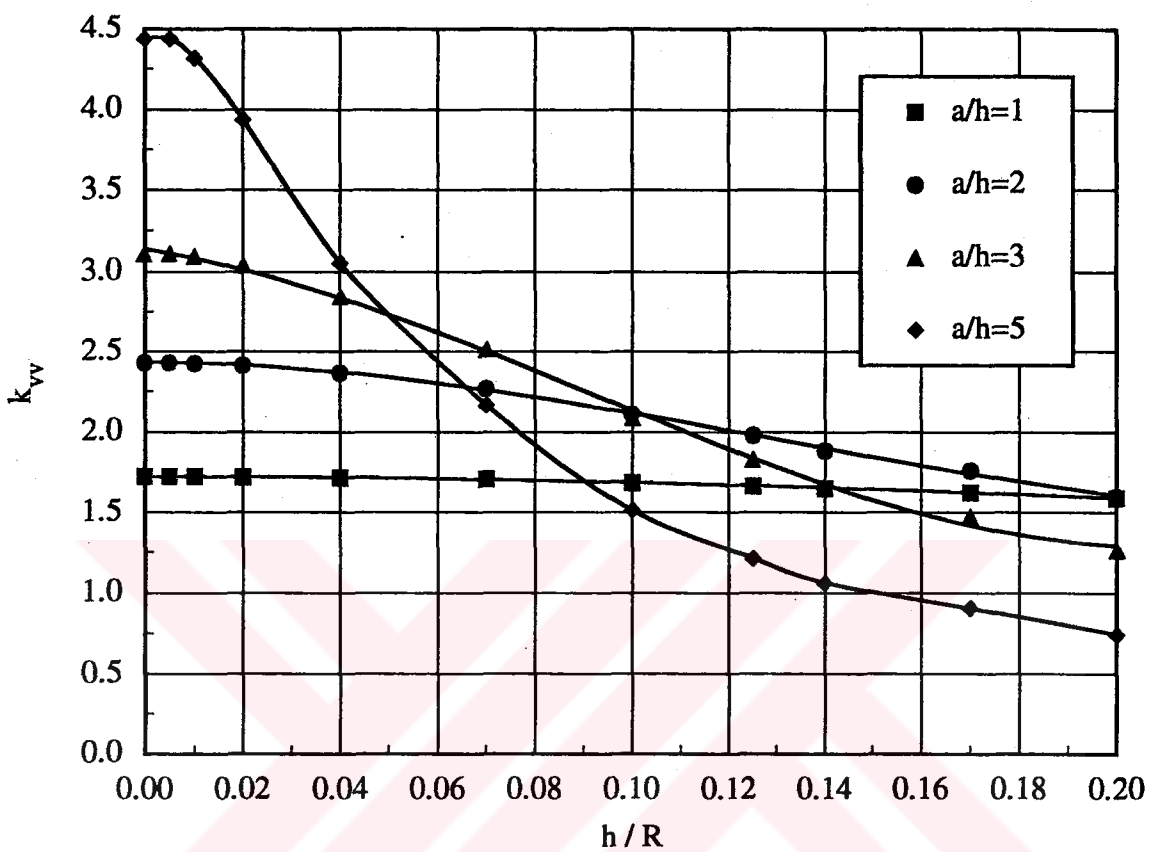

Figure 12. Stress Intensity Factor Ratio k_{vv} in an Isotropic Cylindrical Shell with a Fixed end Containing a Circumferential Through Crack Under Uniform Out-of-Plane Shear Loading; $\nu = 0.3$, $l / a = 0.5$.

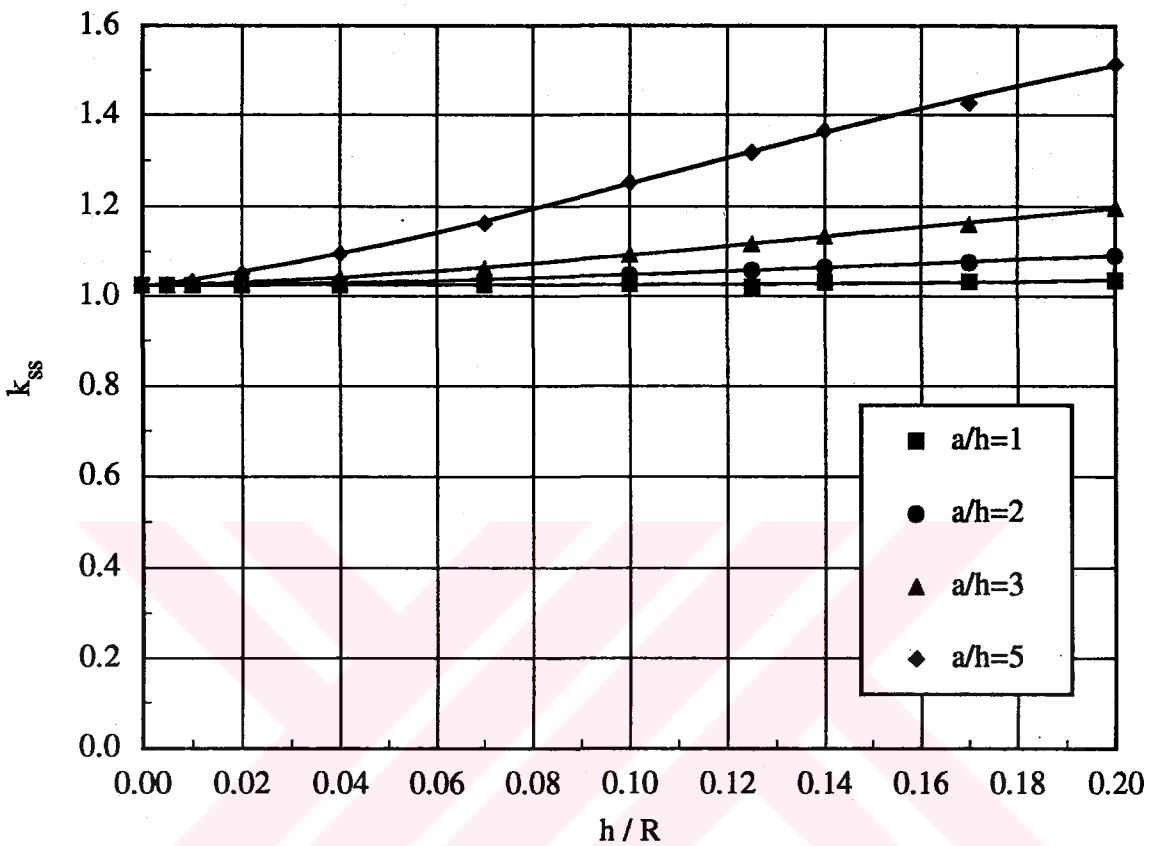

Figure 13. Stress Intensity Factor Ratio k_{ss} in an Isotropic Cylindrical Shell with a Fixed end Containing a Circumferential Through Crack Under Uniform In-Plane Shear Loading; $\nu = 0.3$, $l / a = 0.5$.

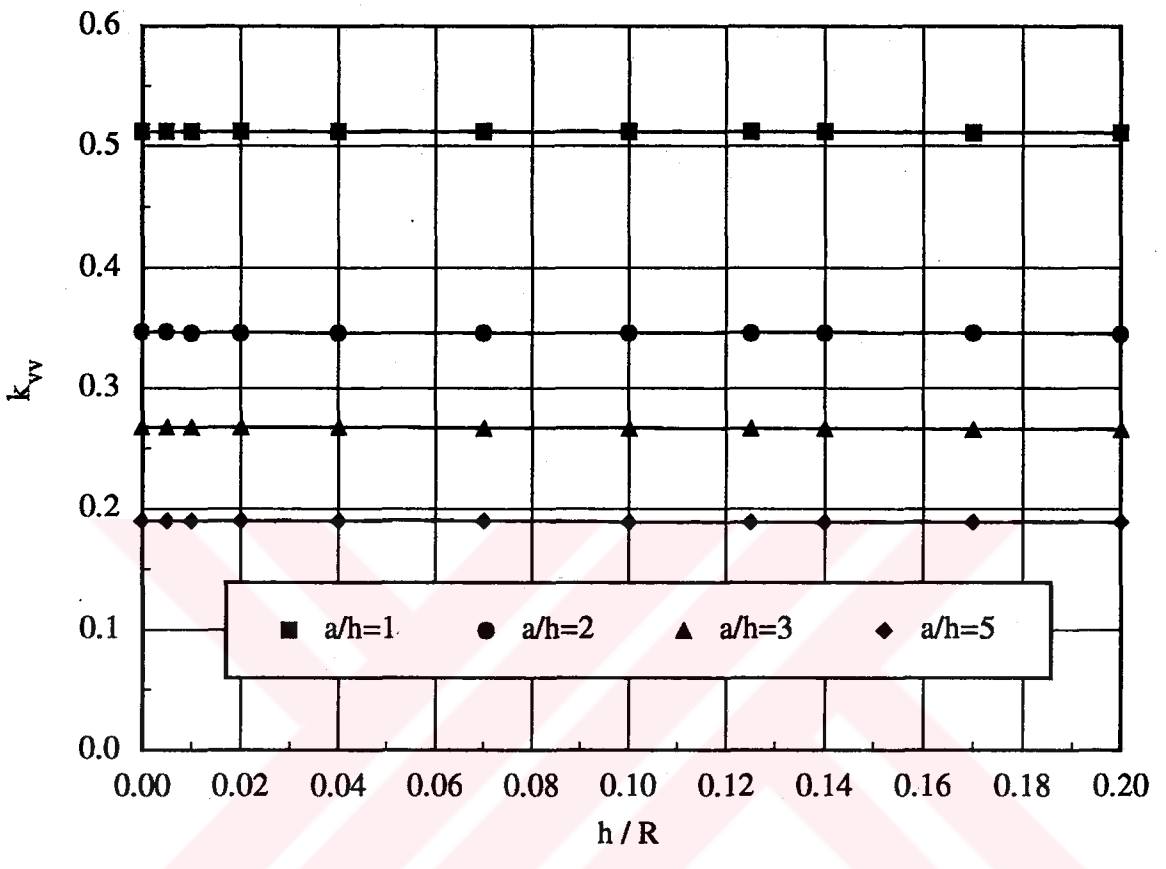

Figure 14. Stress Intensity Factor Ratio k_{II} in an Isotropic Cylindrical Shell with a Fixed end Containing a Circumferential Through Crack Under Uniform Twisting Moment; $\nu = 0.3$, $l / a = 0.5$.

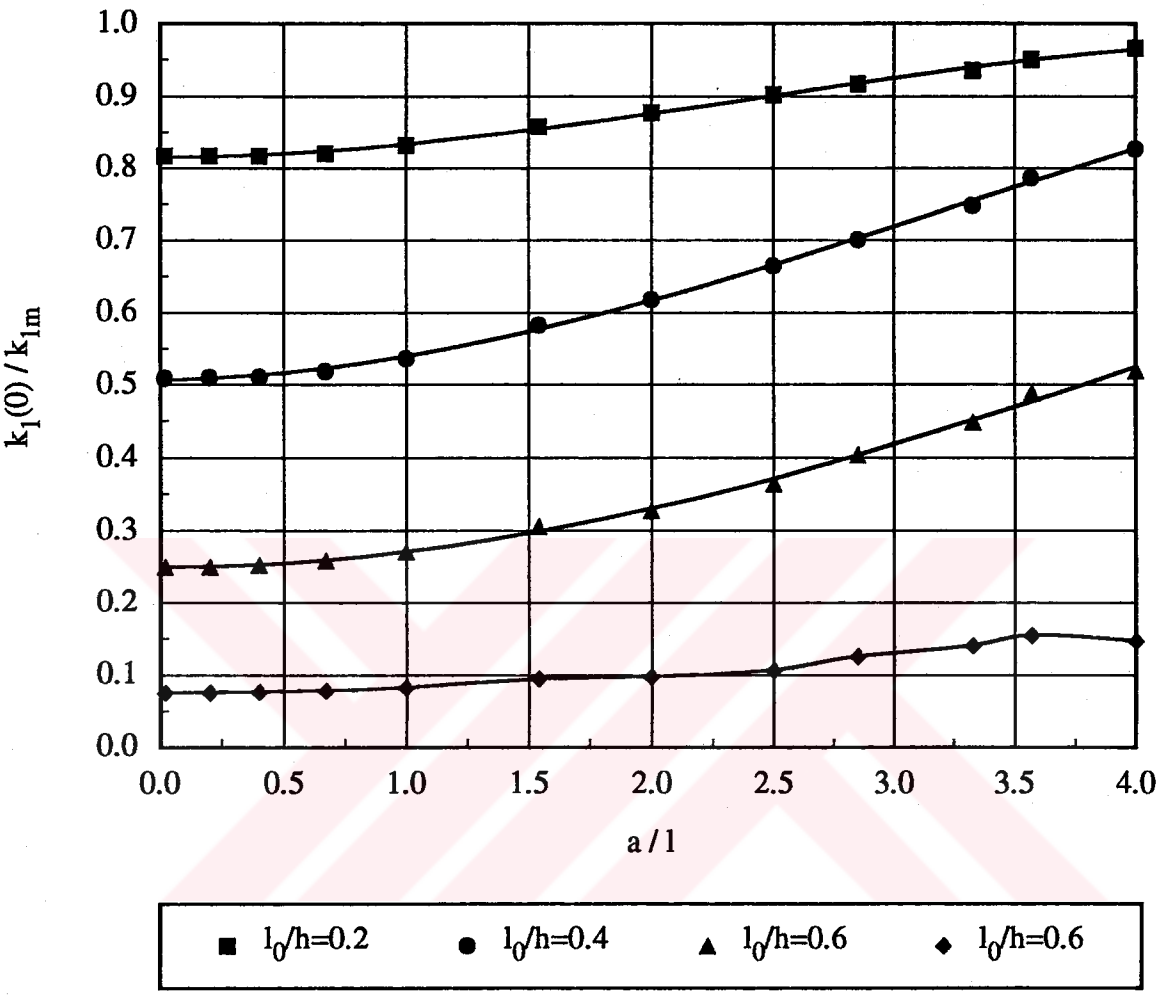

Figure 15. Mode I Normalized Stress Intensity Factor at the Center of a Semi-Elliptic Circumferential Outer Part-Through Crack in an Isotropic Cylindrical Shell with a Fixed End Subjected to Membrane Loading; $\nu = 0.3$, $R/h = 5$, $a/h = 1$.

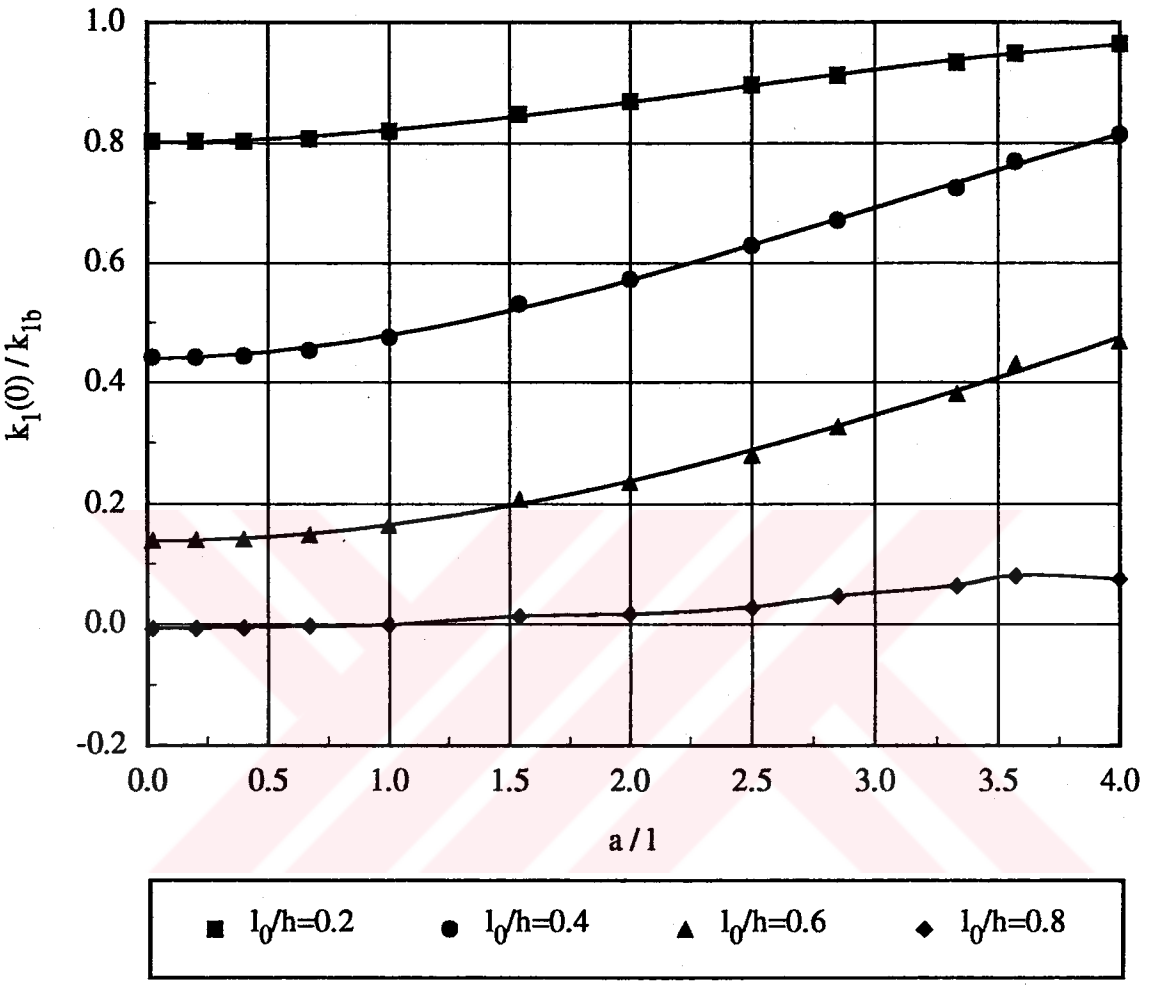

Figure 16. Mode I Normalized Stress Intensity Factor at the Center of a Semi-Elliptic Circumferential Outer Part-Through Crack in an Isotropic Cylindrical Shell with a Fixed End Subjected to Bending Moment; $\nu = 0.3$, $R/h = 5$, $a/h = 1$.

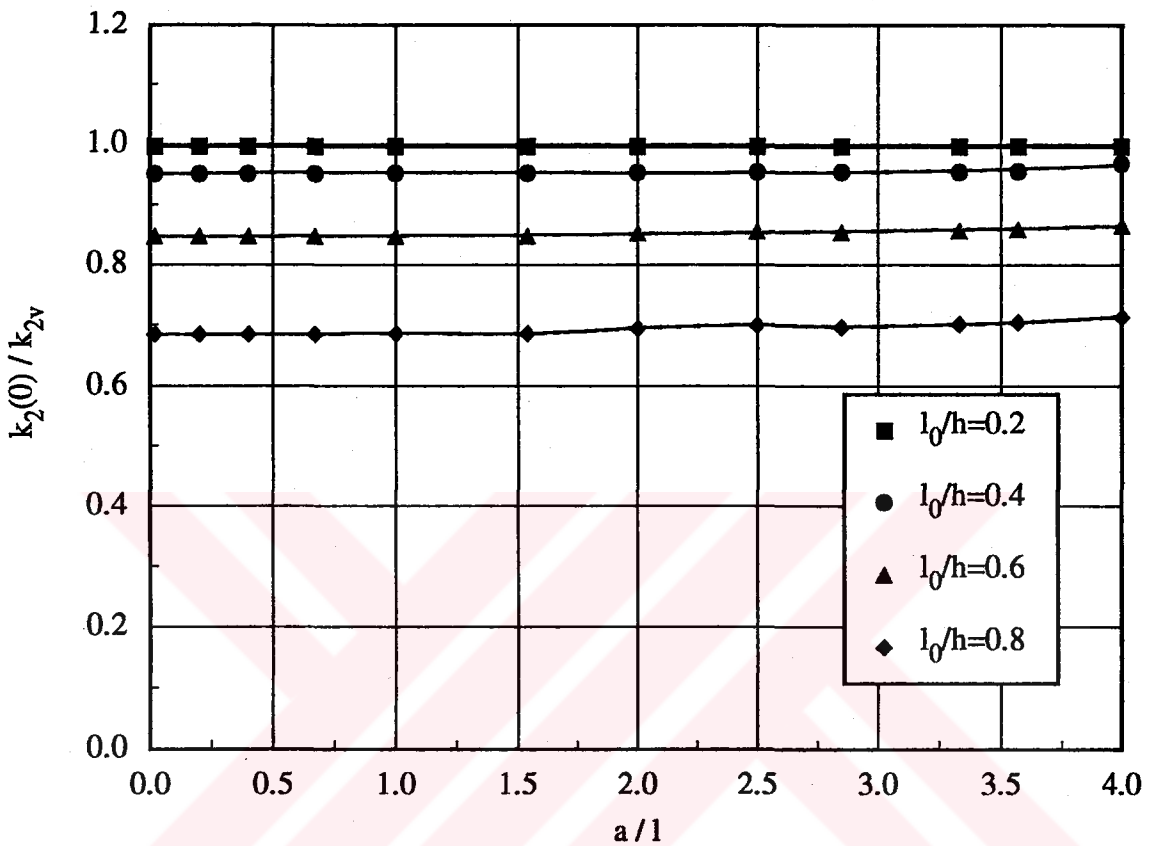

Figure 17. Mode II Normalized Stress Intensity Factor at the Center of a Semi-Elliptic Circumferential Outer Part-Through Crack in an Isotropic Cylindrical Shell with a Fixed End Subjected to Out-of-Plane Shear; $\nu = 0.3$, $R/h = 5$, $a/h = 1$.

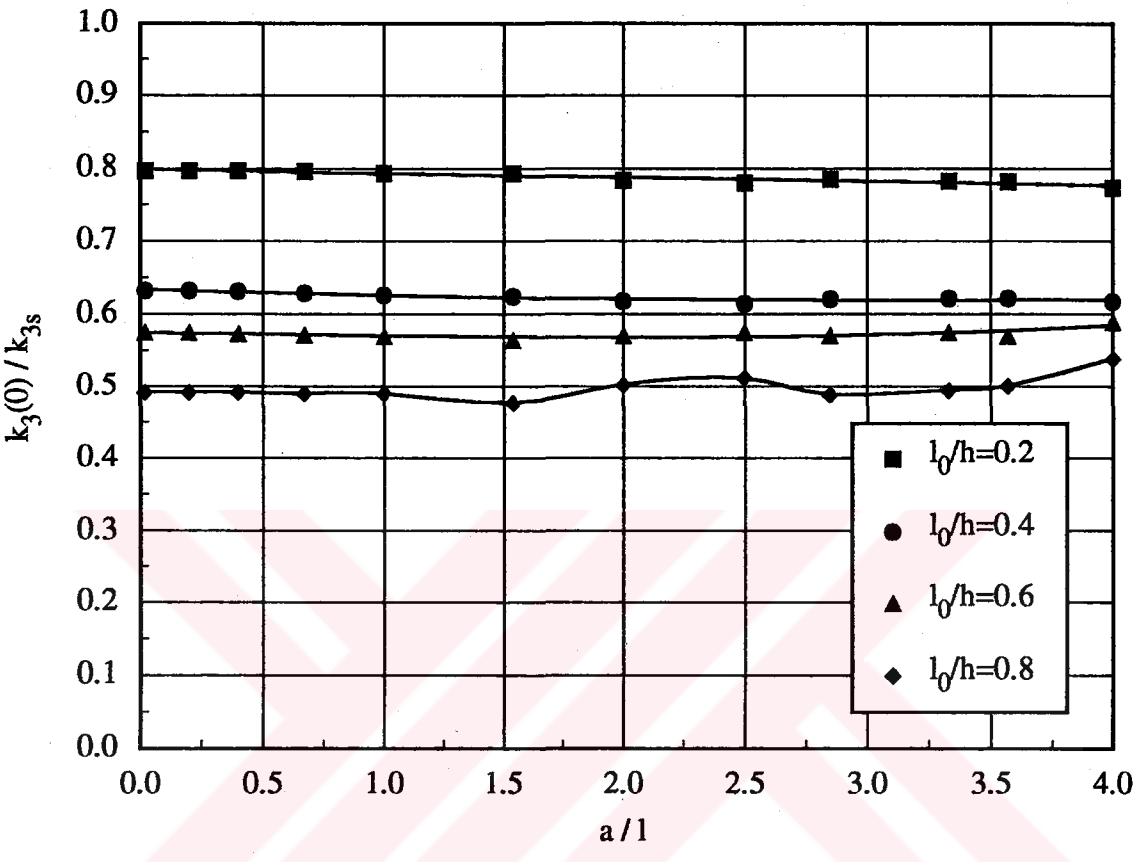

Figure 18. Mode III Normalized Stress Intensity Factor at the Center of a Semi-Elliptic Circumferential Outer Part-Through Crack in an Isotropic Cylindrical Shell with a Fixed End Subjected to In-Plane Shear; $\nu = 0.3$, $R/h = 5$, $a/h = 1$.

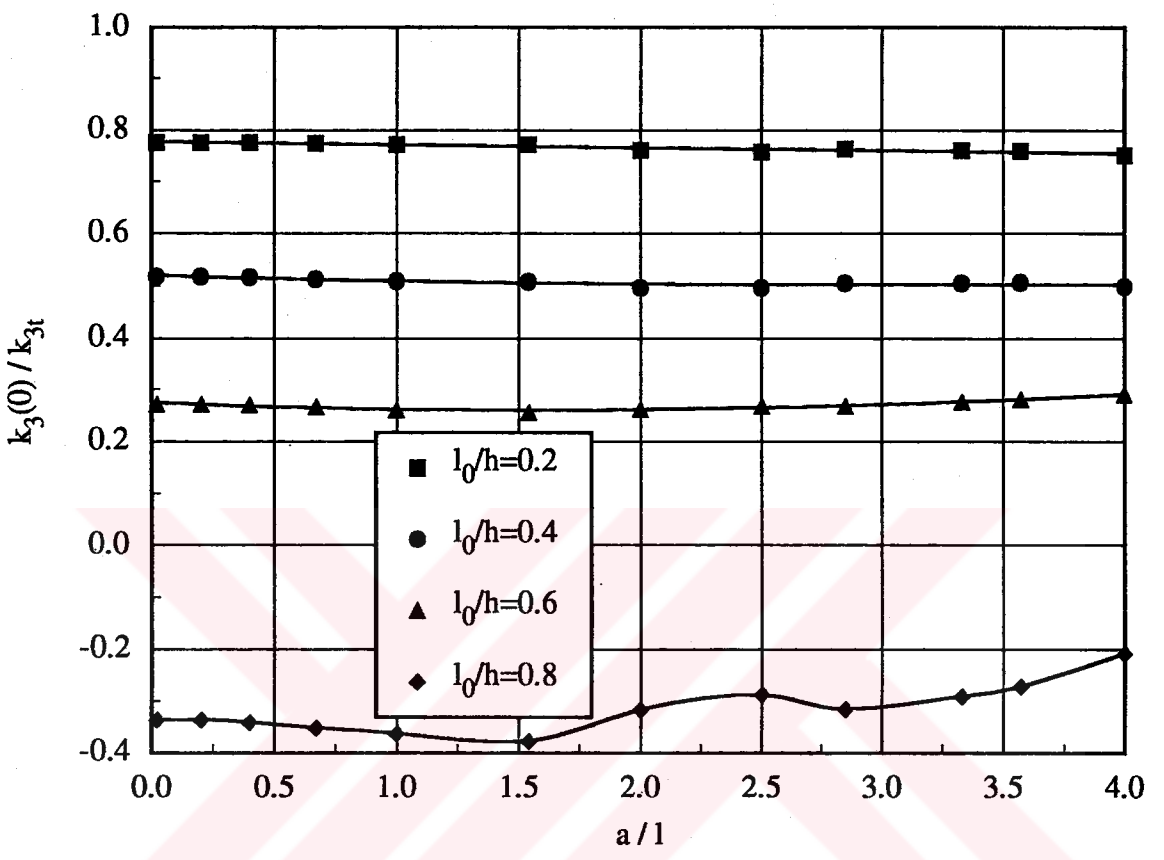

Figure 19. Mode III Normalized Stress Intensity Factor at the Center of a Semi-Elliptic Circumferential Outer Part-Through Crack in an Isotropic Cylindrical Shell with a Fixed End Subjected to Twisting; $\nu = 0.3$, $R/h = 5$, $a/h = 1$.

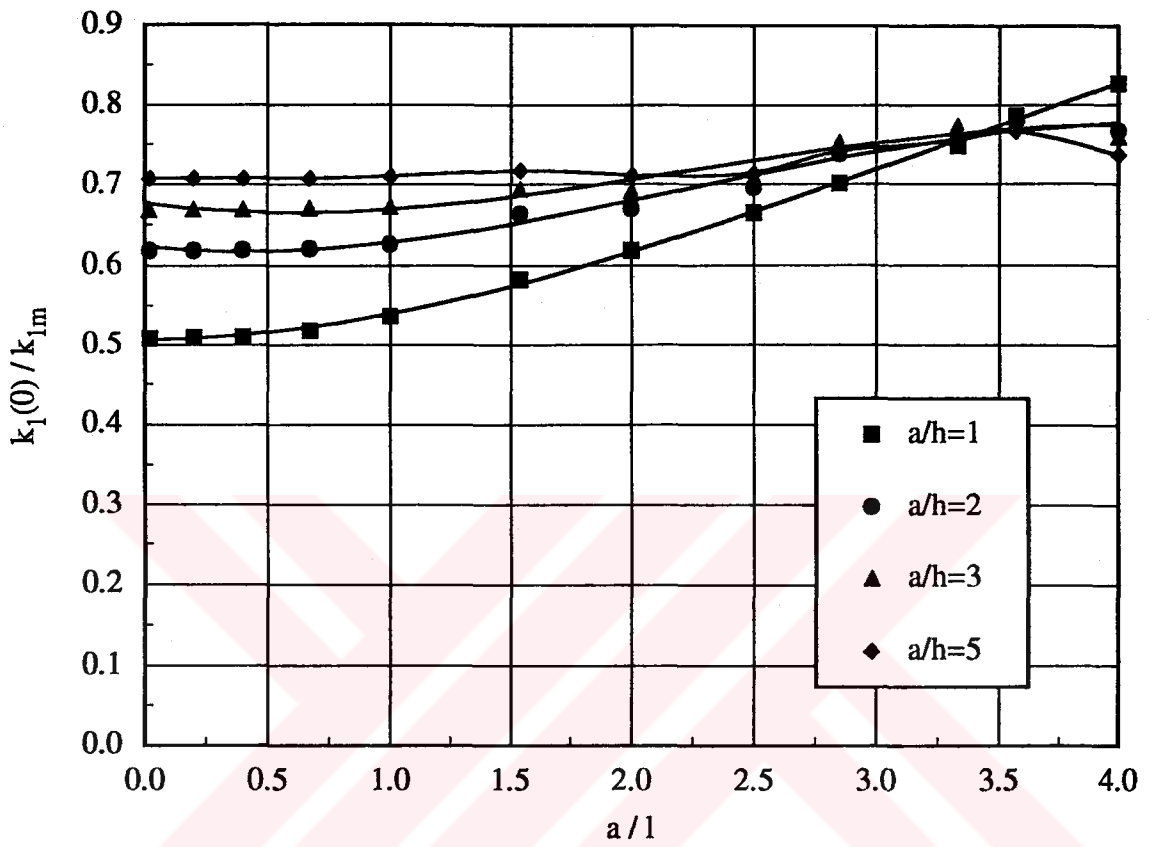

Figure 20. Mode I Normalized Stress Intensity Factor at the Center of a Semi-Elliptic Circumferential Outer Part-Through Crack in an Isotropic Cylindrical Shell with a Fixed End Subjected to Membrane Loading; $\nu = 0.3$, $R/h = 5$, $l_0/h = 0.2$

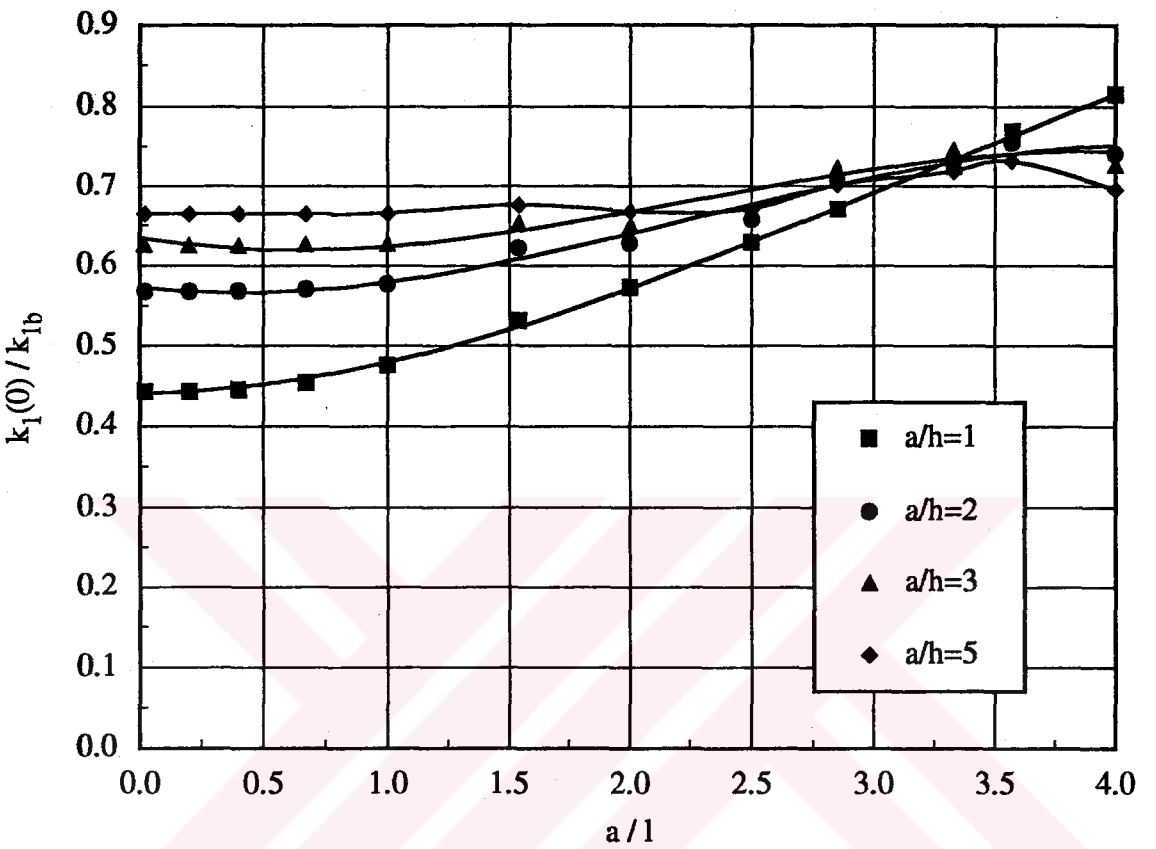

Figure 21. Mode I Normalized Stress Intensity Factor at the Center of a Semi-Elliptic Circumferential Outer Part-Through Crack in an Isotropic Cylindrical Shell with a Fixed End Subjected to Bending Moment; $\nu = 0.3$, $R/h = 5$, $l_0/h = 0.2$

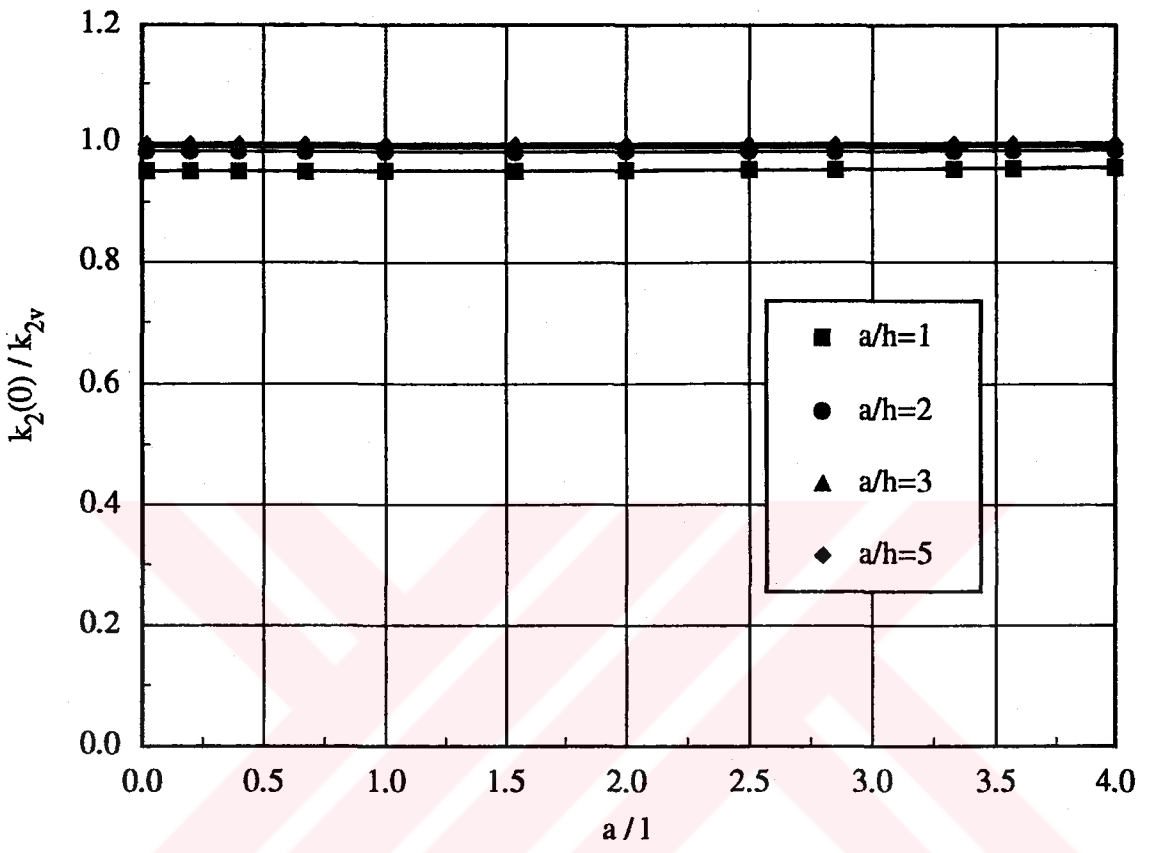

Figure 22. Mode II Normalized Stress Intensity Factor at the Center of a Semi-Elliptic Circumferential Outer Part-Through Crack in an Isotropic Cylindrical Shell with a Fixed End Subjected to Out-of-Plane Shear; $\nu = 0.3$, $R/h = 5$, $l_0/h = 0.2$

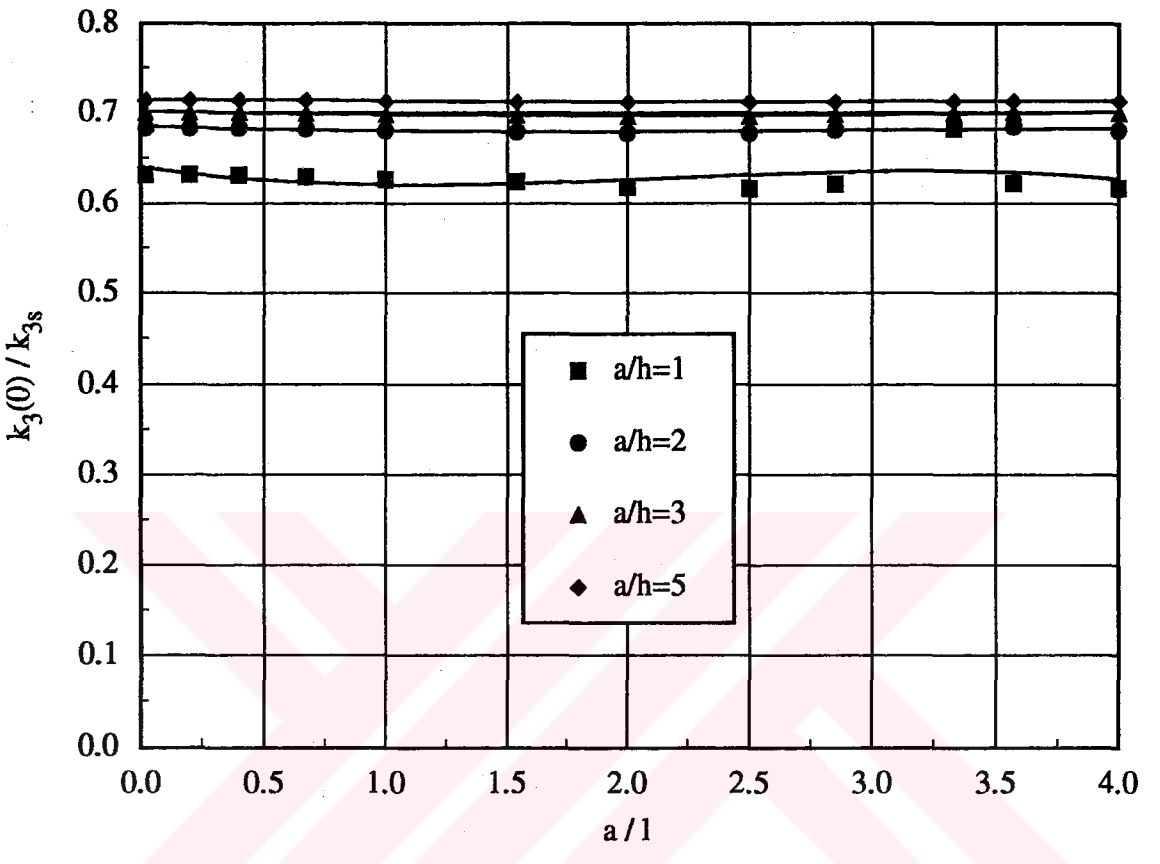

Figure 23. Mode III Normalized Stress Intensity Factor at the Center of a Semi-Elliptic Circumferential Outer Part-Through Crack in an Isotropic Cylindrical Shell with a Fixed End Subjected to In-Plane Shear; $\nu = 0.3$, $R/h = 5$, $l_0/h = 0.2$

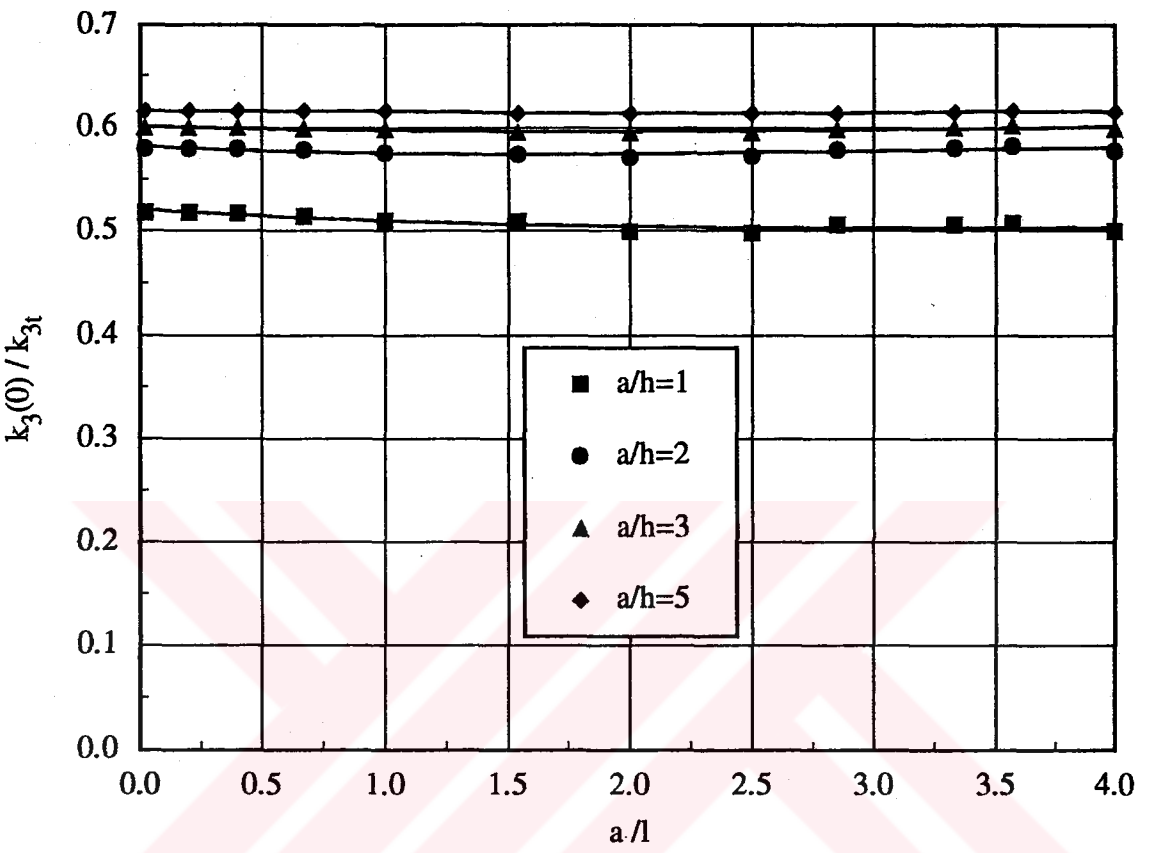

Figure 24. Mode III Normalized Stress Intensity Factor at the Center of a Semi-Elliptic Circumferential Outer Part-Through Crack in an Isotropic Cylindrical Shell with a Fixed End Subjected to Twisting; $\nu = 0.3$, $R/h = 5$, $l_0/h = 0.2$

REFERENCES

[1]. E.S. Folias, Journal of Mathematics and Physics, 44, 165 (1965).

[2]. E.S Folias, International Journal of Fracture Mechanics, 1, 20 (1965).

[3]. E.S Folias, ,International Journal of Fracture Mechanics, .3, 104 (1967).

[4]. E.S. Folias, International Journal of Fracture Mechanics, 3, 1 (1967).

[5]. F. Erdogan and J.J. Kibler, International Journal of Fracture Mechanics, 5,.229 (1969).

[6]. G.C.Sih and H.C.Hagendorf, Thin-Shell Structures: Theory, Experiment and Design, (1974).

[7]. P.M. Naghdi, Quarterly of Applied Mathematics, 14, 331 (1956).

[8]. S. Krenk, International Journal of Fracture Mechanics, 14, 123 (1978).

[9]. F. Delale and F. Erdogan, Quarterly of Applied Mathematics, 37, 239 (1979).

[10]. F. Delale, NASA Project Report, NGR 39-007-011,(July 1981).

[11]. E. Reissner, ASME Journal of Applied Mechanics, 12, A69 (1945).

[12]. E. Reissner, Quarterly of Applied Mathematics, .5, 56 (1947).

[13]. O.S. Yahsi and F. Erdogan, International Journal of Solids and Structures, 19, 955 (1983).

[14]. J.C. Newman and I.S. Raju, NASA Technical Memorandum ,80073, (July 1979).

[15]. J.J. McGowan and M. Raymond, ASTM-STP 677 Fracture Mechanics, (1979).

[16]. J. Heliot, R.C. Labbens and A. Peellisier-Tanou, ASTM-STP 677 Fracture Mechanics, (1979).

[17]. J.R. Rice and N. Levy, ASME Journal of Applied Mechanics, 39, 185 (1972).,

[18]. J.R. Rice, The Surface Crack: Physical Problems and Computational Solutions ASME New York, 171, (1972).

[19]. F. Delale and F. Erdogan, ASME Journal of Applied Mechanics, 49, 97 (1982).

[20]. P.F. Joseph and F. Erdogan, ASME Journal of Applied Mechanics, 55, 195 (1988).
[21]. O.S. Yahsi and F. Erdogan, International Journal of Fracture, 28, 161 (1985).

[22]. F. Erdogan, Journal of Applied Mathematics, 17, 1041 (1969).

[23]. O.S. Yahsi, and M. Gulgec, Proceedings of International Conference on Computational Engineering Science, (1988).

[24]. F. Erdogan, Mixed Boundary Value Problems in Mechanics, Mechanics Today, 4, 1 (1978).

[25]. I.S. Gradshteyn and I.M. Ryzhik, Tables of Integrals, Series and Products, 1965.

APPENDICES

APPENDIX A

Dimensionless Quantities

$$x=\frac{1}{\sqrt{c}}\frac{X_1}{a} \quad , \quad y=\sqrt{c}\frac{X_2}{a} \quad , \quad z=\frac{X_3}{a} \tag{A.1}$$

$$u=\sqrt{c}\frac{u_1}{a} \quad , \quad v=\frac{1}{\sqrt{c}}\frac{u_2}{a} \quad , \quad w=\frac{W}{a} \tag{A.2}$$

$$\beta_x=\sqrt{c}\beta_1 \quad , \quad \beta_y=\frac{1}{\sqrt{c}}\beta_2 \quad , \quad \Phi=\frac{F}{a^2hE} \tag{A.3}$$

$$\sigma_{xx}=\frac{\sigma_{11}}{cE} \quad , \quad \sigma_{yy}=\frac{c\sigma_{22}}{E} \quad , \quad \sigma_{xy}=\frac{\sigma_{12}}{E}$$

$$\sigma_{xz}=\frac{\sigma_{13}}{B\sqrt{c}} \quad , \quad \sigma_{yz}=\frac{\sqrt{c}\sigma_{23}}{B} \tag{A.4}$$

$$N_{xx}=\frac{N_{11}}{chE} \quad , \quad N_{yy}=\frac{cN_{22}}{hE} \quad , \quad N_{xy}=\frac{N_{12}}{hE} \tag{A.5}$$

$$M_{xx}=\frac{M_{11}}{ch^2E} \quad , \quad M_{yy}=\frac{cM_{22}}{h^2E} \quad , \quad M_{xy}=\frac{M_{12}}{h^2E} \tag{A.6}$$

$$V_x=\frac{V_1}{\sqrt{chB}} \quad , \quad V_y=\frac{\sqrt{c}V_2}{hB} \tag{A.7}$$

$$\lambda_2^4=12(1-\nu^2)\frac{a^4}{h^2R_2^2c^2}$$

$$\lambda^4=12(1-\nu^2)\frac{a^2}{h^2}$$

$$\kappa=\frac{E}{B\lambda^4} \tag{A.8}$$

APPENDIX B

ASYMPTOTIC VALUES OF KERNELS OF INTEGRAL EQUATIONS

In this part, asymptotic values of kernels of integral equations (3.1.93)-(3.1.97) for $\alpha \to \infty$ will be given.

Denote the inregrands of the infinite integrals of the integral equations (3.1.93)-(3.1.97) as

$$K_{un,1} = \alpha^2 \sum_{j=1}^{8} K_j R_j \tag{B.1}$$

$$K_{un,2} = \frac{1}{\lambda^4}\left[\sum_{j=1}^{8} \frac{p_j + (1-\nu)\alpha^2}{\kappa p_j - 1} R_j - \frac{\kappa(1-\nu)^2}{2} i\alpha\left(A_1 r_1 + A_2 r_2\right)\right] \tag{B.2}$$

$$K_{un,3} = \sum_{j=1}^{8} \frac{\kappa p_j m_j R_j}{\kappa p_j - 1} - \frac{\kappa(1-\nu)}{2} \alpha i\left(A_1 + A_2\right) \tag{B.3}$$

$$K_{un,4} = i\alpha \sum_{j=1}^{8} K_j m_j R_j \tag{B.4}$$

$$K_{un,5} = \frac{(1-\nu)}{\lambda^4}\left[i\alpha \sum_{j=1}^{8} \frac{m_j R_j}{\kappa p_j - 1} + \frac{\kappa(1-\nu)}{4}\left(\alpha^2 + r_1^2\right)\left(A_1 + A_2\right)\right] \tag{B.5}$$

Let the asymptotic values of $K_{un,i}$ (i=1,...,5) for $\alpha \to \infty$ be $K_{as,i}$ (i=1,...,5), respectively. To be able to evaluate $K_{as,i}$ (i=1,...,5), define the following new auxiliary expressions in terms of B_0, B_1,..., B_8 as follows

$$\sum_{j=1}^{4}\frac{m_j R_j}{p_j^4}-\sum_{j=5}^{8}\frac{m_j R_j}{p_j^4}=B_0$$
$$\sum_{j=1}^{4}\frac{m_j R_j}{p_j^3}-\sum_{j=5}^{8}\frac{m_j R_j}{p_j^3}=B_1$$
$$\vdots$$
$$\sum_{j=1}^{4}m_j p_j^4 R_j-\sum_{j=5}^{8}m_j p_j^4 R_j=B_8 \qquad \text{(B.6)}$$

From equations (3.1.99) and (3.1.100), it is known that

$$m_j\Big|_{\alpha\to\infty}=-|\alpha|\left(1+\frac{a_1 p_j}{\alpha^2}-\frac{a_2 p_j^2}{\alpha^4}+\cdots+\frac{a_n p_j^n}{\alpha^{2n}}\right)\quad j=1,2,3,4$$
$$m_j\Big|_{\alpha\to\infty}=|\alpha|\left(1+\frac{a_1 p_j}{\alpha^2}-\frac{a_2 p_j^2}{\alpha^4}+\cdots+\frac{a_n p_j^n}{\alpha^{2n}}\right)\quad j=5,6,7,8 \qquad \text{(B.7)}$$

If one now substitutes the asymptotic values of $m_j(\alpha)$ given in (B.7) into (B.6) and solves for, $\sum_1^8\frac{R_j}{p_j^4}$, $\sum_1^8\frac{R_j}{p_j^3}$,....., $\sum_1^8 R_j p_j^4$, the following expressions can be found

$$\sum_{j=1}^{8}p_j^4 R_j(\alpha)=-\frac{B_8}{\alpha}$$

$$\sum_{j=1}^{8}p_j^3 R_j(\alpha)=-\frac{B_7}{\alpha}+\frac{B_8}{2\alpha^3}$$

$$\sum_{j=1}^{8}p_j^2 R_j(\alpha)=-\frac{B_6}{\alpha}+\frac{B_7}{2\alpha^3}-\frac{3B_8}{8\alpha^5}$$

$$\sum_{j=1}^{8}p_j R_j(\alpha)=-\frac{B_5}{\alpha}+\frac{B_6}{2\alpha^3}-\frac{3B_7}{8\alpha^5}+\frac{5B_8}{16\alpha^7}$$

$$\sum_{j=1}^{8} R_j(\alpha) = -\frac{B_4}{\alpha} + \frac{B_5}{2\alpha^3} - \frac{3B_6}{8\alpha^5} + \frac{5B_7}{16\alpha^7} - \frac{15B_8}{64\alpha^9}$$

$$\sum_{j=1}^{8} \frac{R_j(\alpha)}{p_j} = -\frac{B_3}{\alpha} + \frac{B_4}{2\alpha^3} - \frac{3B_5}{8\alpha^5} + \frac{5B_6}{16\alpha^7} - \frac{15B_7}{64\alpha^9} + \frac{23B_8}{128\alpha^{11}}$$

$$\sum_{j=1}^{8} \frac{R_j(\alpha)}{p_j^2} = -\frac{B_2}{\alpha} + \frac{B_3}{2\alpha^3} - \frac{3B_4}{8\alpha^5} + \frac{5B_5}{16\alpha^7} - \frac{15B_6}{64\alpha^9} + \frac{23B_7}{128\alpha^{11}}$$

$$\sum_{j=1}^{8} \frac{R_j(\alpha)}{p_j^3} = -\frac{B_1}{\alpha} + \frac{B_2}{2\alpha^3} - \frac{3B_3}{8\alpha^5} + \frac{5B_4}{16\alpha^7} - \frac{15B_5}{64\alpha^9} + \frac{23B_6}{128\alpha^{11}}$$

$$\sum_{j=1}^{8} \frac{R_j(\alpha)}{p_j^4} = -\frac{B_0}{\alpha} + \frac{B_1}{2\alpha^3} - \frac{3B_2}{8\alpha^5} + \frac{5B_3}{16\alpha^7} - \frac{15B_4}{64\alpha^9} + \frac{23B_5}{128\alpha^{11}} \qquad \text{(B.8)}$$

Thus the problem is reduced to the evaluation of B_0, B_1, ..., B_8. From equation (3.1.79), it is seen that

$$B_4 = \sum_{j=1}^{4} m_j R_j(\alpha) - \sum_{j=5}^{8} m_j R_j(\alpha) = -\frac{iq_2}{\alpha} \qquad \text{(B.9)}$$

recalling (3.1.18)

$$K_j = \left(\frac{\lambda_2}{\lambda}\right)^2 \frac{\left(p_j + \alpha^2\right)}{p_j^2} \qquad \text{(B.10)}$$

and using (3.1.78), B_2 and B_3 can be found as

$$B_2 = -\left(\frac{\lambda}{\lambda_2}\right)^2 \frac{iq_1}{\alpha^3}$$

$$B_3 = \left(\frac{\lambda}{\lambda_2}\right)^2 \frac{iq_1}{\alpha^3} \tag{B.11}$$

In a similar way, using (3.1.68)-(3.1.72) and (3.1.78), (3.1.79), B_0, B_1 can be obtained as

$$B_0 = \frac{\kappa(1-\nu)}{\lambda_2^4}\frac{iq_2}{\alpha^3} - \frac{(1-2\nu)}{\lambda_2^4}\frac{iq_2}{\alpha^5} - \left(\frac{\lambda}{\lambda_2}\right)^2 \frac{iq_1}{\alpha^7}$$

$$B_1 = \frac{(1-\nu)}{\lambda_2^4}\frac{iq_2}{\alpha^3} + \left(\frac{\lambda}{\lambda_2}\right)^2 \frac{iq_1}{\alpha^5} \tag{B.12}$$

Also, observing that

$$\kappa\left(\sum_{j=1}^{4}\frac{p_j^{n-3}m_jR_j(\alpha)}{\kappa p_j - 1} - \sum_{j=5}^{8}\frac{p_j^{n-3}m_jR_j(\alpha)}{\kappa p_j - 1}\right) = \left(\sum_{j=1}^{4} p_j^{n-4}m_jR_j - \sum_{j=5}^{8} p_j^{n-4}m_jR_j\right) + \left(\sum_{j=1}^{4}\frac{p_j^{n-4}m_jR_j(\alpha)}{\kappa p_j - 1} - \sum_{j=5}^{8}\frac{p_j^{n-4}m_jR_j(\alpha)}{\kappa p_j - 1}\right), \quad n = 0,1,\ldots,8 \tag{B.13}$$

and referring to (B.6), B_n can also be expressed as,

$$B_n = \kappa\left(\sum_{j=1}^{4}\frac{p_j^{n-3}m_jR_j}{\kappa p_j - 1} - \sum_{j=5}^{8}\frac{p_j^{n-3}m_jR_j}{\kappa p_j - 1}\right) - \left(\sum_{j=1}^{4}\frac{p_j^{n-4}m_jR_j}{\kappa p_j - 1} - \sum_{j=5}^{8}\frac{p_j^{n-4}m_jR_j}{\kappa p_j - 1}\right) \tag{B.14}$$

By substituting the expression of p_j given in (3.1.20) into (3.1.9), it can be shown that

$$\frac{1}{\kappa p_j - 1} = \frac{\lambda_2^4 m_j^4}{p_j^4} \tag{B.15}$$

Using (B.15), (B.14), (B.11) and (B.12), remaining B_j terms can be found as,

$$B_5 = -(1-\nu)\alpha(iq_2) + \kappa\lambda_2^4 \frac{(iq_2)}{\alpha} + \kappa\lambda_2^2\lambda^2\alpha(iq_1)$$

$$B_6 = -\kappa\lambda_2^4(3-\nu)\alpha(iq_2) + \kappa\lambda_2^2\lambda^2\alpha^3(iq_1) + \lambda_2^2\lambda^2(\kappa\lambda_2^4 - 1)\alpha(iq_1)$$

$$B_7 = -\kappa\lambda_2^4(3-2\nu)\alpha^3(iq_2) + (3\kappa^2\lambda_2^4 - 1)\lambda_2^2\lambda^2\alpha^3(iq_1) + O(\alpha^1)$$

$$B_8 = -(1-\nu)\kappa\lambda_2^4\alpha^5(iq_2) + 3\kappa^2\lambda_2^6\lambda^2\alpha^5(iq_1) + O(\alpha^3) \qquad \text{(B.16)}$$

By substituting (B.11), (B.12) and (B.16) into (B.8), one can obtain following results,

$$\sum_{j=1}^{8} \frac{R_j}{p_j^4} = sign(\alpha)\left[-\frac{\kappa(1-\nu)}{\lambda_2^4}\frac{(iq_2)}{\alpha^4} + \frac{(3-5\nu)}{2\lambda_2^4}\frac{(iq_2)}{\alpha^6} + \frac{35}{16}\left(\frac{\lambda}{\lambda_2}\right)^2\frac{(iq_1)}{\alpha^8} + O(\alpha^{-10})\right]$$

$$\sum_{j=1}^{8} \frac{R_j}{p_j^3} = sign(\alpha)\left[-\frac{(1-\nu)}{\lambda_2^4}\frac{(iq_2)}{\alpha^4} - \frac{5(1+3\nu)}{64}\frac{(iq_2)}{\alpha^8} - \frac{15}{8}\left(\frac{\lambda}{\lambda_2}\right)^2\frac{(iq_1)}{\alpha^6} - \frac{15}{64}\kappa\lambda_2^2\lambda^2\frac{(iq_1)}{\alpha^8} + O(\alpha^{-10})\right]$$

$$\sum_{j=1}^{8} \frac{R_j}{p_j^2} = sign(\alpha)\left[\frac{(1+5\nu)}{16}\frac{(iq_2)}{\alpha^6} + \frac{3}{2}\left(\frac{\lambda}{\lambda_2}\right)^2\frac{(iq_1)}{\alpha^4} + \frac{5}{64}\kappa\lambda_2^2\lambda^2\frac{(iq_1)}{\alpha^6} + O(\alpha^{-8})\right]$$

$$\sum_{j=1}^{8} \frac{R_j}{p_j} = sign(\alpha)\left[-\frac{(1+3\nu)}{8}\frac{(iq_2)}{\alpha^4} + \frac{3}{8}\kappa\lambda_2^4\frac{(iq_2)}{\alpha^6} - \left(\frac{\lambda}{\lambda_2}\right)^2\frac{(iq_1)}{\alpha^2} - \frac{1}{16}\kappa\lambda_2^2\lambda^2\frac{(iq_1)}{\alpha^4} + O(\alpha^{-6})\right]$$

$$\sum_{j=1}^{8} R_j = sign(\alpha)\left[\frac{(1+\nu)}{2}\frac{(iq_2)}{\alpha^2} + \frac{\kappa\lambda_2^2\lambda^2}{8}\frac{(iq_1)}{\alpha^2} + O(\alpha^{-4})\right]$$

$$\sum_{j=1}^{8} p_j R_j = sign(\alpha)\left[(1-\nu)(iq_2) - \frac{\kappa\lambda_2^2\lambda^2}{2}(iq_1) + O(\alpha^{-2})\right]$$

$$\sum_{j=1}^{8} p_j^2 R_j = sign(\alpha)\left[-\kappa\lambda_2^2\lambda^2\alpha^2(iq_1) + O(\alpha^0)\right]$$

$$\sum_{j=1}^{8} p_j^3 R_j = O(\alpha^2)$$

$$\sum_{j=1}^{8} p_j^4 R_j = O(\alpha^4) \qquad \text{(B.17)}$$

Similarly, the asymptotic analysis of the terms $\sum_{1}^{8} p_j^{-4} m_j R_j$, $\sum_{1}^{8} p_j^{-3} m_j R_j$,....., $\sum_{1}^{8} p_j^4 m_j R_j$ as $\alpha \to \infty$ have to be evaluated. By denoting

$$\sum_{j=1}^{4}\frac{R_j}{p_j^4} - \sum_{j=5}^{8}\frac{R_j}{p_j^4} = C_0 \quad ,$$

$$\sum_{j=1}^{4}\frac{R_j}{p_j^3} - \sum_{j=5}^{8}\frac{R_j}{p_j^3} = C_1 \quad ,$$

$$\vdots$$

$$\sum_{j=1}^{4} p_j^4 R_j - \sum_{j=5}^{8} p_j^4 R_j = C_8 \qquad \text{(B.18)}$$

also by substituting the expansions for m_j given in (3.1.99) and (3.1.100), asymptotic values of terms $\sum_{1}^{8} p_j^{-4} m_j R_j$, $\sum_{1}^{8} p_j^{-3} m_j R_j$,....., $\sum_{1}^{8} p_j^4 m_j R_j$ as $\alpha \to \infty$ can be expressed in terms of auxiliary expressions $C_0, C_1, \cdots, C_8$ as follows,

$$\sum_{1}^{8}\frac{m_j R_j}{p_j^4}=-|\alpha|\left(C_0+\frac{1}{2\alpha^2}C_1-\frac{1}{8\alpha^4}C_2+\cdots\right)$$

$$\sum_{1}^{8}\frac{m_j R_j}{p_j^3}=-|\alpha|\left(C_1+\frac{1}{2\alpha^2}C_2-\frac{1}{8\alpha^4}C_3+\cdots\right)$$

$$\sum_{1}^{8}\frac{m_j R_j}{p_j^2}=-|\alpha|\left(C_2+\frac{1}{2\alpha^2}C_3-\frac{1}{8\alpha^4}C_4+\cdots\right)$$

$$\sum_{1}^{8}\frac{m_j R_j}{p_j}=-|\alpha|\left(C_3+\frac{1}{2\alpha^2}C_4-\frac{1}{8\alpha^4}C_5+\cdots\right)$$

$$\sum_{1}^{8}m_j R_j=-|\alpha|\left(C_4+\frac{1}{2\alpha^2}C_5-\frac{1}{8\alpha^4}C_6+\cdots\right)$$

$$\sum_{1}^{8}P_j m_j R_j=-|\alpha|\left(C_5+\frac{1}{2\alpha^2}C_6-\frac{1}{8\alpha^4}C_7+\cdots\right) \qquad \text{(B.19)}$$

So, it is required to evaluate $C_0, C_1, \cdots, C_8$. By using (3.1.80)-(3.1.82) and boundary conditions (3.1.68)-(3.1.72), following expressions can be found as

$$C_1=-\frac{iq_3}{\alpha^7}+\left(\frac{\lambda}{\lambda_2}\right)^2\frac{q_4}{\alpha^6}+\frac{(1-\nu)}{\lambda_2^4}\frac{q_5}{\alpha^4}$$

$$C_2=\frac{iq_3}{\alpha^5}-\left(\frac{\lambda}{\lambda_2}\right)^2\frac{q_4}{\alpha^4}$$

$$C_3=-\frac{iq_3}{\alpha^3}+\left(\frac{\lambda}{\lambda_2}\right)^2\frac{q_4}{\alpha^2}$$

$$C_4 = \frac{iq_3}{\alpha} \tag{B.20}$$

The remaining C_j terms can be obtained by using the following identity

$$C_n = \kappa\left(\sum_1^4 \frac{p_j^{n-3}R_j}{\kappa p_j - 1} - \sum_5^8 \frac{p_j^{n-3}R_j}{\kappa p_j - 1}\right) - \left(\sum_1^4 \frac{p_j^{n-4}R_j}{\kappa p_j - 1} - \sum_5^8 \frac{p_j^{n-4}R_j}{\kappa p_j - 1}\right) \tag{B.21}$$

and equation (B.15) as follows

$$C_0 = -\frac{1}{\lambda_2^4}\frac{iq_3}{\alpha^5} + \frac{iq_3}{\alpha^9} - \left(\frac{\lambda}{\lambda_2}\right)^2 \frac{q_4}{\alpha^8} + \frac{\kappa(1-\nu)}{\lambda_2^4}\frac{q_5}{\alpha^4} - \frac{2(1-\nu)}{\lambda_2^4}\frac{q_5}{\alpha^6}$$

$$C_5 = d_1 q_3 - (1-\nu)q_5$$

$$C_6 = d_2\alpha(iq_3) + d_1\alpha^2 q_4 + (d_1 d_2 - \lambda_2^2\lambda^2)q_4 - d_2(1-\nu)q_5$$

$$\begin{aligned} C_7 = {} & d_2\alpha^3(iq_3) + (d_2^2 - \lambda_2^4)(iq_3) + (3d_1 d_2 - \lambda_2^2\lambda^2)\alpha^2 q_4 \\ & + (d_1 d_2^2 - 2d_1\lambda_2^4)q_4 - 2(1-\nu)d_2\alpha^2 q_5 + (1-\nu)(\lambda_2^4 - d_2^2)q_5 \end{aligned}$$

$$\begin{aligned} C_8 = {} & (3d_2^2 - \lambda_2^4)\alpha^3(iq_3) + (d_2^3 - d_2\lambda_2^4)\alpha(iq_3) + 3d_1 d_2\alpha^4 q_4 \\ & (2d_2^2 - 4\lambda_2^4 - 2)d_1\alpha^2 q_4 - (1-\nu)d_2\alpha^4 q_5 \\ & + (1-\nu)(2\lambda_2^4 - 4d_2^2)\alpha^2 q_5 + O(\alpha^0) \end{aligned} \tag{B.22}$$

where

$$\begin{aligned} d_1 &= \kappa\lambda_2^2\lambda^2 \\ d_2 &= \kappa\lambda_2^4 \end{aligned} \tag{B.23}$$

Substituting (B.20) and (B.22) into (B.19), following expressions can be obtained

$$\sum_1^8 \frac{m_j R_j}{p_j^4} = -\alpha\, sign(\alpha)\left[-\frac{1}{\lambda_2^4}\frac{iq_3}{\alpha^5} + \frac{35}{128}\frac{iq_3}{\alpha^9} - \frac{5}{16}\left(\frac{\lambda}{\lambda_2}\right)^2 \frac{q_4}{\alpha^8} + \frac{\kappa(1-\nu)}{\lambda_2^4}\frac{q_5}{\alpha^4} - \frac{3}{2}\frac{(1-\nu)}{\lambda_2^4}\frac{q_5}{\alpha^6} + O(\alpha^{-10})\right]$$

$$\sum_1^8 \frac{m_j R_j}{p_j^3} = -\alpha\, sign(\alpha)\left[-\frac{5}{16}\frac{iq_3}{\alpha^7} + \frac{3}{8}\left(\frac{\lambda}{\lambda_2}\right)^2 \frac{q_4}{\alpha^6} + \frac{(1-\nu)}{\lambda_2^4}\frac{q_5}{\alpha^4} + \frac{5(1-\nu)}{128}\frac{q_5}{\alpha^8} + O(\alpha^{-10})\right]$$

$$\sum_1^8 \frac{m_j R_j}{p_j^2} = -\alpha\, sign(\alpha)\left[+\frac{3}{8}\frac{iq_3}{\alpha^5} - \frac{1}{2}\left(\frac{\lambda}{\lambda_2}\right)^2 \frac{q_4}{\alpha^4} + \frac{3\kappa\lambda_2^2\lambda^2}{128}\frac{q_4}{\alpha^6} - \frac{(1-\nu)}{16}\frac{q_5}{\alpha^6} + O(\alpha^{-8})\right]$$

$$\sum_1^8 \frac{m_j R_j}{p_j} = -\alpha\, sign(\alpha)\left[-\frac{1}{2}\frac{iq_3}{\alpha^3} + \left(\frac{\lambda}{\lambda_2}\right)^2 \frac{q_4}{\alpha^2} - \frac{1}{16}\kappa\lambda_2^2\lambda^2\frac{q_4}{\alpha^4} + \frac{(1-\nu)}{8}\frac{q_5}{\alpha^4} + O(\alpha^{-6})\right]$$

$$\sum_1^8 m_j R_j = -\alpha\, sign(\alpha)\left[\frac{iq_3}{\alpha} + \frac{3}{8}\kappa\lambda_2^2\lambda^2\frac{q_4}{\alpha^2} - \frac{(1-\nu)}{2}\frac{q_5}{\alpha^2} + O(\alpha^{-4})\right]$$

$$\sum_1^8 p_j m_j R_j = -\alpha\, sign(\alpha)\left[\frac{3}{2}\kappa\lambda_2^2\lambda^2 q_4 - (1-\nu)q_5 + O\left(\alpha^{-2}\right) + O\left(\alpha^{-2}\right)\right] \quad \text{(B.24)}$$

To be able to complete the asymptotic analysis, evaluation of the second terms appearing at the righthand side of (B.2), (B.3) and (B.5) as $\alpha \to \infty$ is required. As an example, lets evaluate the following term in (B.2)

$$-\frac{\kappa(1-\nu)}{2}\alpha I\left(A_1 + A_2\right) \quad \text{(B.25)}$$

Recalling equation (3.1.69)

$$-\frac{\kappa(1-\nu)^2\alpha i}{2}r_2\left(A_1+A_2\right)=\sum_1^4\frac{p_j+(1-\nu)\alpha^2}{\kappa p_j-1}R_j-\sum_5^8\frac{p_j+(1-\nu)\alpha^2}{\kappa p_j-1}R_j \quad \text{(B.26)}$$

and multiplying both sides by $1/(1-\nu)r_2$, following expression can be found as

$$-\frac{\kappa(1-\nu)\alpha i}{2}\left(A_1+A_2\right)=\frac{1}{(1-\nu)r_2}\left[\sum_1^4\frac{p_j+(1-\nu)\alpha^2}{\kappa p_j-1}R_j-\sum_5^8\frac{p_j+(1-\nu)\alpha^2}{\kappa p_j-1}R_j\right] \quad \text{(B.27)}$$

Using (B.15), (B.18), (B.20) and (B.22), righthand side of (B.27) can be expressed in terms of q_i as follows

$$-\frac{\kappa(1-\nu)\alpha i}{2}\left(A_1+A_2\right)=\frac{1}{r_2}\left[-\alpha q_3+\kappa(1-\nu)\alpha^2 q_5+q_5\right] \quad \text{(B.28)}$$

Using asymptotic expansion

$$\frac{1}{r_2}=\frac{1}{|\alpha|}\left(1-\frac{1}{\alpha(1-\nu)\alpha^2}+\frac{3}{2\kappa^2(1-\nu)^2\alpha^4}-\cdots\right) \quad \text{(B.29)}$$

and neglecting lower order terms, asymptotic value of (B.25) can be found as follows

$$\lim_{\alpha\to\infty}\left[-\frac{\kappa(1-\nu)\alpha i}{2}\left(A_1+A_2\right)\right]=\text{sign}(\alpha)\left[iq_3+\frac{iq_3}{\kappa(1-\nu)\alpha^2}+\kappa(1-\nu)\alpha q_5+\frac{1}{2\kappa(1-\nu)}\frac{q_5}{\alpha^3}+O(^{-4})\right] \quad \text{(B.30)}$$

In a similar way, also using the asymptotic expansions of r_1 and r_2, given in (3.1.102) and (3.1.103) respectively, asymptotic values of second terms appearing at the righthand side of (B.2) and (B.5) can be written as follows

$$\lim_{\alpha\to\infty}\left[-\frac{\kappa(1-\nu)^2\alpha i}{2}\left(r_1A_1+r_2A_2\right)\right]=sign(\alpha)\left[\kappa(1-\nu)^2\alpha^2(iq_2)+\right.$$
$$\left.(1\quad-\nu)(iq_2)+\frac{1}{2\kappa}\frac{iq_2}{\alpha^2}+O(^{-4})\right]$$

$$\lim_{\alpha\to\infty}\left[\frac{\kappa(1-\nu)\alpha i}{4}(\alpha^2+r_1^2)\left(A_1+A_2\right)\right]=sign(\alpha)\left[(1-\nu)\alpha q_3+\frac{1}{2\kappa^2(1-\nu)}\frac{q_3}{\alpha^3}+\right.$$
$$\left.\kappa(1-\nu)^2\alpha^2(iq_5)+(1-\nu)(iq_5)+\frac{1}{2\kappa}\frac{iq_5}{\alpha^2}+O(^{-4})\right] \qquad \text{(B.31)}$$

Finally, using the results given in (B.17) and (B.24), and following the procedures described above, asymptotic values as $\alpha\to\infty$ for the first terms at the righthand side of (B.1) through (B.5) can be obtained. Combining these and (B.30), (B.31) asymptotic values of $K_{un,i}$ (i=1,...,5) can be found as

$$K_{as,1}=sign(\alpha)\left[\frac{1}{2}(iq_1)+\frac{1}{64}\kappa\lambda_2^4\frac{iq_1}{\alpha^2}-\frac{(1+\nu)}{16}\left(\frac{\lambda_2}{\lambda}\right)^2\frac{iq_2}{\alpha^2}+O(\alpha^{-4})\right]$$

$$K_{as,2}=sign(\alpha)\left[-\frac{(1-\nu^2)}{2\lambda^4}(iq_2)-\frac{1}{2\kappa\lambda^4}\frac{iq_2}{\alpha^2}+\frac{(1+\nu)}{16}\left(\frac{\lambda_2}{\lambda}\right)^2\frac{iq_1}{\alpha^2}+O(\alpha^{-4})\right]$$

$$K_{as,3}=sign(\alpha)\left\{-iq_3+\left[\frac{\kappa\lambda_2^4}{16}+\frac{1}{\kappa(1-\nu)}\right]\frac{iq_2}{\alpha^2}-\frac{3}{8}\kappa\lambda_2^2\lambda^2\frac{q_4}{\alpha}+\right.$$
$$\left.\left[\frac{1}{2\kappa(1-\nu)}-\frac{5\kappa(1-\nu)\lambda_2^4}{128}\right]\frac{q_5}{\alpha^3}+O(\alpha^{-4})\right\}$$

$$K_{as,4} = sign(\alpha)\left\{-\frac{1}{2}iq_4 + \frac{5}{128}\kappa\lambda_2^4\frac{iq_4}{\alpha^2} + \frac{1}{8}\left(\frac{\lambda_2}{\lambda}\right)^2\frac{q_3}{\alpha} + \frac{(1-\nu)}{16}\left(\frac{\lambda_2}{\lambda}\right)^2\frac{iq_5}{\alpha^2} + O(\alpha^{-4})\right\}$$

$$K_{as,5} = sign(\alpha)\left\{\frac{(1-\nu^2)}{2\lambda_2^4}iq_5 + \frac{1}{2\kappa\lambda_2^4}\frac{iq_5}{\alpha^2} + \left[\frac{3(1-\nu)}{128} + \frac{1}{2\kappa^2(1-\nu)}\right]\frac{1}{\lambda_2^4}\frac{q_3}{\alpha^3} + \frac{(1-\nu)}{16}\left(\frac{\lambda}{\lambda_2}\right)^2\frac{iq_4}{\alpha^2} + O(\alpha^{-4})\right\} \quad \text{(B.32)}$$

If the integration is performed from zero to infinity, it can be seen that only the first terms of equations given in (B.32) contribute to Simple Cauchy type singularities. Those terms which are the closed form solutions of the asymptotic integrals are added as singular terms and those asymptotic integrals in the closed form are subtracted from unbounded integrals under the integral sign as mentioned in Section 3.1.

APPENDIX C

KERNELS OF INTEGRAL EQUATIONS

$$k_{11}\left(\sqrt{c}\tau,\sqrt{c}\eta\right)=\int_0^\infty\left[2\alpha^2\,\mathrm{Re}\left(\sum_{j=1}^{8}K_jQ_j-2\sum_{j=5}^{8}K_jQ_je^{-2m_jl'}\right)-1\right]\sin\alpha\sqrt{c}(\tau-\eta)\,d\alpha+2\int_0^\infty\alpha^2\,\mathrm{Im}\left(\sum_{j=1}^{8}K_jQ_j-2\sum_{j=5}^{8}K_jQ_je^{-2m_jl'}\right)\cos\alpha\sqrt{c}(\tau-\eta)\,d\alpha \tag{C.1}$$

$$k_{12}\left(\sqrt{c}\tau,\sqrt{c}\eta\right)=\int_0^\infty 2\alpha^2\,\mathrm{Re}\left(\sum_{j=1}^{8}K_jN_j-2\sum_{j=5}^{8}K_jN_je^{-2m_jl'}\right)\sin\alpha\sqrt{c}(\tau-\eta)\,d\alpha+2\int_0^\infty\alpha^2\,\mathrm{Im}\left(\sum_{j=1}^{8}K_jN_j-2\sum_{j=5}^{8}K_jN_je^{-2m_jl'}\right)\cos\alpha\sqrt{c}(\tau-\eta)\,d\alpha \tag{C.2}$$

$$k_{13}\left(\sqrt{c}\tau,\sqrt{c}\eta\right)=\int_0^\infty 2\alpha^2\,\mathrm{Re}\left(\sum_{j=1}^{8}K_jC_j-2\sum_{j=5}^{8}K_jC_je^{-2m_jl'}\right)\sin\alpha\sqrt{c}(\tau-\eta)\,d\alpha+2\int_0^\infty\alpha^2\,\mathrm{Im}\left(\sum_{j=1}^{8}K_jC_j-2\sum_{j=5}^{8}K_jC_je^{-2m_jl'}\right)\cos\alpha\sqrt{c}(\tau-\eta)\,d\alpha \tag{C.3}$$

$$k_{14}\left(\sqrt{c}\tau,\sqrt{c}\eta\right)=\int_0^\infty 2\alpha^2\,\mathrm{Re}\left(\sum_{j=1}^{8}K_jD_j-2\sum_{j=5}^{8}K_jD_je^{-2m_jl'}\right)\sin\alpha\sqrt{c}(\tau-\eta)\,d\alpha+2\int_0^\infty\alpha^2\,\mathrm{Im}\left(\sum_{j=1}^{8}K_jD_j-2\sum_{j=5}^{8}K_jD_je^{-2m_jl'}\right)\cos\alpha\sqrt{c}(\tau-\eta)\,d\alpha \tag{C.4}$$

$$k_{15}\left(\sqrt{c}\tau,\sqrt{c}\eta\right)=\int_0^\infty 2\alpha^2\,\mathrm{Re}\left(\sum_{j=1}^{8}K_jY_j-2\sum_{j=5}^{8}K_jY_je^{-2m_jl'}\right)$$
$$\sin\alpha\sqrt{c}(\tau-\eta)\,d\alpha+2\int_0^\infty\alpha^2\,\mathrm{Im}\left(\sum_{j=1}^{8}K_jY_j-\right.$$
$$\left.-2\sum_{j=5}^{8}K_jY_je^{-2m_jl'}\right)\cos\alpha\sqrt{c}(\tau-\eta)\,d\alpha \qquad \text{(C.5)}$$

$$k_{21}\left(\sqrt{c}\tau,\sqrt{c}\eta\right)=-\frac{2}{\lambda^4}\int_0^\infty\mathrm{Re}\left[\sum_{j=1}^{8}\frac{p_j+(1-\nu)\alpha^2}{\kappa p_j-1}Q_j-\right.$$
$$\left.2\sum_{j=5}^{8}\frac{p_j+(1-\nu)\alpha^2}{\kappa p_j-1}Q_je^{-2m_jl'}\right]\sin\alpha\sqrt{c}(\tau-\eta)\,d\alpha$$
$$-\frac{2}{\lambda^4}\int_0^\infty\mathrm{Im}\left[\sum_{j=1}^{8}\frac{p_j+(1-\nu)\alpha^2}{\kappa p_j-1}Q_j-\right.$$
$$\left.2\sum_{j=5}^{8}\frac{p_j+(1-\nu)\alpha^2}{\kappa p_j-1}Q_je^{-2m_jl'}\right]\cos\alpha\sqrt{c}(\tau-\eta)\,d\alpha \qquad \text{(C.6)}$$

$$k_{22}\left(\sqrt{c}\tau,\sqrt{c}\eta\right)=-\frac{2}{\lambda^4}\int_0^\infty\mathrm{Re}\left[\sum_{j=1}^{8}\frac{p_j+(1-\nu)\alpha^2}{\kappa p_j-1}N_j-\right.$$
$$\left.2\sum_{j=5}^{8}\frac{p_j+(1-\nu)\alpha^2}{\kappa p_j-1}N_je^{-2m_jl'}\right]\sin\alpha\sqrt{c}(\tau-\eta)\,d\alpha$$
$$-\frac{2}{\lambda^4}\int_0^\infty\mathrm{Im}\left[\sum_{j=1}^{8}\frac{p_j+(1-\nu)\alpha^2}{\kappa p_j-1}N_j-\right.$$
$$\left.2\sum_{j=5}^{8}\frac{p_j+(1-\nu)\alpha^2}{\kappa p_j-1}N_je^{-2m_jl'}\right]\cos\alpha\sqrt{c}(\tau-\eta)\,d\alpha+$$
$$\frac{1}{\lambda^4}\int_0^\infty\left[2\kappa(1-\nu)^2\alpha r_1-(1-\nu^2)\right.$$
$$\left.+4\kappa(1-\nu)^2\alpha r_2e^{-2r_2l'}\right]\sin\alpha\sqrt{c}(\tau-\eta)\,d\alpha \qquad \text{(C.7)}$$

$$k_{23}\left(\sqrt{c}\tau,\sqrt{c}\eta\right)=-\frac{2}{\lambda^4}\int_0^\infty \mathrm{Re}\left[\sum_{j=1}^{8}\frac{p_j+(1-\nu)\alpha^2}{\kappa p_j-1}C_j-\right.$$
$$\left.2\sum_{j=5}^{8}\frac{p_j+(1-\nu)\alpha^2}{\kappa p_j-1}C_j e^{-2m_j l'}\right]\sin\alpha\sqrt{c}(\tau-\eta)\,d\alpha$$
$$-\frac{2}{\lambda^4}\int_0^\infty \mathrm{Im}\left[\sum_{j=1}^{8}\frac{p_j+(1-\nu)\alpha^2}{\kappa p_j-1}C_j-\right.$$
$$\left.2\sum_{j=5}^{8}\frac{p_j+(1-\nu)\alpha^2}{\kappa p_j-1}C_j e^{-2m_j l'}\right]\cos\alpha\sqrt{c}(\tau-\eta)\,d\alpha-$$
$$8(1-\nu)\int_0^\infty \alpha e^{-2r_2 l'}\sin\alpha\sqrt{c}(\tau-\eta)\,d\alpha \qquad \text{(C.8)}$$

$$k_{24}\left(\sqrt{c}\tau,\sqrt{c}\eta\right)=-\frac{2}{\lambda^4}\int_0^\infty \mathrm{Re}\left[\sum_{j=1}^{8}\frac{p_j+(1-\nu)\alpha^2}{\kappa p_j-1}D_j-\right.$$
$$\left.2\sum_{j=5}^{8}\frac{p_j+(1-\nu)\alpha^2}{\kappa p_j-1}D_j e^{-2m_j l'}\right]\sin\alpha\sqrt{c}(\tau-\eta)\,d\alpha$$
$$-\frac{2}{\lambda^4}\int_0^\infty \mathrm{Im}\left[\sum_{j=1}^{8}\frac{p_j+(1-\nu)\alpha^2}{\kappa p_j-1}D_j-\right.$$
$$\left.2\sum_{j=5}^{8}\frac{p_j+(1-\nu)\alpha^2}{\kappa p_j-1}D_j e^{-2m_j l'}\right]\cos\alpha\sqrt{c}(\tau-\eta)\,d\alpha \qquad \text{(C.9)}$$

$$k_{25}\left(\sqrt{c}\tau,\sqrt{c}\eta\right)=-\frac{2}{\lambda^4}\int_0^\infty \mathrm{Re}\left[\sum_{j=1}^{8}\frac{p_j+(1-\nu)\alpha^2}{\kappa p_j-1}Y_j-\right.$$
$$\left.2\sum_{j=5}^{8}\frac{p_j+(1-\nu)\alpha^2}{\kappa p_j-1}Y_j e^{-2m_j l'}\right]\sin\alpha\sqrt{c}(\tau-\eta)\,d\alpha$$
$$-\frac{2}{\lambda^4}\int_0^\infty \mathrm{Im}\left[\sum_{j=1}^{8}\frac{p_j+(1-\nu)\alpha^2}{\kappa p_j-1}Y_j-\right.$$
$$\left.2\sum_{j=5}^{8}\frac{p_j+(1-\nu)\alpha^2}{\kappa p_j-1}Y_j e^{-2m_j l'}\right]\cos\alpha\sqrt{c}(\tau-\eta)\,d\alpha-$$
$$8(1-\nu)\int_0^\infty\left[1+\kappa(1-\nu)\alpha^2\right]e^{-2r_2 l'}\cos\alpha\sqrt{c}(\tau-\eta)\,d\alpha \qquad \text{(C.10)}$$

$$k_{31}\left(\sqrt{c}\tau,\sqrt{c}\eta\right)=-\int_0^{\infty}\mathrm{Re}\left[\sum_{j=1}^{8}\frac{\kappa p_j m_j}{\kappa p_j-1}Q_j-\right.$$
$$\left.2\sum_{j=5}^{8}\frac{\kappa p_j m_j}{\kappa p_j-1}Q_j e^{-2m_j l'}\right]\sin\alpha\sqrt{c}(\tau-\eta)\,d\alpha$$
$$-\int_0^{\infty}\mathrm{Im}\left[\sum_{j=1}^{8}\frac{\kappa p_j m_j}{\kappa p_j-1}Q_j-\right.$$
$$\left.2\sum_{j=5}^{8}\frac{\kappa p_j m_j}{\kappa p_j-1}Q_j e^{-2m_j l'}\right]\cos\alpha\sqrt{c}(\tau-\eta)\,d\alpha \qquad \text{(C.11)}$$

$$k_{32}\left(\sqrt{c}\tau,\sqrt{c}\eta\right)=-\int_0^{\infty}\mathrm{Re}\left[\sum_{j=1}^{8}\frac{\kappa p_j m_j}{\kappa p_j-1}N_j-\right.$$
$$\left.2\sum_{j=5}^{8}\frac{\kappa p_j m_j}{\kappa p_j-1}N_j e^{-2m_j l'}\right]\sin\alpha\sqrt{c}(\tau-\eta)\,d\alpha$$
$$-\int_0^{\infty}\mathrm{Im}\left[\sum_{j=1}^{8}\frac{\kappa p_j m_j}{\kappa p_j-1}N_j-\right.$$
$$\left.2\sum_{j=5}^{8}\frac{\kappa p_j m_j}{\kappa p_j-1}N_j e^{-2m_j l'}\right]\cos\alpha\sqrt{c}(\tau-\eta)\,d\alpha+$$
$$2\kappa(1-\nu)\int_0^{\infty}\alpha e^{-2r_2 l'}\sin\alpha\sqrt{c}(\tau-\eta)\,d\alpha \qquad \text{(C.12)}$$

$$k_{33}\left(\sqrt{c}\tau,\sqrt{c}\eta\right)=-\int_0^{\infty}\mathrm{Re}\left[\sum_{j=1}^{8}\frac{\kappa p_j m_j}{\kappa p_j-1}C_j-\right.$$
$$\left.2\sum_{j=5}^{8}\frac{\kappa p_j m_j}{\kappa p_j-1}C_j e^{-2m_j l'}\right]\sin\alpha\sqrt{c}(\tau-\eta)\,d\alpha$$
$$-\int_0^{\infty}\mathrm{Im}\left[\sum_{j=1}^{8}\frac{\kappa p_j m_j}{\kappa p_j-1}C_j-\right.$$
$$\left.2\sum_{j=5}^{8}\frac{\kappa p_j m_j}{\kappa p_j-1}C_j e^{-2m_j l'}\right]\cos\alpha\sqrt{c}(\tau-\eta)\,d\alpha-$$
$$\int_0^{\infty}\left(1+\frac{\alpha}{r_1}+\frac{2\alpha}{r_2}e^{-2r_2 l'}\right)\sin\alpha\sqrt{c}(\tau-\eta)\,d\alpha \qquad \text{(C.13)}$$

$$k_{34}\left(\sqrt{c}\tau,\sqrt{c}\eta\right)=-\int_0^{\infty}\mathrm{Re}\left[\sum_{j=1}^{8}\frac{\kappa p_j m_j}{\kappa p_j-1}D_j-2\sum_{j=5}^{8}\frac{\kappa p_j m_j}{\kappa p_j-1}D_j e^{-2m_j l'}\right]\sin\alpha\sqrt{c}(\tau-\eta)\,d\alpha$$
$$-\int_0^{\infty}\mathrm{Im}\left[\sum_{j=1}^{8}\frac{\kappa p_j m_j}{\kappa p_j-1}D_j-2\sum_{j=5}^{8}\frac{\kappa p_j m_j}{\kappa p_j-1}D_j e^{-2m_j l'}\right]\cos\alpha\sqrt{c}(\tau-\eta)\,d\alpha \qquad \text{(C.14)}$$

$$k_{35}\left(\sqrt{c}\tau,\sqrt{c}\eta\right)=-\int_0^{\infty}\mathrm{Re}\left[\sum_{j=1}^{8}\frac{\kappa p_j m_j}{\kappa p_j-1}Y_j-2\sum_{j=5}^{8}\frac{\kappa p_j m_j}{\kappa p_j-1}Y_j e^{-2m_j l'}\right]\sin\alpha\sqrt{c}(\tau-\eta)\,d\alpha$$
$$-\int_0^{\infty}\mathrm{Im}\left[\sum_{j=1}^{8}\frac{\kappa p_j m_j}{\kappa p_j-1}Y_j-2\sum_{j=5}^{8}\frac{\kappa p_j m_j}{\kappa p_j-1}Y_j e^{-2m_j l'}\right]\cos\alpha\sqrt{c}(\tau-\eta)\,d\alpha-$$
$$\int_0^{\infty}\left[1+\kappa(1-\nu)\alpha^2\right]\left(\frac{1}{r_1}+\frac{2}{r_2}e^{-2r_2 l'}\right)\cos\alpha\sqrt{c}(\tau-\eta)\,d\alpha \qquad \text{(C.15)}$$

$$k_{41}\left(\sqrt{c}\tau,\sqrt{c}\eta\right)=-\int_0^{\infty}2\alpha\mathrm{Re}\left(\sum_{j=1}^{8}K_j m_j Q_j-2\sum_{j=5}^{8}K_j m_j Q_j e^{-2m_j l'}\right)$$
$$\cos\alpha\sqrt{c}(\tau-\eta)\,d\alpha+2\int_0^{\infty}\alpha\mathrm{Im}\left(\sum_{j=1}^{8}K_j m_j Q_j-\right.$$
$$\left.-2\sum_{j=5}^{8}K_j m_j Q_j e^{-2m_j l'}\right)\sin\alpha\sqrt{c}(\tau-\eta)\,d\alpha \qquad \text{(C.16)}$$

$$k_{42}\left(\sqrt{c}\tau,\sqrt{c}\eta\right)=-\int_0^\infty 2\alpha\mathrm{Re}\left(\sum_{j=1}^{8}K_j m_j N_j-2\sum_{j=5}^{8}K_j m_j N_j e^{-2m_j l}\right)$$
$$\cos\alpha\sqrt{c}(\tau-\eta)\,d\alpha+2\int_0^\infty \alpha\mathrm{Im}\left(\sum_{j=1}^{8}K_j m_j N_j-\right.$$
$$\left.-2\sum_{j=5}^{8}K_j m_j N_j e^{-2m_j l}\right)\sin\alpha\sqrt{c}(\tau-\eta)\,d\alpha \qquad \text{(C.17)}$$

$$k_{43}\left(\sqrt{c}\tau,\sqrt{c}\eta\right)=-\int_0^\infty 2\alpha\mathrm{Re}\left(\sum_{j=1}^{8}K_j m_j C_j-2\sum_{j=5}^{8}K_j m_j C_j e^{-2m_j l}\right)$$
$$\cos\alpha\sqrt{c}(\tau-\eta)\,d\alpha+2\int_0^\infty \alpha\mathrm{Im}\left(\sum_{j=1}^{8}K_j m_j C_j-\right.$$
$$\left.-2\sum_{j=5}^{8}K_j m_j C_j e^{-2m_j l}\right)\sin\alpha\sqrt{c}(\tau-\eta)\,d\alpha \qquad \text{(C.18)}$$

$$k_{44}\left(\sqrt{c}\tau,\sqrt{c}\eta\right)=-\int_0^\infty 2\alpha\mathrm{Re}\left(\sum_{j=1}^{8}K_j m_j D_j-2\sum_{j=5}^{8}K_j m_j D_j e^{-2m_j l}\right)$$
$$\cos\alpha\sqrt{c}(\tau-\eta)\,d\alpha+\int_0^\infty\left[2\alpha\mathrm{Im}\left(\sum_{j=1}^{8}K_j m_j D_j-\right.\right.$$
$$\left.\left.-2\sum_{j=5}^{8}K_j m_j D_j e^{-2m_j l}\right)-1\right]\sin\alpha\sqrt{c}(\tau-\eta)\,d\alpha \qquad \text{(C.19)}$$

$$k_{45}\left(\sqrt{c}\tau,\sqrt{c}\eta\right)=-\int_0^\infty 2\alpha\mathrm{Re}\left(\sum_{j=1}^{8}K_j m_j Y_j-2\sum_{j=5}^{8}K_j m_j Y_j e^{-2m_j l}\right)$$
$$\cos\alpha\sqrt{c}(\tau-\eta)\,d\alpha+\int_0^\infty 2\alpha\mathrm{Im}\left(\sum_{j=1}^{8}K_j m_j Y_j-\right.$$
$$\left.-2\sum_{j=5}^{8}K_j m_j Y_j e^{-2m_j l}\right)\sin\alpha\sqrt{c}(\tau-\eta)\,d\alpha \qquad \text{(C.20)}$$

$$k_{51}\left(\sqrt{c}\tau,\sqrt{c}\eta\right)=\frac{2(1-\nu)}{\lambda^4}\int_0^\infty \alpha \mathrm{Re}\left(\sum_{j=1}^{8}\frac{m_j}{\kappa p_j-1}Q_j-\right.$$
$$\left.2\sum_{j=5}^{8}\frac{m_j}{\kappa p_j-1}Q_j e^{-2m_j l'}\right)\cos\alpha\sqrt{c}(\tau-\eta)\,d\alpha-$$
$$\frac{2(1-\nu)}{\lambda^4}\int_0^\infty \alpha \,\mathrm{Im}\left(\sum_{j=1}^{8}\frac{m_j}{\kappa p_j-1}Q_j-\right.$$
$$\left.2\sum_{j=5}^{8}\frac{m_j}{\kappa p_j-1}Q_j e^{-2m_j l'}\right)\sin\alpha\sqrt{c}(\tau-\eta)\,d\alpha \qquad \text{(C.21)}$$

$$k_{52}\left(\sqrt{c}\tau,\sqrt{c}\eta\right)=\frac{2(1-\nu)}{\lambda^4}\int_0^\infty \alpha \mathrm{Re}\left(\sum_{j=1}^{8}\frac{m_j}{\kappa p_j-1}N_j-\right.$$
$$\left.2\sum_{j=5}^{8}\frac{m_j}{\kappa p_j-1}N_j e^{-2m_j l'}\right)\cos\alpha\sqrt{c}(\tau-\eta)\,d\alpha-$$
$$\frac{2(1-\nu)}{\lambda^4}\int_0^\infty \alpha \,\mathrm{Im}\left(\sum_{j=1}^{8}\frac{m_j}{\kappa p_j-1}N_j-\right.$$
$$\left.2\sum_{j=5}^{8}\frac{m_j}{\kappa p_j-1}N_j e^{-2m_j l'}\right)\sin\alpha\sqrt{c}(\tau-\eta)\,d\alpha-$$
$$\frac{\kappa(1-\nu)^2}{2\lambda^4}\int_0^\infty\left(\alpha^2+r_2^2\right)e^{-2r_2 l'}\cos\alpha\sqrt{c}(\tau-\eta)\,d\alpha \qquad \text{(C.22)}$$

$$k_{53}\left(\sqrt{c}\tau,\sqrt{c}\eta\right)=\frac{2(1-\nu)}{\lambda^4}\int_0^\infty \alpha \mathrm{Re}\left(\sum_{j=1}^{8}\frac{m_j}{\kappa p_j-1}C_j-\right.$$
$$\left.2\sum_{j=5}^{8}\frac{m_j}{\kappa p_j-1}C_j e^{-2m_j l'}\right)\cos\alpha\sqrt{c}(\tau-\eta)\,d\alpha-$$
$$\frac{2(1-\nu)}{\lambda^4}\int_0^\infty \alpha \,\mathrm{Im}\left(\sum_{j=1}^{8}\frac{m_j}{\kappa p_j-1}C_j-\right.$$
$$\left.2\sum_{j=5}^{8}\frac{m_j}{\kappa p_j-1}C_j e^{-2m_j l'}\right)\sin\alpha\sqrt{c}(\tau-\eta)\,d\alpha+$$
$$\frac{(1-\nu)}{\lambda^4}\int_0^\infty\left(\alpha^2+r_2^2\right)\left(\frac{1}{r_1}+\frac{2}{r_2}e^{-2r_2 l'}\right)\cos\alpha\sqrt{c}(\tau-\eta)\,d\alpha \qquad \text{(C.23)}$$

$$k_{54}\left(\sqrt{c}\tau,\sqrt{c}\eta\right)=\frac{2(1-\nu)}{\lambda^4}\int_0^\infty \alpha \mathrm{Re}\left(\sum_{j=1}^{8}\frac{m_j}{\kappa p_j-1}D_j-\right.$$
$$\left.2\sum_{j=5}^{8}\frac{m_j}{\kappa p_j-1}D_j e^{-2m_j l'}\right)\cos\alpha\sqrt{c}(\tau-\eta)\,d\alpha-$$
$$\frac{2(1-\nu)}{\lambda^4}\int_0^\infty \alpha \,\mathrm{Im}\left(\sum_{j=1}^{8}\frac{m_j}{\kappa p_j-1}D_j-\right.$$
$$\left.2\sum_{j=5}^{8}\frac{m_j}{\kappa p_j-1}D_j e^{-2m_j l'}\right)\sin\alpha\sqrt{c}(\tau-\eta)\,d\alpha \qquad \text{(C.24)}$$

$$k_{55}\left(\sqrt{c}\tau,\sqrt{c}\eta\right)=\frac{2(1-\nu)}{\lambda^4}\int_0^\infty \alpha \mathrm{Re}\left(\sum_{j=1}^{8}\frac{m_j}{\kappa p_j-1}Y_j-\right.$$
$$\left.2\sum_{j=5}^{8}\frac{m_j}{\kappa p_j-1}Y_j e^{-2m_j l'}\right)\cos\alpha\sqrt{c}(\tau-\eta)\,d\alpha-$$
$$\frac{2(1-\nu)}{\lambda^4}\int_0^\infty \alpha \,\mathrm{Im}\left(\sum_{j=1}^{8}\frac{m_j}{\kappa p_j-1}Y_j-\right.$$
$$\left.2\sum_{j=5}^{8}\frac{m_j}{\kappa p_j-1}Y_j e^{-2m_j l'}\right)\sin\alpha\sqrt{c}(\tau-\eta)\,d\alpha-$$
$$\frac{(1-\nu^2)}{\lambda^4}\int_0^\infty \sin\alpha\sqrt{c}(\tau-\eta)\,d\alpha-$$
$$\frac{(1-\nu)}{\lambda^4}\int_0^\infty\left[\kappa(1-\nu)\alpha^2+1\right]\left(\frac{\alpha^2+r_2^2}{\alpha}\right)\left(\frac{1}{r_1}+\right.$$
$$\left.\frac{1}{r_2}e^{-2r_2 l'}\right)\sin\alpha\sqrt{c}(\tau-\eta)\,d\alpha \qquad \text{(C.25)}$$

APPENDIX D

EVALUATION OF SINE AND COSINE INTEGRALS

The exponential decaying property of the bounded kernels given in Appendix C is no longer valid as $y \to t$, since the power of exponent terms being almost zero. Thus, some terms obtained in Appendix B, which have been disregarded in the formulation of the problem, i.e. during singularity extraction, will now be considered.

Analyzing B.32, it can be seen that the first terms have already been considered to be able to extract singularities and to satisfy convergence. Their effects were extracted from the unbounded kernels. The lower order terms, i.e. the remaining ones, constitute the subject of this chapter.

Consider. for example, the typical kernel k_{44} which appear in the integral equation (3.1.105). Referring to equation (C.19) in Appendix C, let

$$F_{44}(\alpha) = \sum_{j=1}^{8} \alpha K_j m_j D_j(\alpha)$$
$$= \left(\frac{\lambda_2}{\lambda}\right)^2 \sum_{j=1}^{8} \alpha \frac{m_j(p_j + \alpha^2)}{p_j^2} D_j(\alpha) \qquad \text{(D.1)}$$

The asymptotic values of fourth integral equation were obtained as $k_{as,4}$ in Appendix B. By using (3.1.88) and (B.32), the asymptotic value of F_{44} can be evaluated as

$$F_{44}\Big|_{\alpha\to\infty} = \frac{i}{2\alpha} - \frac{5\kappa\lambda_2^4}{128}\frac{i}{\alpha^2} \qquad \text{(D.2)}$$

Finally, by using equation (B.19), the kernel k_{44} can be expressed as

$$k_{44}\left(\sqrt{c}\tau,\sqrt{c}\eta\right)=-\int_0^A 2\alpha\mathrm{Re}\left(\sum_{j=1}^{8}K_j m_j D_j-2\sum_{j=5}^{8}K_j m_j D_j e^{-2m_j l}\right)$$
$$\cos\alpha\sqrt{c}(\tau-\eta)\,d\alpha+\int_0^A\left[2\alpha\mathrm{Im}\left(\sum_{j=1}^{8}K_j m_j D_j-\right.\right.$$
$$\left.\left.-2\sum_{j=5}^{8}K_j m_j D_j e^{-2m_j l}\right)-1\right]\sin\alpha\sqrt{c}(\tau-\eta)\,d\alpha-$$
$$\frac{5\kappa\lambda_2^4}{64}\int_A^\infty\frac{\sin\alpha\sqrt{c}(\tau-\eta)}{\alpha^2}d\alpha \qquad \text{(D.3)}$$

The value of the last integral is evaluated by using integration by parts as follows

$$\int_A^\infty\frac{\sin\alpha\sqrt{c}(\tau-\eta)}{\alpha^2}\,d\alpha=-\frac{\sin\alpha\sqrt{c}(\tau-\eta)}{\alpha}\Bigg|_A^\infty+\sqrt{c}(\tau-\eta)\int_A^\infty\frac{\cos\alpha\sqrt{c}(\tau-\eta)}{\alpha}\,d\alpha \qquad \text{(D.4)}$$

The integral in (D.4) is given as cosine integral in [25] as follows

$$\int_A^\infty\frac{\cos\alpha\sqrt{c}(\tau-\eta)}{\alpha}\,d\alpha=-Ci\left[A\sqrt{c}(\tau-\eta)\right] \qquad \text{(D.5)}$$

Substituting (D.5) into (D.4), following result can be obtained

$$\int_A^\infty\frac{\sin\alpha\sqrt{c}(\tau-\eta)}{\alpha^2}\,d\alpha=\frac{\sin A\sqrt{c}(\tau-\eta)}{A}-\sqrt{c}(\tau-\eta)Ci\left[A\sqrt{c}(\tau-\eta)\right] \qquad \text{(D.6)}$$

Similar analysis are done for the other kernels and they are reduced into the following form

$$k_{11}\left(\sqrt{c}\tau,\sqrt{c}\eta\right)=\int_0^A\left[2\alpha^2\mathrm{Re}\left(\sum_{j=1}^{8}K_j Q_j-2\sum_{j=5}^{8}K_j Q_j e^{-2m_j l}\right)-\right.$$
$$\left.-1\right]\sin\alpha\sqrt{c}(\tau-\eta)\,d\alpha+2\int_0^A\alpha^2\mathrm{Im}\left(\sum_{j=1}^{8}K_j Q_j-\right.$$

$$-2\sum_{j=5}^{8} K_j Q_j e^{-2m_j l'}\Big)\cos\alpha\sqrt{c}(\tau-\eta)\,d\alpha - \frac{\kappa\lambda_2^4}{32}\int_A^{\infty}\frac{\sin\alpha\sqrt{c}(\tau-\eta)}{\alpha^2}\,d\alpha \tag{D.7}$$

$$k_{12}\left(\sqrt{c}\tau,\sqrt{c}\eta\right) = \int_0^A 2\alpha^2\,\mathrm{Re}\left(\sum_{j=1}^{8} K_j N_j - 2\sum_{j=5}^{8} K_j N_j e^{-2m_j l'}\right) \sin\alpha\sqrt{c}(\tau-\eta)\,d\alpha + 2\int_0^A \alpha^2\,\mathrm{Im}\Big(\sum_{j=1}^{8} K_j N_j - -2\sum_{j=5}^{8} K_j N_j e^{-2m_j l'}\Big)\cos\alpha\sqrt{c}(\tau-\eta)\,d\alpha + \frac{(1+\nu)}{8}\left(\frac{\lambda_2}{\lambda}\right)^2\int_A^{\infty}\frac{\sin\alpha\sqrt{c}(\tau-\eta)}{\alpha^2}\,d\alpha \tag{D.8}$$

$$k_{13}\left(\sqrt{c}\tau,\sqrt{c}\eta\right) = \int_0^A 2\alpha^2\,\mathrm{Re}\left(\sum_{j=1}^{8} K_j C_j - 2\sum_{j=5}^{8} K_j C_j e^{-2m_j l'}\right) \sin\alpha\sqrt{c}(\tau-\eta)\,d\alpha + 2\int_0^A \alpha^2\,\mathrm{Im}\Big(\sum_{j=1}^{8} K_j C_j - -2\sum_{j=5}^{8} K_j C_j e^{-2m_j l'}\Big)\cos\alpha\sqrt{c}(\tau-\eta)\,d\alpha \tag{D.9}$$

$$k_{14}\left(\sqrt{c}\tau,\sqrt{c}\eta\right) = \int_0^A 2\alpha^2\,\mathrm{Re}\left(\sum_{j=1}^{8} K_j D_j - 2\sum_{j=5}^{8} K_j D_j e^{-2m_j l'}\right) \sin\alpha\sqrt{c}(\tau-\eta)\,d\alpha + 2\int_0^A \alpha^2\,\mathrm{Im}\Big(\sum_{j=1}^{8} K_j D_j - -2\sum_{j=5}^{8} K_j D_j e^{-2m_j l'}\Big)\cos\alpha\sqrt{c}(\tau-\eta)\,d\alpha \tag{D.10}$$

$$k_{15}\left(\sqrt{c}\tau,\sqrt{c}\eta\right) = \int_0^A 2\alpha^2\,\mathrm{Re}\left(\sum_{j=1}^{8} K_j Y_j - 2\sum_{j=5}^{8} K_j Y_j e^{-2m_j l'}\right) \sin\alpha\sqrt{c}(\tau-\eta)\,d\alpha + 2\int_0^A \alpha^2\,\mathrm{Im}\Big(\sum_{j=1}^{8} K_j Y_j -$$

$$-2\sum_{j=5}^{8} K_j Y_j e^{-2m_j l}\Bigg)\cos\alpha\sqrt{c}(\tau-\eta)\,d\alpha \qquad \text{(D.11)}$$

$$\begin{aligned}
k_{21}\left(\sqrt{c}\tau,\sqrt{c}\eta\right) = &-\frac{2}{\lambda^4}\int_0^A \mathrm{Re}\left[\sum_{j=1}^{8}\frac{p_j+(1-\nu)\alpha^2}{\kappa p_j-1}Q_j\right.\\
&\left.-2\sum_{j=5}^{8}\frac{p_j+(1-\nu)\alpha^2}{\kappa p_j-1}Q_j e^{-2m_j l}\right]\sin\alpha\sqrt{c}(\tau-\eta)\,d\alpha\\
&-\frac{2}{\lambda^4}\int_0^A \mathrm{Im}\left[\sum_{j=1}^{8}\frac{p_j+(1-\nu)\alpha^2}{\kappa p_j-1}Q_j\right.\\
&\left.-2\sum_{j=5}^{8}\frac{p_j+(1-\nu)\alpha^2}{\kappa p_j-1}Q_j e^{-2m_j l}\right]\cos\alpha\sqrt{c}(\tau-\eta)\,d\alpha\\
&-\frac{(1+\nu)}{8}\left(\frac{\lambda_2}{\lambda}\right)^2\int_A^{\infty}\frac{\sin\alpha\sqrt{c}(\tau-\eta)}{\alpha^2}\,d\alpha
\end{aligned} \qquad \text{(D.12)}$$

$$\begin{aligned}
k_{22}\left(\sqrt{c}\tau,\sqrt{c}\eta\right) = &-\frac{2}{\lambda^4}\int_0^A \mathrm{Re}\left[\sum_{j=1}^{8}\frac{p_j+(1-\nu)\alpha^2}{\kappa p_j-1}N_j\right.\\
&\left.-2\sum_{j=5}^{8}\frac{p_j+(1-\nu)\alpha^2}{\kappa p_j-1}N_j e^{-2m_j l}\right]\sin\alpha\sqrt{c}(\tau-\eta)\,d\alpha\\
&-\frac{2}{\lambda^4}\int_0^A \mathrm{Im}\left[\sum_{j=1}^{8}\frac{p_j+(1-\nu)\alpha^2}{\kappa p_j-1}N_j\right.\\
&\left.-2\sum_{j=5}^{8}\frac{p_j+(1-\nu)\alpha^2}{\kappa p_j-1}N_j e^{-2m_j l}\right]\cos\alpha\sqrt{c}(\tau-\eta)\,d\alpha\\
&+\frac{1}{\lambda^4}\int_0^A\left[2\kappa(1-\nu)^2\alpha r_1-(1-\nu^2)\right.\\
&\left.+4\kappa(1-\nu)^2\alpha r_2 e^{-2r_2 l}\right]\sin\alpha\sqrt{c}(\tau-\eta)\,d\alpha\\
&+\frac{1}{\kappa\lambda^4}\int_A^{\infty}\frac{\sin\alpha\sqrt{c}(\tau-\eta)}{\alpha^2}\,d\alpha
\end{aligned} \qquad \text{(D.13)}$$

$$\begin{aligned}
k_{23}\left(\sqrt{c}\tau,\sqrt{c}\eta\right) = &-\frac{2}{\lambda^4}\int_0^A \mathrm{Re}\left[\sum_{j=1}^{8}\frac{p_j+(1-\nu)\alpha^2}{\kappa p_j-1}C_j\right.\\
&\left.-2\sum_{j=5}^{8}\frac{p_j+(1-\nu)\alpha^2}{\kappa p_j-1}C_j e^{-2m_j l}\right]\sin\alpha\sqrt{c}(\tau-\eta)\,d\alpha
\end{aligned}$$

$$-\frac{2}{\lambda^4}\int_0^A \mathrm{Im}\left[\sum_{j=1}^{8}\frac{p_j+(1-\nu)\alpha^2}{\kappa p_j-1}C_j\right.$$
$$\left.-2\sum_{j=5}^{8}\frac{p_j+(1-\nu)\alpha^2}{\kappa p_j-1}C_j e^{-2m_j l'}\right]\cos\alpha\sqrt{c}(\tau-\eta)\,d\alpha$$
$$-8(1-\nu)\int_0^A \alpha e^{-2r_2 l'}\sin\alpha\sqrt{c}(\tau-\eta)\,d\alpha \qquad \text{(D.14)}$$

$$k_{24}\left(\sqrt{c}\tau,\sqrt{c}\eta\right)=-\frac{2}{\lambda^4}\int_0^A \mathrm{Re}\left[\sum_{j=1}^{8}\frac{p_j+(1-\nu)\alpha^2}{\kappa p_j-1}D_j\right.$$
$$\left.-2\sum_{j=5}^{8}\frac{p_j+(1-\nu)\alpha^2}{\kappa p_j-1}D_j e^{-2m_j l'}\right]\sin\alpha\sqrt{c}(\tau-\eta)\,d\alpha$$
$$-\frac{2}{\lambda^4}\int_0^A \mathrm{Im}\left[\sum_{j=1}^{8}\frac{p_j+(1-\nu)\alpha^2}{\kappa p_j-1}D_j\right.$$
$$\left.-2\sum_{j=5}^{8}\frac{p_j+(1-\nu)\alpha^2}{\kappa p_j-1}D_j e^{-2m_j l'}\right]\cos\alpha\sqrt{c}(\tau-\eta)\,d\alpha \qquad \text{(D.15)}$$

$$k_{25}\left(\sqrt{c}\tau,\sqrt{c}\eta\right)=-\frac{2}{\lambda^4}\int_0^A \mathrm{Re}\left[\sum_{j=1}^{8}\frac{p_j+(1-\nu)\alpha^2}{\kappa p_j-1}Y_j\right.$$
$$\left.-2\sum_{j=5}^{8}\frac{p_j+(1-\nu)\alpha^2}{\kappa p_j-1}Y_j e^{-2m_j l'}\right]\sin\alpha\sqrt{c}(\tau-\eta)\,d\alpha$$
$$-\frac{2}{\lambda^4}\int_0^A \mathrm{Im}\left[\sum_{j=1}^{8}\frac{p_j+(1-\nu)\alpha^2}{\kappa p_j-1}Y_j\right.$$
$$\left.-2\sum_{j=5}^{8}\frac{p_j+(1-\nu)\alpha^2}{\kappa p_j-1}Y_j e^{-2m_j l'}\right]\cos\alpha\sqrt{c}(\tau-\eta)\,d\alpha$$
$$-8(1-\nu)\int_0^A\left[1+\kappa(1-\nu)\alpha^2\right]e^{-2r_2 l'}\cos\alpha\sqrt{c}(\tau-\eta)\,d\alpha \qquad \text{(D.16)}$$

$$k_{31}\left(\sqrt{c}\tau,\sqrt{c}\eta\right)=-\int_0^A \mathrm{Re}\left[\sum_{j=1}^{8}\frac{\kappa p_j m_j}{\kappa p_j-1}Q_j-\right.$$
$$\left.2\sum_{j=5}^{8}\frac{\kappa p_j m_j}{\kappa p_j-1}Q_j e^{-2m_j l'}\right]\sin\alpha\sqrt{c}(\tau-\eta)\,d\alpha$$

$$-\int_0^A \mathrm{Im}\left[\sum_{j=1}^{8}\frac{\kappa p_j m_j}{\kappa p_j - 1}Q_j - 2\sum_{j=5}^{8}\frac{\kappa p_j m_j}{\kappa p_j - 1}Q_j e^{-2m_j t}\right]\cos\alpha\sqrt{c}(\tau-\eta)\,d\alpha \tag{D.17}$$

$$k_{32}\left(\sqrt{c}\tau,\sqrt{c}\eta\right) = -\int_0^A \mathrm{Re}\left[\sum_{j=1}^{8}\frac{\kappa p_j m_j}{\kappa p_j - 1}N_j - 2\sum_{j=5}^{8}\frac{\kappa p_j m_j}{\kappa p_j - 1}N_j e^{-2m_j t}\right]\sin\alpha\sqrt{c}(\tau-\eta)\,d\alpha$$
$$-\int_0^A \mathrm{Im}\left[\sum_{j=1}^{8}\frac{\kappa p_j m_j}{\kappa p_j - 1}N_j - 2\sum_{j=5}^{8}\frac{\kappa p_j m_j}{\kappa p_j - 1}N_j e^{-2m_j t}\right]\cos\alpha\sqrt{c}(\tau-\eta)\,d\alpha +$$
$$2\kappa(1-\nu)\int_0^\infty \alpha e^{-2r_2 t}\sin\alpha\sqrt{c}(\tau-\eta)\,d\alpha \tag{D.18}$$

$$k_{33}\left(\sqrt{c}\tau,\sqrt{c}\eta\right) = -\int_0^A \mathrm{Re}\left[\sum_{j=1}^{8}\frac{\kappa p_j m_j}{\kappa p_j - 1}C_j - 2\sum_{j=5}^{8}\frac{\kappa p_j m_j}{\kappa p_j - 1}C_j e^{-2m_j t}\right]\sin\alpha\sqrt{c}(\tau-\eta)\,d\alpha$$
$$-\int_0^A \mathrm{Im}\left[\sum_{j=1}^{8}\frac{\kappa p_j m_j}{\kappa p_j - 1}C_j - 2\sum_{j=5}^{8}\frac{\kappa p_j m_j}{\kappa p_j - 1}C_j e^{-2m_j t}\right]\cos\alpha\sqrt{c}(\tau-\eta)\,d\alpha$$
$$-\int_0^\infty\left(1+\frac{\alpha}{r_1}+\frac{2\alpha}{r_2}e^{-2r_2 t}\right)\sin\alpha\sqrt{c}(\tau-\eta)\,d\alpha$$
$$-\left[\frac{3(1-\nu)}{64}+\frac{1}{\kappa^2(1-\nu)}\right]\frac{1}{\lambda_2^4}\int_A^\infty\frac{\sin\alpha\sqrt{c}(\tau-\eta)}{\alpha^2}\,d\alpha \tag{D.19}$$

$$k_{34}\left(\sqrt{c}\tau,\sqrt{c}\eta\right)=-\int_0^A \mathrm{Re}\left[\sum_{j=1}^{8}\frac{\kappa p_j m_j}{\kappa p_j-1}D_j -2\sum_{j=5}^{8}\frac{\kappa p_j m_j}{\kappa p_j-1}D_j e^{-2m_j l'}\right]\sin\alpha\sqrt{c}(\tau-\eta)\,d\alpha$$
$$-\int_0^A \mathrm{Im}\left[\sum_{j=1}^{8}\frac{\kappa p_j m_j}{\kappa p_j-1}D_j -2\sum_{j=5}^{8}\frac{\kappa p_j m_j}{\kappa p_j-1}D_j e^{-2m_j l'}\right]\cos\alpha\sqrt{c}(\tau-\eta)\,d\alpha$$
$$-\frac{3\kappa\lambda_2^2\lambda^2}{4}\int_A^{\infty}\frac{\cos\alpha\sqrt{c}(\tau-\eta)}{\alpha}\,d\alpha \qquad \text{(D.20)}$$

$$k_{35}\left(\sqrt{c}\tau,\sqrt{c}\eta\right)=-\int_0^A \mathrm{Re}\left[\sum_{j=1}^{8}\frac{\kappa p_j m_j}{\kappa p_j-1}Y_j -2\sum_{j=5}^{8}\frac{\kappa p_j m_j}{\kappa p_j-1}Y_j e^{-2m_j l'}\right]\sin\alpha\sqrt{c}(\tau-\eta)\,d\alpha$$
$$-\int_0^A \mathrm{Im}\left[\sum_{j=1}^{8}\frac{\kappa p_j m_j}{\kappa p_j-1}Y_j -2\sum_{j=5}^{8}\frac{\kappa p_j m_j}{\kappa p_j-1}Y_j e^{-2m_j l'}\right]\cos\alpha\sqrt{c}(\tau-\eta)\,d\alpha$$
$$-\int_0^A\left[1+\kappa(1-\nu)\alpha^2\right]\left(\frac{1}{r_1}+\frac{2}{r_2}e^{-2r_2 l'}\right)\cos\alpha\sqrt{c}(\tau-\eta)\,d\alpha$$
$$-\left[\frac{1}{\kappa(1-\nu)}-\frac{5\kappa(1-\nu)\lambda_2^4}{64}\right]\int_A^{\infty}\frac{\cos\alpha\sqrt{c}(\tau-\eta)}{\alpha^3}\,d\alpha \qquad \text{(D.21)}$$

$$k_{41}\left(\sqrt{c}\tau,\sqrt{c}\eta\right)=-\int_0^A 2\alpha\,\mathrm{Re}\left(\sum_{j=1}^{8}K_j m_j Q_j-2\sum_{j=5}^{8}K_j m_j Q_j e^{-2m_j l'}\right)$$
$$\cos\alpha\sqrt{c}(\tau-\eta)\,d\alpha+2\int_0^A\alpha\,\mathrm{Im}\left(\sum_{j=1}^{8}K_j m_j Q_j$$
$$-2\sum_{j=5}^{8}K_j m_j Q_j e^{-2m_j l'}\right)\sin\alpha\sqrt{c}(\tau-\eta)\,d\alpha \qquad \text{(D.22)}$$

$$k_{42}\left(\sqrt{c}\tau,\sqrt{c}\eta\right)=-\int_0^A 2\alpha\mathrm{Re}\left(\sum_{j=1}^{8}K_j m_j N_j-2\sum_{j=5}^{8}K_j m_j N_j e^{-2m_j l}\right)$$
$$\cos\alpha\sqrt{c}(\tau-\eta)\,d\alpha+2\int_0^A \alpha\mathrm{Im}\left(\sum_{j=1}^{8}K_j m_j N_j-\right.$$
$$\left.-2\sum_{j=5}^{8}K_j m_j N_j e^{-2m_j l}\right)\sin\alpha\sqrt{c}(\tau-\eta)\,d\alpha \qquad \text{(D.23)}$$

$$k_{43}\left(\sqrt{c}\tau,\sqrt{c}\eta\right)=-\int_0^A 2\alpha\mathrm{Re}\left(\sum_{j=1}^{8}K_j m_j C_j-2\sum_{j=5}^{8}K_j m_j C_j e^{-2m_j l}\right)$$
$$\cos\alpha\sqrt{c}(\tau-\eta)\,d\alpha+2\int_0^A \alpha\mathrm{Im}\left(\sum_{j=1}^{8}K_j m_j C_j\right.$$
$$\left.-2\sum_{j=5}^{8}K_j m_j C_j e^{-2m_j l}\right)\sin\alpha\sqrt{c}(\tau-\eta)\,d\alpha$$
$$-\frac{1}{4}\left(\frac{\lambda_2}{\lambda}\right)^2\int_A^{\infty}\frac{\cos\alpha\sqrt{c}(\tau-\eta)}{\alpha}\,d\alpha \qquad \text{(D.24)}$$

$$k_{44}\left(\sqrt{c}\tau,\sqrt{c}\eta\right)=-\int_0^A 2\alpha\mathrm{Re}\left(\sum_{j=1}^{8}K_j m_j D_j-2\sum_{j=5}^{8}K_j m_j D_j e^{-2m_j l}\right)\times$$
$$\cos\alpha\sqrt{c}(\tau-\eta)\,d\alpha+\int_0^A\left[2\alpha\mathrm{Im}\left(\sum_{j=1}^{8}K_j m_j D_j\right.\right.$$
$$\left.\left.-2\sum_{j=5}^{8}K_j m_j D_j e^{-2m_j l}\right)-1\right]\sin\alpha\sqrt{c}(\tau-\eta)\,d\alpha$$
$$+\frac{5}{64}\kappa\lambda_2^4\int_A^{\infty}\frac{\sin\alpha\sqrt{c}(\tau-\eta)}{\alpha^2}\,d\alpha \qquad \text{(D.25)}$$

$$k_{45}\left(\sqrt{c}\tau,\sqrt{c}\eta\right)=-\int_0^A 2\alpha\mathrm{Re}\left(\sum_{j=1}^{8}K_j m_j Y_j-2\sum_{j=5}^{8}K_j m_j Y_j e^{-2m_j l}\right)\times$$
$$\cos\alpha\sqrt{c}(\tau-\eta)\,d\alpha+\int_0^A 2\alpha\mathrm{Im}\left(\sum_{j=1}^{8}K_j m_j Y_j-\right.$$

$$-2\sum_{j=5}^{8} K_j m_j Y_j e^{-2m_j l'}\Bigg)\sin\alpha\sqrt{c}(\tau-\eta)\,d\alpha$$
$$-\frac{(1-\nu)}{8}\left(\frac{\lambda_2}{\lambda}\right)^2\int_A^{\infty}\frac{\sin\alpha\sqrt{c}(\tau-\eta)}{\alpha^2}\,d\alpha \qquad \text{(D.26)}$$

$$k_{51}\left(\sqrt{c}\tau,\sqrt{c}\eta\right)=\frac{2(1-\nu)}{\lambda^4}\int_0^A \alpha\,\mathrm{Re}\left(\sum_{j=1}^{8}\frac{m_j}{\kappa p_j-1}Q_j-\right.$$
$$\left.2\sum_{j=5}^{8}\frac{m_j}{\kappa p_j-1}Q_j e^{-2m_j l'}\right)\cos\alpha\sqrt{c}(\tau-\eta)\,d\alpha-$$
$$\frac{2(1-\nu)}{\lambda^4}\int_0^A \alpha\,\mathrm{Im}\left(\sum_{j=1}^{8}\frac{m_j}{\kappa p_j-1}Q_j-\right.$$
$$\left.2\sum_{j=5}^{8}\frac{m_j}{\kappa p_j-1}Q_j e^{-2m_j l'}\right)\sin\alpha\sqrt{c}(\tau-\eta)\,d\alpha \qquad \text{(D.27)}$$

$$k_{52}\left(\sqrt{c}\tau,\sqrt{c}\eta\right)=\frac{2(1-\nu)}{\lambda^4}\int_0^A \alpha\,\mathrm{Re}\left(\sum_{j=1}^{8}\frac{m_j}{\kappa p_j-1}N_j-\right.$$
$$\left.2\sum_{j=5}^{8}\frac{m_j}{\kappa p_j-1}N_j e^{-2m_j l'}\right)\cos\alpha\sqrt{c}(\tau-\eta)\,d\alpha-$$
$$\frac{2(1-\nu)}{\lambda^4}\int_0^A \alpha\,\mathrm{Im}\left(\sum_{j=1}^{8}\frac{m_j}{\kappa p_j-1}N_j-\right.$$
$$\left.2\sum_{j=5}^{8}\frac{m_j}{\kappa p_j-1}N_j e^{-2m_j l'}\right)\sin\alpha\sqrt{c}(\tau-\eta)\,d\alpha-$$
$$\frac{\kappa(1-\nu)^2}{2\lambda^4}\int_0^A\left(\alpha^2+r_2^2\right)e^{-2r_2 l'}\cos\alpha\sqrt{c}(\tau-\eta)\,d\alpha \qquad \text{(D.28)}$$

$$k_{53}\left(\sqrt{c}\tau,\sqrt{c}\eta\right)=\frac{2(1-\nu)}{\lambda^4}\int_0^A \alpha\,\mathrm{Re}\left(\sum_{j=1}^{8}\frac{m_j}{\kappa p_j-1}C_j-\right.$$
$$\left.2\sum_{j=5}^{8}\frac{m_j}{\kappa p_j-1}C_j e^{-2m_j l'}\right)\cos\alpha\sqrt{c}(\tau-\eta)\,d\alpha-$$
$$\frac{2(1-\nu)}{\lambda^4}\int_0^A \alpha\,\mathrm{Im}\left(\sum_{j=1}^{8}\frac{m_j}{\kappa p_j-1}C_j-\right.$$

$$2\sum_{j=5}^{8}\frac{m_j}{\kappa p_j-1}C_j e^{-2m_j l'}\Bigg)\sin\alpha\sqrt{c}(\tau-\eta)\,d\alpha+$$
$$\frac{(1-\nu)}{\lambda^4}\int_0^A\left(\alpha^2+r_2^2\right)\left(\frac{1}{r_1}+\frac{2}{r_2}e^{-2r_2 l'}\right)\cos\alpha\sqrt{c}(\tau-\eta)\,d\alpha+$$
$$\left[\frac{3(1-\nu)}{64}+\frac{1}{\kappa^2(1-\nu)}\right]\frac{1}{\lambda_2^4}\int_0^A\frac{\cos\alpha\sqrt{c}(\tau-\eta)}{\alpha^3}\,d\alpha \qquad \text{(D.29)}$$

$$k_{54}\left(\sqrt{c}\tau,\sqrt{c}\eta\right)=\frac{2(1-\nu)}{\lambda^4}\int_0^A\alpha\,\mathrm{Re}\left(\sum_{j=1}^{8}\frac{m_j}{\kappa p_j-1}D_j-\right.$$
$$\left.2\sum_{j=5}^{8}\frac{m_j}{\kappa p_j-1}D_j e^{-2m_j l'}\right)\cos\alpha\sqrt{c}(\tau-\eta)\,d\alpha-$$
$$\frac{2(1-\nu)}{\lambda^4}\int_0^A\alpha\,\mathrm{Im}\left(\sum_{j=1}^{8}\frac{m_j}{\kappa p_j-1}D_j-\right.$$
$$\left.2\sum_{j=5}^{8}\frac{m_j}{\kappa p_j-1}D_j e^{-2m_j l'}\right)\sin\alpha\sqrt{c}(\tau-\eta)\,d\alpha+$$
$$\frac{(1-\nu)}{8}\left(\frac{\lambda}{\lambda_2}\right)^2\int_A^{\infty}\frac{\sin\alpha\sqrt{c}(\tau-\eta)}{\alpha^2}\,d\alpha \qquad \text{(D.30)}$$

$$k_{55}\left(\sqrt{c}\tau,\sqrt{c}\eta\right)=\frac{2(1-\nu)}{\lambda^4}\int_0^A \alpha \mathrm{Re}\left(\sum_{j=1}^{8}\frac{m_j}{\kappa p_j-1}Y_j-\right.$$

$$\left.2\sum_{j=5}^{8}\frac{m_j}{\kappa p_j-1}Y_j e^{-2m_j l'}\right)\cos\alpha\sqrt{c}(\tau-\eta)\,d\alpha-$$

$$\frac{2(1-\nu)}{\lambda^4}\int_0^A \alpha\,\mathrm{Im}\left(\sum_{j=1}^{8}\frac{m_j}{\kappa p_j-1}Y_j-\right.$$

$$\left.2\sum_{j=5}^{8}\frac{m_j}{\kappa p_j-1}Y_j e^{-2m_j l'}\right)\sin\alpha\sqrt{c}(\tau-\eta)\,d\alpha-$$

$$\frac{(1-\nu^2)}{\lambda^4}\int_0^A \sin\alpha\sqrt{c}(\tau-\eta)\,d\alpha-$$

$$\frac{(1-\nu)}{\lambda^4}\int_0^A\left[\kappa(1-\nu)\alpha^2+1\right]\left(\frac{\alpha^2+r_2^2}{\alpha}\right)\left(\frac{1}{r_1}+\right.$$

$$\left.\frac{1}{r_2}e^{-2r_2 l'}\right)\sin\alpha\sqrt{c}(\tau-\eta)\,d\alpha+$$

$$\frac{1}{\kappa\lambda_2^4}\int_A^{\infty}\frac{\sin\alpha\sqrt{c}(\tau-\eta)}{\alpha^2}\,d\alpha \qquad \text{(D.31)}$$

APPENDIX E

EDGE CRACK STRESS INTENSITY FACTOR CURVE FITTING

The line spring model is based on two assumptions. The first, previously stated, involves replacing the net ligament (in which the state of stress is two dimensional), by resultant forces which are functions of y only. The second assumption is that the stress intensity factors along the crack front may be obtained from these resultant forces as though the stress state were one of plane strain.

In order to make use of this analogy, the plane strain stress intensity factor solution for an edge-cracked strip must be available for the five possible loading conditions in a shell on a given surface. These solutions are presented along with a curve fit in the form,

$$p_i(\xi) = \frac{\sqrt{\xi}}{(1-\xi)^{3/2}} \sum_{k=0}^{12} C_{ik} \xi^K \quad , \qquad (i=1,2)$$

$$p_i(\xi) = \frac{\sqrt{\xi}}{(1-\xi)^{1/2}} \sum_{k=0}^{8} C_{ik} \xi^K \quad , \qquad (i=3,4,5)$$

where l is the crack depth, and the variable ξ is the ratio of the depth l to the strip thickness h, i.e. $\xi = l/h$. The constants C_{ik} are given in Table E.1 and Table E.2.

Table E.1. The Compliance Coefficients for $p_1(\xi)$ and $p_2(\xi)$ for tension and bending respectively.

Mode I

k	C_{1k}	C_{2k}
0	1.12152	1.12152
1	-1.67890	-3.04507
2	8.43058	10.49184
3	-29.46644	-36.66780
4	84.43442	110.09900
5	-182.95329	-255.68184
6	274.45012	421.97167
7	-252.12029	-440.50866
8	92.30672	199.37326
9	62.66657	123.93056
10	-88.30652	-237.97164
11	37.54045	136.17068
12	-5.30201	-28.91005

Table E.2. The Compliance Coefficients for $p_i(\xi)$, i=3,4,5, for parabolic in-plane shear, constant out-of-plane shear and twisting, respectively.

Modes II and III

k	C_{3k}	C_{4k}	C_{5k}
0	0.0	1.0	1.0
1	2.73069	-0.4999949	-1.773760
2	-3.44019	0.2860705	0.937496
3	0.33305	-0.2661996	-0.602894
4	2.80514	0.2193511	1.176914
5	-2.94406	-0.1731221	-2.183231
6	0.74775	0.1047768	2.906943
7	0.63860	-0.0418068	-2.121964
8	-0.32028	0.0075456	0.659759

VITA

Müfit Gülgeç was born on March 13, 1959 in Ankara. He graduated in 1980 from Ankara State Academy of Architecture and Engineering with Bachelor of Science in Mechanical Engineering. He worked as a Research Assistant for the Department of Mechanical Engineering, Gazi University until 1988 and earned a Masters of Science Degree in Mechanical Engineering from the Middle East Technical University in 1986. In the same department, he started his Ph.D. study in 1986. He has been working as an Instructor in the Mechanical Engineering Department, Gazi University since 1988.

He is married to Sema Gülgeç and they have a daughter, Sıla.